Universiteit Twente

faculteit der
chemische technologie

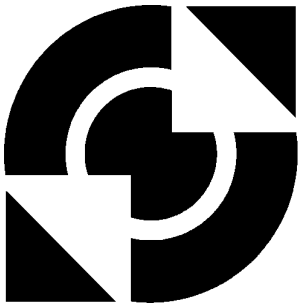

Limit cycles

139923

The elimination of limit cycles in a CISTR through the application of a feedback process controller

Onno Kramer

April 2002

Universiteit Twente

faculteit der
chemische technologie

PO box 217
7500 AE Enschede
The Netherlands
Phone: +31 (0)53 4899111
Internet: http://www.utwente.nl

Limit cycles

Graduate assignment

The elimination of limit cycles in a CISTR through the application of a feedback process controller

Group:
Process development and design
Faculty: Chemical Technology
Head: Prof. dr. ir. G.F. Versteeg

Commission:
Chairman: Prof. dr. ir. G.F. Versteeg (Twente University)
Member: Prof. dr. ir. J.A.M. Kuipers (Twente University)
Mentor: Dr. ir. D.W.F. Brilman (Twente University)
Company Mentor: Dr. ir. E.P. van Elk (Procede Twente b.v.)

Keywords:
CISTR, cooling, limit cycle, bifurcation, stability, control

Author:
Ing. O.J.I. Kramer

Date:
Friday 7 December 2001

SUMMARY

It is possible to eliminate the occurrence of limit cycles in a continuously ideally stirred tank reactor (CISTR), in which an irreversible exothermic reaction $A_{(l)} \rightarrow P_{(l)}$ takes place. This can be done through the application of a traditional feedback process controller, which regulates the extent of cooling. Controlling the throughput is possible, however nevertheless or the reactor temperature or the conversion can be preserved, not both.

Problem Analyses

Due to the interaction between the heat withdrawal and the heat generation in the CISTR, dynamical instability can appear. The resulting oscillating behaviour is generally unwanted and must therefore be eliminated. The scope of this report is to determine whether a process controller can fulfil this assignment. In addition, a second objective of this report is to acquire knowledge with respect to the dynamical behaviour in relation with the controller and phenomenon like the presumed delay.

Solving Method

The key to success is the use of the bifurcation program LOCBIF. This software package has numerical routines, which can contribute to the construction of distinct stability maps. These stability maps provide full information with regards to the static and dynamical behaviour of a particular process. Through a formulated mathematical model, describing the actual physical process and the intervening process controller, the dynamical behaviour is examined for several distinguished parameters. These parameters can be both process parameters, like the cooling capacity or throughput, as well as controller parameters like the proportional gain or the integral time. Three different control methods have been selected: coolant temperature control, coolant flowrate control and throughput control. All three types are investigated on their dynamical behaviour for both proportional and for proportional-integral control. For every specific case, the sensitivity of relevant parameters like the cooling capacity and the presumed delay is considered.

Results

Changes in continuous process operation are due to internal changes (limit cycles) and external changes (disturbances). A process, which exhibits distinct dynamical unstable behaviour, can be controlled through increasing the proportional gain. In many cases, limit cycles shrink and stability is acquired. However, precaution must always be taken for the processes in which multiplicity exists. Controllers with large proportional gain values can unmistakably manipulate a process variable (like the coolant flowrate) too far away from the desired set point. Consequently, transition can be inevitable. Therefore, the choice of the magnitude of the controller parameters has to be done deliberately. In case of controlling the extent of cooling, this is certainly possible. Nevertheless, in spite of an appropriate controller configuration, large disturbances in particular if also the system is dynamical unstable, transition remains apparent. In case of controlling the throughput, the restriction appears that the deviancy is in view of reactor design is limited. Therefore, large proportional gain values, which are required to eradicate both limit cycles as perturbations, are often not feasible. Moreover, in case of flowrate control, the risk of extinction or runaway is to be concerned with due to multiplicity. The implementation of the integral action in the mathematical controller model results in the offset being eliminated. To increase the physical realism of the mathematical model, the presumed delay is introduced. Small delay cannot destabilise a proper controlled process. Conversely, large delay provokes dynamical instability. Traditional control configuration tuning methods like the Ziegler and Nichols technique are not appropriate to deal with dynamical instabilities. Large cooling capacity, in general has a positive effect on the stability of a process in particular in combination with a suitable proportional gain.

OVERVIEW

Table 1 Suitable base case controller configuration to eliminate limit cycles and preserve stability.

Description	Coolant temperature control	Coolant flowrate control	Throughput control
Presumed delay	τ_d = 30 [s]	τ_d = 30 [s]	τ_d = 30 [s]
Perturbation	ΔT = 20 [K]	ΔT = 20 [K]	ΔT = 2 [K]
Inlet coolant temperature	-	$T_{cool,0}$ = 303 [K]	-
Proportional gain	K_c = 5 [-]	K_c = 0.0003 [m^3 s^{-1} K^{-1}]	K_c = 0.01 [m^3 s^{-1} K^{-1}]
Integral time	τ_I = 600 [s]	τ_I = 600 [s]	τ_I = 600 [s]
Desired base case reactor temperature	T = 468 [K]	T = 468 [K]	Φ_V = 0.012 [m^3 s^{-1}] T = 468 [K] with ζ = 0.48 [-]
Required conversion	ζ = 0.68 [-]	ζ = 0.68 [-]	Φ_V = 0.002 [m^3 s^{-1}] ζ = 0.72 with T = 454 [K]

VOORWOORD

Een voorwoord in een afstudeerverslag is doorgaans bedoeld om o.a. de afstudeercommissie, het afstudeerbedrijf en de mentor te bedanken. Het bedanken komt straks uitgebreid aan bod, maar eerst zou ik van de gelegenheid gebruik willen maken om eens te verwoorden waarom ik pas op 34 jarige leeftijd afstudeer. De primaire oorzaak ligt voor mij zeker bij het feit dat ik een visuele handicap heb. Mensen vragen altijd: "Wat kan je nou wel of niet zien?" Dat is lastig. Leg maar eens uit aan een persoon die gewoon alles kan zien wat 10% zicht is waarbij constant alles heen en weer beweegt zonder perspectief en ook nog eens wazig. "Draai een verrekijker maar eens om want dan krijg je een idee", zeg ik meestal. Mijn handicap zie ik niet als een excuus voor het feit dat dit studeren zo'n enorm lang traject werd, wel een belangrijke oorzaak.
Toen ik een klein jongetje was adviseerden medici mijn ouders om mij naar een school voor slechtzienden te sturen. Gelukkig zagen mijn vader en moeder in dat ik dat niet wilde en ging ik naar een normale basisschool. Al vanaf de basisschool werd mij meerdere malen dringend verzocht ander onderwijs te nemen. Daarom maar naar de HAVO in plaats van het VWO, waar ik koos voor wis-, natuur- en scheikunde en economie. Er werd mij op het hart gedrukt dat het geen verstandige keuze was om al deze β-vakken te kiezen. Talen, tekenen e.d. was het advies. Ik liet als compromis economie vallen voor biologie. Zonder doubleren haalde ik de eindstreep. Op de HTS werd mijn handicap steeds meer een probleem. Ik bleef voor de tweede maal zitten. Het advies was om te stoppen. Maar ik wilde toch verder en dat was zeer ongebruikelijk. Dankzij de docenten Bronkhorst en van der Meij mocht ik blijven. Door een nieuw medicijn en in combinatie met een bril met kijker kon ik weer de lessen volgen. Wederom ging alles daarna op rolletjes. Mijn stages bij de Akzo, de afdeling procesontwikkeling en techniek bij de Gemeentewaterleidingen Amsterdam o.l.v. Eric Baars en de Heidemij-Arcadis ingenieursbureau waren uiterst succesvol. Voor mijn afstuderen haalde ik 2 maal een 9 en een 10. Toen ik het beste afstudeerverslag had van regio Amsterdam en omstreken en mee deed met de afstudeerprijsvraag van de ingenieursvereniging NIRIA en 4^{e} werd van Nederland begon ik toch in te zien dat je met een handicap en wilskracht een heel eind kan komen. Iedereen adviseerde mij om door te gaan voor de hoofdprijs te weten de Universiteit. Deze stap nam ik in 1991 zonder echt goed na te denken of ik dat nou wel wilde. Nu ik dit voorwoord een week voor mijn afstudeerpraatje schrijf maakt het mij allemaal niet zoveel meer uit. Toch heb ik eerlijkheidshalve mijzelf wel duizend keer afgevraagd waarom ik dit ben gaan doen. Een heel belangrijk argument is voor mij dat ik volgens de vele oogartsen de enige ben met zo'n handicap die zover is gekomen. Als ik zou stoppen kunnen de ooit toekomstige studenten met dergelijke handicaps te horen krijgen dat zelfs die hardnekkige Onno Kramer uiteindelijk afhaakte. Nee, dat nooit. Ik wil niet op mijn geweten hebben dat anderen daarom wellicht negatief advies zouden kunnen krijgen. Een ander argument is dat ik vind dat je iets moet afmaken waar je aan begint. Wat heb ik dan gedaan al die tijd? In mijn studieperiode zit een gat van 6 jaar waarvan ik 1½ jaar heb gewerkt bij Gelink Adviesbureau als IT'r. Veel gesport: wedstrijdroeien, buitenlandse wedstrijden (topsport), marathons lopen. Zeker 5 jaar heb ik besteed aan mijn muzikale carrière (veel optredens etc.). De kans is groot dat de beurs die ik heb aangevraagd wordt toegewezen zodat ik naar Sevilla kan gaan om mijn muzikale kennis te verfijnen. In deze tussenperiode van weinig studeren, moest ik erachter komen hoe ik in deze wereld sta. De door mijn ouders met de paplepel ingegoten normen en waarden, klaar staan voor anderen e.d. is voor mij de rode draad in mijn leven. Toen ik besloot de draad weer op te pakken en begon met de literatuuropdracht bij professor Kuipers en deze afsloot met een 9 kwam het geloof weer terug. Professor Versteeg liet met het vak Inleiding procesontwikkeling en ontwerp zien dat je twee uiterste bij elkaar kan brengen: van fundamenteel wetenschappelijk tot met je schoenen in de mest-praktijk. Chemie is dus niet stoffig en saai. Niet geheel toevallig zitten deze twee heren in mijn afstudeercommissie. De eerder goedgekeurde afstudeeropdracht bij de GW-Amsterdam-Kiwa werd niet meer geaccepteerd. Mij werd een alternatieve opdracht aangeboden bij Edwin van Elk werkzaam bij Procede Twente B.V. Zo gezegd, zo gedaan. De commissie moest nog een vierde lid bevatten en dat werd Wim Brilman. Het avontuur was lang en ik heb naast de chemische technologie heel veel geleerd, én, ben benaderd voor een baan bij, DSM, AKZO en Arcadis. Dus het doorzetten heeft toch nut gehad. Het lijkt er een beetje op dat ik mijzelf aan het verdedigen ben met dit voorwoord. Ten dele is dat ook waar, omdat ik zo vaak met onbegrip en kortzichtigheid ben geconfronteerd. Als je probeert om 'normaal' te functioneren vergeten men dat alles mij meer moeite kost en dat terwijl ik best weinig om hulp vraag.
En nu het bedanken van de mensen die mij hebben begeleid. Ik wil Geert Versteeg bedanken voor het laten zien dat je onder andere met gezond verstand en een goede planning zelfs de meest saaie en moeilijke opdrachten leuk en interessant kunt maken. Hans Kuipers wil ik bedanken voor de positieve ondersteuning die hij aan mij heeft gegeven. Wim Brilman bedank ik voor zijn altijd vriendelijk doch zeer kritische feedback. Edwin heeft meerdere malen bewezen niet alleen superhandig te zijn met computers maar ook zijn enorme kennis en inzicht hierin te kunnen vertalen. Een ding vraag ik mij eigenlijk al een hele tijd af: "Waarom houd je niet van sporten maar loop je wel van Oost naar West Engeland? Dat moet je na 7 december maar eens uitleggen". Edwin heel erg bedankt.

Dit verslag draag ik volledig op aan mijn ouders, omdat zij mij altijd onvoorwaardelijk hebben gesteund en altijd in mij hebben geloofd.

Onno Kramer
Amsterdam, november 2001

TABLE OF CONTENTS

PART II

LIST OF STABILITY MAPS

Table 2 Base case stability maps for no control

Stability map	Reference	
T versus T_{cool} (varying UA)	Figure 19	p30
T versus T_{cool} (varying Φ_V)	Figure 20	p31
T_{cool} versus UA (varying Φ_V)	Figure 21	p32

Table 3 Reactor designer stability maps (proportional control)

Stability map	Reference					
	Coolant temperature		**Coolant flowrate**		**Throughput**	
T versus T_{cool}	Figure 23	p37	Figure 43 ($T_{cool,0}$ = 303 [K])	p45	-	-
T versus UA	Figure 24	p38	Figure 44 ($T_{cool,0}$ = 303 [K]) Figure 45 ($T_{cool,0}$ = 400 [K]) Figure 49 ($T_{cool,0}$ = 435 [K])	p46 p47 p49	Figure 67	p56
T versus $\Phi_{V,cool}$	-	-	Figure 28 (0 – 0.005 [m^3 s^{-1}]) Figure 41 (0 – 0.02 [m^3 s^{-1}]) Figure 42 (0 – 0.1 [m^3 s^{-1}])	p41 p43 p44	Figure 50 ($K_c \geq 0$) Figure 54 ($K_c \leq 0$)	p51 p53

Table 4 Reactor controller stability maps

Stability map	Reference					
	K_c versus τ_I		**K_c versus UA**		**K_c versus UA**	
Controller	**Proportional-integral**		**Proportional**		**Proportional-integral**	
Coolant temperature control	Figure 74	p62	Figure 71	p58	Figure 79	p64
Coolant flowrate control	Figure 80a ($T_{cool,0}$ = 303 [K]) Figure 80b ($T_{cool,0}$ = 400 [K]) Figure 80c ($T_{cool,0}$ = 435 [K])	p65	Figure 72	p59	Figure 82 ($T_{cool,0}$ = 303 [K]) Figure 83 ($T_{cool,0}$ = 400 [K]) Figure 84 ($T_{cool,0}$ = 435 [K])	p66 p67 p68
Throughput control	Figure 85	p69	Figure 73	p60	Figure 86	p70

Table 5 Reactor controller stability maps regarding delay

Stability map	Reference			
K_c versus τ_d	**Proportional control**		**Proportional-integral control**	
Coolant temperature control	Figure 88	p73	Figure 103	p80
Coolant flowrate control	Figure 94a ($T_{cool,0}$ = 303 [K]) Figure 94b ($T_{cool,0}$ = 400 [K]) Figure 94c ($T_{cool,0}$ = 435 [K])	p76 p76 p76	Figure 106 ($T_{cool,0}$ = 303 [K])	p82
Throughput control	Figure 95	p77	Figure 107	p84

Stability map	Reference	
Process capacity	**Proportional control**	
K_c versus τ_R	Figure 108	p85
K_c versus τ_{cool}	Figure 110	p87
K_c versus τ_{cool}	Figure 113 ($T_{cool,0}$ = 303 [K]) Figure 114 ($T_{cool,0}$ = 400 [K]) Figure 115 ($T_{cool,0}$ = 435 [K])	p88 p89 p89

Chapter I

1 INTRODUCTION

This report is part of the research into the stability of process-operation of gas-liquid reactors performed at the research group 'Industrial process development and design' of the University of Twente. In gas-liquid reactors, it appears that at specific conditions sustained temperature oscillations, which are called limit cycles, occur. In plant operation, these conditions have to be avoided, because they may adversely affect product quality, catalyst stability and downstream operations and can lead both to serious difficulty in process control and unsafe reactor operations. In some extraordinary cases[67] limit cycles are useful, namely when they serve as a driving force for a second reactor in series.

It is known from literature that limit cycles do not only occur in gas-liquid reactors, but in many distinguished processes. The phenomenon of limit cycles is very similar for these processes despite the different reaction mechanisms, values of system variables, process parameters and conceivably control-method. Due to these similarities, it was decided to study the relatively simple case of limit cycle in a CISTR. The results and obtained knowledge of this study can subsequently be used to study processes that are more complicated.

To be able to study limit cycles, a mathematical description is required. The mathematical description of the system of a controlled reactor contains two or more differential equations, which cannot be solved satisfactory through traditional analytical or graphical methods. With the introduction of the software package LOCBIF, a new approaching strategy seems to exist.

LOCBIF was already used in other fields than the chemical industry and science. It is capable of interpreting mathematical problems involving differential equations far more easily than existing methods could, by supplying stability maps. Thereby it made it possible to study problems which could not be studied before because of the mathematically complexity. The first results were very promising. The construction of a stability map by van Elk *et.al.*[22] of the system of a reactor with LOCBIF showed good agreement with the results obtained by method developed by Heiszwolf and Fortuin[36] and Vleeschhouwer and Fortuin[77]. But moreover LOCBIF did this in a much more efficient way.

Although the results were very promising, more investigation had to be done to prove the applicability and reliability of LOCBIF. Van Elk investigated a system with proportional control, but did not account for integral control and delay, of which the latter improves the simulation of the real physical process.

In the present report, these aspects are investigated. Thereby, next to the control of the coolant temperature, also the control of the coolant flowrate and the throughput is investigated with LOCBIF.

As a consequence, the following research objectives can be formulated:

- Can limit cycles be predicted for certain reactor design and specific circumstances?
- If they can be predicted, can they be prevented?
- If they can be prevented, can they be prevented by applying a certain process controller?
- If the controller is not configured adequately, what are the consequences for the operating process?

The resulting outcome of the research is presented in two main parts. The first part discusses the theory of the reactor system described by mathematical equations. Thereafter, the current status of research is presented, which is the starting point of the simulations done in the second part.

Chapter II

2 MODEL OF A COOLED CISTR

2.1 Introduction

Although this report is part of the research to the stability of process-operation of gas-liquid reactors, due to the coincidence of the phenomenon of limit cycles, a relatively simple case of limit cycle in a cooled CISTR with first order irreversible exothermic reaction is considered. In this chapter, the apparent mass and heat balance will be postulated.

2.2 The mass and heat balance of the reaction mixture

Consider the reactor shown in Figure 1.

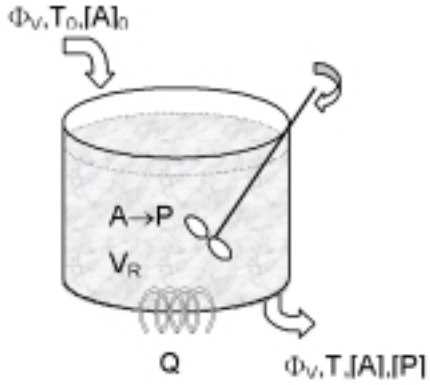

Figure 1 Schematic drawing of a cooled or heated CISTR.

A simple irreversible exothermic reaction 1 takes place in the reactor.

$$A_{(l)} \xrightarrow{k_R} P_{(l)} \qquad \text{Reaction: } \mathbf{1}$$

With the following overall reaction rate expression for reaction 1:

$$r = -r_A = k_R[A] = k_0 e^{-E_{act}/RT}[A] \qquad (1)$$

A liquid enters the reactor with a flow rate of Φ_V [$m^3\ s^{-1}$] and a temperature T_0 [K]. This feed flow contains component A with concentration $[A]_0$. The tank is considered to be ideally mixed, which implies that the temperature and concentration of the effluent is equal to the temperature and concentration of the liquid in the tank Φ_V, T, [A] and [P]. The reactor is cooled by a coolant that for example flows through a jacket around the reactor or flows through a construction of cooling pipes.

The dynamic behaviour of a first-order reaction system in a continuously ideally stirred tank reactor (CISTR) can be described with a process model consisting of two differential equations based on a material balance and an energy balance. The mathematical model of the process consists of mass and energy balances and introducing appropriate constitutive equations. For a complete mathematical derivation, the reader is referred to Appendix 1.

The general form of the non-stationary transient mass and energy balance for the CISTR is represented by state equations 2 and 3:

$$V_R \frac{d[A]}{dt} = \Phi_V \left([A]_0 - [A]\right) - V_R k_0 e^{-E_{act}/RT}[A] \tag{2}$$

$$\rho C_P V_R \frac{dT}{dt} = \rho C_P \Phi_V \left(T_0 - T\right) + \left(-\Delta H_R\right) V_R k_0 e^{-E_{act}/RT}[A] - UA\left(T - T_{cool}\right) \tag{3}$$

- Both equations 2 and 3 contain non-linear functions of T.
- Equations 2 and 3 are coupled, in the sense, that it not possible to solve one equation independently of the other.

Commonly, dimensionless numbers have been introduced to simplify the set of equations (2 and 3) and making it more generally applicable. The Uppal *et.al.* notation[75] is commonly applied in this field of research in which the following specific numbers and dimensionless variables are essential:

Average residence time:

$$\tau_R = \frac{V_R}{\Phi_V} \tag{4}$$

Conversion:

$$\zeta = 1 - \frac{[A]}{[A]_0} \tag{5}$$

The number of transport units which in the literature often is called the Stanton number St':

$$NTU = \frac{UA}{\Phi_V \rho C_p} \tag{6}$$

Adiabatic temperature rise:

$$\Delta T_{ad} = \frac{-\Delta H_R}{\rho C_P}[A]_0 \tag{7}$$

The adiabatic temperature rise or adiabatic factor is the extent of adiabatic temperature change if it is assumed that the reaction goes to completion i.e. ζ=1, The mass balance 2 and heat balance 3 can be rewritten into respectively equation 8 and 9 implementing equations: 4, 5, 6 and 7,

$$\frac{d\zeta}{dt} = (1-\zeta) k_0 e^{-E_{act}/RT} - \frac{\zeta}{\tau_R} \tag{8}$$

$$\frac{dT}{dt} = \frac{\left(T_0 - T\right) - NTU\left(T - T_{cool}\right)}{\tau_R} + \Delta T_{ad} k_0 e^{-E_{act}/RT}\left(1-\zeta\right) \tag{9}$$

The steady state solution of the CISTR can be found if the left-hand side of equation 2 or 8 and 3 are set equal to zero i.e. d[A]/dt or dζ/dt = 0 and dT/dt = 0.

$$[A] = [A]_0 \left(\frac{\Phi_V}{\Phi_V + V_R k_0 e^{-E_{act}/RT}} \right) \tag{10}$$

$$\zeta = \frac{1}{1 + \dfrac{1}{k_0 \tau_R \, e^{-E_{act}/RT}}} \tag{11}$$

2.3 Modelling of the Cooling

2.3.1 Coolant heat balance

In the literature of process-control, the assumption can be made that the temperature of the cooling fluid can be described, using the CISTR concept resulting in one extra differential equation (equation 12).

$$\rho_{cool} C_{P,cool} V_{cool} \frac{dT_{cool}}{dt} = \rho_{cool} C_{P,cool} \Phi_{V,cool} \left(T_{cool,0} - T_{cool}\right) + UA(T - T_{cool}) \tag{12}$$

The left term in equation 12 represents the accumulation term in the cooling apparatus with volume V_{cool}. The middle term is the difference in heat per unit of time by coolant convection and the right term is the transferred heat per unit of time from the reactor. In expression 12 the same assumptions are used for the heat balance of the reaction mixture (Appendix 1). In the steady state situation equation 12 becomes in terms of the coolant flowrate:

$$\Phi_{V,cool} = \frac{UA\left(T - T_{cool}\right)}{\rho_{cool} C_{P,cool} \left(T_{cool} - T_{cool,0}\right)} \tag{13}$$

The coolant flowrate can also be determined using equations 2, 3 and 12 resulting in:

$$\Phi_{V,cool} = \frac{\rho C_P \Phi_V \left(T_0 - T\right) + \left(-\Delta H_R\right) k_0 V_R e^{-E_{act}/RT} [A]}{\rho_{cool} C_{P,cool} \left(T_{cool} - T_{cool,0}\right)} \tag{14}$$

Correlations 13 and 14 can henceforth be used to determine the required extent of flowrate in the steady state situation, or to determine the required extent in case of changed process state.
Aris *et.al.*[2] and Ogunnaike *et.al.*[60] formulated the number of transport units for the coolant, similar to equation 6 considering the cooled CISTR:

$$NTU_{cool} = \frac{UA}{\rho_{cool} C_{P,cool} \Phi_{V,cool}} \tag{15}$$

2.3.2 Coolant temperature expression

When modelling the cooling of the reactor one should chose an expression for the coolant temperature, while the latter is not constant. To acquire a value for T_{cool}, several methods have been described in the literature.

1. Average temperature value assumption

The simplest expression for T_{cool} is the mean of the inlet and outlet cooling fluid temperature:

$$T_{cool} = \overline{T}_{cool} = \frac{T_{cooli,0} + T_{cool,1}}{2} \tag{16}$$

2. Logarithmic temperature mean

According to Westerterp[80] and Roffel[68] an expression for T_{cool} is the logarithmic temperature mean:

$$\Delta T_{\log} = T - T_{cool,\log} = \frac{\left(T - T_{cool,0}\right) - \left(T - T_{cool,1}\right)}{\ln\left(\frac{T - T_{cool,0}}{T - T_{cool,1}}\right)} \tag{17}$$

Approximation 1 is preferred because of its mathematical simplicity and is a good approximation when $T_{cool,0} \approx T_{cool,1}$. Expression 17 is used when high accuracy is required.

Chapter III

3 BEHAVIOUR OF THE MODEL

3.1 Introduction

In the following chapter, the static and dynamic behaviour of a cooled CISTR will be discussed. Firstly, the static behaviour is examined, including the concept of multiplicity. Thereafter, various types of dynamic behaviour including the phenomenon limit cycles will be studied.

3.2 Static behaviour of the cooled CISTR

The static thermal behaviour of a cooled CISTR in which an irreversible exothermic reaction A $\rightarrow$ P takes place can be presented schematically by Figure 3. The heat of reaction is removed by a coolant medium, which flows through a jacket around the reactor (Figure 2).

The curve that describes the amount of heat released by the exothermic reaction is a sigmoidal or *S*-shape function of the temperature T in the reactor (curve A in Figure 3). On the other hand, the heat removed by the coolant is a linear function of the temperature T (curve B in Figure 3). When more than one intersection of the energy and mass balance curves appears, there is more than one set of conditions that satisfies both the energy and mass balance and consequently there will be multiple steady states at which the reactor can be operated. This is called multiplicity.

When the CISTR is at steady state i.e. nothing is changed, the heat produced by the reaction should be equal to the heat removed by the coolant. This requirement yields the steady states P_1, P_2 and P_3 at the intersection of curves A and B in Figure 3. Steady states P_1 and P_3 are called *stable* [34], whereas P_2 is *unstable*. To understand the concept of stability, steady state P_2 will be considered. Assume that the reactor is started at temperature T_2 and corresponding concentration $[A]_2$. Consider the temperature of the feed T_i increases. This will cause an increase in the temperature of the reacting mixture T_2'. At T_2' the heat released by the reaction Q_2' is more than the heat removed by the coolant, Q_2'' consequently leading to higher temperatures in the reactor and consequently to increased rates of reaction. Increased rates of reaction produce larger amounts of heat released by the exothermic reaction, which in turn lead to higher temperatures, and so on. Therefore, an increase in T_i takes the reactor temperature away from steady state P_2 and the temperature will eventually reach the value of steady state P_3. Similarly, if T_i were to decrease, the temperature of the reactor would take off from P_2 and end up at P_1. By contrast, if the reactor is operating at steady state condition P_3 or P_1 and the operation of the reactor is perturbed, it would return naturally back to point P_1 or P_3 from which it started. Sometimes one would like to operate the CISTR at the middle unstable steady state e.g. the upper-temperature steady state P_3 may be very high, causing unsafe conditions, destroying the catalyst for a catalytic reactor and degrading the product P. In such a particular case, a controller is required to ensure the stability of the operation at the middle steady state P_2. It is of practical importance to carry out a stability analyse to determine which of the steady states can be realised i.e. stable and which are unstable; any infinitesimal disturbance will move the reactor away from such an unstable steady state.

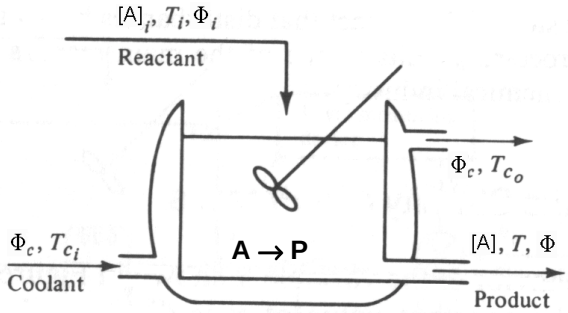

Figure 2 CISTR with cooling jacket.

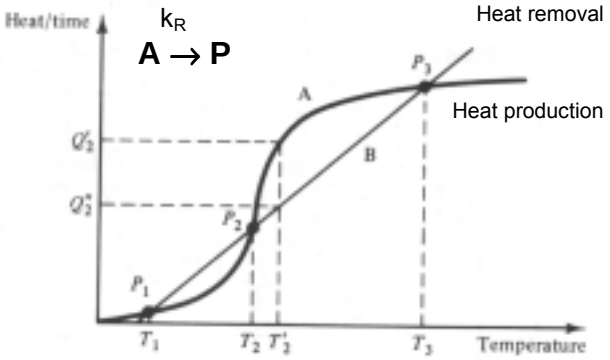

Figure 3 The thermal behaviour of an irreversible, exothermic reaction A → P in a CISTR under non-isothermal conditions (three steady states).

3.3 Dynamic behaviour of the cooled CISTR

Through creating a chart of a chemical process like Figure 3, one can determine whether a process is operated in a statically stable region. Disadvantage of Figure 3 is that no information is supplied regarding the dynamics of the process. Therefore, it is uncertain whether a statically stable steady state is also dynamically stable. If a steady state is statically and dynamically stable, the process can be operated in this steady state (preferably at high conversion). It will return to the steady state after a sufficiently small perturbation. If a steady state is only statically stable, the process can only be operated in the neighbourhood of the steady state. Then, several situations can be distinct: These will be discussed below:

3.3.1 Stable self-regulating process

Consider the behaviour of a process variable, such as temperature, concentration or flowrate, shown in Figure 4. Notice that at time t = t_0 the process variable is disturbed by some external factors, but that as time progresses its value returns to the initial value and stays there. One can say that the process (Figure 4a and b) is *stable* or *self-regulating* and needs no external intervention for its stabilisation. It is clear that no control mechanism is needed to force the process variable to return to its initial value. If the process of returning back to its initial value evolves smoothly, it is called *asymptotic damping* (Figure 4a). On the other hand, the process variable can, if it returns to its initial value, also exhibit considerable oscillations, which is often called a *spiral point* (Figure 4b).

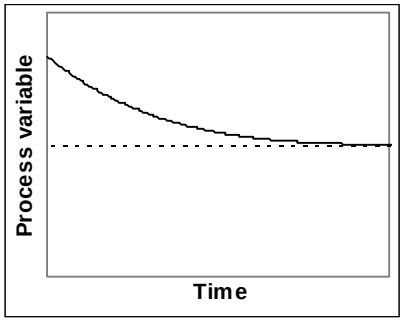

Figure 4a Asymptotic damping of a stable system after a perturbation. (See also Table 6). Type 1. Area Ia.

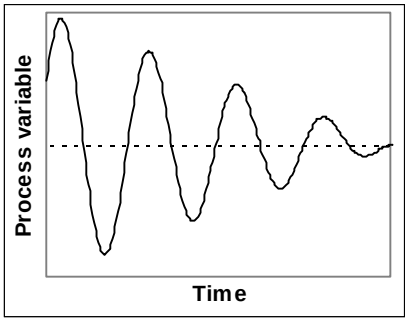

Figure 4b Oscillating response (spiral point) of a stable system after a disturbance. Type 2. Area Ib.

3.3.2 Unstable process

In contrast to the behaviour described above, it is probable that the process variable does not return to its initial value after it has been disturbed by external influences (Figure 4c-i). Processes whose variables follow this pattern are called *unstable* processes and require external control for the stabilisation of their behaviour. If the response of a process is unstable, the distinction can be made between *run away* e.g. if too less superfluous reaction heat is removed (Figure 4f and g), or extinguishes e.g. if the cooling is too strong (Figure 4h and i).

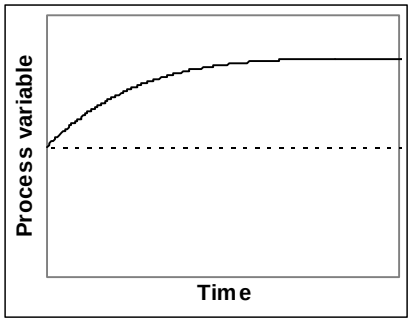

Figure 4f Response of an unstable system i.e. Ignition or runaway. Type 5+6. Area III.

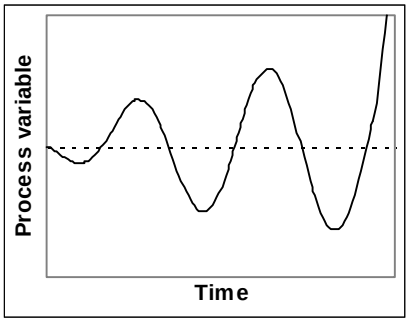

Figure 4g Response of an oscillating unstable system causing runaway. Type 5+6. Area III.

In Figure 4f and h the process variable changes equally until the maximum or minimum value has been reached. If the response of the process however, is oscillatory (Figure 4g and i) in which the amplitude is increasing, eventually the process state transverse to another equilibrium state. Therefore, the amplitude of the peaks is decisive and can cause transition i.e. run away (Figure 4g) or extinction (Figure 4i).

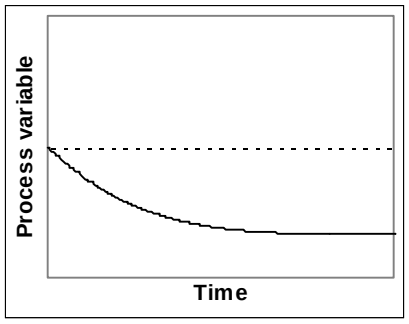

Figure 4h Unstable system. Extinction. Type 5+6. Area III.

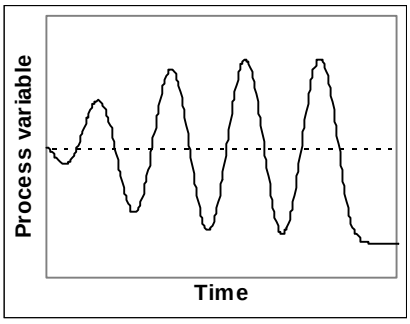

Figure 4i At first the response shows limit cycles; nevertheless, the overshoot causes eventually extinction. Type 5+6. Area III.

Finally, due to the distinguishing characteristic of the kinetic rate term in state equations 2 and 3, and to the introduction of model extensions i.e. extra differential equations, initially, the response can be in the opposite direction to where it eventually ends up. This is called *inverse response* (Figure 4g).

3.3.3 Limit cycles

Next to being stable or unstable as described above, another dynamic mode is possible. Figure 4c-e shows the phenomenon of self-sustained oscillations. Because this phenomenon occurs in principle spontaneously (Figure 4d), a constrained perturbation is not inevitable to acquire these limit cycles (Figure 4c). Therefore: "The occurrence of limit cycles is not exclusively dependent of a disturbance."
Additionally, the pattern of the limit cycles can vary. The process variable can expose a symmetric sinusoid curve (Figure 4c) or an asymmetric curve (Figure 4e). The symmetry increases in case the process state is located towards the transition between dynamic stability and instability.

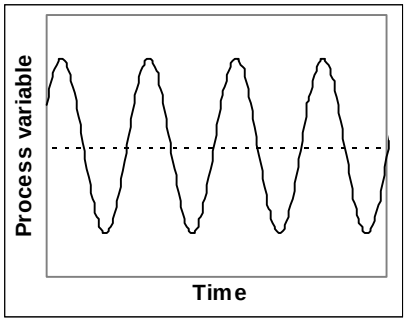

Figure 4c Stable self sustained oscillations (limit cycles) after a perturbation. Close to Hopf (§4.5.3). Type 3. Area II.

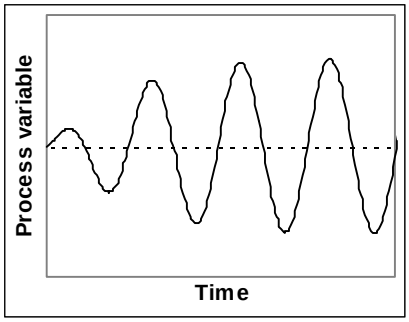

Figure 4d Limit cycles, which occur naturally without a perturbation. Type 3. Area II.

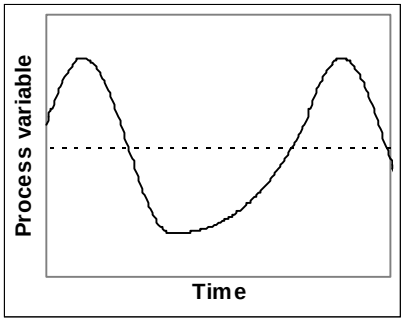

Figure 4e Asymptotic oscillations (limit cycles). Unstable system. Type 3. Area II.

The process will start oscillating forever in a limit cycle around the statically stable operating point at a fixed frequency and fixed amplitude (Figure 5). The following example will illustrate the phenomenon limit cycles more.

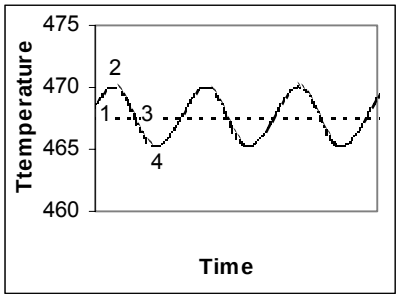

Figure 5a Self-sustained reactor temperature oscillations (limit cycles).

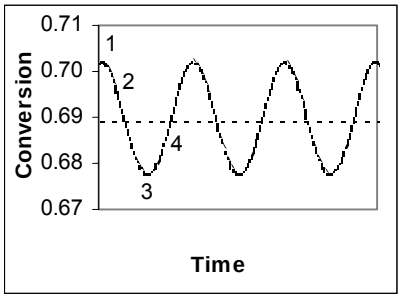

Figure 5b Conversion limit cycles.

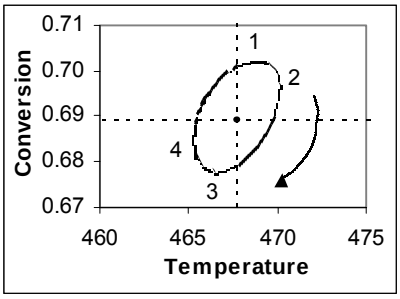

Figure 5c Limit cycle around a static stable but dynamic unstable steady state. Composition of Figure 4a and b.

Assume that the CISTR conditions are represented by point 1. Here T and ζ are higher than corresponds to the stable operating point (dotted in Figure 5), which can be derived if the ODE system 2 and 3 is solved (steady state P_3 in Figure 3). Therefore, the reaction rate is too high; the reaction mixture is heated up, the temperature increases and simultaneously ζ is reduced. When point 2 is reached, r_A has been reduced already in such an extent that the reaction mixture starts to be cooled by the cold feed, however r_A is still so high that the consumption of reactant A is still higher than the supply of fresh A with the feed. In point 3 ζ reaches a minimum, r_A is now so low that build-up of A in the reaction mixture, which is still being cooled by the cold feed and the cooling equipment, starts again. When point 4 is reached sufficient A has been built up to increase the reaction rate in such an extent that the reaction heat evolution is now so high that the cooling of the reaction mixture stops and the heating up is renewed again. The build-up of A continues until point 1 is reached, then the whole cycle starts again.

Chapter IV

4 THEORETICAL PREDICTION OF LIMIT CYCLES

4.1 Introduction

The stability of a process is important for both uncontrolled and controlled processes. Disturbances can adversely affect the stability of a process and accordingly result in decreased performance or in worst-case scenario imply malfunctioning. Therefore, since long one has attempted to predict the process stability theoretically. In this chapter, the bifurcation theory which provides the theoretical background to predict limit cycles, and its application by means of software package LOCBIF, is presented. This yields the basis to construct and interpret stability maps.

4.2 Linearised perturbation method

One approach to predict the process-stability is the linearised perturbation method. It has been developed by Himmelblau and Bischoff[37] [68] and offers a simple, analytical approach to analyse stability using linearised versions of differential equations. It can solve up to two differential equations. In this report, the mathematical description of the problem demands more than just two differential equations. Whereas the underlying theory is beyond the scope of this report, its outcome is useful for the understanding of the report and will therefore be presented in §4.5.5 Table 6.

4.3 Bifurcation theory

Although only in simple cases, the analytical method mentioned above could provide some useful information pertaining to the stability of a process. Advanced methods are required in case more complex systems are involved. In reactor dynamics, it is particularly important to find if multiple stationary points exist or if sustained oscillations (limit cycles) can arise. The bifurcation theory contains distinct curves, which provide useful information about the boundary between stability and instability.

The bifurcation theory of time-depended differential equations have found application in many fields of research, including chemical reactor engineering, mathematical biochemistry and combustion. The bifurcation theory provides several methods in which static and dynamical behaviour of processes can be analysed. The exact definition of bifurcation has been given by Kuznetsov[48]:

> "Bifurcation has been defined as the appearance of topological phase portraits under variation of parameters. A bifurcation is a change of the topological type of the system as its parameters pass through a bifurcation."

A bifurcation analysis is aimed at locating the set of parameter values for which multiple steady states will occur. According to Kuznetsov[48] a bifurcation point i.e. critical value, is a point at which two branches of a curve coalesce as a parameter is varied (point B in Figure 6). Consider function $f(x,\lambda)$ in which x is a scalar variable and λ is a parameter. Figure 6 shows curves AB, BC and BD for which:

$$f(x,\lambda) = 0 \tag{18}$$

is satisfied. In case λ is increased along AB, there is only one value of x for a given λ that will satisfy equation 18. However, if λ is continued to be increased along AB, a bifurcation point λ^* is reached beyond

which there are two values of x that satisfy equation 18 for a given value of λ. Consequently, the system contains multiple solutions i.e. multiplicity.

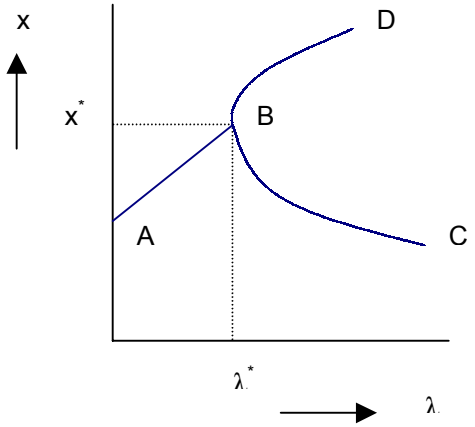

Figure 6 Bifurcation diagram.

In a bifurcation diagram in fact a curve, which represents the dynamical behaviour of a system (e.g. reactor temperature), is examined in relation which a distinguished parameter (e.g. cooling capacity). The bifurcation diagram classifies in a very condensed way all possible modes of behaviour of the system and transitions between them i.e. bifurcations, under parameter variation. It is desirable to obtain the bifurcation diagram as a result of the qualitative analyses of a given dynamical system. The bifurcation diagram, which is a called a stability map, can provide important information about the behaviour of the system being studied. This stability map will be discussed elaborately in paragraph 4.5.

Suitable methods are available e.g. bifurcation software package LOCBIF (see §4.4). Creating stability maps using LOCBIF does require neither special scientific skills, nor knowledge of complex non-linear mathematics or numerical methods. The only condition is that the engineer is capable of describing the dynamic behaviour of the reaction system using a set of differential and algebraic equations e.g. mass and energy balances 2 and 3.

4.4 LOCBIF

This chapter reviews the general features of the LOCBIF bifurcation program. The review is limited to the parts of LOCBIF that are relevant for the analysis of the dynamic and static behaviour of CISTRs. For other LOCBIF features, the reader is referred to the LOCBIF manual[45]. LOCBIF has been developed at the Institute of Mathematical Problems of Biology of the Russian Academy of Sciences in the Moscow Region in 1992. A. Khibnik and E. Nokolaev[45] developed the numerical algorithms. LOCBIF has no special system requirements and runs on any modern PC system.

LOCBIF is a very useful tool, which has the numerical routines to explore the existence and stability of equilibria in dynamic models and to generate stability maps with limited effort. Once familiar with LOCBIF, it is straightforward to create a LOCBIF input file and analyse the dynamic and static behaviour of a typical system instead of producing a complete perturbation analyses which is very profoundly and therefore laboriously. Another advantage is that the linearising of the differential equations, needed for the process controller, can be skipped. The mathematical equations describing a particular process can directly be implemented in a LOCBIF source code called RHS (right hand side).

A dynamical system described with one ore more differential equations can be programmed in a LOCBIF source, in a specific Right Hand Side source code. This subject is discussed comprehensively in the LOCBIF manual[45]. In Appendix 7, LOCBIF "*right hand side*' source codes are included and in Appendix 6 the accompanying nomenclature.

LOCBIF is a scientific tool for bifurcation analysis of systems of differential equations, which depend upon parameters. It helps to explore interactively the existence and stability of equilibria (*steady states*) of dynamical models. LOCBIF supports systems of up to 10 differential equations.

LOCBIF is based on continuation procedures for relevant local bifurcation curves up to co dimension three. This means that LOCBIF can calculate bifurcation curves in a multi-dimensional space and can do it very fast thanks to the efficient continuation algorithms. LOCBIF plots two-dimensional projections of the bifurcation curves during the computations. The numerical background of the LOCBIF continuation methods is discussed extensively in the LOCBIF manual.

Besides calculation of bifurcation curves, LOCBIF can also solve the differential equations with respect to time, like any other ODE solver e.g. Maple. This option is very useful to check the predicted dynamic behaviour or to find stable steady state solutions. Four different LOCBIF versions exist, but for the application of interest here, LBEP.EXE is the only LOCBIF version needed.

LOCBIF supports about 15 different curves, however only four of them are of direct interest for our application i.e: the equilibrium curve, the fold curve, the Hopf curve and the orbit curve.
Some restrictions regarding the LOCBIF program:

- LOCBIF cannot deal with integral equations or partial differential equations.
- Maximum number of differential equations, which can be implemented.
- Very limited possibilities to extend the RHS with mathematical disparities.
- Occasionally, LOCBIF has noticeable troubles finding an initial point.

```
TIME variable declaration
PHASE variable declaration
PAR parameter declaration
FUN function declaration
COMMON variable declaration
function definition(s)
RHS definition(s)
INIT initial values computations
```

LOCBIF rhs 1 Structure of ODEs specification in LOCBIF.

4.5 Stability map

A *stability map* characterises the dynamic behaviour of a system, as a function of important system parameters like the cooling capacity or the temperature of the coolant. A stability map can be very convenient to determine quickly whether or not a particular system proceeds to instability. Such a stability map is composed of equilibrium curves and/or Hopf and/or Fold curves and must be checked by means of orbit curves. For a good understanding of these stability maps, firstly the main ideas of the above mentioned curves are discussed after which an example of constructing a stability map will be given.

4.5.1 Equilibrium curve

The equilibrium curve is for chemical reactors also known as the S-curve (Q-T in Figure 3 here T-T_{cool}) and represents the solution to:

$$f(x, p) = 0 \tag{19}$$

All parameters in equation 19 but p_1 are fixed. This is the steady state solution of the ODE system as a function of one active parameter. The curve can for example describe the steady state solution (concentrations and temperature(s)) of a reactor system as a function of the coolant temperature.

4.5.2 Fold bifurcation curve

According to Kuznetsov[48] this bifurcation has many names i.e. limit point, saddle node bifurcation and turning point. The fold bifurcation curve represents the boundary between static stability and static instability as a function of two active parameters and is defined by:

$$f(x, p) = 0$$
$$\lambda_1(x, p) = 0 \quad (20)$$

In equation 20 all parameters but p_1 and p_2 are fixed. The fold curve is characterised by one zero Eigenvalue λ_1. The projection of a fold bifurcation defines a curve on which a pair of equilibrium points appears or disappears when parameters are changed in such a way to cross this curve transversally.
The curve can for example define the border between static stable and static unstable steady states of a reactor system as a function of the coolant temperature and the cooling capacity.

4.5.3 Hopf bifurcation curve

The Hopf bifurcation curve represents the border between dynamic stability and dynamic instability as a function of two active parameters and is defined by:

$$f(x, p) = 0$$
$$\lambda_1(x, p) + \lambda_2(x, p) = 0 \quad (21)$$

In equation 21 all parameters but p_1 and p_2 are fixed. The Hopf curve is characterised by two equal Eigenvalues of opposite sign. This can be achieved in two different ways:

$$\lambda_1(x, p) = -\lambda_2(x, p) \quad (22)$$
$$\lambda_{1,2}(x, p) = \pm i\omega \ (\omega > 0) \quad (23)$$

Neutral saddle, real Eigenvalues (equation 22) and Andronov-Hopf bifurcation, imaginary Eigenvalues pair (equation 23). The last situation is of special interest and will result in an oscillating system. The period of the oscillation being about $t = 2\pi/\omega$. The Hopf bifurcation can for example define the border between dynamic stability and dynamic instability of a reactor system as a function of the coolant temperature and the cooling capacity.

4.5.4 Orbit curve

Whereas a stability map contains the above equilibrium, Fold and the Hopf curves it does not contain orbit curves, because it represents the solution of the ODE system with respect to time and no parameters are active except the time, so that all system parameters and an initial condition have to be specified. Orbit curves are useful to investigate or to verify the dynamical behaviour and stability of a particular chosen point.

$$\dot{x} = f(x, p) \quad (24)$$

All parameters p in equation 24 are fixed. The computation of the curve means numerical integration of the system in time.

4.5.5 Constructing the stability map

The distinct curves explained above can be drawn in a bifurcation diagram often called stability map, consisting of several equilibrium curves ($dT/dt = 0$ and $d\zeta/dt = 0$) (in which an active bifurcation parameter is varied), Fold curve (border between static stability and static instability) and the Hopf curve (border between dynamic stability and dynamic instability). The behaviour of the considered system is different (stable/unstable) at both sides of the bifurcation curves. A bifurcation diagram can provide useful information about the stability and is therefore called a stability map.

Primarily the stability maps have a rather complex structure. Therefore, the following explicating stability map is constructed. The example provides a clear perceptive of the influence of process parameters like cooling capacity or coolant temperature and becomes comprehensible but moreover, in a certain particular case, the actual problem of limit cycles becomes clear. In the stability map, the coolant temperature T_{cool} is drawn on the abscissa and the active reactor temperature T on the ordinate. The axes-scale is in accordance with the figures printed in the article by van Elk *et.al.*[22] resulting in Figure 7 in which ⊕ represents a particular process value (in this report the base case).

- Initially, one equilibrium curve is drawn for one particular active parameter value (cooling capacity) (Figure 7a).
- To examine the influence of the cooling capacity on the process, a number of equilibrium curves is appended (Figure 7b).
- The Fold curve is plotted, in which the boundary between static stability and instability becomes visible (Figure 7c). The base case ⊕ is drawn which apparently is located in the static stable region i.e. no multiplicity in this particular case.
- The Hopf curve is plotted, in which the boundary between dynamic stability and instability can be determined (Figure 7d). The base case ⊕ is located between the Fold and Hopf curve. Consequently, its dynamical behaviour is unstable: sustained oscillations i.e. limit cycles.
- In Figure 7e the $T_{reactor} = T_{cool}$ curve has been added. It is obvious that the reactor temperature should be larger than the coolant temperature. The equilibrium curve corresponding the cooling capacity for exclusively the reactor wall i.e. no cooling device, is drawn.
- Figure 7f portrays clearly the distinct regions. In subsequent stability maps, these coloured regions will be indicated with I, II or III. Although perhaps more regions can be identified, merely the most relevant regions will be considered.

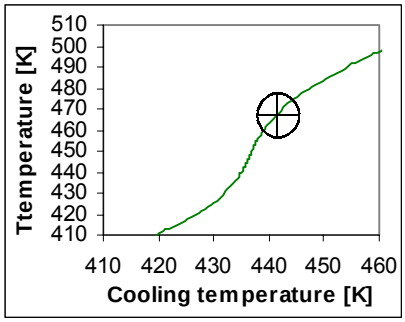

Figure 7a Equilibrium curve through base case value. ⊕ represents the base case.

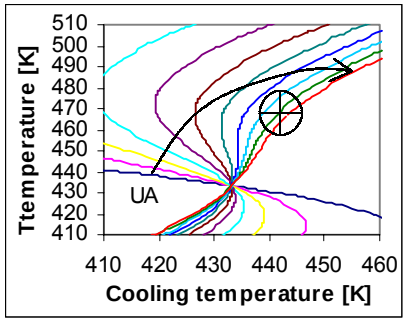

Figure 7b Additional equilibrium curves for varying values of cooling capacities.

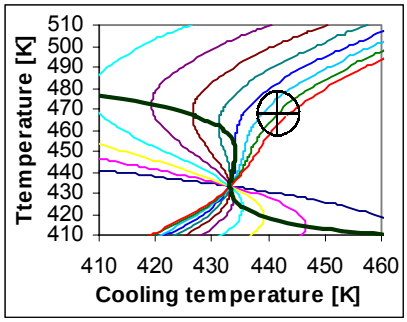

Figure 7c Addition Fold curve, transition between static stability (right) and unstable (left).

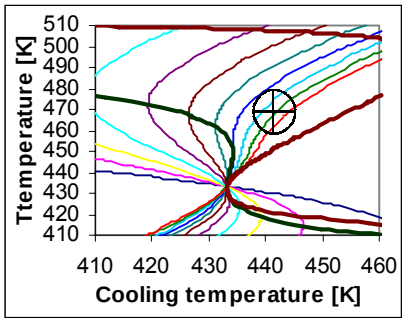

Figure 7d Addition Hopf curve, transition between dynamic stability and unstable.

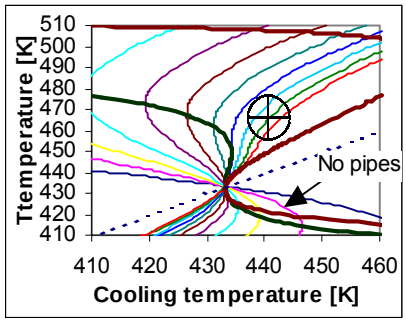

Figure 7e Addition $T = T_{cool}$ curve and equilibrium curve concerning no cooling pipes.

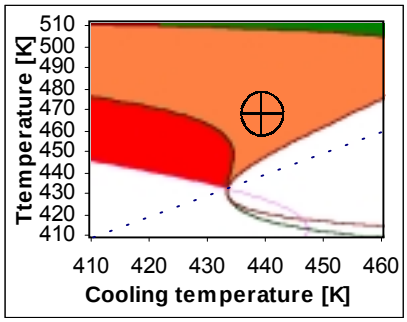

Figure 7f Indicating regions. • region I: stable. • region II: limit cycle. • region III: instability.

Due to the complex structure of a stability map, it is not clear at once whether a region indicates stability or instability. Therefore, a particular case has to be verified through producing some curves. In case multiplicity is involved, a region II can seemingly point towards dynamical instability, which would imply

limit cycles. However, sometimes the existence of static instability 'overrules' the existence of a limit cycle, which means transition and no sustained oscillations. In many articles, this process is a result of a strong attracter, which forces a process towards transition. Summarising: the labelling procedure of a particular process regarding dynamical behaviour and stability must be carried out with caution. A check with orbit curves is indispensable.

The stability map is divided in marked regions:

Region I: The dynamical behaviour of the system is considered as stable. After a constrained disturbance, the process variable returns to its steady state value (Figure 4a and b).
Region II: In the area enclosed between the Fold and Hopf curve, the system is dynamically unstable i.e. limit cycles can exhibit (Figure 4c-e).
Region III: The system is statically unstable due to multiplicity (extinguish or runaway) (Figure 4f and i).

Table 6 Various types of behaviour based on linearised perturbation analyses (Himmelblau *et.al.* [37]).

Behaviour after perturbation	Area	Figure 4
Asymptotic damping	Ia (point stable)	a
Spiral point	Ib (point stable)	b
Stable oscillations, close from Hopf (§4.5.3)	II (limit cycle)	c and e
Asymptotic oscillations, far from Hopf	II (limit cycle)	d
Transition	III (static unstable)	f and g
Transition	III (static unstable)	h and i

4.5.6 Classification of the stability maps

In the literature[22], in general stability maps can be found in which the reactor temperature is plotted against one or more important process variables. A common plot is the $T\text{-}T_{cool}$ stability map in which the reactor designer adequately can determine the stable and unstable regions. However, in case of process control, which involves extra mathematical correlations, this type of stability map is not suitable anymore to determine stability. This is because too many relevant variables have to be analysed simultaneously. For proportional-integral control, the process engineer is in particular interested in the relationship between the proportional gain and the cooling capacity, or the proportional gain and the integral time. If additionally delay is studied, the $T\text{-}T_{cool}$ stability map is certainly not useful. Therefore, the following stability map classification is proposed:

1. Reactor designer stability map
2. Reactor controller stability map

1. Reactor designer stability map

In this type of stability map, the reactor temperature is always drawn on the y-axis. At the x-axis one important process variable, like the coolant temperature is drawn by means of equilibrium curves. The latter is done, several times in relation with another process parameter, e.g. the cooling capacity, to study the effect. Through changing the process variables and parameters, the reactor designer can determine the reactor temperature and the conversion with respect to the behaviour and furthermore the stability.

2. Reactor controller stability map

The reactor control engineer is mainly interested in how to solve and/or prevent unwanted unstable reactor behaviour. Through creating reactor controller stability maps, one can very easy determine for instance the new controller configuration. Therefore, the reactor temperature is not drawn on the axes, but in general one of the crucial process parameters (UA) or the controller parameters (K_c and τ_I). The reactor controller stability map consist no equilibrium, Fold or orbit curves, merely Hopf curves, in which the stable and unstable region clearly can be located and indicated.

4.5.7 Interpreting stability map

Reactor designer stability map

The same stability map will be considered as in §4.5.5. The regions I, II and II indicating respectively stability, limit cycles and instability have been marked (Figure 8a). The reactor engineer is for instance interested in the dynamical behaviour of the process for T_{cool} = 450 [K] for three different cooling capacities. These points have additionally been drawn in (Figure 8a) and examined for their dynamical behaviour through orbit curves.

Table 7 Data regarding the examined points in stability map Figure 8a.

Point	Coolant temperature T_{cool} [K]	Cooling capacity UA [kW K^{-1}]	Perturbation ΔT	Orbit curve	stst reactor temperature T [K]	stst conversion ζ [-]	Region	Behaviour
1	450	35	+20	Figure 9a	510	0.94	I	Stable
1	450	35	-20	Figure 9b	510	0.94	I	Stable
2	450	38	0	Figure 10a	505	0.92	II	Limit cycles
2	445	38	0	Figure 10b	499	0.90	II	Limit cycles
3	420	25	+10	Figure 11a	509	0.94	II	Limit cycles
3	420	25	-10	Figure 11b	401	004	I	Transition

The steady state values, derived from the equations 2 and 3 (or 8 and 9) have been displayed in Table 7. As initial point, the steady state value will be taken. If necessary, a perturbation is constrained.

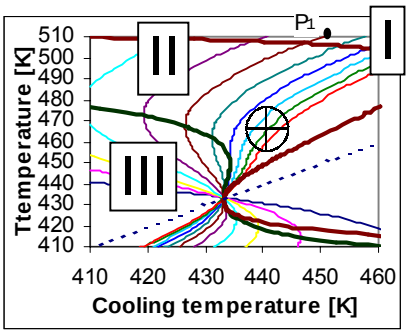

Figure 8a Reactor designer stability map. Point 1 is located above the Hopf curve in region I.

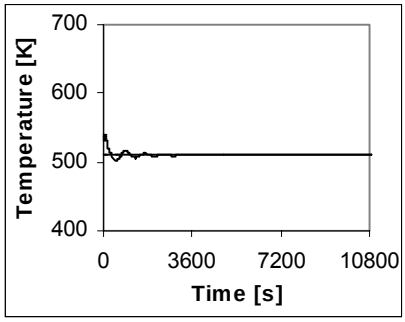

Figure 9a Orbit curve for a disturbance ΔT = 20 [K] becomes a spiral point.

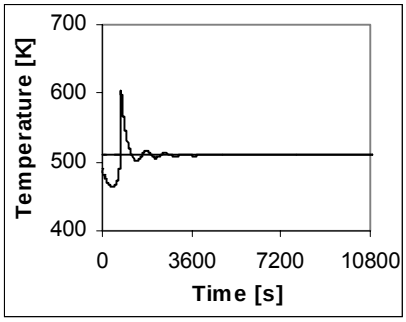

Figure 9b Orbit curve for a disturbance ΔT = -20 [K]. Point 1 returns to its steady state (spiral point).

P_1 Point 1 in Figure 8a, is located in region I. From Figure 9a and Figure 9b it can be seen that after a step disturbance the system returns to P_1.

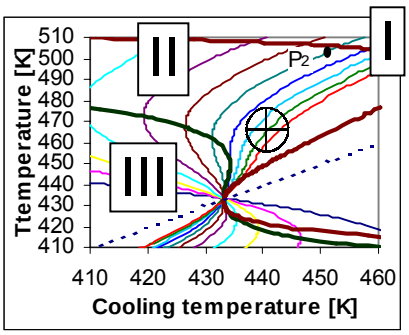

Figure 8b Reactor designer stability map. Point 2 is located beneath the Hopf curve in region II.

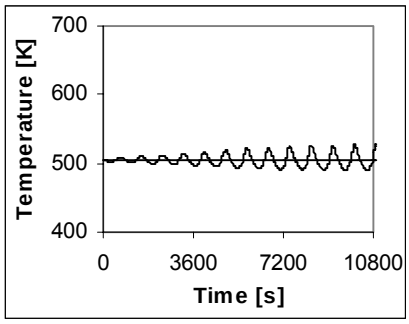

Figure 10a Orbit curve. Point 2 in Figure 8a is located beneath the Hopf curve in region II accordingly limit cycles.

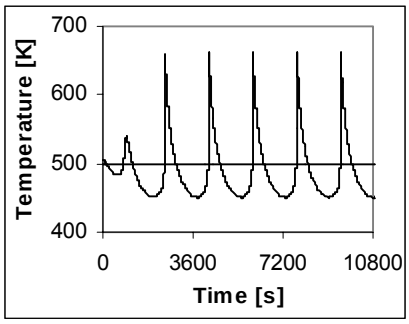

Figure 10b Lowering the coolant temperature 5 [K] results in strong limit cycles.

P_2 Point P_2 in Figure 8a is located just beneath the Hopf curve in region II. Figure 10a demonstrate that limit cycles emerge from the steady state without a perturbation. If the coolant temperature is slightly decreased ΔT_{cool} = -5 [K], Figure 10b shows that limit cycles appear strongly.

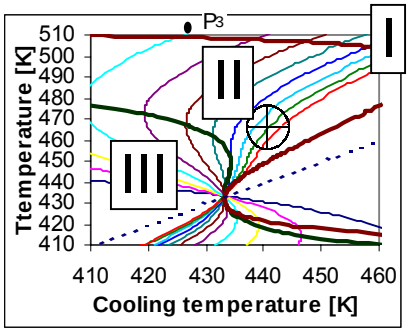

Figure 8c Reactor designer stability map. Point 3 is located above the Hopf curve in region I, however with multiplicity.

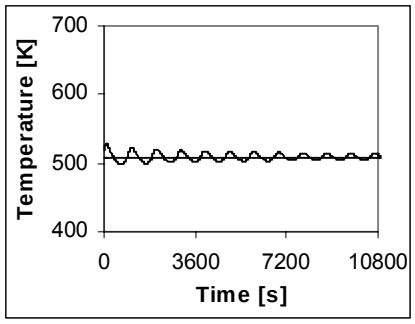

Figure 11a Orbit curve. Point 3 in Figure 8a is located above the Hopf curve in region II. ΔT = +10 [K] limit cycles.

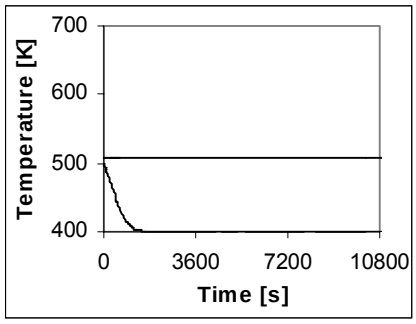

Figure 11b Point 3 in Figure 8a. Disturbance ΔT = -10 [K] results in T = 401 [K], ζ=0.04 reaction extinguishes due to the existence of multiplicity.

P_3 Point P_3 in Figure 8a is as point P_1 located above the Hopf curve within region I. Therefore, stability is to be expected. Nonetheless, after a disturbance ΔT = 10 [K], the temperature will slightly decrease and then pursue the limit cycle which becomes clear in Figure 11a. After a disturbance ΔT = -10 [K] the temperature will decrease to the lowest steady state i.e. the reaction extinguishes (Figure 11b). Point P_3 with UA = 25 [kJ s^{-1} K^{-1}] exhibits multiplicity and is very receptive for disturbances. Even a small deviation from the steady state of 10 [K] forces the system to the lowest steady state.

Although the regions in a reactor designer stability map perhaps point towards a stable dynamical behaviour, disturbances can force a system towards a dynamical unstable region or even in case of multiplicity to a lower or higher steady state vale. By means of creating orbit curves, the latter must be verified.
In the reactor designer stability map in a 2D plot, more than two variables are varied. Therefore, it will be clear that the reactor designer stability maps are in fact 2D-presemntation of 3D phenomena and is therefore sometimes difficult to interpret. In Figure 8 T, T_{cool}, and UA have been varied. Moreover, the complexity is become worse, if also more ordinary differential equations are added to the mathematical model.

Reactor controller stability map

In reactor controller stability maps, exclusively the Hopf curves are drawn. Equilibrium curves and Fold curves like in reactor designer stability maps are excluded. Subsequently, the acquired plots remains well ordered and clear to interpret. Moreover, in cases like the delay or integral time are considered, no Fold curves exist. The latter are described mathematically by differential equation in which in the infinity (in the steady state) the time aspect is eliminated and static instability is then not anymore concerned with. The Fold curve is then merely a dot (solely one steady state solution of the ODE-system) and does therefore not make any useful contribution to the stability map. Another explanation is that the equilibrium curves do not diverge for varying integral times or delay and therefore no Fold curve exists. The advantage of the reactor controller stability maps is the simplicity, ordered structure and easy to interpret the dynamical behaviour. Once the Hopf curve has been drawn, the regions with respect to (in)stability have only to be marked. In most cases, one or two orbit curves for both sides of the Hopf curve provide enough information about the actual stability.

Consider the following example. The reactor engineer is for instance interested in the dynamical behaviour of a particular process in relation with the delay. Therefore, a reactor controller stability map is created with a Hopf curve for parameters K_c and τ_d. In Figure 12, the asymptotic values are visible. Beyond a certain delay τ_d > 108 [s] apparently the process cannot anymore become stable. If $\tau_d \rightarrow 0$ the minimum proportional gain can be found, whose value precisely should preserve stability in case delay is not

concerned with. It is obvious that delay makes a process less stable because the controller can be too late with correcting a certain disturbance. Therefore, the right-hand side of the Hopf curve is region II (or III if multiplicity is involved) and the left-hand side is region I. Large K_c values can eliminate limit cycles and preserve stability.

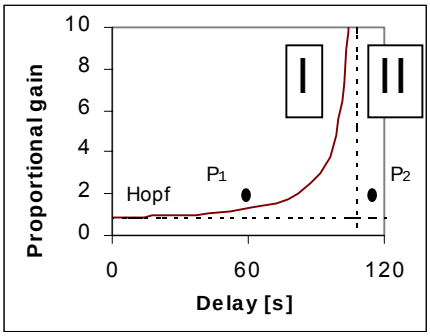

Figure 12a Reactor designer stability map. At the left-hand side, the system behaves stable, at the right-hand side unstable. Two orbit curves are needed to verify the behaviour.

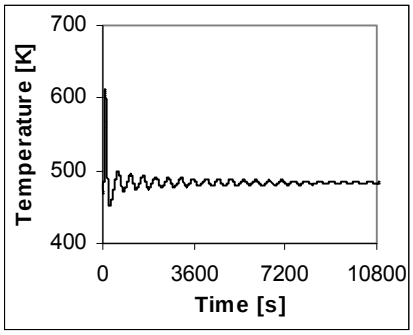

Figure 12b Orbit curve. Point 1, behaves stable after a disturbance $\Delta T = +20$ [K], spiral point.

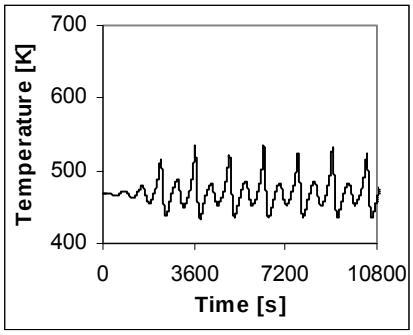

Figure 12c Point 2 behaves unstable (limit cycles) from the initial steady state. Beyond the asymptotic delay, instability is inevitable.

Point 1 shows that after a disturbance, the controller ($K_c = 2$) is robust enough to reduce the limit cycles, even with a delay $\tau_d = 60$ [s]. The same $K_c = 2$ with a delay $\tau_d = 110$ [s], which is slightly larger than the asymptotic value $\tau_d = 108$ [s] implies definitely an unstable process. Suppose a delay $\tau_d = 80$ [s], the engineer can effortlessly read from Figure 12a that $K_c = 3$ signifies no more limit cycles.

4.6 Theoretical prevention and elimination of limit cycles

According to Westerterp *et.al.*[80] the heat capacity of the reactor and in particular in relatively small reactors, has to be taken into account if limit cycles are to be considered. Westerterp postulated in general that limit cycles will not occur if, in a high conversion reactor, a combination of the following factors coincide:

- A weak temperature dependence of the reaction rate (E/R low).
- A low reactant concentration in the feed (ΔT_{ad}) low.
- A low heat effect (ΔT_{ad}) low.
- A high reactor temperature (T_s high).
- A not too high conversion ($1-\zeta_s$ relatively large).
- A long residence time (τ_R high).
- A preferable small reactor (A/V_R large).
- Good heat transfer coefficient or heat capacity (UA large).

In case more advanced processes are considered, these points are conversely not sufficient enough to solve a limit cycle appearance and more knowledge about the process is required.

Chapter V

5 PROCESS CONTROL

5.1 Introduction

During the process of a chemical reactor, several requirements such as safety, production specifications, operational constrains and economics must be satisfied, in the presence possible external disturbances. These requirements dictate the need for continuous monitoring of the operation of a chemical reactor and external intervention i.e. control, to guarantee achieving the operational objectives. This is accomplished through a rational arrangement of measuring devices, valves, controllers, computers etc., which constitutes the control system. There are three general classes of needs, which a control system is required to satisfy:

1. Suppressing the influence of external disturbances
2. Ensuring the stability of a chemical process
3. Optimising the performance of a chemical process

5.2 Feedback controllers

In every control configuration, the controller is the active element that receives the information from the measurements and takes appropriate control actions to adjust the values of the manipulated variables. Consider the generalised process shown in Figure 13. It has an output y, a potential disturbance d also known as *process load* and an available manipulated variable m. The disturbance changes in an unpredictable manner and the control objective is to keep the value of the output y at desired levels.
A feedback control action can take the following steps:

1. Measure the value of the output using the appropriate measuring device. Let y_m be the value indicated by the measuring device.
2. Compare the indicated value y_m to the desired value y_{sp} (*set point*) of the output. Let the deviation (*error*) be $\varepsilon = y_{sp} - y_m$.
3. The value of the deviation ε is supplied to the main controller. The controller in turn changes the value of the manipulated variable m in such a way as to reduce the magnitude of the deviation ε. Usually, the controller does not affect the manipulated variable directly but through another device known as the *final control element*.

The system in Figure 13 is known as feedback-controlled or closed loop system and pictorially summarises the foregoing three steps.

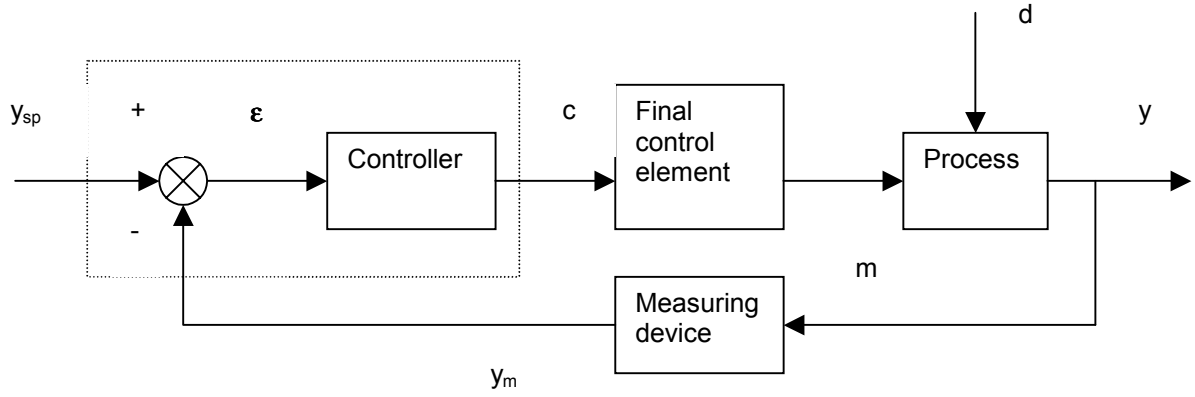

Figure 13 Process and corresponding feedback loop. Y_{sp} = set point or desired value ε = error d = disturbance m = measured value c = controlled value.

The controller comes between the measuring device and the final control element. Its function is to receive the measured output signal $y_m(t)$ and after comparing it with the set point y_{sp} to produce the actuating signal c(t) in such a way as to return the output to the desired value y_{sp}. Therefore, the input to the controller is the error $\boldsymbol{\varepsilon}(t) = y_{sp} - y_m(t)$, while its output is c(t). The various types of continuous feedback controllers differ in the way they relate $\boldsymbol{\varepsilon}(t)$ to c(t). Four basic types of feedback controllers can be distinguished:

1. Proportional (P controller)
2. Proportional integral (PI controller)
3. Proportional derivative (PD controller)
4. Proportional Integral derivative (PID controller)

Due to the scope of this report, exclusively the proportional and the integral action will be examined.

5.2.1 Proportional control

The principle of the P-controller is the proportional correction of the error. The response has a high maximum deviation and there is a significant time of oscillation. The period of this oscillation is moderate. For a sustained change in load, the controller variable is not returned to its original value i.e. the desired value, but attains a new equilibrium value termed the *control point*. The difference between desired value and control point is called the *offset* or *droop*. Its actuating output is proportional to the error:

$$c(t) = K_c \boldsymbol{\varepsilon}(t) + c_s \tag{25}$$

In equation 25 parameter K_c is called the *proportional gain* of the controller and c_s = controller bias signal i.e. its actuating signal when $\varepsilon = 0$. A proportional controller is described by the value of its proportional gain K_c or equivalently by its proportional band PB, where $PB=100/K_c$. The proportional band characterises the range over which the error must change in order to drive the actuating signal of the controller over its full range. Usually ($1 \leq PB \leq 50$). The larger the gain K_c or equivalently, the smaller the proportional band, the higher the sensitivity of controller's actuating signal to deviations ε will be.
Define the deviation c'(t) of the actuating signal by

$$\begin{aligned} c'(t) &= c(t) - c_s \\ &= K_c \boldsymbol{\varepsilon}(t) \end{aligned} \tag{26}$$

5.2.2 Proportional-Integral control

Considerable improvements in the quality of the resulting control can be obtained if a different control law is used known as *proportional-integral control* or *proportional-plus-reset* controller where the proportional and the integral action are combined. Its actuating signal is related to the error by equation 27:

$$c(t) = K_c \boldsymbol{\varepsilon}(t) + \frac{K_c}{\tau_I} \int_0^t \boldsymbol{\varepsilon}(t) dt + c_s \tag{27}$$

where τ_I is the *integral time constant* or reset time often expressed in minutes. The reset time is the time needed by the controller to repeat the initial proportional acting change in its output. The reset time is an adjustable parameter and is usually varied in the range ($0.1 \leq \tau_I \leq 50$ [min]). The integral action causes the controller output c(t) to change as long as an error exists in the process output. Therefore, such a controller can eliminate even small errors. The maximum deviation of the controlled variable is determined by the settings of both K_c and τ_I, The integral term of a PI controller causes its output to continue changing as long as there is a non-zero error. Often the errors cannot be quickly eliminated and given enough time they produce larger and larger values of the integral term, which in turn keeps increasing the control action

until it is saturated (e.g. the valve completely open or closed). This condition is called *integral windup*. Then, even if the error returns to zero, the control action will remain saturated. A PI controller needs special provisions to cope with integral windup.

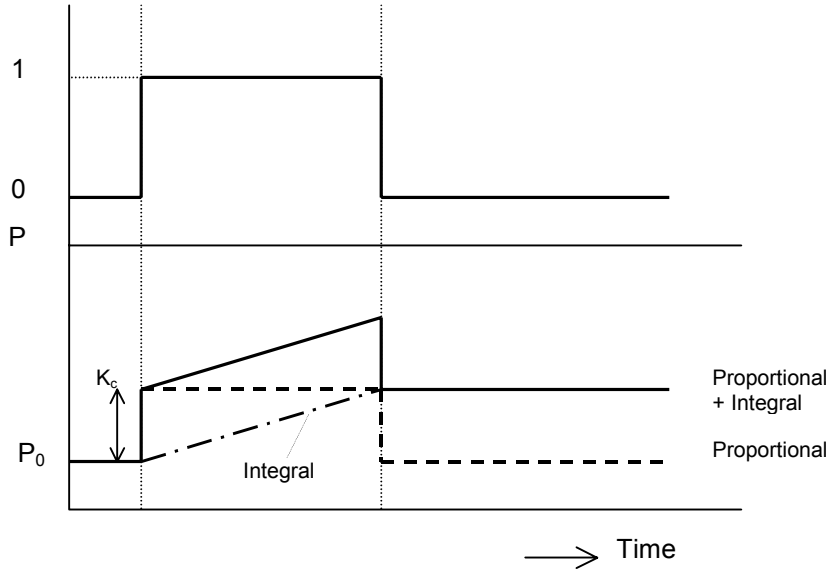

Figure 14 Response of PI controller to unit step change in error.

5.2.3 Offset

The question arises: Why does proportional feedback control result in steady state offset unequal to zero? The proportional controller operates according Equation 26 so that in the transient state, while things are still changing, the rate at which the process input is being changed is given by:

$$\frac{dc'(t)}{dt} = K_c \frac{d\varepsilon(t)}{dt} \tag{28}$$

It is obvious that at steady state, all the derivates will vanish, however is it possible for dε(t)/dt to be zero without ε(t) itself being zero? The answer, of course, as soon as ε(t) becomes constant, whether at zero, or at a nonzero value, steady state is achieved. Observe from equation 26 that for ε(t) to be zero, c'(t) must be zero. From the process model it is obvious that c'(t) will never be zero for non-zero set-point or non-zero disturbance i.e. there will always be a discrepancy i.e. steady state offset.

Offset = (new set point) – (ultimate value of the response)

The offset is the characteristic effect of proportional control. It decreases as K_c becomes larger and theoretically: offset $\rightarrow$ 0 if $K_c \rightarrow \infty$.

Another question arises: Why does PI control not result in steady state offset? For the PI controller, control action is determined according to equation 27. Under transient conditions, the rate at which c'(t) changes is given by equation 29 by differentiating equation 27.

$$\frac{dc'(t)}{dt} = K_c \frac{d\varepsilon(t)}{dt} + \frac{K_c}{\tau_I}\varepsilon(t) \tag{29}$$

Regardless of controller parameters, or the specific process in question, whenever steady state is achieved, all the derivatives in equation 29 will vanish and ε(t) will always be zero i.e. no steady state offset. Therefore, integral action eliminates any offset.

5.2.4 Comparison P and PI controller

The advantage of the PI-controller is the offset removing characteristic. However, the disadvantages of PI control are that it gives rise to a higher maximum deviation, a longer response time and a longer period of oscillation than with proportional action only. This type of control action is therefore used when the above can be tolerated and offset is undesirable. It is however a very frequently used combination.

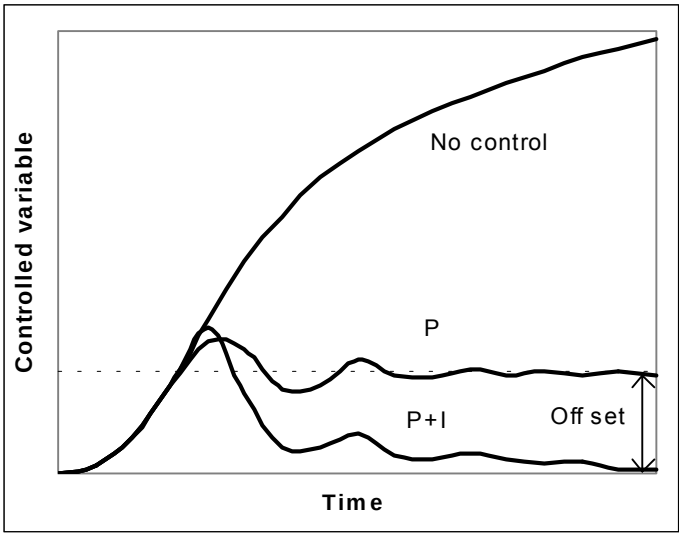

Figure 15 Response of controlled variable to step disturbance in load.

5.3 Disturbances

Changes in continuous process operation can generally be divided into the following categories:

1. Dynamic operations
2. Internal changes
3. External changes

Dynamic operations

Dynamic operations take place when the process is not operated under constant conditions e.g. during start-up or switchover to other conditions.

Internal disturbances

Due to changes in one or more state variables like T and or ζ, without any external disturbances, the process can become dynamical unstable (limit cycles). Drastic internal changes can be caused by failures in process equipment or control instrumentation in which the state variable change. In addition a process can become gradually dynamical unstable by the slow change of conditions of a continuous process by fouling, poisoning of catalyst, coke depositing in furnace tubes etc. Henson *et.al.* [35].

External disturbances

For this type of change, continuous operation is disturbed by external influences. In many cases, it is a matter of disturbances, which enter the process by feed, heating, catalyst flows etc. Here disturbances mean relatively small changes in process conditions without malfunctioning of process apparatus and control instruments.

Process behaviour

Because all disturbances from internal and external causes are undesirable at constant operation, the process has to be corrected (process control to be examined in chapter 5). These disturbances or perturbations cause changes in the dynamical behaviour of a process.

5.4 Concept of dead time

Whenever an input variable of a system changes, there is a time interval during which no effect is observed on the outputs of the system. This time interval is called dead time or delay. This response poses a difficult problem for a feedback controller, because its next move depends on the response of the process to its most recent move. The presence of dead time can easily destabilise the dynamic behaviour of a controlled system to an external perturbation.

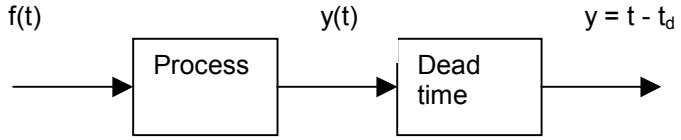

Figure 16 Process with dead time.

$$y_{out}(t) = y_{in}(t - t_d) \tag{30}$$

When a time-delay element is present in a feedback control loop, the following obvious control problems arise:

- With a delay, control action will be based on delayed, hence obsolete process information that is usually not representative of the current situation within the process.
- If the process has an input delay, then the effect of the control action will not be immediately felt by the process, compounding the problem even further.

Virtually all physical processes will involve some dead time between the input and the output. The passing through the core of a measuring device, the controlling process, the transfer of heat from a heating device to the reactor etc., will take time.
To avoid the use of complex mathematical descriptions of every process, which contributes to delay and due to the lack of physical information regarding dead time, the following overall equation can be used:

$$\tau_d \frac{dy_d}{dt} = y - y_d \tag{31}$$

In equation 31, all the different kind of delay is allowed for by means of the parameter τ_d.

5.5 Process capacity

Capacity is where a process stores variable amounts of mass or energy. If the flowrate of mass or energy into and out of a process are not equal, then their difference accumulates within the capacity of the process[1] i.e. the process act as a buffer. If a variable x is a measure of that accumulation, the following general differential equation can be formulated:

[1] Liquid level is an indication of the variable volume of liquid stored in the capacity of a tank, temperature is a measure of the energy contained in the heat capacity of a mass of material and stream composition is also indicative of a particular species accumulating in a mixed vessel such as a reactor or mass transfer process.

$$\tau \frac{dx}{dt} = \Phi_{in} - \Phi_{out} \tag{32}$$

5.5.1 Process time constant

In equation 32 Φ_{in} and Φ_{out} are inflow and outflow respectively and τ the *time constant* of the capacity in the same units as time. The time constant of a process is a measure of the time necessary for the process to adjust to a change in its input. The smaller the value of τ, the steeper the initial response of the system. Consequently, capacity plays a certain role in the dynamical behaviour and stability of a process, which will be examined in next sections. According to Stephanopoulos[74] the CISTR can be observed as a multi capacity process of mass and energy. By dividing differential equations 2 and 3 with $\rho\ C_P\ \Phi_V$, equations 33 and 34 are obtained.

$$\frac{V_R}{\Phi_V}\frac{d[A]}{dt} = ([A]_0 - [A]) - \frac{V_R}{\Phi_V} k_0 e^{-E_{act}/RT}[A] \tag{33}$$

$$\frac{V_R}{\Phi_V}\frac{dT}{dt} = (T_0 - T) + \frac{V_R}{\Phi_V}\frac{(-\Delta H_R)}{\rho C_P} k_0 e^{-E_{act}/RT}[A] - \frac{UA}{\Phi_V \rho C_P}(T - T_{cool}) \tag{34}$$

It is obvious that in this particular case the time constant represents the *average residence time* τ_R of the CISTR according to:

$$\tau_R = \frac{V_R}{\Phi_V} \tag{4}$$

If one takes into account also the heat capacity of the equipment present in the reactor (i.e. stirrer etc.) the equation can be extended to

$$\tau_R = \frac{V_R}{\Phi_V} + \frac{m_{equipment} C_{P,equipment}}{\rho C_P \Phi_V} + \ldots \tag{35}$$

5.5.2 Cooling time constant

If equation 12 is divided by $\rho_{cool}\ C_{P,cool}\ \Phi_{V,cool}$, than equation 36 is obtained:

$$\tau_{cool}\frac{dT_{cool}}{dt} = (T_{cool,0} - T_{cool}) + \frac{UA}{\rho_{cool} C_{P,cool} V_{cool}}(T - T_{cool}) \tag{36}$$

In which τ_{cool} is:

$$\tau_{cool} = \frac{V_{cool}}{\Phi_{V,cool}} \tag{37}$$

In fact, τ_{cool} is partially composed of the time constant of the coolant and additionally partially composed of the physical properties of the equipment. Analogue to equation 35 one can write the coolant time constant correlation 38 according:

$$\tau_{cool} = \frac{V_{cool}}{\Phi_{V,cool}} + \frac{m_{equipment} C_{P,equipment}}{\rho_{cool} C_{P,cool} \Phi_{V,cool}} + \ldots \quad (38)$$

5.6 Controller tuning

Generally, when a set point changes, the response of the process deviates and the controller tries to bring the output again close to the desired set point (Figure 15). The distinguished controllers have different effects on the response of the controlled process. The following questions arise:

- What type of feedback controller should be used to control the process?
- What are the best values for the adjustable parameters of the selected controller?
- What performance criteria should be used for the selection and the tuning of the chosen controller?

5.6.1 Performance criteria

Even though specific details of what is considered acceptable performance can be interpreted throughout a different perspective, some general principles can be applied universally. An effective close loop system is expected to be stable and to be capable of causing the system output ultimately to attain its desired set point value. In addition, the approach of this system output to the desired set point should be neither too sluggish, nor too oscillatory. A careful examination of criteria by which closed-loop system performance may be assessed in general:

- Stability criteria
- Steady state criteria
- Dynamic response criteria

Of these, the first two are very easy to specify. The only reasonable specification is that the system must be stable. Also the key steady state criteria is that there be little or no steady state offset i.e. the error is brought close to zero at steady state. The third class of criteria specifies how the system responds under closed-loop control. The evaluation of the dynamic performance of a closed loop system is based on the following types of commonly used performance criteria:

- *Overshoot* Keep the maximum deviation (*error*) of the response as small as possible.
- *Rise time* Check the time needed to reach the desired value for the first time.
- *Settling time* Return to the desired level of operation as soon a possible (or within ±5%).
- *Decay ratio* Verify if the ration between the first and the second peak is approximately 4:1.
- *Windup* Minimize the integral of the errors until the process has settled to its desired set point and prevent integral windup.

All of the mentioned characteristics above could be used by the designer as the basic criteria for selecting the controller and the values of its adjusted parameters. It must be emphasised, though, that one simple characteristic does not suffice to describe the desired dynamic response. Usually, more satisfied objectives are required i.e. minimum overshoot, minimum settling time etc. Unfortunately, controller designs based on multiple criteria lead to conflicting response characteristics.

5.6.2 Methods of adjusting feedback controller settings

Many procedures exist for estimating optimum settings for controllers:

1. Ratio-overshoot method (Stephanopoulos[74])
   One of the usual bases employed is that the system response should have a decay of ¼ i.e. the ratio of overshoot of the first peak to the overshoot of the second peak is 4:1 (Figure 17). There is no direct mathematical justification for this but it is a compromise between a rapid initial response and a short *response time*. The response time is the time required for the absolute value of the system response to come within a small-specified amount of the final value of the response.
2. Ziegler and Nichols method (Ziegler *et.al.* [81])
   This method is often applied and will be discussed in the next paragraph.
3. Process response methods
   Common methods are e.g. the Loop tuning method by Erickson *et.al.*[25], the Cohen Coon method[11], the Integral relation method by Murrill[56] and many more which are not suitable for the propose of this report due to the fact that a process response is practically obtained.
4. Remainder tuning methods
   Other tuning methods are the Nyquist stability criteria[74] and non-linear process control methods[35]. Many more methods are available in the literature.

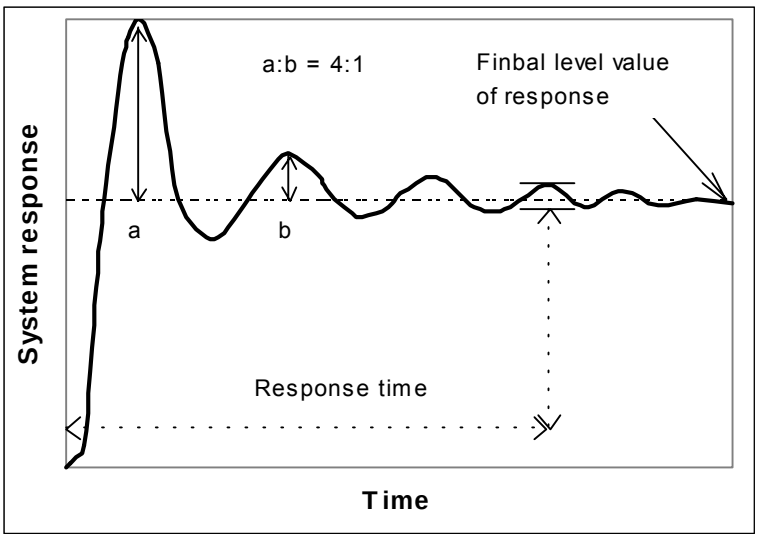

Figure 17 System response with ¼ decay ratio.[14 25 74 60].

5.6.3 Ziegler and Nichols method

This method is characterised by finding the gain at which the system is marginally stable and the frequency of oscillation at this point. From these two parameters, the controller parameters are calculated. The Ziegler Nichols tuning technique[81] is intended to produce a closed-loop damping ration of 1:4.
It goes through the following steps:

1. Bring the system to the desired operational level i.e. design condition.
2. Using proportional control only (or with maximum τ_I) and with the feedback loop closed, introduce a set point change and vary the proportional gain until the system oscillates continuously i.e. limit cycle. The frequency of continuous oscillation is the crossover frequency ω_{co}. Let M be the amplitude ratio of the system's response at the crossover frequency.
3. Compute the following two quantities:
   The ultimate gain or proportional gain for sustained oscillations:

$$K_U = 1/M \tag{39}$$

The ultimate period of sustained cycling [minutes]:

$$P_U = \frac{2\pi}{\omega_\infty} \tag{40}$$

4. Using the values of K_U and P_U, Ziegler Nichols recommended the following settings for feedback controllers:

Table 8 Ziegler Nichols controller settings.

Control action	Controller settings	
	K_c	τ_I [min]
P	K_U / 2	-
PI	K_U / 2.2	τ_U / 1.2

The settings above reveal the rationale of the Ziegler Nichols methodology.

1 For proportional control alone, a gain margin equal to 2 is recommended.
2 For PI control, a lower proportional gain is advised because the presence of the integral control mode introduces additional phase lag in all frequencies with destabilizing effects on the system. Therefore, lower K_c maintains approximately the same gain margin.

5.6.4 Controller configuration

The remaining question is, which one to select first: K_c or τ_I? According to Stephanopoulos[74] in general the proportional gain is selected first, in such way that the controller has the necessary strength to repress disturbances. Afterwards a suitable integral time is chosen for offset elimination. Together K_c and τ_I must satisfy the control performance criteria e.g. the ¼ decay ratio.

In case a system is not exclusively concerned with external disturbances but additionally is concerned with dynamical instability, the mentioned tuning methods have to be interpreted with caution and it is not certain if these methods are still valid. Inevitably, a more robust control action is needed i.e. K_c has to increase. This might have sincere consequences for the e.g. Ziegler Nichols controller settings. Therefore, the following strategy is suggested to acquire stability through searching and optimising controller configuration parameters.

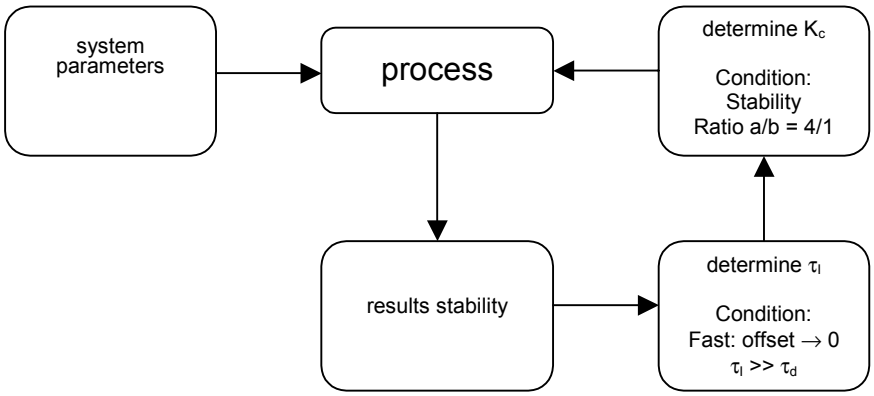

Figure 18 Strategy to acquire stability through searching and optimising controller parameters.

Chapter VI

6 STARTING POINT OF RESEARCH

6.1 Introduction

In this chapter, the current level of research of limit cycles is examined. Therefore, two distinctive reactor designer stability maps and one reactor controller stability map will be considered conjoined with accompanying orbit curves. To apply the theory, a certain system has to be chosen. In this report, a system previously studied by Van Elk *et.al.*[22], is selected. Primarily, in the next paragraph, this system will be quantified. Subsequently, a method to study the stability will be presented. Then, the resulting stability maps will elaborately be presented and discussed.

6.2 Base case definition

Despite that the numerical values are taken from the article presented by Van Elk, the system studied in this report does differ from the system studied by van Elk. He studied the stability and dynamic behaviour of gas-liquid reactors extensively. Adopting a rigorous gas-liquid reactor model, he demonstrated the possible existence of dynamic instability (limit cycles) in gas-liquid processes. Since limit cycles can already emerge in a system that can be described with merely two differential equations i.e. mass and energy balance, some adaptations can be been made to simplify the model. Primarily, non-relevant aspects with regards to limit cycles have been removed from the model. The simplest case will be considered because more detailed issues, through adding more mathematical equations to the model, can be concerned with afterwards.

The first simplification for the base case model is that the reactor of interest in this report is a homogeneous liquid phase reactor. Therefore, all the parameters needed for the description of two-phase reactors and mass transfer (like hold-up and the Hatta number) can be ignored. Because van Elk used a pseudo-first order reaction constant approximation, therefore the same constant k_0 can be used for the first order reaction of the present case. It is assumed that the liquid is completely saturated with component A. As a result the concentration of reactant A, can be considered as constant and accordingly be included in the value of k_0 (Appendix 3).
The simplified model based on van Elk will be called the "*base case*". The required values of the parameters are listed in Table 9.

Table 9 Main system parameters (van Elk *et.al.* [22]).

Parameter	Symbol	Value	Unit
System conditions			
Liquid flow rate	Φ_v	0.005	$[m^3\ s^{-1}]$
Reactor volume	V_R	5	$[m^3]$
Feed concentration	$[A]_0$	5000	$[mol\ m^{-3}]$
	$[P]_0$	0	$[mol\ m^{-3}]$
Feed temperature	T_0	303	[K]
Important base case variables			
Heat transfer coefficient × (transfer) area or cooling capacity	UA	55	$[kJ\ s^{-1}\ K^{-1}]$
Reactor temperature	T	468	[K]
Coolant temperature	T_{cool}	441	[K]
Fixed parameters			
Density	ρ	800	$[Kg\ m^{-3}]$
Heat capacity	C_P	2	$[kJ\ kg^{-1}\ K^{-1}]$
Reaction enthalpy	ΔH_R	-160	$[kJ\ mol^{-1}]$
Activation energy	E_{act}	90	$[kJ\ mol^{-1}]$
Arrhenius frequency factor	k_0	2.505×10^7	$[s^{-1}]$

Additional data			
Density coolant	ρ_{cool}	1000	[Kg m^{-3}]
Heat capacity coolant	$C_{P,cool}$	4.2	[kJ kg^{-1} K^{-1}]
Feed temperature coolant	$T_{cool,0}$	303, 400, 435	[K]

If the mass and heat balance are solved for the steady state situation using the values portrayed in Table 9, a small dissimilarity can be noticed: T = 466 [K] instead of T = 468 [K]. Because the latter should imply an initial perturbation of ΔT = 2 [K], if necessary the exact numerical solution of the mass and heat balance is used for the simulations in this report. In Appendix 3, the magnitude concerning the base case values presented in Table 9 has been evaluated.

6.3 Stability of the base case

The following stability naps will be considered:

Table 10 Base case stability maps.

Stability map	Reference
T versus T_{cool} varying UA	Figure 19
T versus T_{cool} varying Φ_V	Figure 20
T_{cool} versus UA varying Φ_V	Figure 21

Although, in fact Figure 21, which will be discussed later, is sufficient to prove the unstable character of the base case, likewise, the traditional stability maps Figure 19 (and Figure 20) will be presented. Similar stability maps like Figure 19 have been printed in the article by van Elk *et.al.*[22]. To be able to compare the stability maps of this report easily, the axes-scale is as much as possible in accordance with the figures printed in the article.

6.3.1 Reactor designer stability maps

The following stability maps (theory discussed in §4.5) will be considered: Reactor temperature versus coolant temperature for initially (UA variation) and afterwards (Φ_V variation). The mathematical base case model discussed in §2.2 states:

$$V_R \frac{d[A]}{dt} = \Phi_V \left([A]_0 - [A]\right) - V_R k_0 e^{-E_{act}/RT}[A] \tag{2}$$

$$\rho C_P V_R \frac{dT}{dt} = \rho C_P \Phi_V \left(T_0 - T\right) + \left(-\Delta H_R\right) V_R k_0 e^{-E_{act}/RT}[A] - UA\left(T - T_{cool}\right) \tag{3}$$

Reactor temperature versus coolant temperature (UA variation)

The first base case designer stability map is created (Figure 19) in which the coolant temperature is drawn on the abscissa and the active reactor temperature on the ordinate. The stability map consists of equilibrium curves (dT/dt = 0 and $d\zeta/dt$ = 0) as a function of one active parameter, which is in this case the coolant temperature. Several equilibrium curves have been plotted, for various values of UA with the intention that the influence of the cooling capability becomes more comprehensible. Additionally the Fold and Hopf curves are included as a function of two active parameters, which are the coolant temperature and the cooling capacity UA. Eventually the stability map is divided into marked regions. This marking process, of the particular regions in the stability map, is sometimes easy and sometimes vague due to the existence of multiplicity. Then it is a matter of trial and error. However, through creating orbit curves, the dynamical behaviour can be determined or verified.

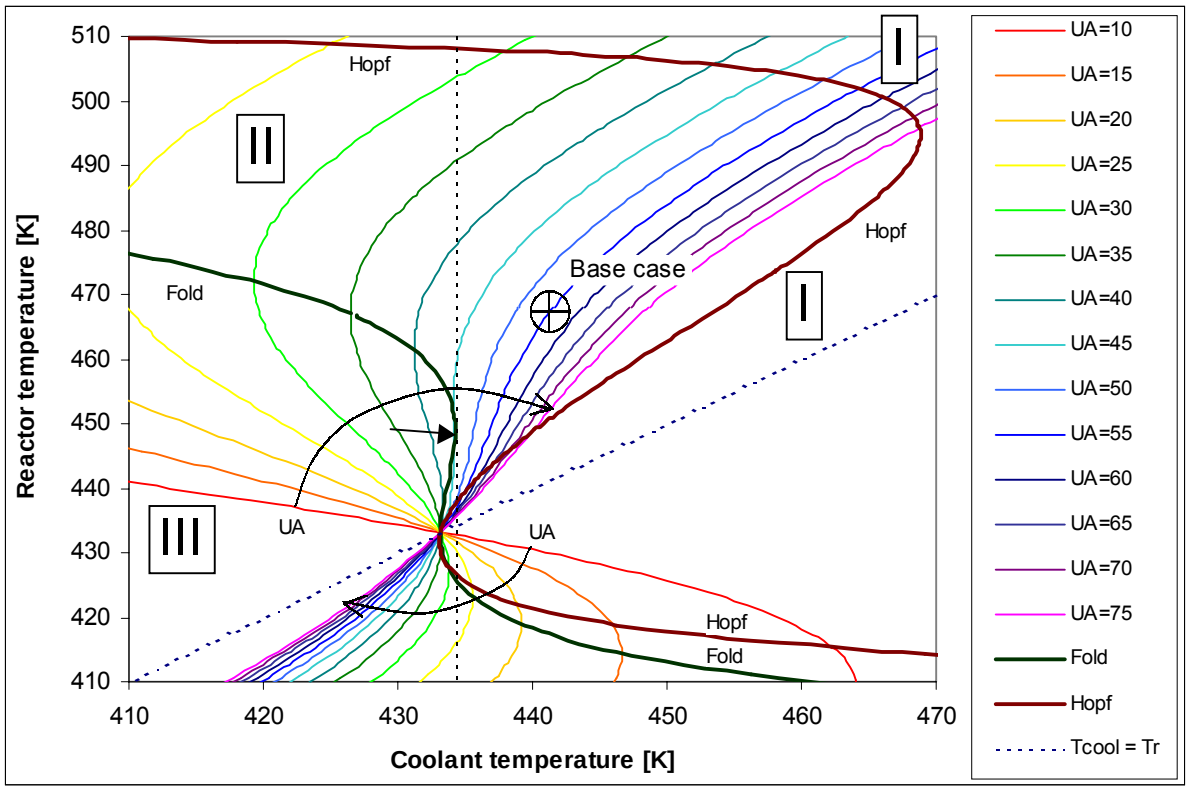

Figure 19 Reactor designer stability map for the base case model considering the irreversible exothermic reaction A → P in a cooled CISTR. The steady state temperature is plotted as function of the coolant temperature in which the cooling capacity is varied. The symbol ⊕ points towards the base case value. The LOCBIF source LOCBIF rhs 2 is included in Appendix 7. The base case is located in a region II which points towards dynamical instability.

Discussion of the reactor designer stability map:

- In Figure 19 a dotted line $T=T_{cool}$ has been drawn which indicate that the reactor temperature cannot decrease beneath the coolant temperature curve.
- LOCBIF provides the bifurcation maximum and minimum values of the cooling capacity and the coolant temperature in the Hopf and Fold curve. In case: UA > 45 [kJ s^{-1} K^{-1}] and $T_{cool} = T_{cool}$ (base case) or T_{cool} > 434 [K] and UA = UA (base case), no multiplicity will occur.
- In Figure 19 the transition from the region in which multiplicity occurs and the region with one operation point is marked with an arrow. –►.
- Absolutely no limit cycles exists in Figure 19 provided that UA > 105 [kJ s^{-1} K^{-1}] (Hopf maximum) irrespective of the coolant temperature.
- It is obvious that the relevant base case, symbolised with ⊕, is located in region II in which undesired limit cycles can emerge.

Reactor temperature versus coolant temperature (Φ_V variation)

In the following designer stability map, instead of the cooling capacity, the throughput is considered. Firstly, the equilibrium curves are drawn as a function of one active bifurcation parameter T_{cool} for increasing flowrate values. Subsequently, the Fold and Hopf curves are added as a function of two active parameters T_{cool} and Φ_V.

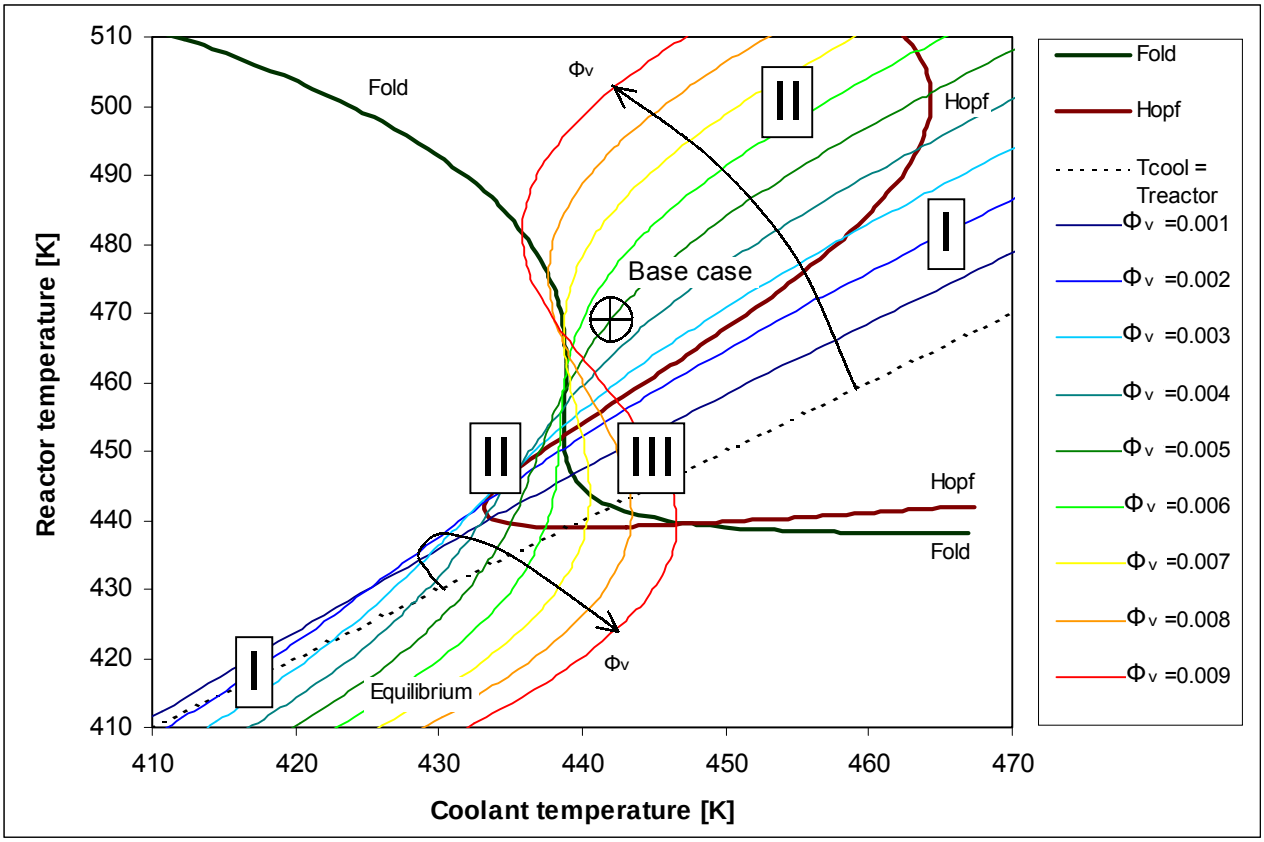

Figure 20 Reactor designer stability map of the base case model considering the irreversible exothermic reaction A → P in a cooled CISTR. The steady state temperature is plotted as function of the coolant temperature in which the flowrate value is varied. For $\Phi_V > 0.006$ [$m^3\ s^{-1}$] (Fold maximum) the equilibrium curve exhibit multiplicity which means that extinction is also possible.

Discussion of the reactor designer stability map:

- If the dotted line $T=T_{cool}$ in Figure 20 is taken as the reference point and the flowrate is increased to $\Phi_V = 0.0014$ [$m^3\ s^{-1}$], the Hopf curve is intercepted at $T_{cool} = 434$ [K] which is according to LOCBIF a Hopf maximum. Up to this flowrate, the system is stable. Larger flowrate values imply dynamical instability.
- If the flowrate is increased, the equilibrium curves increase virtually counter clockwise up to $\Phi_V = 0.006$ [$m^3\ s^{-1}$] from where multiplicity is involved.
- If $\Phi_V > 0.007$ [$m^3\ s^{-1}$] the system is unstable because the reaction extinguishes. Apparently too much heat is withdrawn from the CISTR.
- LOCBIF provides the Fold and Hopf maximum and minimum values. According to LOCBIF two multiplicity transitions exist close to one another ($T_{cool} = 439$ [K]) i.e. no multiplicity stands for a flowrate $\Phi_V < 0.006$ [$m^3\ s^{-1}$]. The existence of multiplicity can be clarified by the fact that in case the flowrate is considerably increased, this implies that on the one hand, the reaction increases due to the supply of fresh feed, on the other hand the reactor is also cooled by the cold feed inlet. If for instance too much cold feed enters the reactor, it can conversely remove too much reaction heat causing the reaction to slow down and eventually extinguish.
- LOCBIF also found the minimum Fold in which certainly no limit cycles occur: $T_{cool} > 464$ [K]. The base case indicated with symbol ⊕ is obviously also in this stability map located in region II in which certainly limit cycles exhibit.

6.3.2 Reactor controller stability maps

In reactor controller stability maps, not the reactor temperature but a process controller parameter is concerned with. Because in this chapter the process controller is not present, the stability map is adapted and examined for as well UA, T_{cool} as Φ_V.

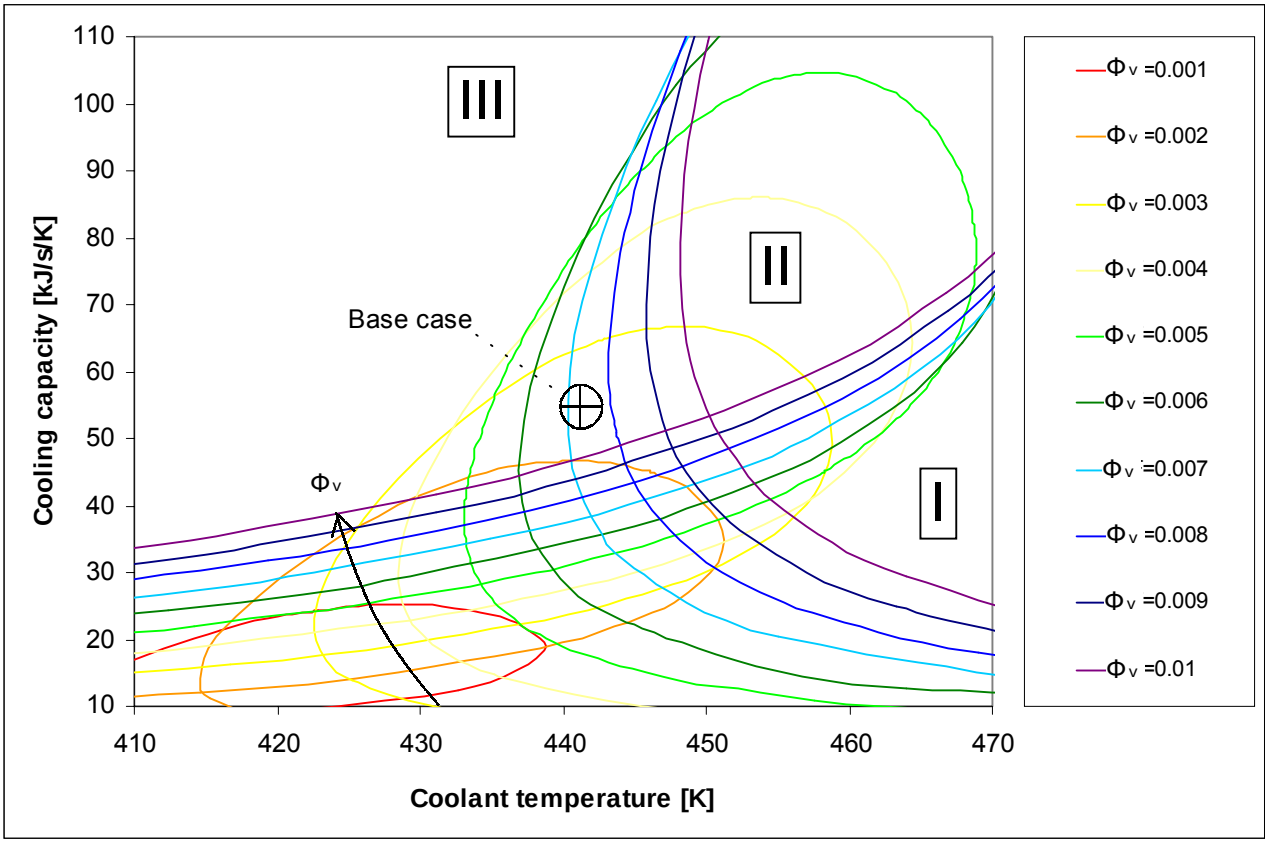

Figure 21 The stability map concerning the base case. Select one particular flowrate. The inside of the loops (Hopf curves) point towards limit cycles, the left hand side of the curves indicate multiplicity and the right hand side means stability.

Discussion of the stability map:

- In Figure 21 the Hopf curves have been drawn for active LOCBIF parameters UA and T_{cool}.
- The stability map provides in one plot, useful process information with regards to as well the cooling capacity, coolant temperature as well as the throughput.
- The inside of all the loops point towards limit cycles, the left hand side of the curves indicate multiplicity, often this means instability and the right hand side means stability.
- A stable operating point can easily be located. For instance, consider the base case with a fixed UA and Φ_V, T_{cool} shifts to region I in case $T_{cool} > 464$ [K].

6.4 Overview

Table 11 Base case relevant stability values (no control). Static and dynamical behaviour.

System variable Dimension	Cooling capacity variation	Coolant temperature variation	Throughput variation	Behaviour
Cooling capacity [kJ s^{-1} K^{-1}]	15 < UA < 45	55	55	Multiplicity
	45 < UA < 78	55	55	Limit cycles
	UA > 78	55	55	Stability
Coolant temperature [K]	441	410 < T_{cool} < 434	441	Multiplicity
	441	434 < T_{cool} < 464	441	Limit cycles
	441	T_{cool} > 464	441	Stability
Throughput [m^3 s^{-1}]	0.005	0.005	0 < Φ_V < 0.0014	Stability
	0.005	0.005	0.0014 < Φ_V < 0.006	Limit cycles
	0.005	0.005	Φ_V > 0.007	Instability

6.5 Base case limit cycles

Primarily, the orbit curve for the base case reactor temperature is created with LOCBIF, which results in Figure 22a and the orbit curve pertaining to the conversion in Figure 22b.
The mathematical steady state solution of the mass and heat balance (ODE 2 and 3) has been chosen as initial point, which is represented by the dotted line. The abscissa of Figure 22a and Figure 22b are identical. The figures conversely can be combined to phase plot Figure 22c in which the principle of the phenomenon limit cycle can be elucidated. No perturbation is necessary to initiate the self-sustained oscillations. The system variables (conversion and the reactor temperature) will cycle around the steady state point however the steady state itself will never be reached.

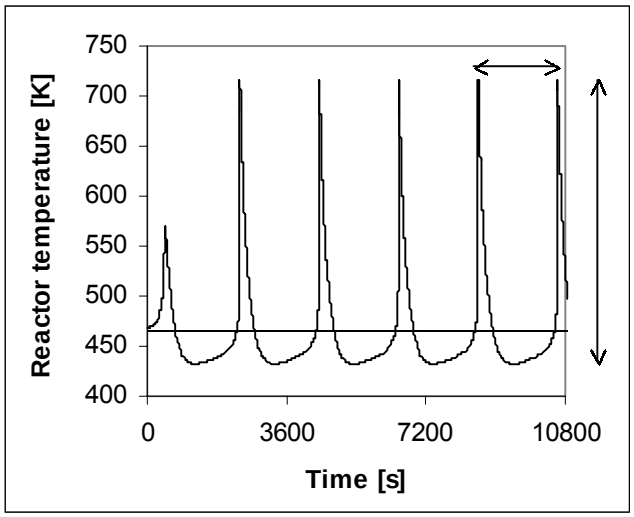

Figure 22a Orbit curve for the exothermic reaction A → P in a CISTR. The initial condition is the steady state situation. The limit cycles occur consistently with a temperature deviation $\Delta T = 284$ [K] in a cycle time $\Delta t \approx 34$ [min].

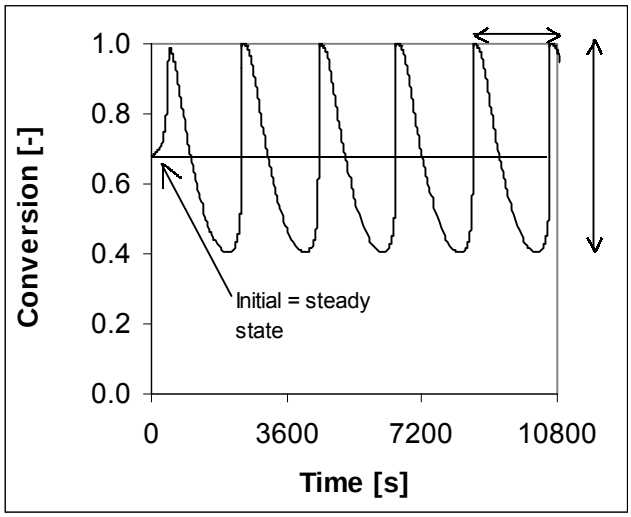

Figure 22b Orbit curve for the base case definition in case limit cycles emerge. The conversion deviation due to the limit cycles appears to be $\Delta\zeta \approx 0.6$ every $\Delta t \approx 34$ [min].

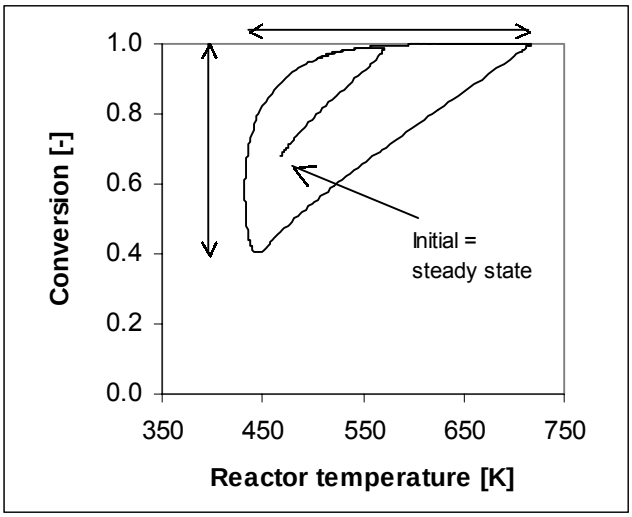

Figure 22c After approximately t = 8 [min], the maximum conversion has been reached i.e. $\zeta \approx 0.98$ and decreases to $\zeta \approx 0.40$ and so on. Subsequently, the system is proverbially dragged into the limit cycle.

Table 12 The base case value (from Table 9).

Variable	Value	Dimension
UA	55	[kJ s^{-1} K^{-1}]
T_{cool}	441	[K]
Φ_V	0.005	[m^3 s^{-1}]
T_{stst}	466	[K]
ζ_{stst}	0.68	[-]

Chapter VII

7 STRUCTURE AND OBJECTIVES OF PART II

Part II, will have the following elements in every chapter.

It will make the difference in two kinds of stability-maps:

1. Reactor designer stability maps: These are indispensable when designing a new reactor. In this case reactor- and coolant-temperature, cooling capacity, coolant flowrate and throughput dependence of the process stability are indispensable parameters for the designer to develop a new reactor. Due to the number of relevant parameters and their dependence, this kind of stability maps have a complex nature and are often difficult to interpret.

2. Reactor controller stability maps: These are useful simplifications of the reactor designer stability maps which focus on a particular case in which reactor- and coolant-temperature, cooling capacity, coolant flowrate and throughput are already fixed (no degrees of freedom) and stability only can be attained by applying process control.

The reactor controller stability maps are an extension of the use of data generated with LOCBIF and are a major improvement in handling stability data and obtaining a profound idea of stability-dependence of the base case (or any other existing or hypothetical possible reactor).

Therefore the objectives of part two are:

1. Providing indispensable information for the design of a new reactor
2. Providing a practical tool to configure the controller in which reactor stability can be guaranteed

The base case model will initially be examined with respect to its dynamical behaviour in the absence of a controller. Subsequently the control system is implemented in the model. The control method can be subdivided into the proportional and the proportional-integral control action. Although the derivative control action is widely used in the process control, this type of control is not suitable for the use in particular bifurcation software packages and will therefore not be considered. Three different control methods have been selected and investigated on its influence on the dynamical behaviour. The system can be controlled adjusting the temperature of the cooling fluid, adjusting the coolant flowrate or the throughput.
The next step is to analyse every situation for sensitivity of relevant parameters respectively

1. The cooling capacity UA
2. The proportional gain K_c
3. The integral time τ_I
4. The presumed delay τ_d

For as well the control of cooling temperature as coolant flowrate and throughput, the following will be presented:

1. Mathematical system will be given
2. Reactor designer stability maps will be given
3. Reactor controller stability maps will be given (to monitor the improvement of the base case due to process control)
4. Conclusion concerning the being of the base case (this being changes as a result of applied process control)

Chapter VIII

8 PRELIMINARY CONSIDERATION CONTROLLABILITY

8.1 Controlling the coolant temperature

In paragraph 5.2 the default controller correlation has been given. In case of coolant temperature control the controller correlation becomes:

$$T_{cool} = T_{cool,sp} + K_c\left(T_{sp} - T\right) \tag{41}$$

This mathematical description is easy to comprehend. If the process is disturbed and the reactor temperature should for instance rise, it is obvious that the coolant temperature has to be decrease to return the reactor temperature to its steady state (set point) value. The magnitude of the proportional gain amounts to $K_c \approx 1$ [-].

8.2 Controlling the coolant flowrate

In case of flowrate control, a reactor temperature increase has the consequence that the coolant flowrate has to be enlarged to increase the heat transfer from the reactor. Therefore, to maintain positive K_c values, the controller equation becomes:

$$\Phi_{V,cool} = \Phi_{V,cool,sp} - K_c\left(T_{sp} - T\right) \tag{42}$$

The proportional gain K_c in equation 42 is not dimensionless as in equation 41. The magnitude of the proportional gain value states $K_c \approx 0.0001$ [$m^3\ s^{-1}\ K^{-1}$]

8.3 Controlling the throughput

In case of throughput control, there are two possibilities available: Suppose the reactor temperature increases, on the one hand increasing the throughput means quenching with the cold feed, but on the other hand increasing the reactant concentration in which subsequently more heat will be produced due to the increased conversion.

$$\Phi_V = \Phi_{V,sp} + K_c\left(T_{sp} - T\right) \tag{43a}$$

$$\Phi_V = \Phi_{V,sp} - K_c\left(T_{sp} - T\right) \tag{43b}$$

Both controller equations are possible. Nevertheless, it is uncertain which one can provide stability. If the proportional gain is too large, the reaction can run away or extinguishes dependent on the K_c sign. This will be clear in the following chapter.
The proportional gain value in equation 43 roughly is $K_c \approx 0.001$ [$m^3\ s^{-1}\ K^{-1}$] which is slightly larger than in case of coolant flowrate control.

Chapter IX

9 PROPORTIONAL CONTROL

In this section, the effect of the proportional controller on the stability of the cooled CISTR with irreversible exothermic reaction is studied.

9.1 Reactor designer stability maps

The following stability maps will be examined:

Table 13 Stability maps P-controlled coolant temperature.

Stability map	Reference
T versus T_{cool}	Figure 23
T versus UA	Figure 24

Table 14 Stability maps P-controlled coolant flowrate.

Stability map	$T_{cool,0}$ = 303 [K]	$T_{cool,0}$ = 400 [K]	$T_{cool,0}$ = 435 [K]
T versus $\Phi_{V,cool}$	Figure 28 0 – 0.005 [m^3 s^{-1}]	Figure 41 0 – 0.02 [m^3 s^{-1}]	Figure 42 0 – 0.1 [m^3 s^{-1}]
T versus T_{cool}	Figure 43	-	-
T versus UA	Figure 44	Figure 45	Figure 49

Table 15 Stability maps P-controlled throughput.

Stability map	Reference
T versus Φ_V ($K_c \geq 0$)	Figure 50
T versus Φ_V ($K_c \leq 0$)	Figure 54
T versus UA	Figure 67

9.1.1 Controlling the coolant temperature

In the industry, the concept of *master-slave* control is often applied[74 71 55 59]. The main and deciding process variable (master) is often the yield of the reaction. Although eventually this quantity is deciding for the complete process, the determination of the magnitude is often very dilatory and therefore in general not the active manipulated controller variable, which preserves stability. Mostly, a CISTR with exothermic reaction is controlled through adjusting the degree of cooling (slave) which response is considerably faster. The coolant temperature in heat balance 3 expresses together with the cooling capacity the extent of cooling. The value of the cooling capacity UA is mostly fixed and determined during the design of the process. Commonly, cooling is realised through the application of cooling pipes or a cooling jacket. The coolant is pumped into the cooling device in which heat is transferred from the reactor content through the wall towards the coolant. To describe the temperature of the cooling fluid accurate, information is needed about the flowrate pattern and mixing behaviour, which in many cases is not available or incomplete. According to Ratto *et.al.*[64] and Uppal *et.al.*[75] the assumption is made that the coolant temperature is constant and can be constrained virtually instantaneously. This assumption is permitted in case the coolant flowrate is considerably large i.e. the average residence time of a coolant particle $\tau_{coolant}$ is rather short compared to the average residence time τ_R of a particle in the CISTR:

$$\tau_R >> \tau_{coolant} \tag{44}$$

1. Reactor temperature versus cooling temperature

Mathematical model

Equations 2, 3 and 41 mathematically describe the proportional controlled base case in which the coolant temperature is manipulated.

$$V_R \frac{d[A]}{dt} = \Phi_V \left([A]_0 - [A]\right) - V_R k_0 e^{-E_{act}/RT}[A] \tag{2}$$

$$\rho C_P V_R \frac{dT}{dt} = \rho C_P \Phi_V \left(T_0 - T\right) + \left(-\Delta H_R\right) V_R k_0 e^{-E_{act}/RT}[A] - UA\left(T - T_{cool}\right) \tag{3}$$

$$T_{cool} = T_{cool,sp} + K_c \left(T_{sp} - T\right) \tag{41}$$

A designer stability map is created (Figure 23) in which the coolant temperature (set point) and the proportional gain are the active LOCBIF bifurcation parameters.

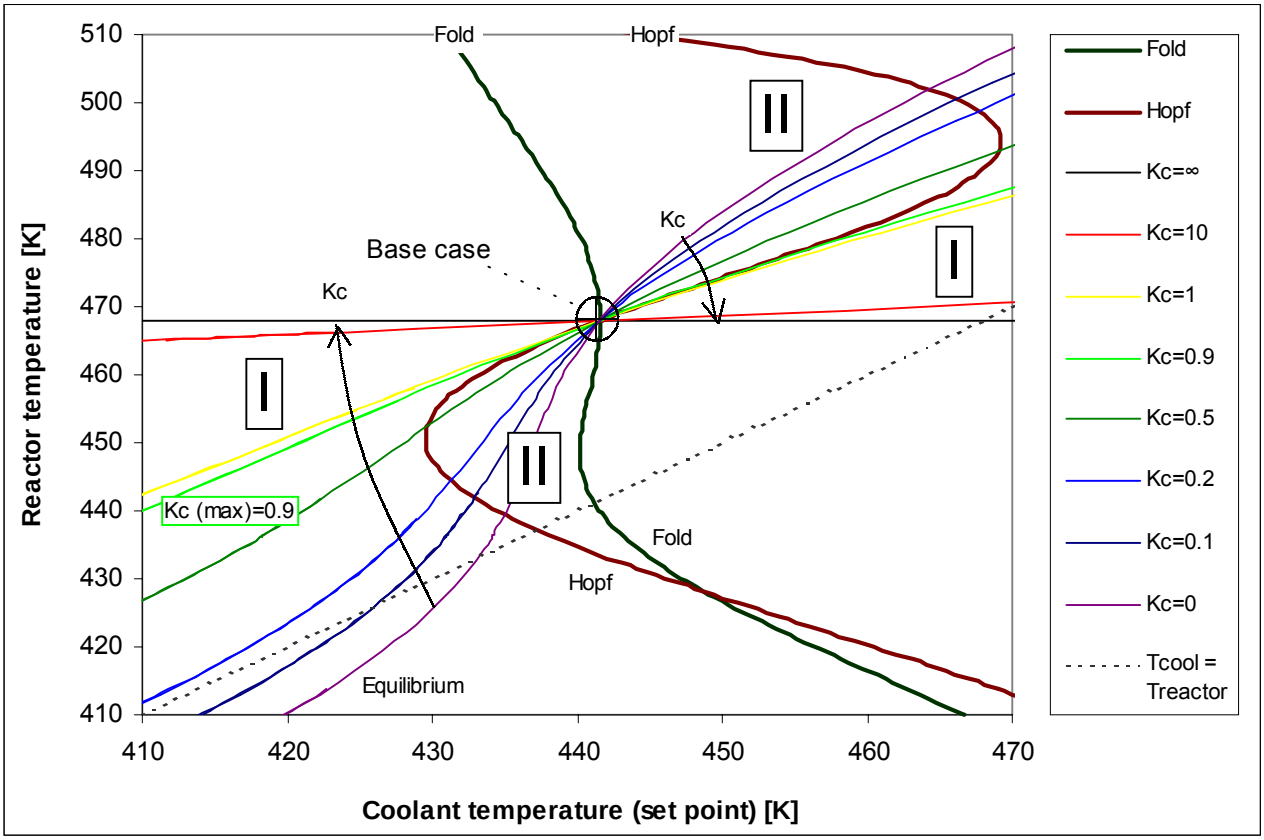

Figure 23 Reactor designer stability map of the coolant temperature proportional controlled base case model. The steady state reactor temperature is plotted as function of the coolant temperature (set point) in which the gain value K_c is varied. If $K_c > 0.9$ no limit cycles will exhibit. The LOCBIF source LOCBIF rhs 3 is included in Appendix 7.

Discussion of the reactor designer stability map:

- In case the proportional gain is increased, the equilibrium curves rotate clockwise and switch from region II towards stable region I in case $K_c > 0.9$.
- Considered the base case coolant temperature, multiplicity does not occur over the examined range ($410 \leq T_{cool} < 470$ [K]), which means that static instability will not take place, merely dynamical instability i.e. the occurrence of limit cycles.

- In Figure 23 the dotted line $T=T_{cool}$ has been drawn which indicating the lowest possible reactor temperature.
- Also previous stability map (Figure 19) demonstrated that in case T_{cool} > 469 [K] no limit cycles can appear. With regard to stability map (Figure 23) no limit cycles will emerge in case T_{cool} < 430 [K] and T_{cool} > 469 [K] which are the acquired Hopf maximum values.

Table 16 Hopf maximum of Figure 23.

Variable	Value	Dimension
K_c (max)	0.9	[-]
T_{cool} (min)	430	[K]
T_{cool} (max)	469	[K]

2. Reactor temperature versus cooling capacity

In this section, it will be demonstrated that increasing cooling capacity improves the stability of the process.

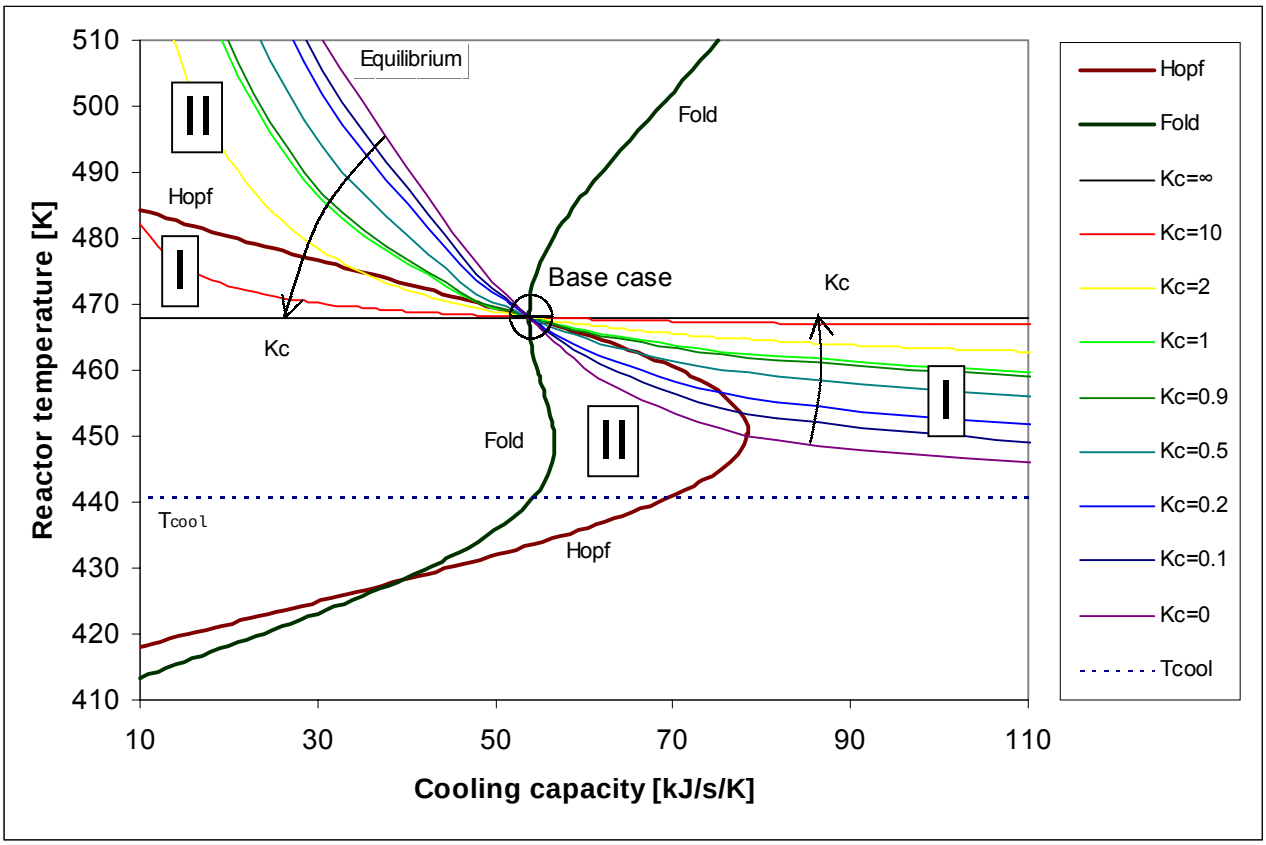

Figure 24 Reactor designer stability map of the proportional controlled base case model. The steady state reactor temperature is plotted as function of the cooling capacity in which the gain value K_c is varied. The base case shifts from region II to stable region I for K_c > 0.9.

Discussion of the reactor designer stability map:

- The subsequent stability map Figure 24, with active LOCBIF bifurcation parameters: UA and K_c, confirm that if UA > 78 [kJ s^{-1} K^{-1}] in view of the base case coolant temperature T_{cool} = 441 [K], absolutely no limit cycles will occur. Compare this fact with the results retrieved from stability map Figure 19 in which for any arbitrarily T_{cool} a cooling capacity UA > 105 [kJ s^{-1} K^{-1}] will prevent limit cycles completely.
- A significantly large cooling capacity improves the overall stability of the process. This has been confirmed by Westerterp *et.al.*[80] (§4.6).
- Figure 23 and Figure 24 confirm that no limit cycles will occur if K_c > 0.9 (Figure 27). Nevertheless, too large UA forces the reactor temperature towards the coolant temperature

because the heat removal becomes significant. Therefore, a considerable cooling capacity combined with a suitable proportional gain can maintain sufficient stability. In this report it is not addressed whether or not a considerable cooling capacity is practically achievable. However, if the implementation of a suitable controller is conceivable, less cooling area A is needed which can yield a cost reduction. The choice of UA and K_c is up to the reactor designer and controller. Appendix 3 provides information about the required cooling pipes in case this cooling device is applied.

- For the reactor designer, the stability map shows for one particular K_c in what extent the process can be changed and what the consequences are for the stability. Take for instance K_c = 1 which means stability. If the cooling capacity is decreased to for example 40 [kJ s^{-1} K^{-1}] then the process is located in a dynamical unstable region.

Orbit curves

Orbit curves have been made for three increasing proportional gain values. Figure 25 shows that a relative small K_c value hardly has any effect on the appearing limit cycles. Increasing K_c slightly dims the overshoot (Figure 26) and finally increasing K_c will eradicate the limit cycles (Figure 27). The orbit simulations demonstrated that actually for a K_c = 0.9 the limit cycle is converted into a spiral point (consistent with Figure 27) which means stability.

Table 17 Data regarding orbit curves for increasing K_c.

Proportional gain K_c [-]	Average reactor temperature T [K]	Average conversion ζ [-]	Figure
0.5	467	0.680	Figure 25
0.8	467	0.686	Figure 26
0.9	468	0.688	Figure 27

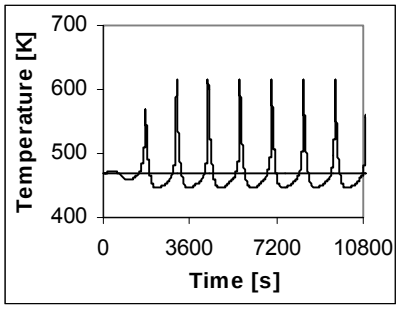

Figure 25 Small K_c values do not affect the emerging limit cycles tremendously compared to not controlled base case according Figure 22.

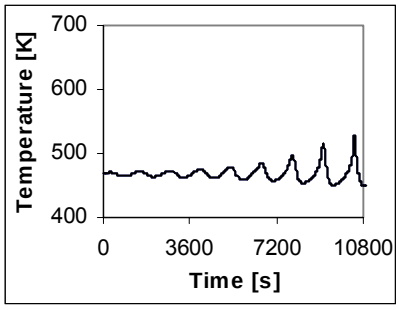

Figure 26 The proportional gain is not robust enough in which limit cycles still emerge.

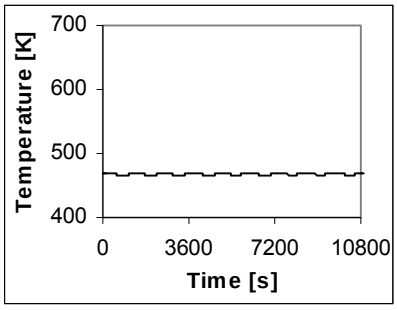

Figure 27 K_c = 0.9 determined from Figure 23 can hardly eliminate limit cycles.

Moreover, the average conversion (Table 17) is slightly increased in case K_c rises. Figure 25 with the strongest limit cycles has a conversion approximately 1% lesser than the conversion of Figure 27.It is not clear if this is the result of inaccuracy of the LOCBIF simulations or this is due to the strong oscillations.

Summarising

A considerable large cooling capacity can contribute to the decline of limit cycles. In case UA > 78 [kJ s^{-1} K^{-1}] no limit cycles will emerge at all for the base case. Nevertheless, very large UA values push the reactor temperature towards the coolant temperature. Therefore, a considerable cooling capacity combined with a suitable proportional gain is required to preserve a stable system.
A proportional controller, which affects the coolant temperature, assuming that the coolant temperature can be instantaneously constrained, can easily eliminate limit cycles. In this particular situation, it counts that the height of K_c determines the stability. The stability maps provide the information that for the specific base case situation a proportional gain: K_c > 0.9 is suitable to eliminate the self-sustained oscillations. For any other cooling capacity a K_c = 5.7 is enough for an absolute stable base case.

9.1.2 Controlling the coolant flowrate

In many industrial processes, reactors in which exothermic chemical reactions take place are cooled continuously. The produced heat is removed from the reactor through for instance a cooling jacket or through a composition of cooling pipes. This section is concerned with the question if limit cycles can be prevented by applying a controller, which manipulates the cooling fluid flowrate. Although various procedures exist in which a reactor can be cooled e.g. cooling water, pressurised steam, reflux vaporiser etc., the objective of this report is to study the fundamental principles of the cooling effect on the CISTR stability, not the practical applied method. This implies that matters as ΔH_{vap}, are not concerned with if for instance heated water under pressure is assumed as cooling fluid.
The coolant heat balance 12, which describes the coolant flowrate as function of the coolant temperature will be implemented in the existing mathematical base case model. The use of the cooling differential equation is justified if the coolant temperature is considered constant in the cooling device. If a liquid with no vapour is used in combination with a recycle stream, the latter assumption is justified. A major recycle stream means that a cooling fluid particle, which carries transferred heat, can be transported and replaced by the cold coolant feed in a very short time. If the recycle stream is large enough, a less significant temperature profile is then acquired, which has the advantage that the temperature of the coolant can be assumed equal. Stephanopoulos[74] reports that a recycle stream improves the heat transfer in general. Furthermore, according to Shinskey[71] the dynamical system response is improved, after the process controller has intervened. This is due to the faster coolant substitution i.e. less delay. Additionally Roffel[68] argued that the use of a recycle stream is practically indispensable. This is because if the coolant velocity becomes too small, heavy fouling can emerge. (In Appendix 5 more about the size of the recycle stream).
The logarithmic temperature mean (expression 17) could be introduced to improve the model accuracy. Despite this improvement, ΔT_{log} will not be considered in this report due to the implicit character of equation 17 which is not solvable in the bifurcation package LOCBIF.

Mathematical model

The base case mass and heat balance and the coolant temperature balance represented by respectively equations 2, 3, 12 and 42 describe the proportional controlled base case according:

$$V_R \frac{d[A]}{dt} = \Phi_V \left([A]_0 - [A]\right) - V_R k_0 e^{-E_{act}/RT}[A] \tag{2}$$

$$\rho C_P V_R \frac{dT}{dt} = \rho C_P \Phi_V \left(T_0 - T\right) + \left(-\Delta H_R\right) V_R k_0 e^{-E_{act}/RT}[A] - UA\left(T - T_{cool}\right) \tag{3}$$

$$\rho_{cool} C_{P,cool} V_{cool} \frac{dT_{cool}}{dt} = \rho_{cool} C_{P,cool} \Phi_{V,cool} \left(T_{cool,0} - T_{cool}\right) + UA(T - T_{cool}) \tag{12}$$

$$\Phi_{V,cool} = \Phi_{V,cool,sp} - K_c \left(T_{sp} - T\right) \tag{42}$$

Using the base case values printed in Table 9 the steady state coolant flowrate (set point) can be calculated with correlations 13 and 14.
Moreover, there is one degree of freedom in the system model which is the inlet coolant temperature $T_{cool,0}$. To acquire knowledge regarding the influence of the inlet coolant temperature, three distinct values have been chosen: (Table 18). These values have been chosen arbitrary and vary from ‘cold’ to ‘average’ and ‘high’ in which for the latter no multiplicity is possible.
Several reactor designer stability maps can provide useful information about the stability of this case. The active LOCBIF parameters are: the coolant flowrate (set point) and the proportional gain K_c.
It is however, possible that the controller calculates negative coolant flowrate values, which in fact means that heat is generated (perpetual mobile). Therefore, restrictions have been implemented In the LOCBIF models ($\Phi_{V,cool} \geq 0$). Practically this should mean that the coolant throughput supply is halted temporarily.

Table 18 Coolant flowrate.

$T_{cool,0}$ [K]	$\Phi_{V,cool}$ [m^3 s^{-1}]
303	0.00241
400	0.00811
435	0.05540

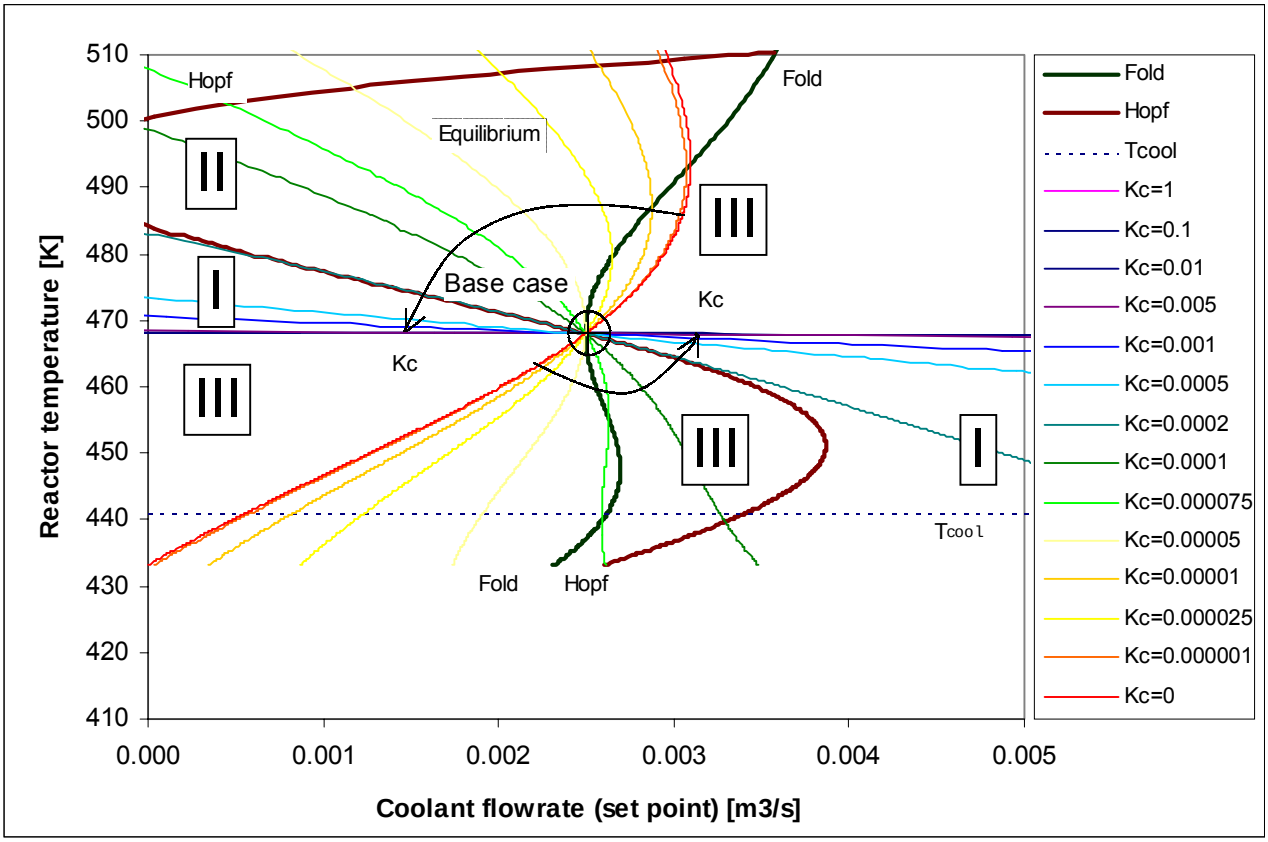

Figure 28 Reactor designer stability map. Proportional controlled coolant flowrate. $T_{cool,0}$ = 303 [K]. Active LOCBIF bifurcation parameters: $\Phi_{V,cool}$ (set point). K_c > 0.00025 [m^3 s^{-1} K^{-1}] (Hopf maximum) means more stability. Fold maximum K_c > 0.000067 [m^3 s^{-1} K^{-1}].

Discussion of the reactor designer stability map:

- The equilibrium curves in stability map (Figure 28) rotate counter clockwise if the proportional gain is increased. The existence of multiplicity in the stability map (Figure 28) is conspicuous.
- In case K_c > 0.000067 [m^3 s^{-1} K^{-1}] i.e. Fold maximum, the hazard for multiplicity near the base case situation is reduced. Nevertheless, still extinction is possible although Figure 28 does not provide that information.
- If K_c > 0.00025 [m^3 s^{-1} K^{-1}] i.e. Hopf maximum, the equilibrium curves traverse region I instead of region II which implies that stability is possible. Through the following orbit curves, this will be demonstrated.
- The marking process i.e. region I, II and III in Figure 28 must be interpreted with caution. Because extinction is always possible in the system is large disturbed. Then, region I indicates actually a region III. In case a region is indicated as region I this implies that stability is possible, even if the process it slightly disturbed, however it must be considered with caution.

Orbit curves

Orbit curves have been created for increasing K_c values for both the reactor temperature and the coolant flowrate. Concerning the first orbit curve (Figure 29) no controller action is applied and a strong limit cycle system should be expected due to the fast temperature rise (like Figure 22). Nevertheless, due to the existence of multiplicity, the reactor temperature is in fact attracted towards a higher steady state value after the first peak and the limit cycles disappear. Figure 32 is the accompanying coolant flow flowrate curve, which shows that the coolant flowrate remains at the same value, which is obvious because the controller does not intervene.

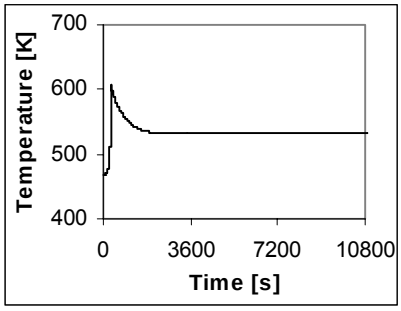

Figure 29 **$K_c = 0$** [$m^3 s^{-1} K^{-1}$]. $\Delta T = 0$ [K] transition to higher steady state.

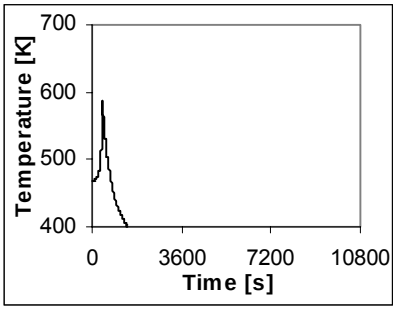

Figure 30 **$K_c = 0.00006$** [$m^3 s^{-1} K^{-1}$] derived from equation 13. $\Delta T = 0$ [K] extinction.

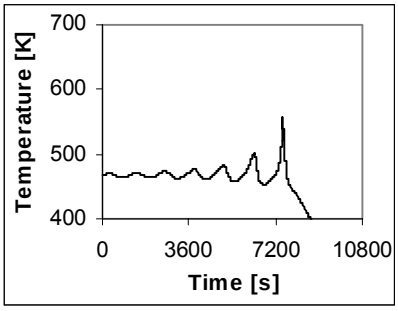

Figure 31 **$K_c = 0.00019$** [$m^3 s^{-1} K^{-1}$]. $\Delta T = 0$ [K]. Instability and extinction.

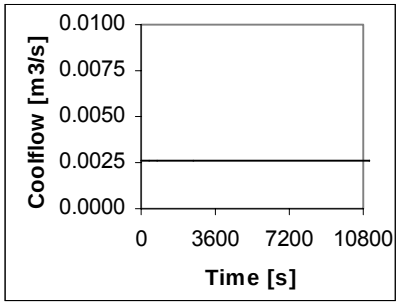

Figure 32 **$K_c = 0$** [$m^3 s^{-1} K^{-1}$]. $\Delta T = 0$ [K] Coolant flow is not adjusted.

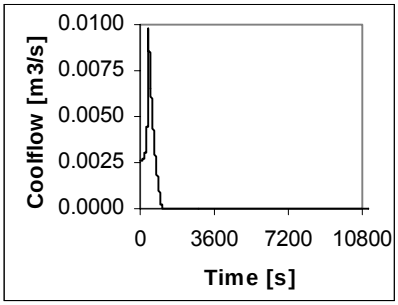

Figure 33 **$K_c = 0.00006$** [$m^3 s^{-1} K^{-1}$] derived from equation 13. $\Delta T = 0$ [K] extinction.

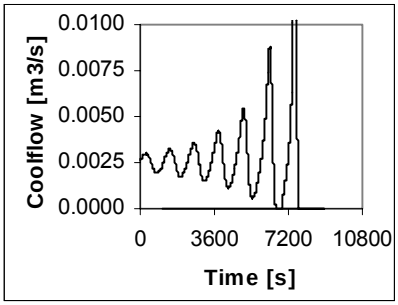

Figure 34 **$K_c = 0.00019$** [$m^3 s^{-1} K^{-1}$]. $\Delta T = 0$ [K]. Instability and extinction.

Using equation 13 a first approximation can be made to determine the proportional gain: $K_c = 0.00006$ [$m^3 s^{-1} K^{-1}$]. Figure 30 clearly shows that with this K_c the proportional controller is not robust enough to restrict the evolving limit cycles. After the first peak, which in fact is a limit cycle, transition towards another steady state is inevitable causing i.e. extinction. In the stability map Figure 28, for this particular K_c value, the multiple steady states are visible. The latter can be explained because the flowrate manipulation is not accurate. The initial temperature rise has to be repressed through increasing the coolant flowrate. This has the consequence that the reactor temperature drops distinguished. To halt the temperature decline, the proportional gain of Figure 30 and Figure 33 is not robust enough resulting in extinction i.e. too much heat has removed from the system. If K_c is increased, Figure 31 shows that still the proportional gain is not powerful enough to suppress the self-sustained oscillations (Figure 34). After approximately two hours, the overshoot is considerably enlarged and the temperature is again attracted to a lower steady state i.e. extinction towards the feed temperature. Again increasing K_c means stability, nonetheless small temperature limit cycles emerge and considerable for the manipulated coolant flowrate (Figure 35). If for the same K_c value a disturbance is constrained, due to the large overshoot extinction is inevitable (Figure 36 and Figure 39).

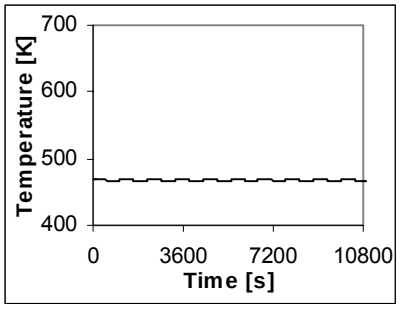

Figure 35 **$K_c = 0.0002$** [$m^3 s^{-1} K^{-1}$]. $\Delta T = 0$ [K]. Limit cycles.

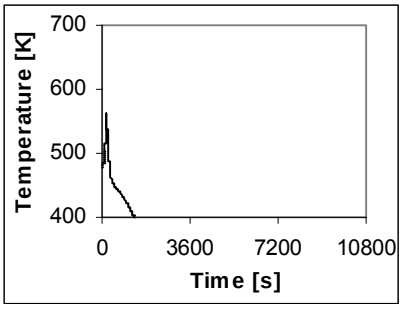

Figure 36 **$K_c = 0.0002$** [$m^3 s^{-1} K^{-1}$]. $\Delta T = +10$ [K]. Extinction $T \rightarrow T_0$.

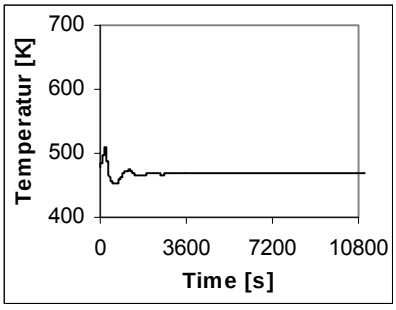

Figure 37 **$K_c = 0.00025$** [$m^3 s^{-1} K^{-1}$]. $\Delta T = +10$ [K]. Spiral point.

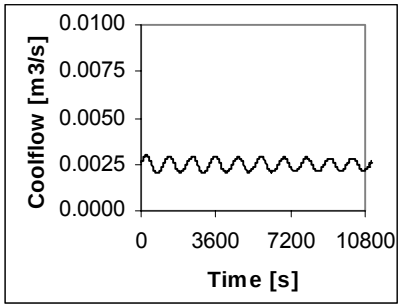

Figure 38 $K_c = 0.0002$ [$m^3\ s^{-1}\ K^{-1}$] $\Delta T = 0$ [K]. Limit cycles.

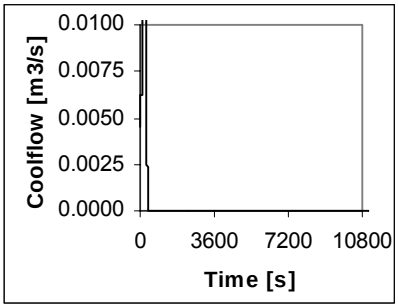

Figure 39 $K_c = 0.0002$ [$m^3\ s^{-1}\ K^{-1}$]. $\Delta T = +10$ [K]. Extinction T $\rightarrow T_0$.

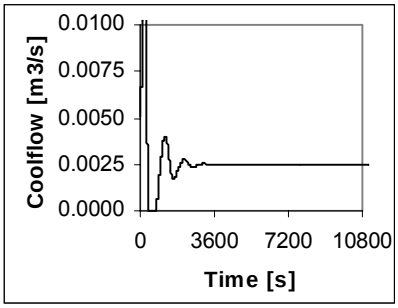

Figure 40 $K_c = 0.00025$ [$m^3\ s^{-1}\ K^{-1}$]. $\Delta T = +10$ [K]. Spiral point.

A proportional gain larger than the Hopf maximum accomplishes a stable system after a step disturbance (Figure 37). The controlled coolant flowrate varies however extraordinary (Figure 40) and besides has to be halted for a particular period. Proportional controlling the coolant flowrate can provide a stable process. However, the severe coolant flowrate variation is disputed. Consider a recycle stream which is applied with a recycle flow which is 10 times the throughput (Appendix 5), the maximum fluid velocity after $t \approx 4$ [min] (Figure 40) becomes v_{cool} =1.2 [m s^{-1}] which is permitted.

The next stability map (Figure 41) with a less cooler inlet coolant temperature $T_{cool,0}$ = 400 [K] is basically similar to the Figure 28. The main difference is the range on the abscissa, which is obvious because in case the coolant temperature is higher, the temperature difference is smaller; consequently, more coolant throughput is required to transfer the surplus heat.

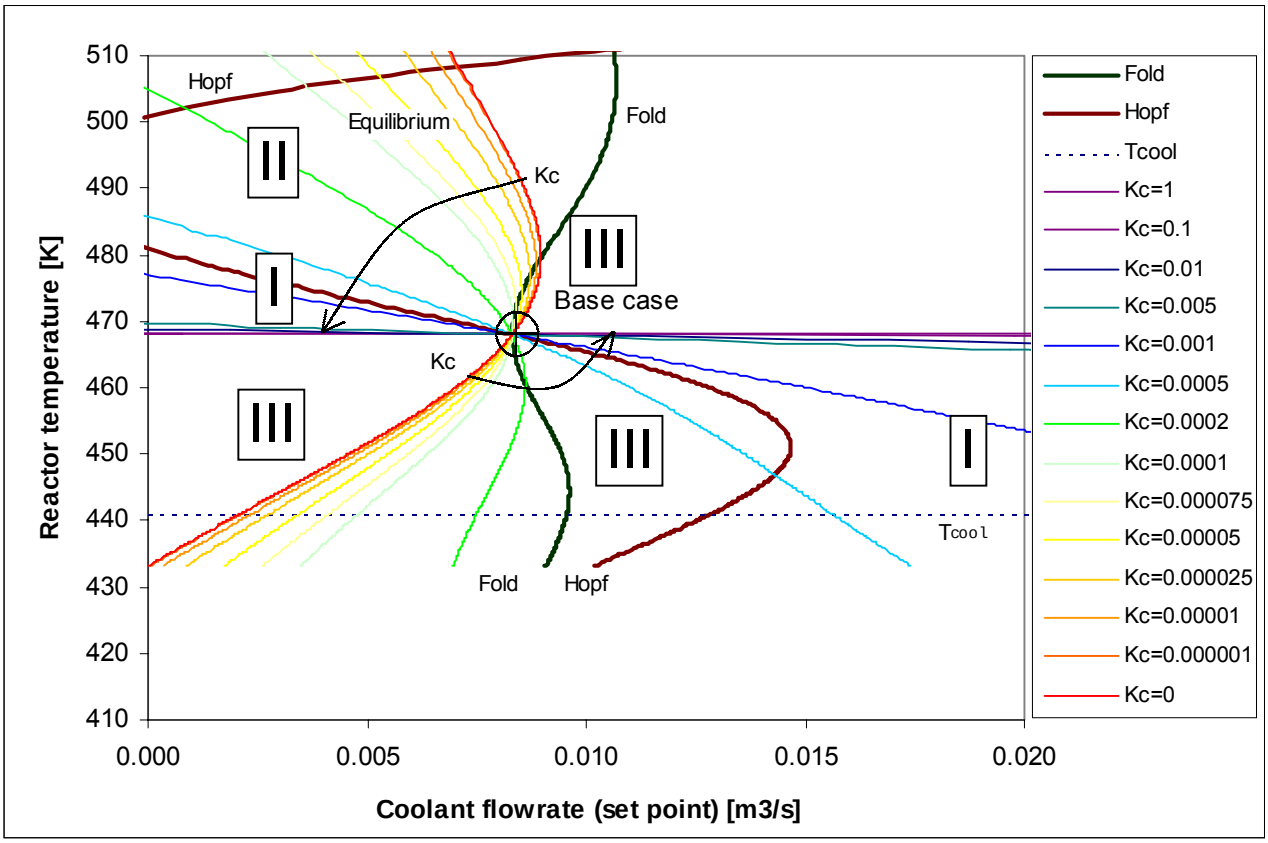

Figure 41 Reactor designer stability map. Proportional control on coolant flowrate. $T_{cool,0}$ = 400 [K]. Active parameters: $\Phi_{V,cool}$ (set point) and K_c. Hopf maximum $K_c > 0.00078$ [$m^3\ s^{-1}\ K^{-1}$]. Fold maximum $K_c > 0.00026$ [$m^3\ s^{-1}\ K^{-1}$].

Discussion of the reactor designer stability map:

- The equilibrium curves in Figure 41 rotate likewise counter clockwise if the proportional gain is increased. The existence of multiplicity in Figure 28 is evident.
- In case $K_c > 0.00026$ [m^3 s^{-1} K^{-1}] i.e. Fold maximum, multiplicity is less dangerous because the controller cooling is stronger and prevent too large overshoot caused by the limit dynamical instability. If $K_c > 0.00078$ [m^3 s^{-1} K^{-1}] i.e. Hopf maximum, region II in which limit cycles emerge, is excluded. The gain is apparently large enough to restrict the limit cycles. Nevertheless, large external disturbances can always cause the transition towards the lower steady state.
- The equilibrium curves intersect regions I and III. Once again, region I implies that the controller can stabilise the process accurately, although extinction remains thinkable possibility in case of large perturbations. Region III refers to extinction.

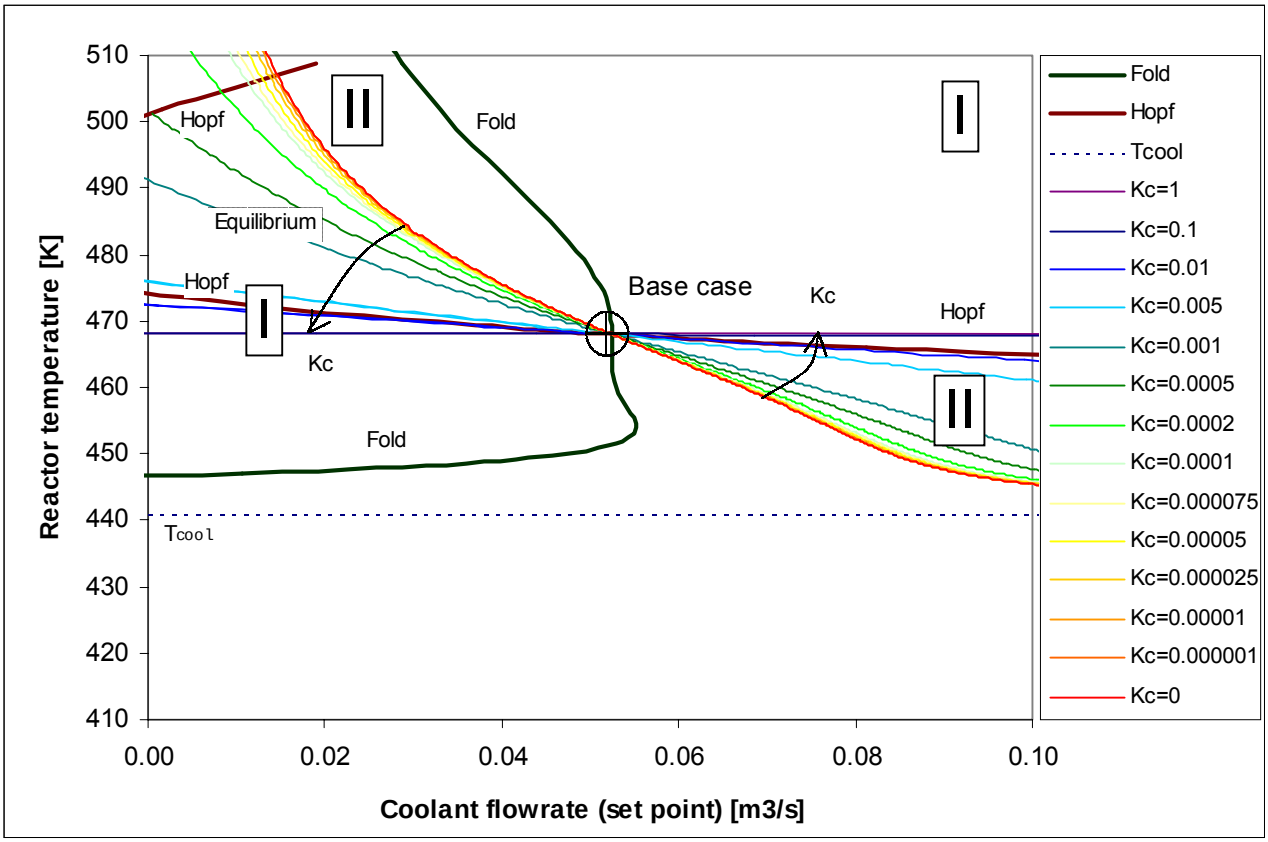

Figure 42 Reactor designer stability map. Proportional control on coolant flowrate. $T_{cool,0}$ = 435 [K]. Active bifurcation parameters: $\Phi_{V,cool}$ (set point) and K_c. Hopf maximum $K_c > 0.012$ [m^3 s^{-1} K^{-1}]. No multiplicity is involed.

Discussion of the reactor designer stability map:

- If the inlet coolant temperature is enlarged to $T_{cool,0}$ = 435 [K], multiplicity near the base case value which has formerly been found in (Figure 19), is not an issue according to Figure 42. Nevertheless, due to the relatively small temperature difference between the reactor temperature and the coolant temperature, a considerable coolant throughput is needed to cool the reactor i.e. about 20 times larger than Figure 28 $T_{cool,0}$ = 303 [K]. Despite the advantage that multiplicity is less prominent, too large fluid velocity in the cooling apparatus can be an impediment.
- Differential equation 12 describes the dynamical behaviour of the coolant temperature in which the assumption has been made that the temperature difference between the coolant inlet and exit is negligible. This assumption is merely acceptable if a recycle stream is involved in which the recycle flow is several times the throughput. If due to the minor temperature difference a large coolant throughput is needed and additionally a substantial recycle stream is required, the coolant velocity can practically be too large.
- Finally, LOCBIF noticed the Hopf maximum K_c = 0.012 [m^3 s^{-1} K^{-1}], which means that larger values involve stability and no hazard of extinction is possible because no multiplicity is involved.

Table 19 Proportional gain values P-control coolant flowrate.

Description	$T_{cool,0}$ = 303 [K]	$T_{cool,0}$ = 400 [K]	$T_{cool,0}$ = 435 [K]
Fold maximum	K_c > 0.00067 [m^3 s^{-1} K^{-1}]	K_c > 0.00026 [m^3 s^{-1} K^{-1}]	Not existing: no multiplicity
Hopf maximum	K_c > 0.00025 [m^3 s^{-1} K^{-1}]	K_c > 0.00078 [m^3 s^{-1} K^{-1}]	K_c > 0.012 [m^3 s^{-1} K^{-1}]

Summarising

On the one hand, a low inlet coolant temperature has the advantage that superfluous heat can be withdrawn from the reactor very easy and that coolant fluid velocities are not too large. The disadvantage is that multiplicity in case of improper proportional control can be inevitable, in particular, if the process is considerable disturbed. On the other hand, a rather high inlet coolant temperature has the advantage that multiplicity is less dangerous, but in combination with a recycle stream, too large coolant fluid velocities can be a hindrance. Therefore, the choice of reactor designer for $T_{cool,0}$, Depends greatly on the safety of the process and in second place on economic aspects e.g. reproduction of heat.

Comparison coolant temperature and coolant flowrate control (T_0=303 K)

In previous paragraph, the stability map (Figure 23) for coolant temperature control has been drawn with active parameters T_{cool} and K_c. In this chapter, in which coolant flowrate is concerned with, the same stability map is drawn to investigate the effect of the introduction of the extra differential equation 36. The implementation implies that multiplicity is probable. The latter is not the case in case the coolant temperature proportional is controlled.

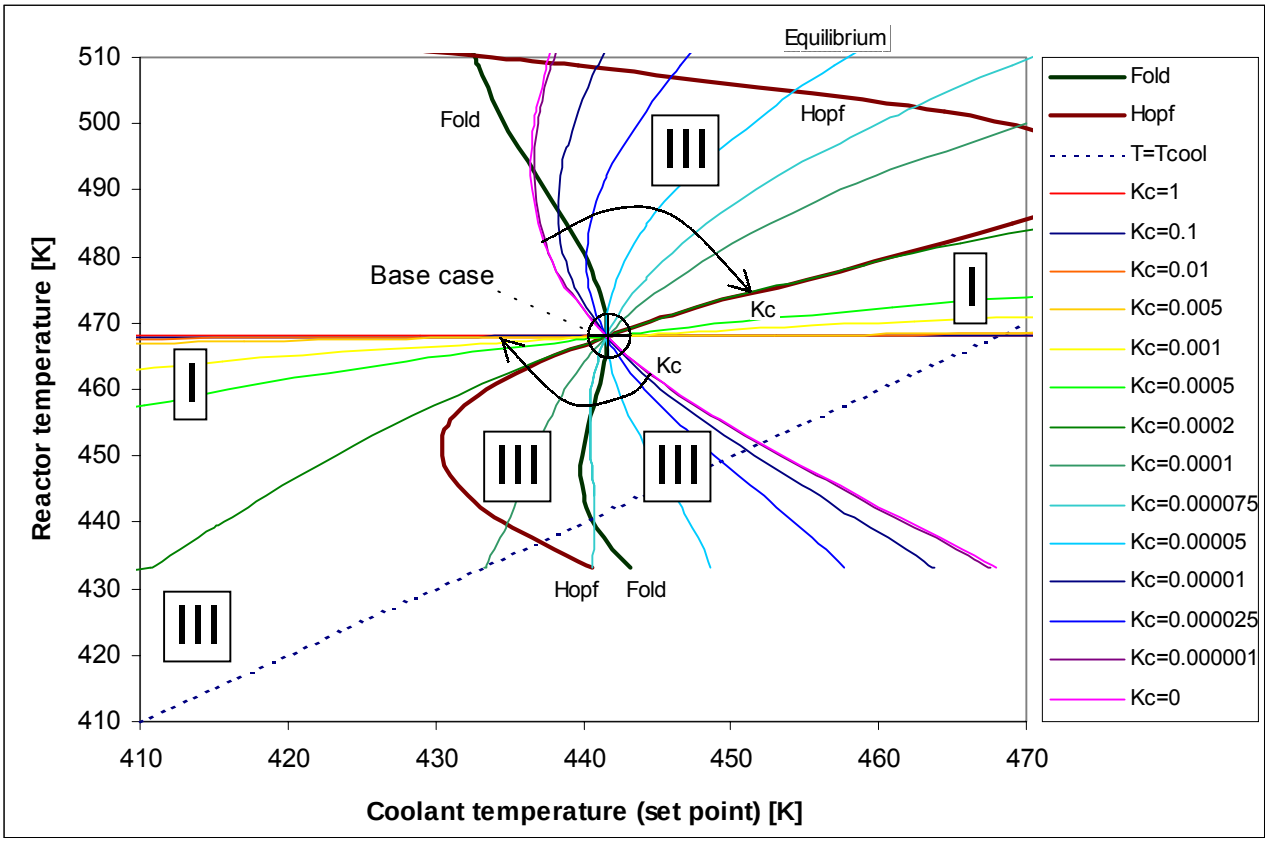

Figure 43 Reactor designer stability map. Proportional control on coolant flowrate. $T_{cool,0}$ = 303 [K]. Active LOCBIF bifurcation parameters: T_{cool} (set point) and K_c. Hopf maximum K_c > 0.00025 [m^3 s^{-1} K^{-1}]. Fold maximum K_c > 0.000079 [m^3 s^{-1} K^{-1}]. Compare this stability map with Figure 19. The LOCBIF source LOCBIF rhs 5 is included in Appendix 7.

Discussion of the reactor designer stability map:

- Figure 43 show clearly that for $K_c < 0.000079$ [m^3 s^{-1} K^{-1}] more steady state solutions are possible.
- The main difference between Figure 23 and Figure 43 is the shape or trajectory of the drawn equilibrium curves. In case of coolant temperature control, increasing the proportional gain causes the equilibrium curves to move towards the stable region and prevents the occurrence of limit cycles. In case of coolant flowrate control, the risk for multiplicity is always a point of concern, despite a dynamically stable behaviour. The stable and unstable regions in Figure 23 are very clear in contrast to Figure 43 in which, due to multiplicity, these regions are more complicated to interpret.
- According to Figure 23 the (Hopf) maximum T_{cool} = 469 [K]. Beyond this coolant temperature, instability is impossible. According Figure 43 this maximum is considerable higher: T_{cool} = 477 [K]. Again, this can be explained through the fact that, in case of coolant temperature control multiplicity can cause instability, which is not possible if the coolant temperature is controlled i.e. only limit cycles.

Reactor temperature versus coolant capacity (T_0=303 K)

In previous chapters, it has been found that the cooling capacity, in combination with a suitable proportional gain, has a stabilising effect on the dynamical behaviour of the concerned base case process. The following stability maps, in which the coolant inlet temperature is varied, respectively Figure 44, Figure 45 and Figure 49 will be examined.

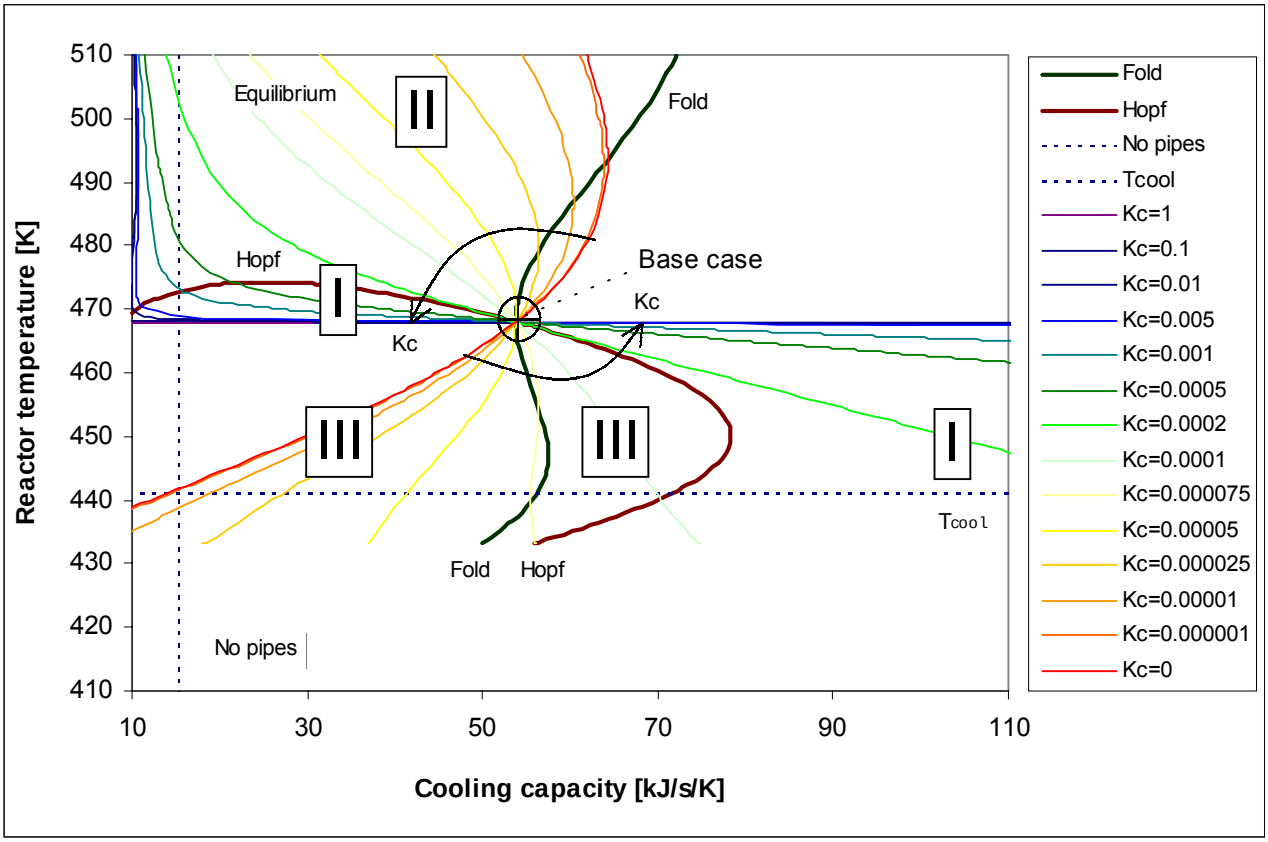

Figure 44 Reactor designertability map. Proportional control on coolant flowrate. $T_{cool,0}$ = 303 [K]. Active parameters: UA and K_c. Hopf maximum K_c > 0.00025 [m^3 s^{-1} K^{-1}]. Fold maximum K_c > 0.000079 [m^3 s^{-1} K^{-1}]. UA_{max} = 78 [kJ s^{-1} K^{-1}].

Discussion of the reactor designer stability map:

- In Figure 44 the equilibrium curves rotate counter clockwise if the proportional gain is increased. In this stability map the existence of multiplicity is visible.
- In case $K_c > 0.00025$ [m^3 s^{-1} K^{-1}] a dynamically stable system is possible. Nevertheless, extinction is still probable if the appropriate proportional gain is not used.
- Suppose that the reactor designer decides to change the set point reactor temperature, through following the equilibrium curves the consequences regarding the stability can be determined.
- In case UA > 79 [kJ s^{-1} K^{-1}] stability is more certain, although in case of large disturbances, extinction still is a risk, besides the disadvantage of the economical aspects of the application of large cooling capacity. A suitable combination of UA and K_c is required.

Table 20 Survey stability P-control coolant flowrate. $T_{cool,0}$ = 303 [K].

Cooling capacity [kJ s^{-1} K^{-1}]	Dynamical behaviour	Explanation
0 ≤ UA < 15	Not existing	UA of the reactor > 0
15 ≤ UA < 65	Dangerous region	Multiplicity can disturb the stability
65 ≤ UA < 78	Moderate safe region	Stability if $K_c > K_c$ (Hopf)
UA > 78	Stable region, no limit cycles	Stability if $K_c > K_c$ (Hopf)

Reactor temperature versus cooling capacity (T_0=400 K)

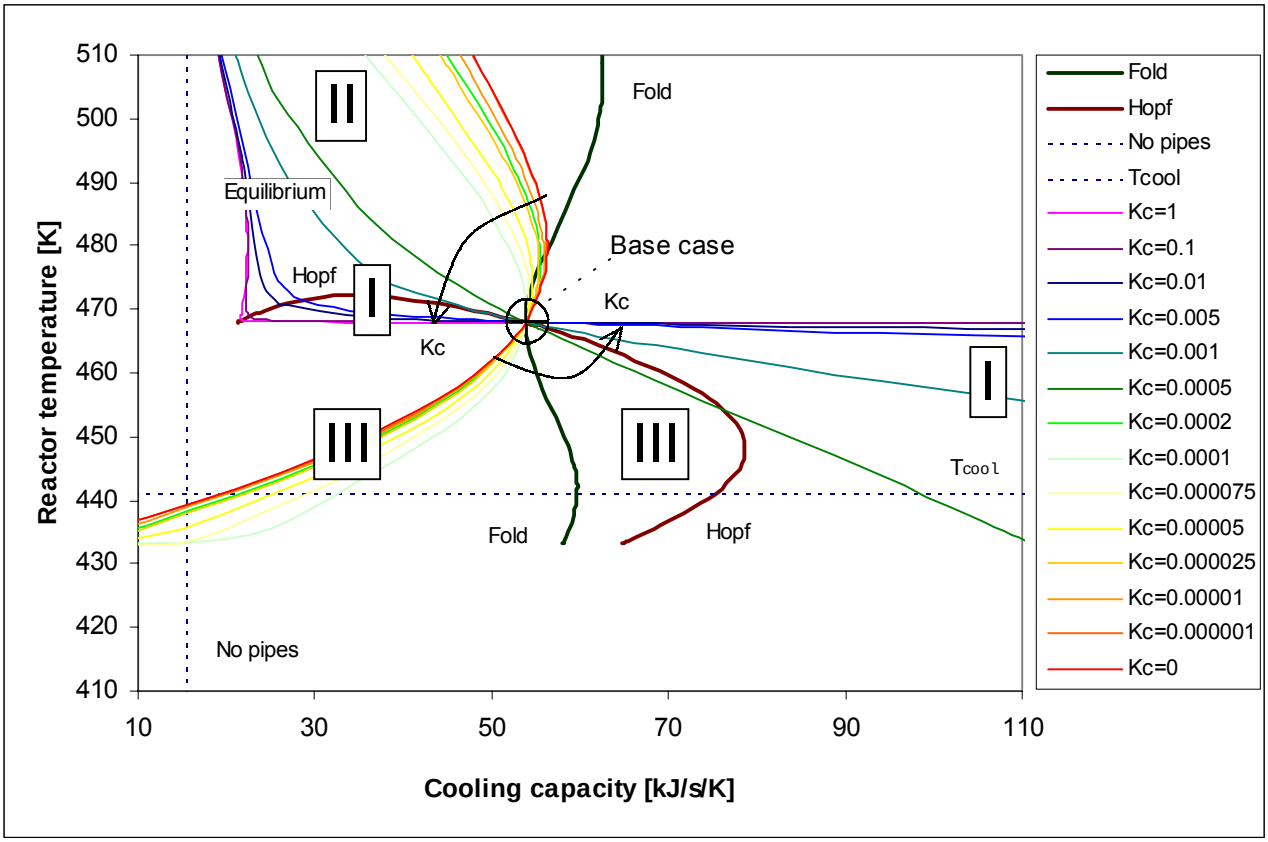

Figure 45 Reactor designer stability map. Proportional control on coolant flowrate. $T_{cool,0}$ = 400 [K]. Active parameters: UA and K_c. Hopf maximum $K_c > 0.00078$ [m^3 s^{-1} K^{-1}]. Fold maximum $K_c > 0.00026$ [m^3 s^{-1} K^{-1}]. UA_{max} = 79 [kJ s^{-1} K^{-1}].

Discussion of the reactor designer stability map:

- Like, Figure 44 the equilibrium curves in Figure 45 rotate counter clockwise if the proportional gain is increased. In case $K_c > 0.00078$ [m^3 s^{-1} K^{-1}] a dynamically stable system is possible.
- In Figure 45 in case $K_c > 0.00026$ [m^3 s^{-1} K^{-1}] (Fold maximum) it seems that the cooling capacity is limited $UA_{min} \approx 22$ [kJ s^{-1} K^{-1}]. For the base case temperature T = 468 [K] this is the minimum attainable cooling capacity.
- Apparently, as the inlet coolant temperature is increased the minimum cooling capacity shifts upwards.
- In case UA > 79 [kJ s^{-1} K^{-1}] stability is more certain, although in case of large disturbances, extinction still can emerge.

Table 21 Survey stability P-control coolant flowrate. $T_{cool,0}$ = 400 [K].

Cooling capacity [kJ s^{-1} K^{-1}]	Dynamical behaviour	Explanation
$0 \leq UA < 15$	Not existing	UA of the reactor > 0
$15 \leq UA < 22$	Not existing	Minimum Hopf UA for base case
$22 \leq UA < 56$	Dangerous region	Multiplicity can disturb the stability
$56 \leq UA < 78$	Moderate safe region	Stability if $K_c > K_c$ (Hopf)
UA > 78	Stable region, no limit cycles	Stability if $K_c > K_c$ (Hopf)

Orbit curves

The influence of UA on the stability is demonstrated through of the following orbit curves with equal K_c value and varying UA values. In Figure 46, UA = 45 [kJ s^{-1} K^{-1}] the proportional gain is not powerful enough resulting in exhibiting limit cycles. If the cooling capacity is increased to the base case value, the cooling capacity is considerably large i.e. much more heat can be transferred, however the overshoot cannot be restrained, which causes the reaction to extinguish. (Figure 47). If the cooling capacity is even larger, the overshoot can be shortened, in which the transition towards the lower steady state is excluded (Figure 48).

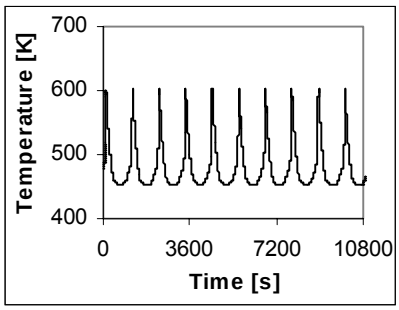

Figure 46 $T_{cool,0}$ = 400 [K], K_c = 0.001 [m^3 s^{-1} K^{-1}], **UA = 45** [kJ s^{-1} K^{-1}], ΔT = +10 [K]. Limit cycles.

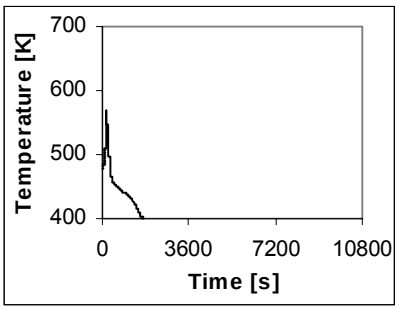

Figure 47 $T_{cool,0}$ = 400 [K], K_c = 0.001 [m^3 s^{-1} K^{-1}], **UA = 55** [kJ s^{-1} K^{-1}], ΔT = +10 [K]. Extinction $T \rightarrow T_0$.

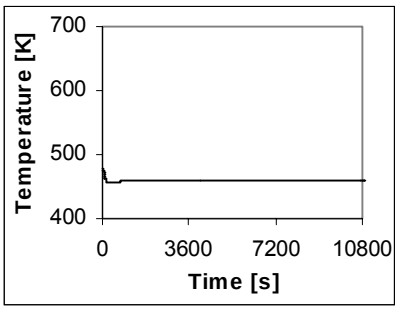

Figure 48 $T_{cool,0}$ = 400 [K], K_c = 0.001 [m^3 s^{-1} K^{-1}], **UA = 95** [kJ s^{-1} K^{-1}], ΔT = +10 [K]. Stable system.

Reactor temperature versus cooling capacity (T_0=435 K)

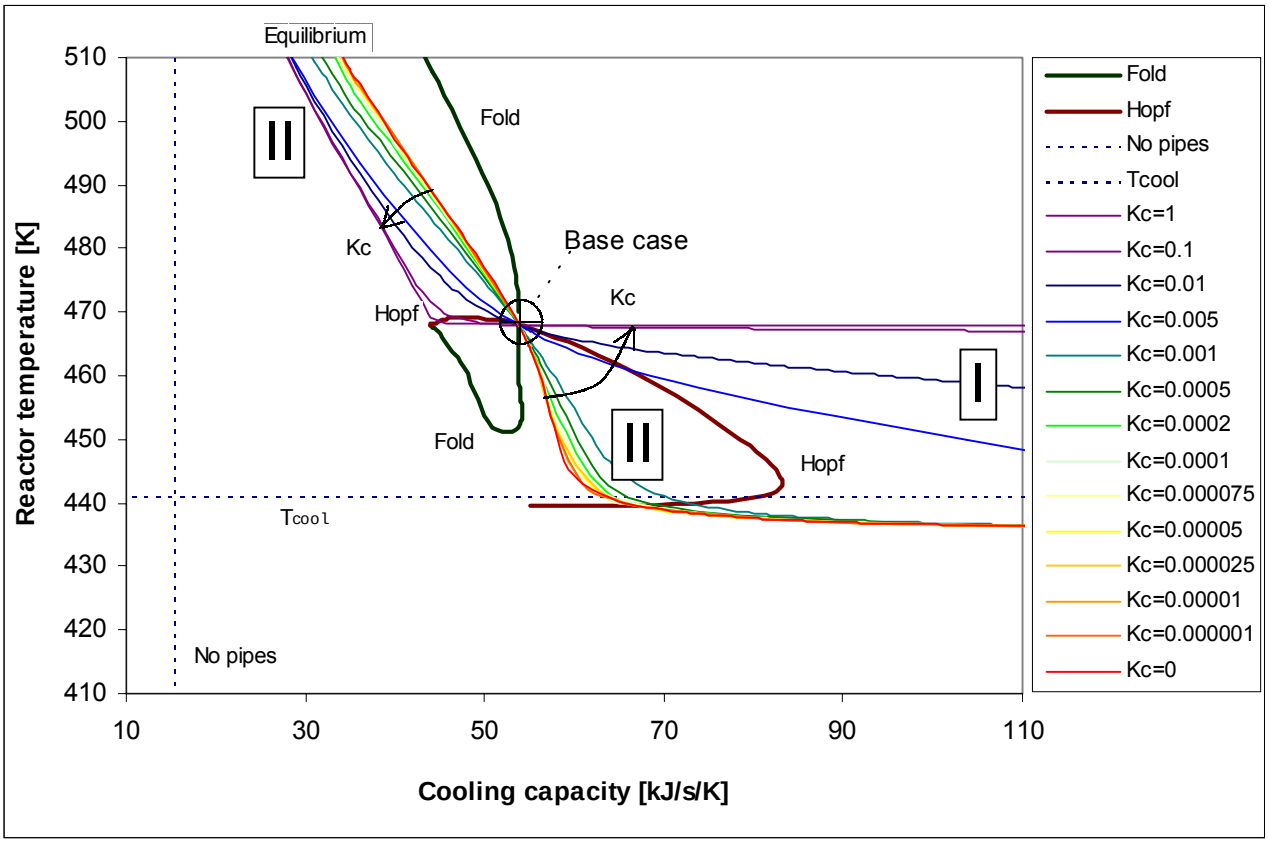

Figure 49 Reactor designer stability map. Proportional control on coolant flowrate. $T_{cool,0}$ = 435 [K]. Active parameters: UA and K_c. Hopf maximum K_c > 0.012 [m^3 s^{-1} K^{-1}]. UA_{max} = 83 [kJ s^{-1} K^{-1}].

Discussion of the reactor designer stability map:

- In Figure 49 for the base case temperature the minimum cooling capacity is $UA_{min} \approx 46$ [kJ s^{-1} K^{-1}]. This means that for lower UA values, the reactor temperature increases distinctive, no matter the proportional gain and strong limit cycles occur.
- In Figure 49 it is evident that multiplicity near the base case value is not anymore concerned. Increasing the proportional gain again rotates counter clockwise the equilibrium curves. In case K_c > 0.012 [m^3 s^{-1} K^{-1}] the system behaves dynamically stable.
- In case UA > 83 [kJ s^{-1} K^{-1}] stability is guaranteed.

Table 22 Survey stability P-control coolant flowrate. $T_{cool,0}$ = 435 [K].

Cooling capacity [kJ s^{-1} K^{-1}]	Dynamical behaviour	Explanation
0 ≤ UA < 15	Not existing	UA of the reactor > 0
15 ≤ UA < 46	Not existing	Minimum Hopf UA for base case
46 ≤ UA < 82	Moderate safe region	Stability if K_c > K_c (Hopf)
UA > 82	Stable region, no limit cycles	Stability if K_c > K_c (Hopf)

Table 20, Table 21 and Table 22 provide a survey of the dynamical behaviour for several cooling inlet temperatures. A system that appears to be stable can become unstable after a considerable perturbation. Therefore, these tables have to be examined with caution.

9.1.3 Controlling the throughput

In the process industry where one aims to operate at maximum yield, where primarily the process conditions based on process design are in general fixed, it is not likely that tremendous changes in flowrate are permitted. In case slight changes (i.e. in between a range of a few per cent) are allowable, it can be interesting to study if the residence time or throughput control can contribute to the possibilities of eliminating limit cycles.

Mathematical model

Equations 2 and 3 are similar regarding coolant temperature control, except the controller correlation 43:

$$V_R \frac{d[A]}{dt} = \Phi_V \left([A]_0 - [A]\right) - V_R k_0 e^{-E_{act}/RT}[A] \tag{2}$$

$$\rho C_P V_R \frac{dT}{dt} = \rho C_P \Phi_V \left(T_0 - T\right) + \left(-\Delta H_R\right) V_R k_0 e^{-E_{act}/RT}[A] - UA\left(T - T_{cool}\right) \tag{3}$$

$$\Phi_V = \Phi_{V,sp} \pm K_c \left(T_{sp} - T\right) \tag{43}$$

Both the possibilities will be examined i.e.: $K_c > 0$ and $K_c < 0$.

Comparison coolant temperature and flowrate control

The main difference between coolant temperature control and flowrate control is explained by the fact that changing the coolant temperature affects directly the heat balance, which has, due to the fact that the balances are coupled, indirectly consequences for the conversion. Flowrate alteration affects both directly the heat and mass balance. It changes the existing situation in the CISTR whereas the coolant temperature can be seen more as an external parameter. Cooling a reactor by decreasing the coolant temperature mainly implies a larger driving force to heat transfer. Controlling a reactor for instance by increasing the flowrate will on the one hand decrease the reactor temperature due to the supply of cold feed flow, but on the other hand it will increase the reactor temperature due to the increasing heat production by the chemical reaction. Thereby, flowrate control is more complicated due to the existence of multiplicity, which is not the case for coolant temperature control regarding the base case. This role of multiplicity will be demonstrated in a later stadium in this chapter. Although the mathematical description does not differ, the impact on the reactor temperature and conversion is considerably different.

Positive K_c value

The controller equation becomes:

$$\Phi_V = \Phi_{V,sp} + K_c \left(T_{sp} - T\right) \tag{43a}$$

A reactor designer stability map is created (Figure 50) applying positive proportional gain values ($K_c > 0$). The active bifurcation parameters are: the flowrate (set point) and the proportional gain.

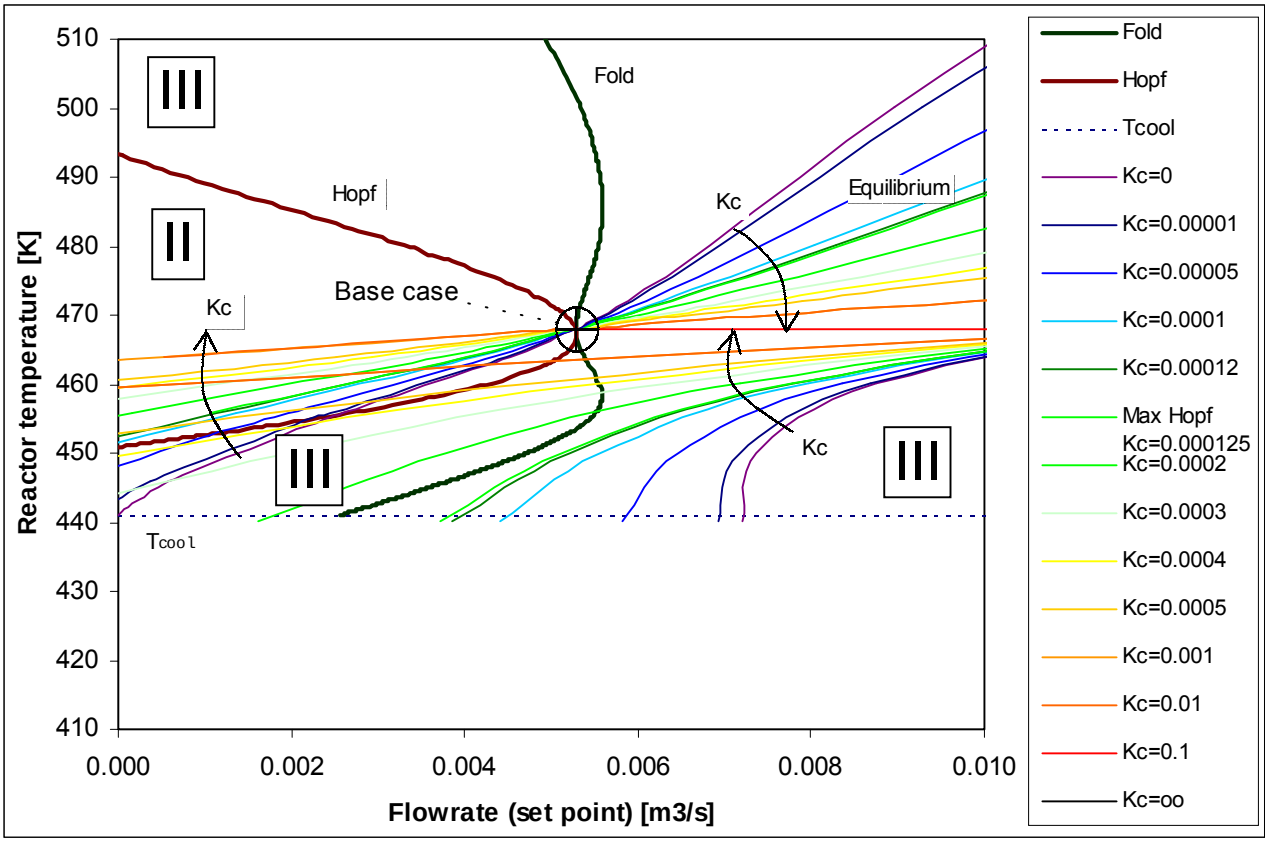

Figure 50 Reactor designer stability map proportional controlled flowrate ($K_c > 0$). The considered base case model exhibiting limit cycles cannot be controlled satisfactorily due to unstable regions in the vicinity of the base case. The region II in fact is a III region because too large K_c values can cause the reaction to extinct, however for low K_c values limit cycles exhibit. Hopf maximum $K_c = 0.000125$ [$m^3\ s^{-1}\ K^{-1}$].

Discussion of the reactor designer stability map:

- In case the proportional gain is increased, the equilibrium curves rotate a little clockwise.
- In view of the controlled flowrate, multiplicity is of significance over the entire range ($0 \leq \Phi_V < 0.01$ [$m^3\ s^{-1}$]), which is clearly visible in the stability map because of the equilibrium curves.
- The equilibrium curves alter due to the increased proportional gain nevertheless cannot prevent the process to behave unstable. No region I can be observed.

Orbit curves

Considered positive K_c values the following orbit curves have been drawn to demonstrate that for $K_c > 0$ throughput control is not applicable.

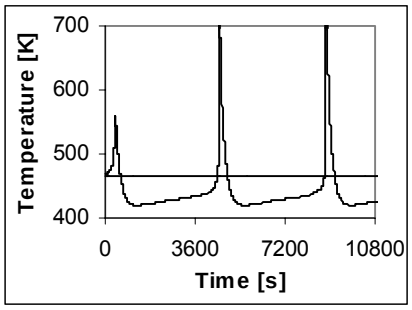

Figure 51 $K_c = 0.00007$ [m^3 s^{-1} K^{-1}]. The proportional controller can't eradicate the evolving limit cycles.

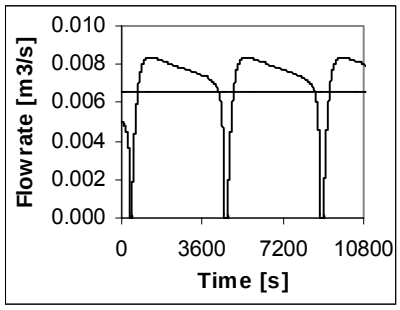

Figure 52 $K_c = 0.00007$ [m^3 s^{-1} K^{-1}]. The flowrate varies exceedingly which is presumable unwanted.

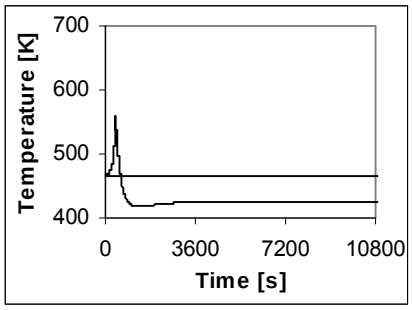

Figure 53 In case the controller gain is slightly increased towards $K_c = 0.00008$ [m^3 s^{-1} K^{-1}] the reaction extinguishes.

Using the steady state solution of the mass and heat balance 2 and 3, a proportional gain can be estimated: $K_c = 0.00007$ [m^3 s^{-1} K^{-1}]. Apparently, this value is too small to elucidate the limit cycles, which is confirmed through Figure 51. A larger K_c however cannot achieve the desired steady state; actually, a steady state with a much lower conversion is reached (T_{cool}) (Figure 53). Figure 52 displays the eminent variation of the throughput, which is in industrial process unacceptable.

The question arises: "Why can't the process be controlled?" In case a disturbance occurs, due to external factors or due to the self-sustained oscillations, the proportional controller determines the corrected flowrate, which should adapt the process towards the set point. On the one hand, a large K_c value is required to repress the evolving limit cycles causing overshoot. On the other hand, small K_c values are inevitable to regulate the process mildly and not to disrupt the actual process. Too rigorous flowrate variations, however causes the process to jump (attract) to other steady state situations. In case too less heat is withdrawn runaway occurs and if the throughput is too large the reaction extinguishes called the blow-out velocity (Fogler[26]).
Based on stability map (Figure 50) and displayed orbit curves one can conclude that it is dissuadable to control the base case applying a proportional controller with positive values for K_c.

Negative K_c value

Using the steady state solution of the mass and heat balance 2 and 3, a proportional gain can be estimated: $K_c = -0.0007$ [m^3 s^{-1} K^{-1}]. Therefore, due to the negative sign equation 43 changes into:

$$\Phi_V = \Phi_{V,sp} - K_c\left(T_{sp} - T\right) \tag{43b}$$

A new stability map (like Figure 50 for $K_c > 0$) is created for $K_c < 0$ (Figure 67).

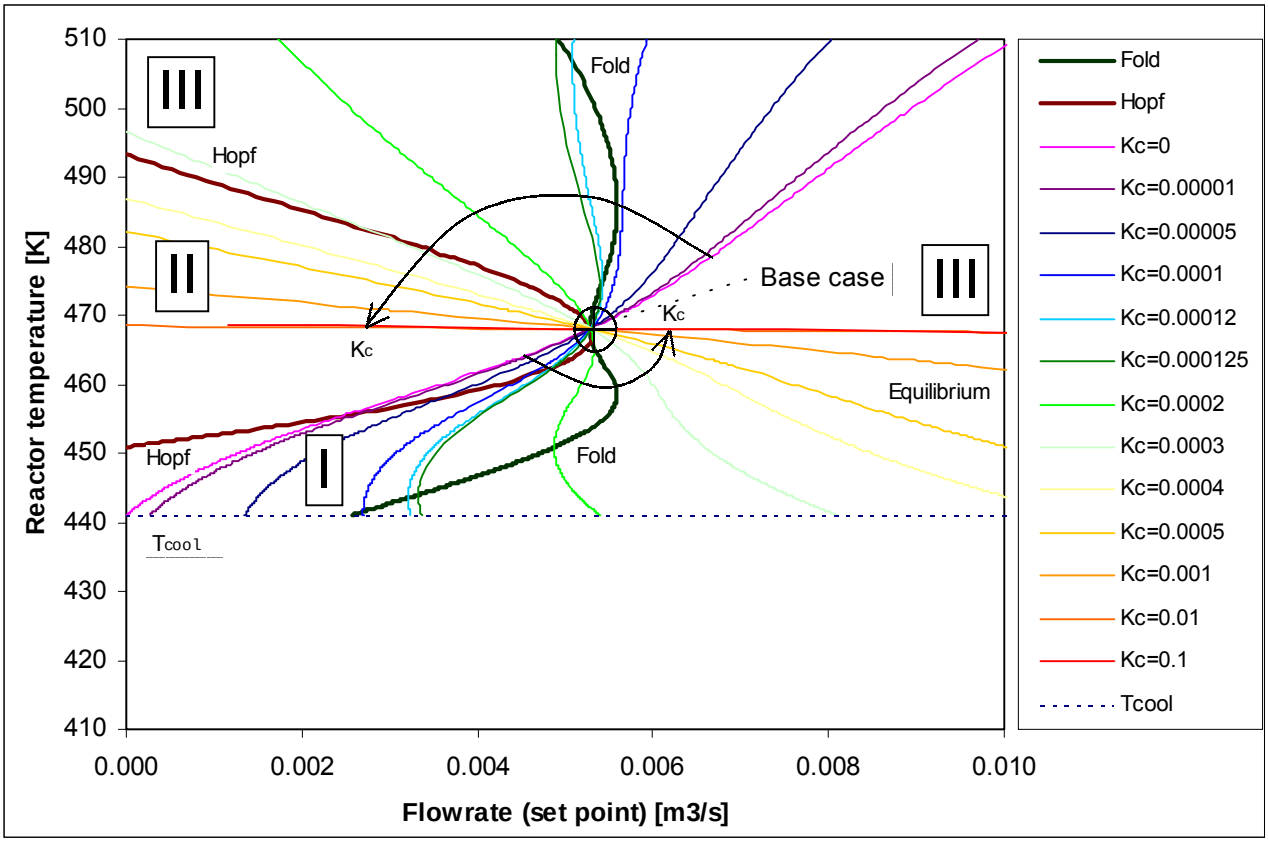

Figure 54 Reactor designer stability map. Proportional controlled flowrate ($K_c < 0$). Hopf maximum $K_c = 0.000125$ [$m^3\ s^{-1}\ K^{-1}$]. The region marked II is actually a region III because the limit cycles can cause extinction or runaway but is marked with II because the base case exhibits limit cycles in case no controller is interfering.

Discussion of the reactor designer stability map:

- The Hopf and Fold curves are similar like Figure 50.
- The equilibrium curves rotate counter clockwise in case the proportional gain is increased.
- A particular small region marked I is found which implies that the process may behave stable. The consequences are that the desired set point T = 468 [K] cannot be maintained, through following the equilibrium curves. If however, it is not allowed to change this temperature, one has to accept a lower conversion. $\zeta = 0.47$ instead of $\zeta = 0.69$.

Orbit curves

For region I in Figure 54 the dynamical behaviour is studied. A proportional gain $K_c = 0.000124$ [$m^3\ s^{-1}\ K^{-1}$] slightly smaller than the Hopf maximum value $K_c = 0.000125$ [$m^3\ s^{-1}\ K^{-1}$] clearly shows limit cycles (Figure 55). The maximum Hopf K_c value (Figure 56) shows that the process behaves stable after a step disturbance of $\Delta T = 10$ [K] through a spiral point, nevertheless with higher temperature and conversion. Conversely, K_c is not large enough to maintain the set point steady state. Increasing K_c results in the first place runaway (Figure 57) and subsequently realises stability (Figure 58). Very large K_c values with a positive temperature disturbance preserve the stability and the desired set point (Figure 59). However, in case the disturbance is negative, it is apparent that K_c causes the temperature to drop to the coolant temperature (Figure 60).

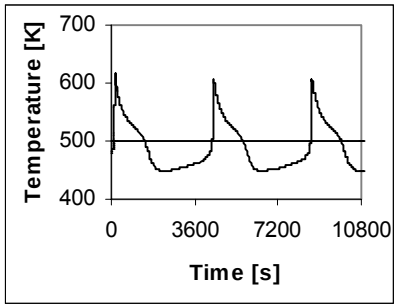

Figure 55 **K_c = 0.000124** [m^3 s^{-1} K^{-1}] and ΔT = 10 [K]. A limit cycle evolves around a different steady state.

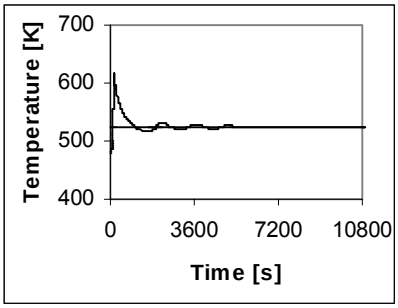

Figure 56 **K_c = 0.000125** [m^3 s^{-1} K^{-1}] and ΔT = 10 [K]. The system is stable (spiral point) but jumps to a higher steady state i.e. $T \rightarrow 524$ [K]. $\zeta = 0.92$.

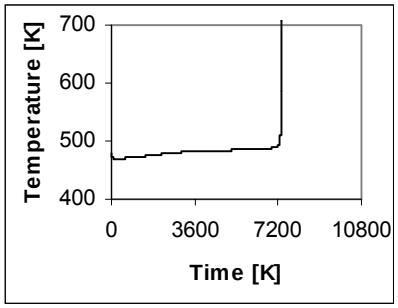

Figure 57 **K_c = 0.00139** [m^3 s^{-1} K^{-1}] and ΔT = 10 [K]. Slightly higher K_c values cause runaway. $T \rightarrow 774$ [K].

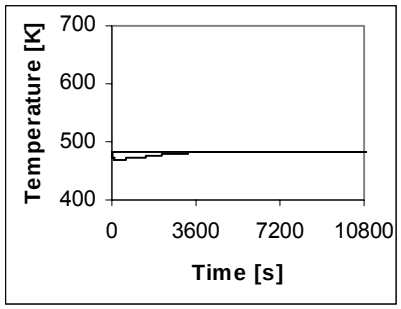

Figure 58 **K_c = 0.00140** [m^3 s^{-1} K^{-1}]. Step disturbance ΔT = 10 [K]. The process behaves stable. However with a lower conversion $\zeta = 0.47$ instead of $\zeta = 0.69$.

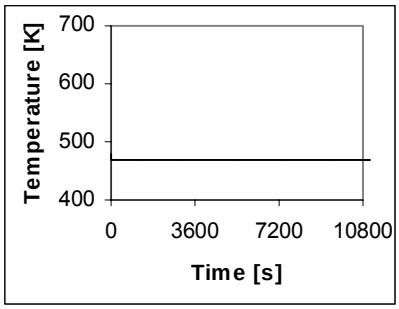

Figure 59 **K_c = 0.01** [m^3 s^{-1} K^{-1}]. If ΔT = 10 [K] stable system, nevertheless the set point T can be maintained, not the conversion.

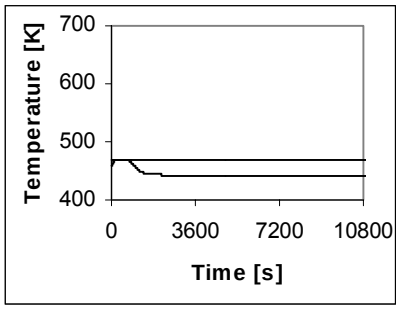

Figure 60 **K_c = 0.01** [m^3 s^{-1} K^{-1}]. Step disturbance ΔT = -10 [K]. The process behaves unstable. The temperature drops to the coolant temperature due to the too rigorous control.

Figure 60 demonstrated another complication. It is remarkable that a disturbance ΔT = +10 [K] (Figure 59) can be controlled, however it makes the system to extinguish in case ΔT = -10 [K] as is illustrated in Figure 60. The sign of the offset is evidently decisive. In case the offset > 0 the reaction appears to extinguish ($T \rightarrow T_{cool}$) i.e. the controllers manipulates with the wrong sign, the same phenomenon as in case $K_c > 0$. If the sign is reverse, the controller will decrease the flowrate causing temperature drop eventually until the coolant temperature is reached (extinction). Because $\Phi_V \rightarrow 0$ the controller cannot anymore manipulate (multiply) the flowrate and the reactor is actually halted.

Modification:

- Downwards approaching temperature disturbance i.e. offset < 0: sign > 0.
- Upwards approaching temperature disturbance i.e. offset > 0: sign < 0.

Disadvantage of this trick is the virtually endless converging process around the set point. Nonetheless, an adaptation in the LOCBIF source achieves Figure 60 to become like Figure 59.
The problems caused by the sign of the offset can be solved using a gimmick but is not a very scientifically solution. A controller with knowledge of the process in which the K_c value is fitted to the particular situations e.g. ($K_c < 0$ / $K_c > 0$) or (K_c robust / K_c gentle) can help to improve the controlling procedure. In this case, non-linear process control could be an option.

Conversion versus reactor temperature

If not the reactor temperature but the base case conversion has to be remained, the proportional controller equation becomes:

$$\Phi_V = \Phi_{V,sp} - K_c\left(\zeta_{sp} - \zeta\right) \tag{45}$$

The controller changes the flowrate to acquire a base case conversion ζ = 0.68 which has the corollary that the reactor temperature decreases and finally another steady state is reached.

Orbit curves

Orbit curves will be created applying controller equation 45. Due to proportional control, steady state offset however is inevitable.

Table 23 Stability maps P-control throughput.

Proportional gain K_c [$m^3\ s^{-1}$]	Final conversion ζ [-]	Final reactor temperature T [K]	Final flowrate Φ_V [$m^3\ s^{-1}$]	Dynamical behaviour	Reference
5×10^{-6}	$\zeta_{average} \rightarrow 0.84$	$T_{average} \rightarrow 464$	0.0027	Limit cycles	Figure 61, Figure 62
6×10^{-6}	0.72	454	0.0021	Spiral point	Figure 63, Figure 64
10×10^{-6}	0.91	444	0.0003	Asymptotic damping	Figure 65, Figure 66

Figure 61 demonstrates that the proportional controller is not powerful enough to eradicate emerging limit cycles. Both conversion and temperature (Figure 62) still exhibits sustained oscillations. Increasing K_c implies stability (Figure 63 and Figure 64) nevertheless with an offset. The conversion finally becomes ζ = 0.72 [-] with an accompanying temperature T = 454 [K].

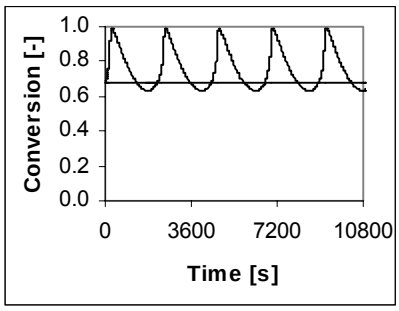

Figure 61 $K_c = 5 \times 10^{-6}$ [$m^3\ s^{-1}$].

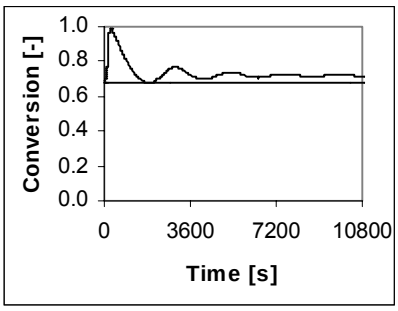

Figure 62 $K_c = 6 \times 10^{-6}$ [$m^3\ s^{-1}$].

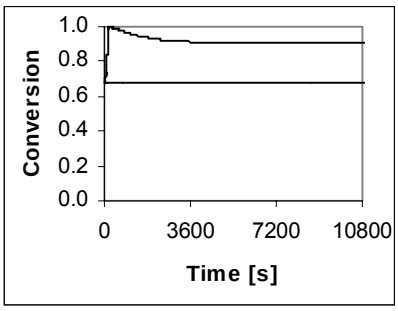

Figure 63 $K_c = 1 \times 10^{-5}$ [$m^3\ s^{-1}$].

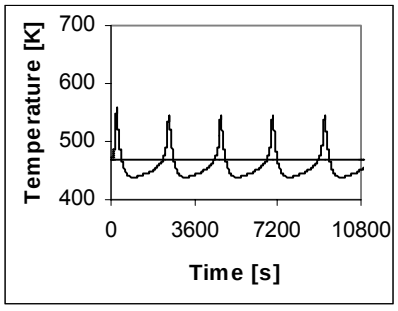

Figure 64 $K_c = 5 \times 10^{-6}$ [$m^3\ s^{-1}$].

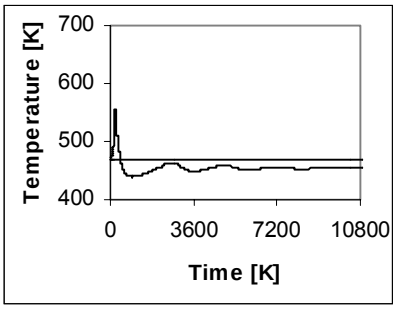

Figure 65 $K_c = 6 \times 10^{-6}$ [$m^3\ s^{-1}$].

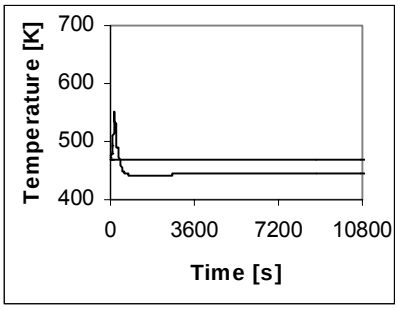

Figure 66 $K_c = 1 \times 10^{-5}$ [$m^3\ s^{-1}$].

If throughput control is applied, the reactor designer and controller have to decide which process variable (temperature or conversion) is decisive.

Reactor temperature versus cooling capacity

A significant large cooling capacity can have a positive effect on the stability of the process. The study to the not controlled base case resulted in a stable region, in which no limit cycles exhibit, in case UA > 78 [kJ s^{-1} K^{-1}] viewed in Figure 24. Hence the effect of the cooling capacity is examined for the base case + proportional controller on the flowrate. A stability map is created regarding active parameters, which are the proportional gain and the cooling capacity resulting in Figure 67.

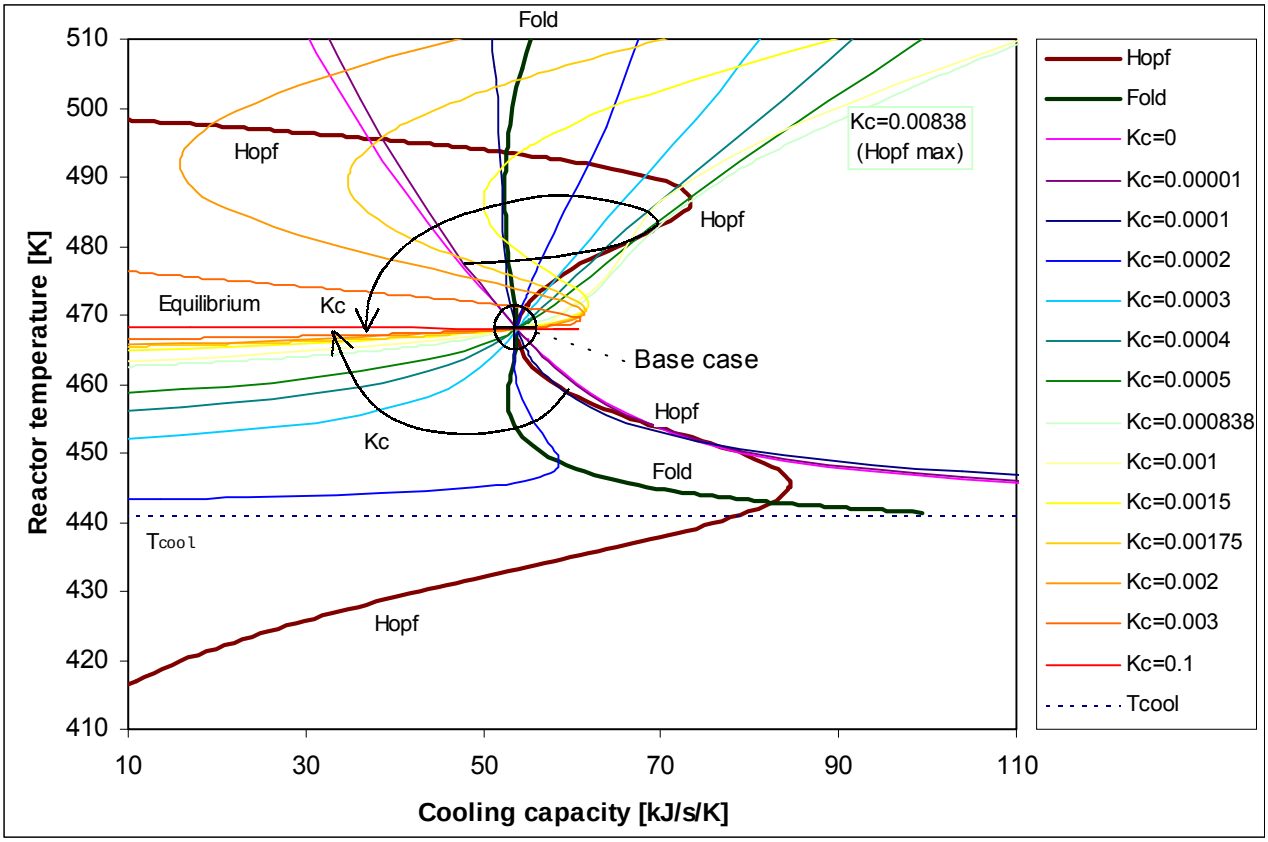

Figure 67 Reactor designer stability map. Proportional controlled flowrate. Hopf maximum UA > 84 [kJ s^{-1} K^{-1}]. Fold maximum K_c = 1.05 $\times 10^{-4}$ and Fold minimum K_c = 2.2 $\times 10^{-4}$ [m^3 s^{-1} K^{-1}].

Discussion of the reactor designer stability map:

- The 3D effect is here clearly visible, therefore,
- In case the proportional gain is increased, the equilibrium curves at first rotate clockwise until K_c = 0.00838 [m^3 s^{-1} K^{-1}] then the equilibrium curves are indented and resemble a parabolic shape. It is apparent to perceive in Figure 67 that more than one steady state solution is possible and definitely with respect to the base case.
- Multiplicity is of significance over the entire examined range. Therefore, the region marked with I must be considered with the knowledge that runaway or extinction is probable in case an external disturbance is eminent. In case the simulation is started from the base case steady state situation, the system behaves stable.
- In the contrary, to the stability maps formerly created in, (e.g. T_{cool} control) in which the stable region could be marked clearly, is in case of flowrate control due to the prominent existing of multiplicity much more complicated. A specific chosen K_c could mean that a point is stable throughout the perspective of the base case, however can make a system to become unstable in case a external disturbance is imposed.
- LOCBIF found the Hopf maximum for UA = 73 [kJ s^{-1} K^{-1}], which is almost the same value UA = 75 [kJ s^{-1} K^{-1}] as for coolant temperature control (Figure 24) which has formerly been found.

Orbit curves

If the cooling capacity UA = 73 [kJ s^{-1} K^{-1}] derived from the Hopf maximum value. Limit cycles appear in case no controller is correcting (Figure 68). In case K_c is increased the limit cycles are visibly shrinking (Figure 69). For slightly larger K_c values limit cycles, vanish (Figure 70).

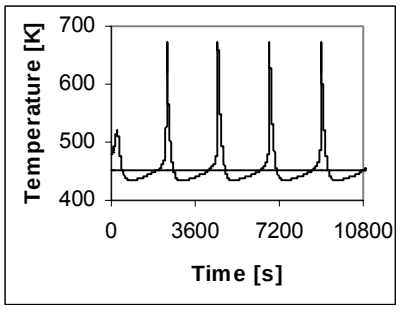

Figure 68 UA = 73 [kJ s^{-1} K^{-1}] **K_c = 0** [m^3 s^{-1} K^{-1}]. ΔT = 10 [K]. Limit cycles. ζ = 0.50, T = 452 [K].

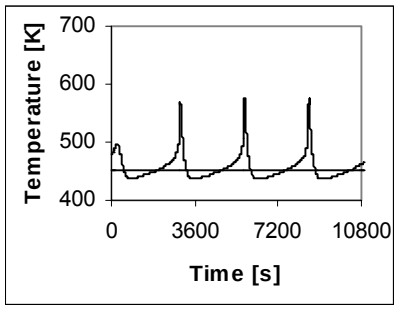

Figure 69 UA = 73 [kJ s^{-1} K^{-1}] **$K_c = 3 \times 10^{-5}$** [m^3 s^{-1} K^{-1}]. ΔT = 10 [K]. Fading limit cycles. ζ = 0.52, T = 452 [K].

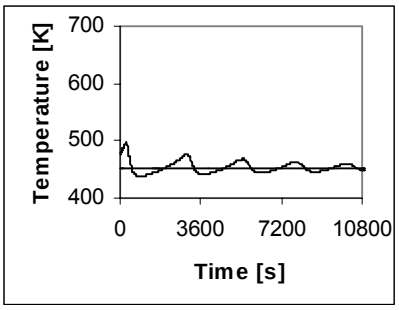

Figure 70 UA = 73 [kJ s^{-1} K^{-1}]. **$K_c = 3.1 \times 10^{-5}$** [m^3 s^{-1} K^{-1}]. ΔT = 10 [K]. Spiral point. ζ = 0.53, T = 451 [K].

With the base case cooling capacity UA = 55 [kJ s^{-1} K^{-1}], stability can be acquired if $K_c > 0.002$ [m^3 s^{-1} K^{-1}] although with lower conversion. The choice of the proportional gain must be done with caution in consideration of instability.

Summarising

Based on the stability map and orbit curves it can be noted that proportional control is possible. Nevertheless, suitable choice of the proportional gain is necessary to avoid unstable situations. The acquired K_c values through the bifurcation software program LOCBIF can merely indicate that K_c must be strong enough to exclude the self-sustained limit cycles but cannot be too large to prevent instability due to the existence of multiplicity. The choice has to be made to, or to preserve the reactor temperature or the conversion. In case the proportional controller is applied which regulated the throughput, both cannot simultaneously be maintained. An advanced controller with knowledge of the process device is therefore recommended. With regards to the cooling capacity, larger UA values have a stabilising effect. The LOCBIF source LOCBIF rhs 7 is included in Appendix 7.

9.2 Reactor controller stability map

The following stability maps will be examined:

Table 24 Reactor controller stability maps P-control.

Stability map	Reference
K_c versus UA Controlling T_{cool}	Figure 71
K_c versus UA Controlling $\Phi_{V,cool}$	Figure 72
K_c versus UA Controlling Φ_V	Figure 73

9.2.1 Controlling the coolant temperature

Mathematical model

The mathematical model with regards to the coolant temperature P-controlled base case states:

$$V_R \frac{d[A]}{dt} = \Phi_V \left([A]_0 - [A]\right) - V_R k_0 e^{-E_{act}/RT}[A] \tag{2}$$

$$\rho C_P V_R \frac{dT}{dt} = \rho C_P \Phi_V \left(T_0 - T\right) + \left(-\Delta H_R\right) V_R k_0 e^{-E_{act}/RT}[A] - UA\left(T - T_{cool}\right) \tag{3}$$

$$T_{cool} = T_{cool,sp} + K_c \left(T_{sp} - T\right) \tag{41}$$

A very distinct stability map can be created using active LOCBIF bifurcation parameters UA and K_c resulting in Figure 71.

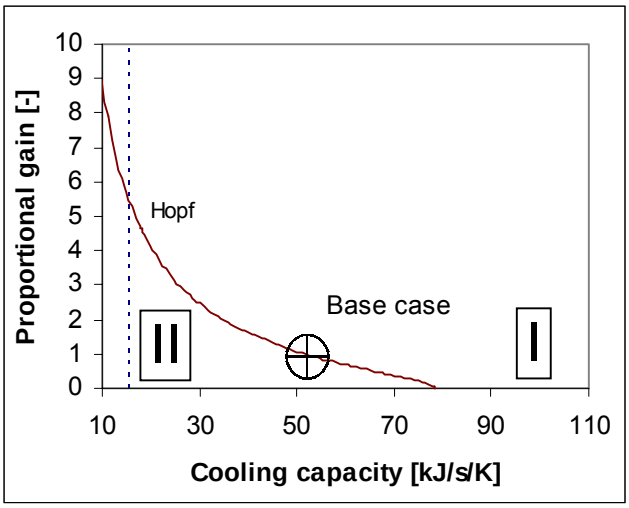

Figure 71 The reactor controller stability map of the proportional controlled base case model. To obtain a stable process, a larger proportional gain has to be chosen in case UA decreases. UA_{max} (Hopf) = 78 [kJ s^{-1} K^{-1}] and $K_{c,\,max}$ = 5.7 [-].

Discussion of the reactor controller stability map:

- The same Hopf maximum can be found values as for the reactor designer stability map Figure 24.
- The stability map shows that K_c decreases when the cool capacity increases.
- The dotted line represents the UA pertaining to the reactor with no cooling pipes. Through Figure 71, the maximum required proportional controller gain could accordingly be derived. If K_c = 5.7, the base case will never exhibit limit cycles no matter the extent of cooling capacity, provided that the coolant temperature can be controlled instantaneously, which in practise is not completely the case. Nevertheless, for this particular dealing scenario it is wise to choose a K_c as large as possible.
- By means of increasing the cooling capacity, less proportional gain is required to prohibit limit cycles.
- The reactor controller stability map is a very useful tool to determine an appropriate K_c value in case for instance the cooling capacity is changed. Therefore, a particular UA value is chosen, e.g. UA = 40 [kJ s^{-1} K^{-1}], to acquire a stable process, K_c = 1.8 to shift from region II to stable region I.

9.2.2 Controlling the coolant flowrate

Mathematical model

The mathematical model with regards to the coolant flowrate P-controlled base case states:

$$V_R \frac{d[A]}{dt} = \Phi_V ([A]_0 - [A]) - V_R k_0 e^{-E_{act}/RT}[A] \quad (2)$$

$$\rho C_P V_R \frac{dT}{dt} = \rho C_P \Phi_V (T_0 - T) + (-\Delta H_R) V_R k_0 e^{-E_{act}/RT}[A] - UA(T - T_{cool}) \quad (3)$$

$$\rho_{cool} C_{P,cool} V_{cool} \frac{dT_{cool}}{dt} = \rho_{cool} C_{P,cool} \Phi_{V,cool} (T_{cool,0} - T_{cool}) + UA(T - T_{cool}) \quad (12)$$

$$\Phi_{V,cool} = \Phi_{V,cool,sp} - K_c (T_{sp} - T) \quad (42)$$

For coolant flowrate control, the following reactor controller stability map is created, similar as for coolant temperature control (Figure 71).

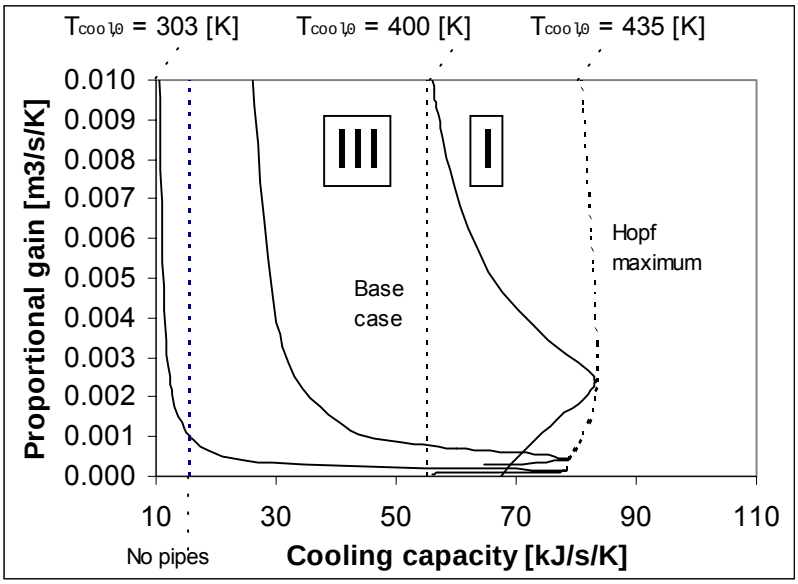

Figure 72 The reactor controller stability map. Hopf curves using active bifurcation parameters UA and K_c for various coolant inlet temperatures. For each Hopf curve, the process is stable at the right-hand side and unstable at the left-hand side.

Discussion of the reactor controller stability map:

- Although In the stability map Figure 72 different axes are used, compared to Figure 71, The stability map shows again that K_c decreases when the cool capacity increases.
- The stable region I is clearly appearing, besides for every $T_{cool,0}$ the minimum and the maximum cooling capacity.
- The introduction of the coolant differential equation, which implies multiplicity, is clearly visible. For $T_{cool,0}$ = 435 [K], one can see that multiplicity is not anymore existing with regards to the base case.
- The stability map demonstrates that the maximum UA Hopf value is dependent of the inlet coolant temperature.

9.2.3 Controlling the throughput

Mathematical model

The mathematical model with regards to the proportional controlled throughput base case states:

$$V_R \frac{d[A]}{dt} = \Phi_V \left([A]_0 - [A]\right) - V_R k_0 e^{-E_{act}/RT}[A] \tag{2}$$

$$\rho C_P V_R \frac{dT}{dt} = \rho C_P \Phi_V \left(T_0 - T\right) + \left(-\Delta H_R\right) V_R k_0 e^{-E_{act}/RT}[A] - UA\left(T - T_{cool}\right) \tag{3}$$

$$\Phi_V = \Phi_{V,sp} - K_c \left(T_{sp} - T\right) \tag{43b}$$

The subsequent reactor controller stability map is drawn to investigate the influence the relationship between the cooling capacity and the proportional gain with respect to the stability.

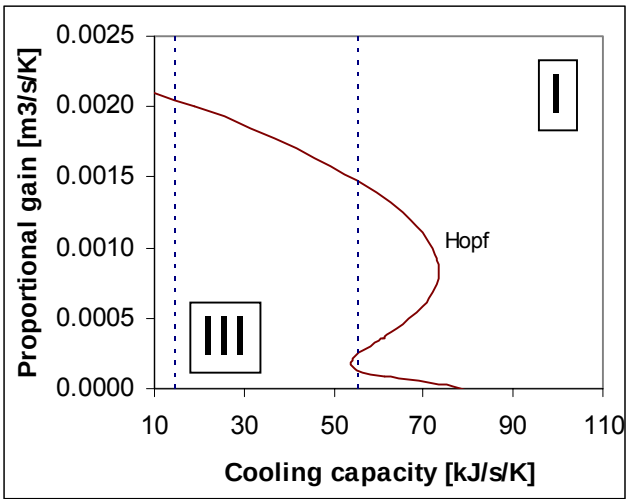

Figure 73 Reactor controller stability map. Proportional controlled throughput. Hopf maximum UA > 73 [kJ s^{-1} K^{-1}] and K_c = 0.00084 [m^3 s^{-1} K^{-1}]. In case the cooling capacity UA > 78 [kJ s^{-1} K^{-1}] or K_c > 0.002 [m^3 s^{-1} K^{-1}] stability is certain, nevertheless with lower conversion.

Discussion of the reactor controller stability map:

- Analogous to previous stability maps (Figure 71 and Figure 72), Figure 73 the clearly demonstrates the problem with multiplicity.
- The same Hopf maximum values have been acquired as for reactor designer stability map Figure 67 in which the latter is rather complicated to interpret.
- A clear stable region I is however located on the right hand side of the Hopf curve, however with lower conversion.

Summarising

Proportional controlling the throughput is possible. Disadvantage is that or the reactor temperature or the conversion must be chosen as a set point. Both contemporaneous is not possible because due to the existence of multiplicity the process is forced to one steady state situation. Due to the dynamical unstable situation of the base case, a certain proportional gain has to be chosen to resist the limit cycles. And here the problem arises, that too large K_c values cause inevitable transition towards other steady states and in particular if the process is also disturbed. Therefore, if only one reactant is involved, like the base case, controlling the throughput is not a suitable controlling method if both the reactor temperature as well the conversion must be maintained.

Chapter X

10 PROPORTIONAL-INTEGRAL CONTROL

In this section, it is considered to what extent the proportional + integral controller affects the stability of the cooled CISTR with exothermic reaction.

10.1 Reactor designer stability maps

The integral action merely eliminates the offset in which eventually a particular process variable coincides with the controller set point. Therefore, the equilibrium, Fold and Hopf curves remain unchanged. Therefore, the reactor designer stability maps of proportional control and proportional-integral control are similar.

10.2 Reactor controller stability maps

The following reactor controller stability maps will be examined:

Table 25 Stability maps PI-control coolant temperature.

Stability map	Reference
K_c versus τ_I	Figure 74
K_c versus UA	Figure 79

Table 26 Stability maps PI-control coolant flowrate.

Stability map	$T_{cool,0}$ = 303 [K]	$T_{cool,0}$ = 400 [K]	$T_{cool,0}$ = 435 [K]
K_c versus τ_I	Figure 80a	Figure 80b	Figure 80c
K_c versus UA	Figure 82	Figure 83	Figure 84
K_c versus τ_{cool}	Figure 113	Figure 114	Figure 115

Table 27 Stability maps PI-control throughput.

Stability map	Reference
K_c versus τ_I	Figure 85
K_c versus UA	Figure 86

10.2.1 Controlling the coolant temperature

The mathematical notation by means of equations 8, 9 and 46 is:

$$V_R \frac{d[A]}{dt} = \Phi_V \left([A]_0 - [A]\right) - V_R k_0 e^{-E_{act}/RT}[A] \tag{2}$$

$$\rho C_P V_R \frac{dT}{dt} = \rho C_P \Phi_V \left(T_0 - T\right) + \left(-\Delta H_R\right) V_R k_0 e^{-E_{act}/RT}[A] - UA\left(T - T_{cool}\right) \tag{3}$$

$$T_{cool} = T_{cool,sp} + K_c \left(T_{sp} - T\right) + \frac{K_c}{\tau_I}\int_0^1 \left(T_{sp} - T\right)dt \tag{46}$$

The first interesting issue is to find out in what way the integral time τ_I is related with the proportional gain K_c. Therefore a stability map is created with the proportional gain at the ordinate and the integral time at the abscissa (Figure 74).

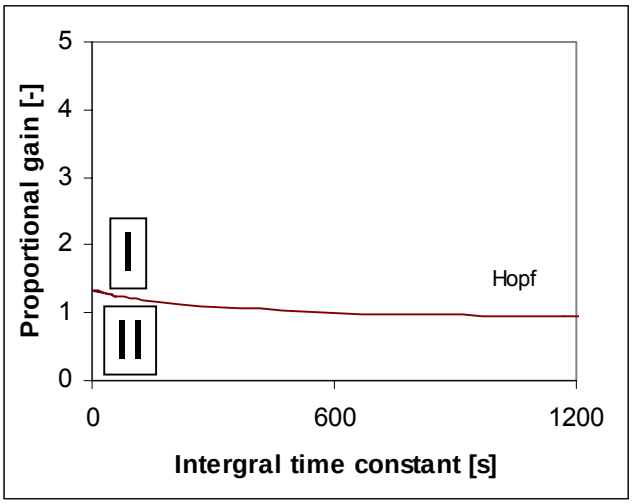

Figure 74 Reactor controller stability map with Hopf curve in which the active parameters are K_c and τ_I. $K_c(\tau_I \rightarrow 0)$ = 1.35 and $K_c(\tau_I \rightarrow \infty)$ = 0.9.

Discussion of the reactor controller stability map:

- K_c is apparently not very dependent on the magnitude of τ_I. In case $\tau_I \rightarrow 0$, K_c = 1.35 and when $\tau_I \rightarrow \infty$, K_c = 0.9 which is in fact the K_c for the solely proportional controlled base case.
- In Figure 74 the Hopf curve is plotted indicating the transition between dynamically stable and unstable.
- Figure 74 demonstrates that increasing the integral time, in fact slightly improves the stability.

Orbit curves

The following step is to examine the dynamic behaviour for one selected proportional gain K_c = 1 and varying integral time. Figure 75a with an integral time τ_I = 60 [s] displays that limit cycles emerge. In case a proportional controlled has exclusively been applied K_c = 0.9 was sufficient to eliminate limit cycles. Evidently, small integral times imply larger K_c values to provide stability. Figure 75a-e show that increasing the integral time is causing the originating of the limit cycles is to be postponed. If τ_I = 600 [s] no limit cycles will arise according to Figure 75f.

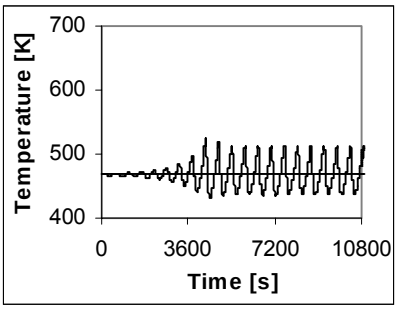

Figure 75a K_c = 1 τ_I = **60** [s].

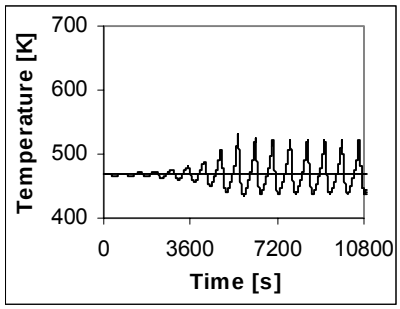

Figure 75b K_c = 1 τ_I = **120** [s].

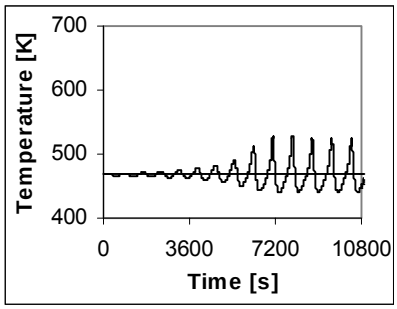

Figure 75c K_c = 1 τ_I = **180** [s].

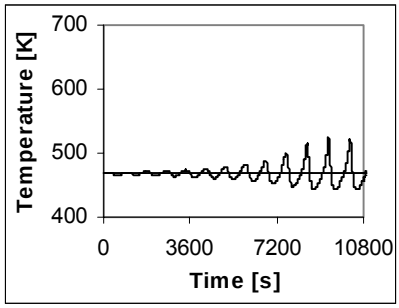

Figure 75d $K_c = 1$ τ_I = **240** [s].

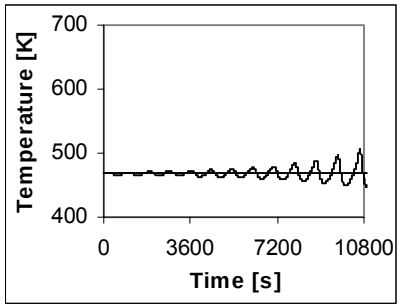

Figure 75e $K_c = 1$ τ_I = **300** [s].

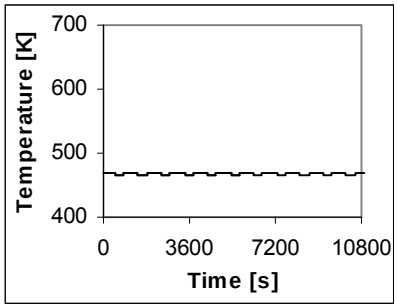

Figure 75f $K_c = 1$ τ_I = **600** [s].

In previous sections it has been found that K_c = 0.9 could narrowly preserve stability. Figure 76a-c demonstrate that τ_I have to be increased to acquire a stable system.

In fact: $K_c(\mathrm{P}) = K_c\big|_{\tau_I \to \infty}(\mathrm{PI})$.

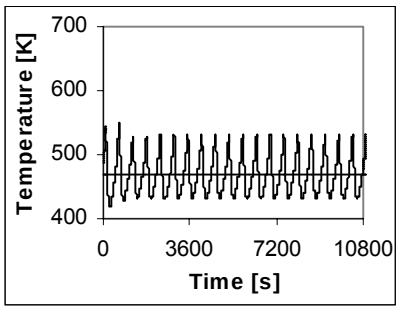

Figure 76a $K_c = 0.9$ τ_I = **60** [s].

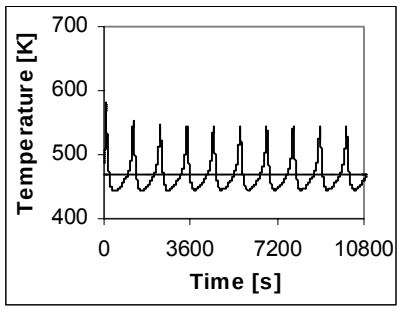

Figure 76b $K_c = 0.9$ τ_I = **600** [s].

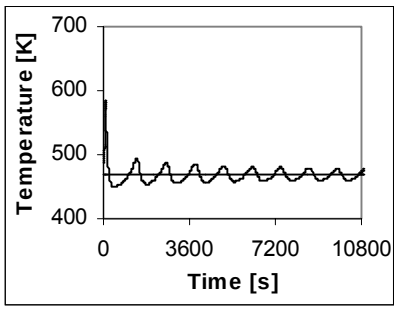

Figure 76c $K_c = 0.9$ τ_I = **3600** [s].

For the next case the proportional gain is selected which provides stability for every chosen integral time K_c = 1.35 (value derived from Figure 74). Figure 77a demonstrates that the limit cycles vanish after a temperature disturbance ΔT = 20 [K], although despite the long lasting spiral point. Decreasing the integral time will not change the stability in general (Figure 77b), primarily the oscillation time will be decreased. A large K_c accomplishes the desired steady state value within a few minutes and not too large overshoot (Figure 78).

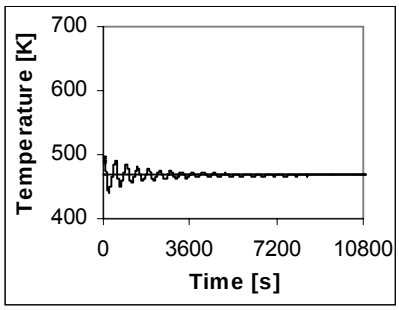

Figure 77a $K_c = 1.35$, τ_I = **60** [s] derived from Figure 74. Constrained temperature disturbance ΔT = 20 [K].

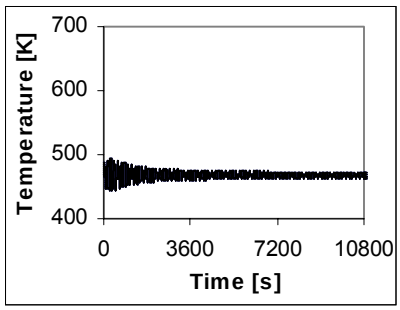

Figure 77b $K_c = 1.35$, τ_I = **5 [s]** derived from Figure 74. Constrained temperature disturbance ΔT = 20 [K].

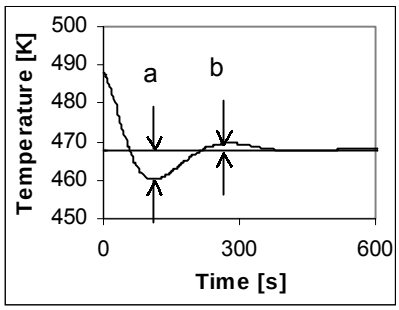

Figure 78 $K_c = 4$ τ_I = 60 [s]. Constrained temperature disturbance ΔT = 20 [K]. Ratio a/b = 4/1 discussed in §5.6.2 (Figure 17).

The LOCBIF source LOCBIF rhs 4 is included in Appendix 7.

Proportional gain versus cooling capacity

In previous section in which exclusively the proportional gain has been considered, the cooling capacity, in combination with a suitable proportional gain, had a stabilising effect on the process stability (Figure 71). Regarding the PI-controller, the cooling capacity still has this positive consequence alomst irrespective of the integral action. Figure 79 represents the stability map with applied active parameters UA and K_c in relation with several values of the integral time.

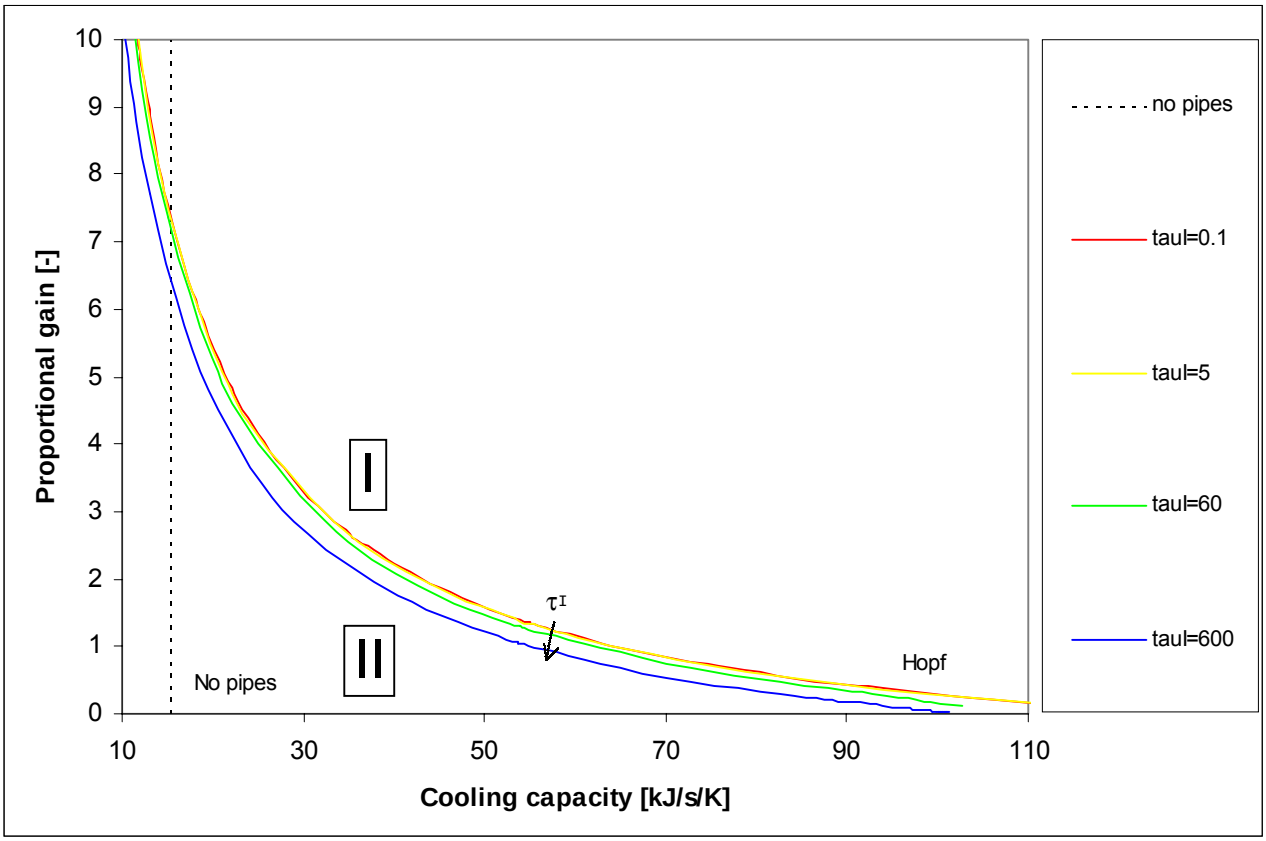

Figure 79 Reactor controller stability map of the proportional-integral controlled base case model. If the cooling capacity decreases, a larger K_c value has to be chosen. The integral time constant has a minor influence. If $\tau_I \rightarrow \infty$ the stability map matches with the proportional controlled base case showed in Figure 71.

Discussion of the reactor controller stability map:

- The Hop curves are similar to the curves for proportional control only (Figure 71). In case the cooling capacity decreases, a larger proportional gain must be selected to preserve stability.
- The integral time constant has little influence on the stability. K_c is mainly decisive.
- The reactor controller can easily determine or a suitable combination of UA and K_c in which stability is guaranteed.

Summarising

In case the base case is proportional-integral controlled through regulating the coolant temperature, the integral action has the advantage that the offset is eliminated, however short integral times has to be avoided because then the process behaves less stable. The controller stability maps K_c-UA can be used to effortless determine a stable process.

10.2.2 Controlling the coolant flowrate

Equations 2, 3, 36 and 47 mathematically describe the proportional + integral controlled base case.

$$V_R \frac{d[A]}{dt} = \Phi_V ([A]_0 - [A]) - V_R k_0 e^{-E_{act}/RT}[A] \quad (2)$$

$$\rho C_P V_R \frac{dT}{dt} = \rho C_P \Phi_V (T_0 - T) + (-\Delta H_R) V_R k_0 e^{-E_{act}/RT}[A] - UA(T - T_{cool}) \quad (3)$$

$$\rho_{cool} C_{P,cool} V_{cool} \frac{dT_{cool}}{dt} = \rho_{cool} C_{P,cool} \Phi_{V,cool} (T_{cool,0} - T_{cool}) + UA(T - T_{cool}) \quad (12)$$

$$\Phi_{V,cool} = \Phi_{V,cool,sp} - K_c (T_{sp} - T) - \frac{K_c}{\tau_I} \int_0^1 (T_{sp} - T) dt \quad (47)$$

In Table 19 the proportional gain values regarding the P-control have been printed. These values are again obtained if ($\tau_I \rightarrow \infty$) is taken in the Hopf curves of Figure 80a,b and Figure 80c.

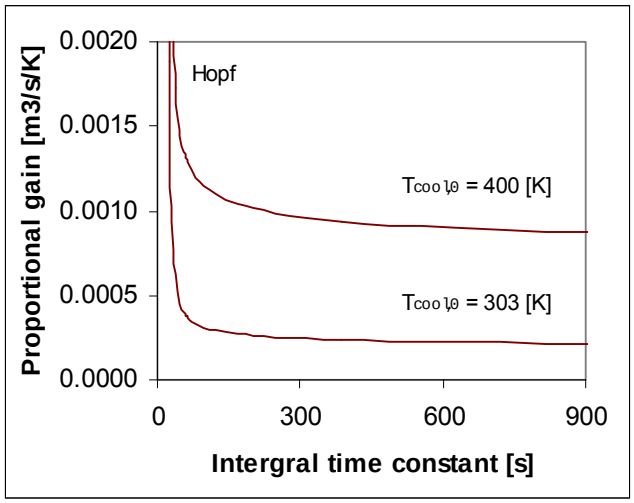

Figure 80a,b Reactor controller stability map with Hopf curves for $T_{cool,0}$ = 303 [K] and $T_{cool,0}$ = 400 [K]. Proportional gain versus integral time. For each Hopf curve the upper area I refers to stability and the lowest region II to instability.

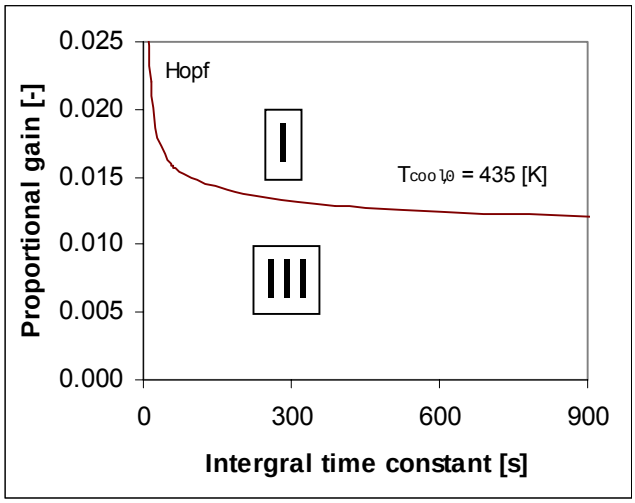

Figure 80c Reactor controller stability map with Hopf curves for $T_{cool,0}$ = 435 [K]. Proportional gain versus integral time.

Discussion of the reactor controller stability maps:

- For each Hopf curve the upper region points towards a stable region I and the lower region means instability. Moreover, due to the existence of multiplicity, transition to another steady state remains present, in particular if the process is considerably disturbed. Therefore, the stable regions always have to be interpreted with caution.
- The stability maps show that for short integral times, for instance if the process response has to be fast, the proportional gain must be selected considerably larger to maintain stability.
- If τ_I > 300 [s] the problem of integral windup almost not anymore exists.
- If $\tau_I \rightarrow \infty$ the same values are obtained:
  For $T_{cool,0}$ = 303 [K]: K_c > 0.00025 [m^3 s^{-1} K^{-1}] retrieved from Figure 28,
  For $T_{cool,0}$ = 400 [K]: K_c > 0.00078 [m^3 s^{-1} K^{-1}] retrieved from Figure 41,
  For $T_{cool,0}$ = 435 [K]: K_c > 0.012 [m^3 s^{-1} K^{-1}] retrieved from Figure 42.

Orbit curves

The following orbit curves demonstrate the influence of the integral time on the stability for a particular proportional gain (Hopf maximum value).

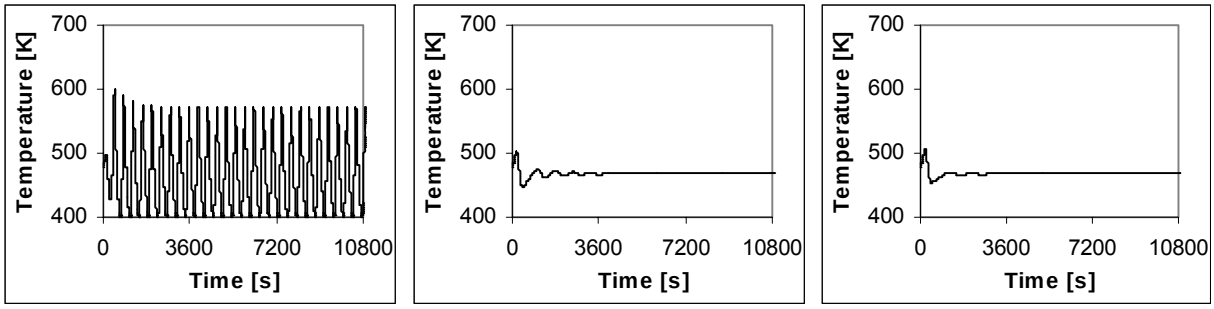

Figure 81a $T_{cool,0}$ = 303 [K], K_c = 0.00025 [m^3 s^{-1} K^{-1}], **τ_I = 60** [s] ΔT = +10 [K]. Limit cycles.

Figure 81b $T_{cool,0}$ = 303 [K], K_c = 0.00025 [m^3 s^{-1} K^{-1}], **τ_I = 600** [s] ΔT = +10 [K]. Spiral point.

Figure 81c $T_{cool,0}$ = 303 [K], K_c = 0.00025 [m^3 s^{-1} K^{-1}], **τ_I = 3600** [s] ΔT = +10 [K]. Stable spiral point.

That a large integral time improves the stability can be confirmed through the orbit curves Figure 81a-c. Small τ_I make the system unstable in which substantial limit cycles emerge. A larger integral time makes the process more stable (Ratto *et.al.*[66]) (Figure 81b) and a very large τ_I (Figure 81c) is similar to Figure 36 in which merely proportional control is concerned. The LOCBIF source LOCBIF rhs 6 is included in Appendix 7.

Proportional gain versus cooling capacity

In previous chapters, it has been found that the cooling capacity, in combination with a suitable proportional gain, has a stabilising effect on the dynamical behaviour of the concerned base case process. In the following stability maps, the cooling capacity has been drawn at the abscissa and the proportional gain at the ordinate for various integral times.

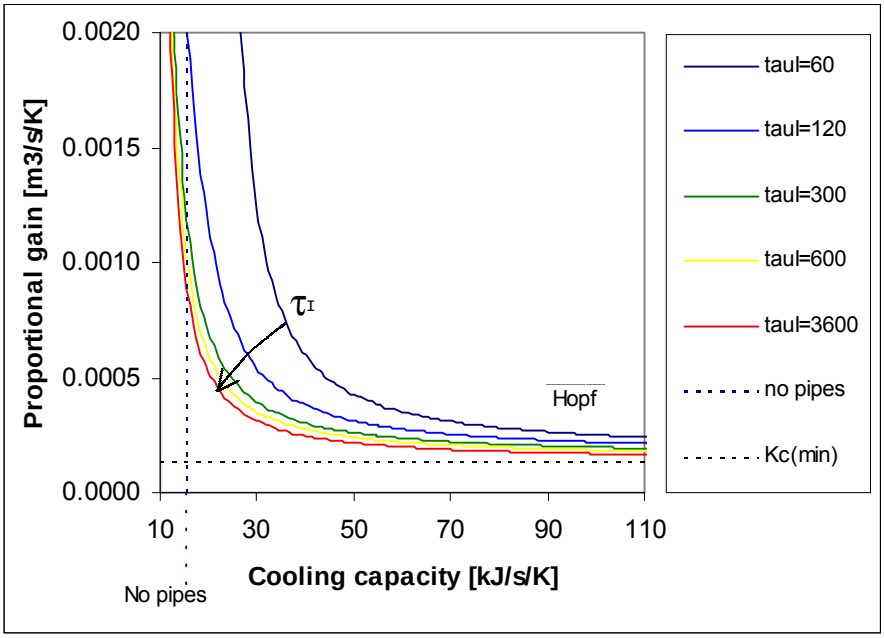

Figure 82 Reactor controller stability map. Hopf curves with bifurcation parameters: Proportional gain and the cooling capacity for $T_{cool,0}$ = 303 [K]. For each Hopf curve the stable region I is located at the right hand side and the unstable at the left hand side.

Discussion of the reactor controller stability maps:

- Figure 82 ($T_{cool,0}$ = 303 [K]) proves that the cooling capacity has a stabilising effect on the dynamical behaviour of the process. In case a larger integral time is chosen, the stability is even increased. This is also the case for Figure 83 ($T_{cool,0}$ = 400 [K]) and Figure 84 ($T_{cool,0}$ = 435 [K]).
- Typical for the considered stability maps is the fact that beneath a specific cooling capacity, the proportional gain increases severely. This can be explained through the fact that the controller ought to increase the coolant flowrate in case less heat can be transferred through the wall.
- In Figure 82 ($T_{cool,0}$ = 303 [K]) $K_c \uparrow$ if UA < 40 [kJ s^{-1} K^{-1}]. $UA_{min} \approx UA_{vessel}$ = 15 [kJ s^{-1} K^{-1}].
  In Figure 83 ($T_{cool,0}$ = 400 [K]) $K_c \uparrow$ if UA < 50 [kJ s^{-1} K^{-1}]. $UA_{min} \approx$ 30 [kJ s^{-1} K^{-1}].
  In Figure 84 ($T_{cool,0}$ = 435 [K]) $K_c \uparrow$ if UA < 60 [kJ s^{-1} K^{-1}]. $UA_{min} \approx$ 50 [kJ s^{-1} K^{-1}].
- The stability maps as function of the inlet coolant temperature confirm that the stable region increases for a low inlet coolant temperature. This is due to the larger temperature driving force in the coolant differential equation. In situations in which the cooling capacity could decline, the lowest inlet coolant temperature provides the best stability. Although still large perturbations can cause extinction.

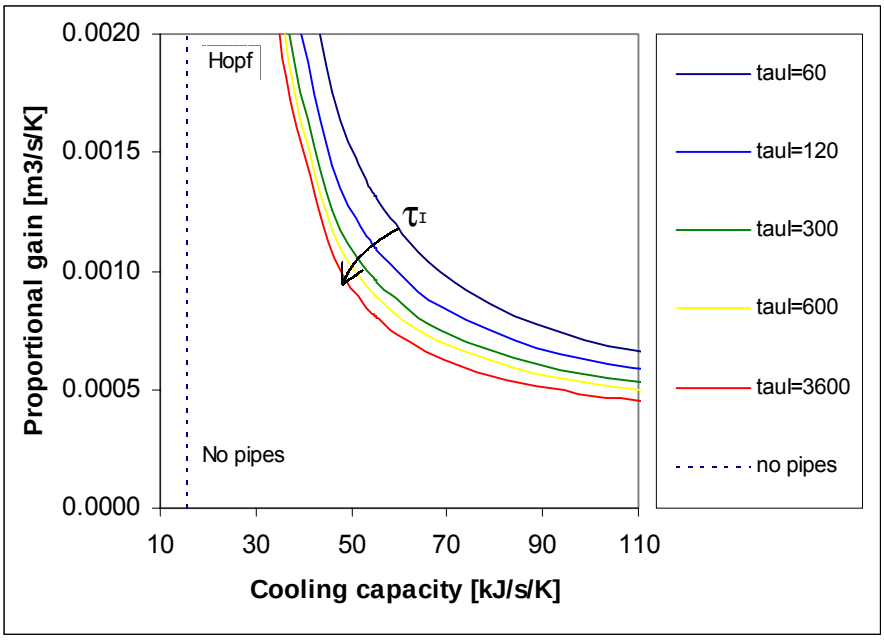

Figure 83 Reactor controller stability map. Hopf curves with bifurcation parameters: Proportional gain and the cooling capacity for $T_{cool,0}$ = 400 [K]. For each Hopf curve the stable region I is located at the right hand side and the unstable at the left hand side.

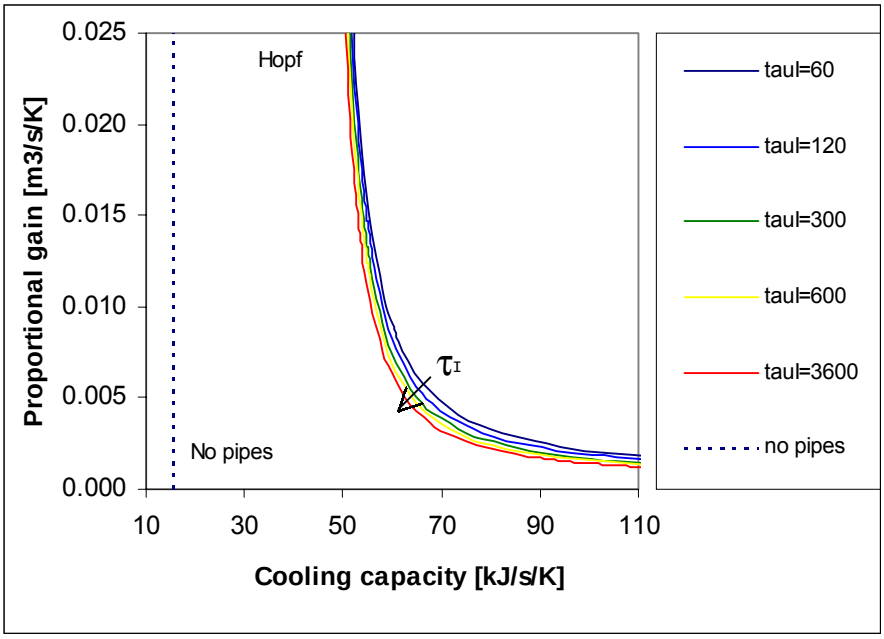

Figure 84 Reactor controller stability map. Hopf curves with bifurcation parameters: Proportional gain and the cooling capacity for $T_{cool,0}$ = 435 [K]. For each Hopf curve the stable region I is located at the right hand side and the unstable at the left hand side.

Summarising

In case the base case is proportional-integral controlled through regulating the coolant flowrate, like with coolant temperature control, the same integral action has the advantage that the offset is eliminated, however short integral times has to be avoided because the process behaves then less stable. The controller stability maps K_c-UA can be used to determine effortless a stable process. A low inlet coolant temperature implies that instability is less prominent. However again, large external disturbances can force the process to a lower steady state.

10.2.3 Controlling the throughput

Mathematical model

Equations 2, 3 and 48 describe the proportional + integral controlled base case.

$$V_R \frac{d[A]}{dt} = \Phi_V \left([A]_0 - [A]\right) - V_R k_0 e^{-E_{act}/RT}[A] \tag{2}$$

$$\rho C_P V_R \frac{dT}{dt} = \rho C_P \Phi_V \left(T_0 - T\right) + \left(-\Delta H_R\right) V_R k_0 e^{-E_{act}/RT}[A] - UA\left(T - T_{cool}\right) \tag{3}$$

$$\Phi_V = \Phi_{V,sp} - K_c\left(T_{sp} - T\right) - \frac{K_c}{\tau_I}\int_0^1 \left(T_{sp} - T\right) dt \tag{48}$$

In the previous section, the influence of a proportional controller is examined. It was found that controlling through regulating the flowrate is possible, however, a suitable K_c is necessary and a lower conversion is inevitable.
An integral action causes the controller output to change as long as an error exists in the process output. In the vicinity of the constrained set point, the integral action eliminates the offset. However, in case K_c has not been chosen properly or the offset becomes substantial, the integral action can make the process even more unstable i.e. integral wind-up.
In previous section, it was also found that the way a considered disturbance is introduced in the model is of concern. In case a higher temperature perturbation is imposed i.e. offset < 0 the P-controller could

stabilise the system. However, if the temperature was lower than the set point, the controller could regulate in the wrong direction. The applied trick in which the sign is reversed caused the process variable the virtually endless revolve around the set point. It could be expected that, due to the offset removing ability off the I-action, the wobbling effect would decline. Unfortunately, this is not the case according to several simulations.
The next step is to examine the relation between the proportional gain and the integral time by creating a suitable stability map in which K_c at the ordinate was viewed versus τ_I at the abscissa.

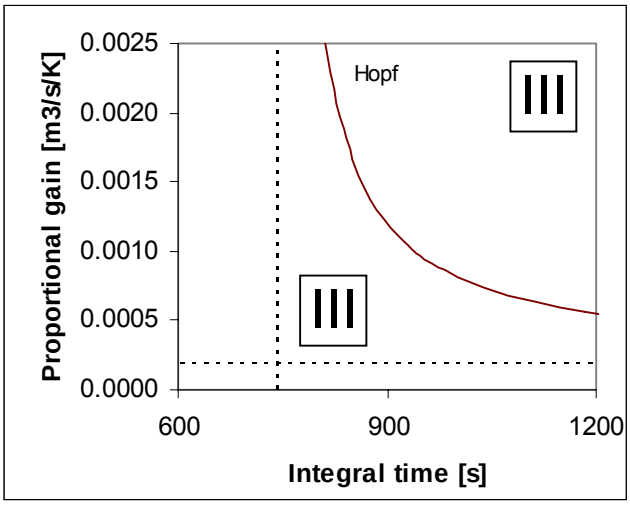

Figure 85 Process controller stability map with Hopf curves. The proportional gain versus integral time is asymptotic shaped in which $K_c \downarrow 0.0002$ [$m^3\ s^{-1}\ K^{-1}$] and $\tau_I \uparrow 740$ [s].

Discussion of the reactor controller stability maps:

- The same pattern arises for this particular stability map: smaller integral time means larger proportional gain values.
- At both sides of the Hopf curve, the system behaves unstable. Compared to Figure 73 in which K_c has been drawn against UA, it became clear that for $K_c > 0.000$ [$m^3\ s^{-1}\ K^{-1}$] stability is possible, although with lower conversion. LOCBIF did not generate such curve or maximum value.
- LOCBIF could not find any solutions for small integral time i.e. $\tau_I < 740$ [s].
- According to the attained Hopf curve, $K_c = 0.0002$ [$m^3\ s^{-1}\ K^{-1}$] if $\tau_I \rightarrow \infty$ which also will be confirmed in case K_c is drawn against τ_d (Figure 95). Because both sides of the curve are indicated as III, this value is not relevant anymore.
- Figure 85 demonstrates once again that a larger integral time has an increasing stabilising effect. Nevertheless, merely the integral action cannot provide absolute stability i.e. region I.
- Still the same disadvantage stands for that or the reactor temperature or the conversion has to be chosen.

The proportional gain must be robust enough to be able to adjust the flowrate into the right direction i.e. set point after both a external disturbance and both to restrain the evolving limit cycles. This has the disadvantageous effect that even a slight correction has a tremendous effect on the system. The latter is with respect to the obligation that the throughput variation must be in between a few percent not any more valid.
The stabilising effect of a large integral time can be explained as follows: apparently, large integral times make this process executing more smoothly. Consider a small integral time and a large proportional gain. After a disturbance, the controller determines the new e.g. higher flowrate and because the integral time is small, in a very short time the flowrate is adjusted. The fresh supported cold feed lowers the reactor temperature (decreased reaction rate) resulting in fast blow out and subsequently lower conversion. If the progress of this process is too hasty, extinction is the unwanted and inevitable result. The LOCBIF source LOCBIF rhs 8 is included in Appendix 7.

Proportional gain versus cooling capacity

In the previous section in which merely proportional gain was concerned, LOCBIF had severe problems finding a solution (Figure 73). Adding the integral action does not improve this solving process.
Based on previous chapters an increasing cooling capacity can have a stabilising effect on the process, however too large UA can cause extinction T towards T_{cool} or T_0 which can be explained by the fact that a tremendous amount of heat quickly can be removed from the system which implies fast temperature drop and consequently reaction extinction.

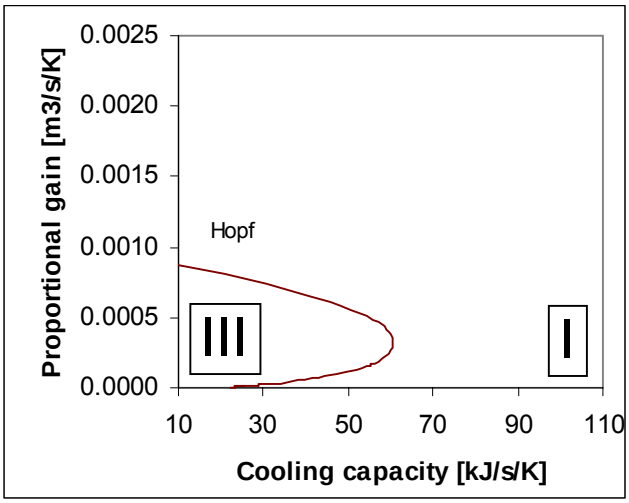

Figure 86 Reactor controller stability map. Hopf curve: proportional gain versus cooling capacity.

Discussion of the reactor controller stability map:

- In view of the base case, once more the existence of multiplicity is confirmed. A large K_c value is needed to stay away from region III.
- The same maximum Hopf value is found as for P-control (Figure 73) K_c = 0.00084 [m^3 s^{-1} K^{-1}]. Nevertheless the maximum Hopf value with regards to the cooling capacity is considerably lower UA = 60 [kJ s^{-1} K^{-1}] compared to the previously found UA = 73 [kJ s^{-1} K^{-1}].
- Although region I means stability. The same disadvantage of the lower conversion for one particular reactor temperature is involved.

Summarising

If the base case is proportional-integral controlled through regulating the throughput, no stable system can be obtained for small integral time values. Still the same disadvantage stand for that or the reactor temperature or the conversion has to be chosen. In general, controlling the throughput is compared to regulating the extent of cooling not preferable.

10.3 Alternatives

In previous section, the influence of the cooling capacity is examined. Additionally, the study to the effects on the stability of the feed temperature and the coolant temperature can perhaps contribute to the search for stability. In case the coolant temperature is decreased from T_{cool} = 441 [K] toward T_{cool} = 438 [K] the stability map like Figure 54 changes sincere in which the stable region I is slightly increased. Decreasing T_{cool} = 441 [K] beneath T_{cool} = 435 [K] which represents the transition to the region exhibiting multiplicity (Figure 19), deteriorate the stability. Increasing T_{cool} > 441 [K] diminish the stable region. The effect of the feed temperature on the process is minor. Decreasing T_0 to environmental temperature slightly increases the stable region. In fact the complete stability map are translated upwards in view of the abscissa. Finally, the introduction of a recycle stream can be useful, because the cooling effect of the fresh feed supply can be repressed which has its effect on the controller equation. (Fogler[26 76]).

Chapter XI

11 CONTROLLED SYSTEM WITH DELAY

In this chapter, the effect of delay on the overall stability (explained in paragraph 5.4) is to be considered. Due to the ease of LOCBIF, a presumed delay correlation can effortless be implemented to an existing mathematical model.

The following reactor controller stability maps will be examined:

Table 28 Stability maps delay

Stability map	**Reference**	
K_c versus τ_d	**Proportional control**	**Proportional-integral control**
Coolant temperature	Figure 88	Figure 103
Coolant flowrate	Figure 94a ($T_{cool,0}$ = 303 [K]) Figure 94b ($T_{cool,0}$ = 400 [K]) Figure 94c ($T_{cool,0}$ = 435 [K])	Figure 106 ($T_{cool,0}$ = 303 [K])
Throughput	Figure 95	Figure 107

Stability map	**Reference**
Process capacity	**Proportional control**
Kc versus τ_R	Figure 108
Kc versus τ_{cool}	Figure 110
Kc versus τ_{cool}	Figure 113 ($T_{cool,0}$ = 303 [K]) Figure 114 ($T_{cool,0}$ = 400 [K]) Figure 115 ($T_{cool,0}$ = 435 [K])

11.1 Proportional control

11.1.1 Controlling the coolant temperature

Mathematical model

The mathematical system consist of the following equations:

$$V_R \frac{d[A]}{dt} = \Phi_V \left([A]_0 - [A]\right) - V_R k_0 e^{-E_{act}/RT}[A] \tag{2}$$

$$\rho C_P V_R \frac{dT}{dt} = \rho C_P \Phi_V \left(T_0 - T\right) + \left(-\Delta H_R\right) V_R k_0 e^{-E_{act}/RT}[A] - UA\left(T - T_{cool}\right) \tag{3}$$

$$T_{cool} = T_{cool,sp} + K_c \left(T_{sp} - T_d\right) \tag{41}$$

$$\tau_d \frac{dT_d}{dt} = T - T_d \tag{49}$$

The overall value of τ_d will be estimated, considering the following partial τ_d 's:

- Measuring device and transmitter. According to Roffel[68] and Ding *et.al.*[17], the delay caused by the measuring device varies commonly between 5-10 [s] for liquid reactors and 10-30 [s] for gas-liquid reactors. According to Marlin[53] the typical dynamical response is generally about 0-5 [s].
- Heat transfer through pipes. The delay caused by heat transfer process is relatively small due to the assumption that the heat transfer coefficient for the steel cooling pipes is high and is probably 5-10 [s]. The delay by the controller device is assumed to be 0-5 [s].

- Control valve and activator response time. The valve response time according to Shinskey[71] is practically 0-5 [s]. According to Marlin[53] the final control element response time is 1-4 [s] and for signal conversion about 0.5 – 1.0 [s].
- Coolant residence time. The cooling fluid is rapidly pumped through the cooling pipes or jacket and is estimated 0-5 [s] based on §2.3.2 and calculation made in Appendix 3.
- Dead zone. Additionally, industrial reactors often are concerned with the existence of a dead zone in the reactor, in which apparently nothing happens. For this case i.e. the CISTR, it is assumed that no dead zone exists.

Consequently, the value of the presumed delay can be composed from the points mentioned above. Roughly $10 < \tau_d < 60$ [s]. In the succeeding paragraphs $\tau_d \approx 30$ [s] is presupposed. It is not necessary to determine the exact magnitude of τ_d, primarily due to the lack in information. Furthermore, the purpose of the introduction of delay is to obtain qualitative comprehension about the effect on the dynamical behaviour. To determine the effect of the delay on the dynamical behaviour several orbit curves have been created.

Orbit curves

Primarily, the proportional gain is taken $K_c = 0$. Figure 87 demonstrates that in case the delay is increased, the appearance of the oscillations change i.e. the peaks of the measured temperature T_d are dimmed and stretched in which the maximum amplitude emerges later in time than the maximum of the actual reactor temperature (Figure 89). For very large delay (Figure 87f) the measured reactor temperature is almost completely diminished i.e. $T_{d(t_d \to \infty)} = \overline{T}$.

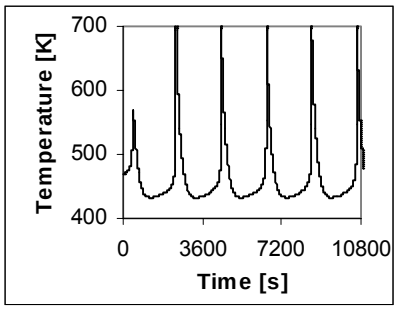

Figure 87a The measured (delayed) reactor temperature. $K_c = 0$, $\tau_d = 5$ [s].

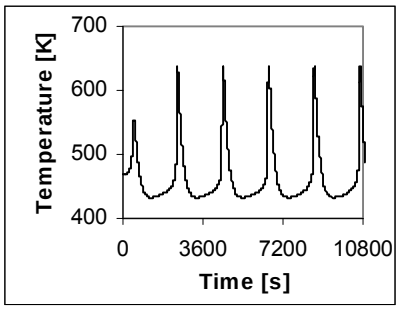

Figure 87b $K_c = 0$, $\tau_d = 30$ [s].

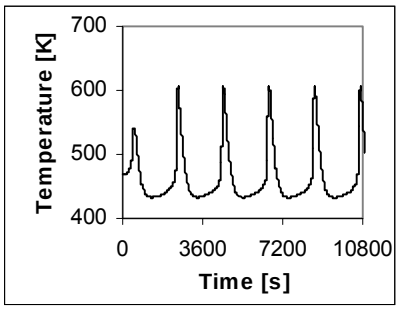

Figure 87c $K_c = 0$, $\tau_d = 60$ [s].

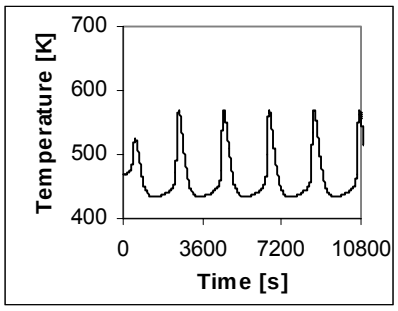

Figure 87d $K_c = 0$, $\tau_d = 120$ [s].

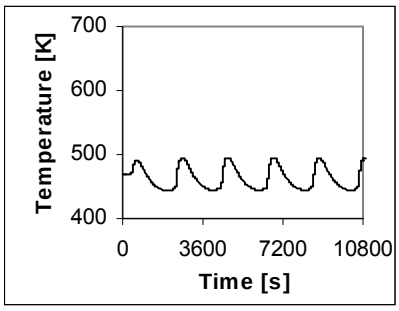

Figure 87e $K_c = 0$, $\tau_d = 600$ [s].

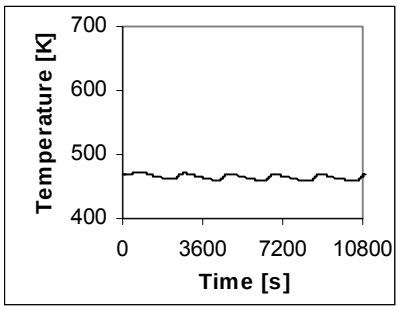

Figure 87f $K_c = 0$, $\tau_d = 3600$ [s]. $T_d \to 468$ [K].

According Equation 49 it is presumed that the reactor temperature is delayed in time. If instead of the reactor temperature, conversely the coolant temperature is delayed in time according equation 50 the same results have been obtained. Moreover, the fundamental principle of delay remains the same.

$$\tau_{cool,d}\frac{dT_{cool,d}}{dt} = T_{cool} - T_{cool,d} \qquad (50)$$

The following reactor controller stability map is created using active LOCBIF bifurcation parameters τ_d and the proportional gain K_c.

Reactor controller stability map

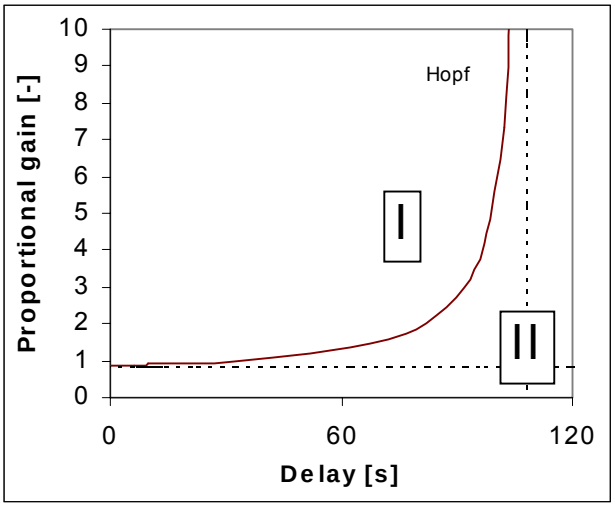

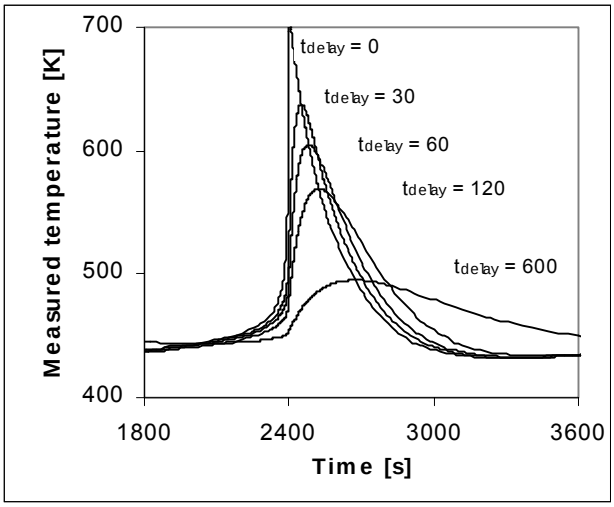

Figure 88 Reactor controller stability map Hopf curves active parameters K_c and τ_d. If τ_d > 108 [s] limit cycles will certainly appear.

Figure 89 Orbit curves of the delayed (measured) reactor temperature base case K_c = 0. The LOCBIF rhs 13 is included in Appendix 7.

Discussion of the reactor controller stability map:

- The stability map (Figure 88) unmistakably confirms that in case the apparent delay is increasing the proportional gain has to be taken considerably larger to preserve stability i.e. no limit cycles.
- If τ_d > 108 [s] which is apparently an asymptotic value, limit cycles will certainly exhibit, no matter the magnitude of K_c, unless the initial point is exactly the steady state, than the temperature remains unaffected. The critical value has been confirmed by Giona and Paladino[29].
- From Figure 88 the minimum proportional gain can be derived $K_c(\tau_d \to 0)$ = 0.9, the same value which has been found in preceding stability maps (e.g. Figure 23 and Figure 24).

Orbit curves

For the subsequent orbit curves, the minimum proportional gain is taken which would provide precise stability in case the base case is considered without presumed delay.

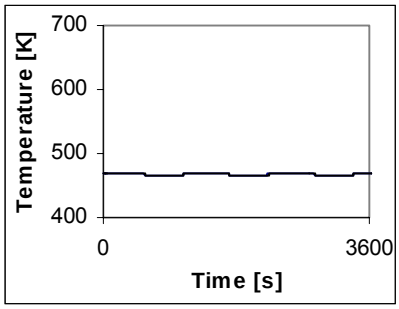

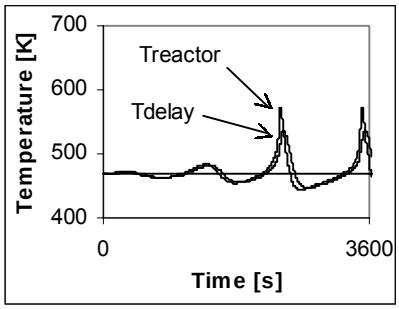

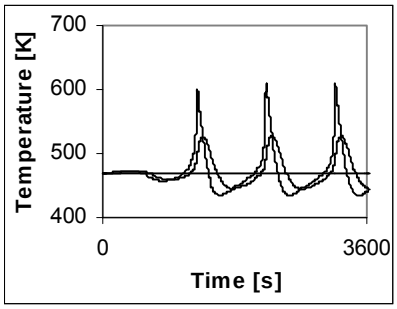

Figure 90a K_c = 0.9. τ_d = **10** [s].

Figure 90b K_c = 0.9. τ_d = **60** [s].

Figure 90c K_c = 0.9. τ_d = **120** [s].

A relatively short delay cannot provoke a stable, minimal controlled system to become unstable, according to Figure 90a. Increased delay makes the process less stable i.e. limit cycles will exhibit (Figure 90b) which are originated earlier in case delay is further increased (Figure 90c). In case a very high proportional gain is selected K_c > 100 and a long delay is presumed τ_d = 120 [s] the system will be absolutely unstable i.e. limit cycles will occur. This is because this particular base case coolant temperature multiplicity is not in question. Therefore, extinction or runaway will not take place. The most unstable situation to fall into is the occurrence of limit cycles.
Stability map (Figure 88) shows that an estimated delay τ_d < 60 [s] has no dramatically effect on the stability of the process i.e. the proportional gain has only to be slightly increased. For a significantly longer delay τ_d, the proportional gain has to be considerably larger to avoid limit cycles. If the non-ideal aspect can be translated into a delay $\tau_d \approx 60$ [s] a proportional gain K_c = 1.3 would be sufficient to eliminate limit cycles. In this particular case, the larger K_c, the more stability is acquired. In next chapter on the other hand, it will be shown that in other cases too large K_c causes conversely instability, especially if multiplicity is considered. Another noticeably effect is the fact that the oscillation frequency increases in case K_c is increased.

Summarising

Consequently, delay makes a process less stable. In case the non-ideal presumed delay equation is implemented in the model, the proportional gain has to be increased to remove limit cycles. However, too large delay cannot be controlled properly to prevent instability.

11.1.2 Controlling the coolant flowrate

Mathematical model

The delay is mathematically described with equation 49 and appended to the mathematical models of the proportional controlled coolant flowrate.

$$V_R \frac{d[A]}{dt} = \Phi_V \left([A]_0 - [A]\right) - V_R k_0 e^{-E_{act}/RT}[A] \tag{2}$$

$$\rho C_P V_R \frac{dT}{dt} = \rho C_P \Phi_V \left(T_0 - T\right) + \left(-\Delta H_R\right) V_R k_0 e^{-E_{act}/RT}[A] - UA\left(T - T_{cool}\right) \tag{3}$$

$$\rho_{cool} C_{P,cool} V_{cool} \frac{dT_{cool}}{dt} = \rho_{cool} C_{P,cool} \Phi_{V,cool} \left(T_{cool,0} - T_{cool}\right) + UA(T - T_{cool}) \tag{12}$$

$$\Phi_{V,cool} = \Phi_{V,cool,sp} - K_c \left(T_{sp} - T_d\right) \tag{42}$$

$$\tau_d \frac{dT_d}{dt} = T - T_d \tag{49}$$

Orbit curves

Lets consider the proportionally controlled base case, which behaves narrowly dynamically stable. If the delay is implemented, primarily limit cycles emerge (Figure 91a and b), which eventually causes extinction for a slightly larger delay (Figure 91c). A very small different initial condition can drastically affect the behaviour of a system. This has been confirmed by Doherty and Ottino[21].

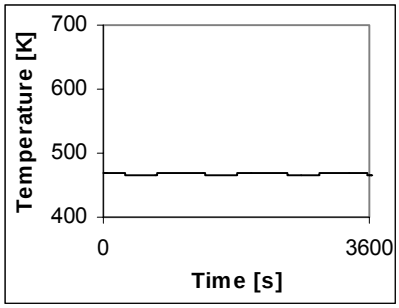

Figure 91a $T_{cool,0}$ = 303 [K], K_c = 0.0002 [$m^3\ s^{-1}\ K^{-1}$], τ_d **= 1** [s]. Small limit cycles.

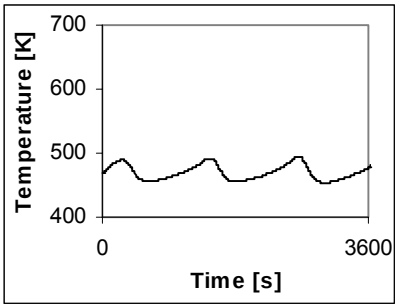

Figure 91b $T_{cool,0}$ = 303 [K], K_c = 0.0002 [$m^3\ s^{-1}\ K^{-1}$], τ_d **= 9** [s] limit cycles.

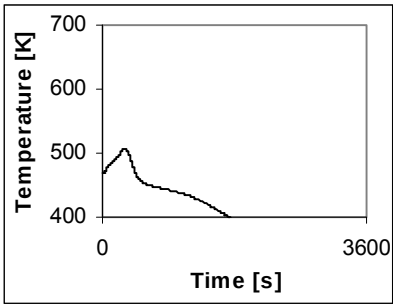

Figure 91c $T_{cool,0}$ = 303 [K], K_c = 0.0002 [$m^3\ s^{-1}\ K^{-1}$], τ_d **= 10** [s]. Extinction.

For the following orbit curves, the non-ideal behaviour has been arbitrarily chosen and presumed to be $\tau_d \approx 30$ [s]. The choice of the proportional gain is rather complicated. In Figure 92a, K_c is evidently not large enough causing extinction. In Figure 92b K_c is however, more robust though still limit cycles emerge. In Figure 92c K_c is too strong, in which the combination with delay eventually leads to the lower steady state i.e. extinction. This is due to the too late intervention of the controller.

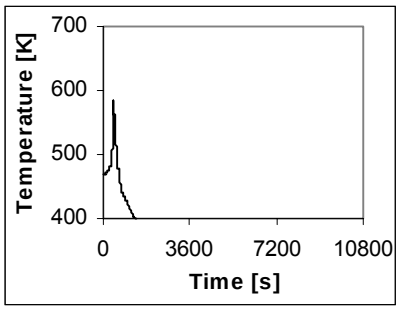

Figure 92a $T_{cool,0}$ = 303 [K], τ_d = 30 [s], K_c = **0.0001** [$m^3\ s^{-1}\ K^{-1}$],. Extinction

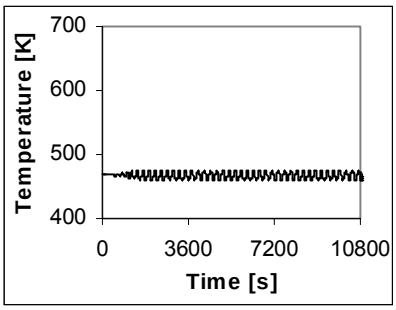

Figure 92b $T_{cool,0}$ = 303 [K], τ_d = 30 [s], $\mathbf{K_c = 0.001}$ [$m^3\ s^{-1}\ K^{-1}$], limit cycles.

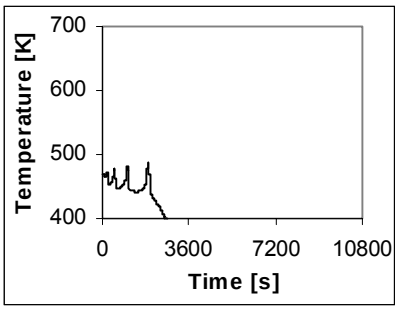

Figure 92c $T_{cool,0}$ = 303 [K], τ_d = 30 [s], $\mathbf{K_c = 0.01}$ [$m^3\ s^{-1}\ K^{-1}$], Extinction.

In Figure 93a the K_c value is sufficient enough to preserve stability after a disturbance. The disadvantage is that the stability is very unsteady and additionally the settling time is considerably long and the coolant flowrate varies enormously to eventually obtain a stable system (Figure 93b and c).

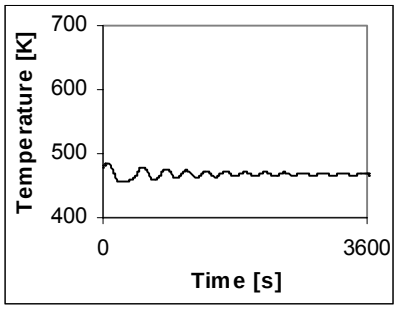

Figure 93a $T_{cool,0}$ = 303 [K], τ_d = 30 [s], $\mathbf{K_c = 0.0006}$ [$m^3\ s^{-1}\ K^{-1}$], Stable system. ΔT = +10 [K].

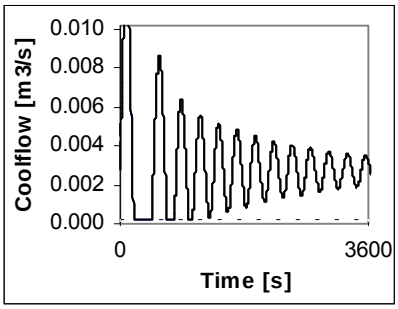

Figure 93b The Coolant flowrate fluctuates fairly. The valve actually has to be halted for several periods.

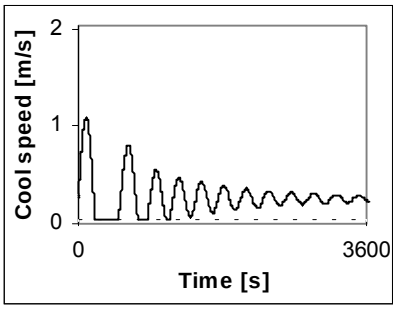

Figure 93c Coolant fluid velocity supposed the recycle stream = 10 × throughput (equation 84)

Reactor controller stability map

The following reactor controller stability maps have been constructed using active parameters K_c and the delay τ_d. These stability maps provide useful information with regard to the stability of the system. In Figure 94a,b the Hopf curves have been plotted for respectively $T_{cool,0}$ = 303 [K] and $T_{cool,0}$ = 400 [K].

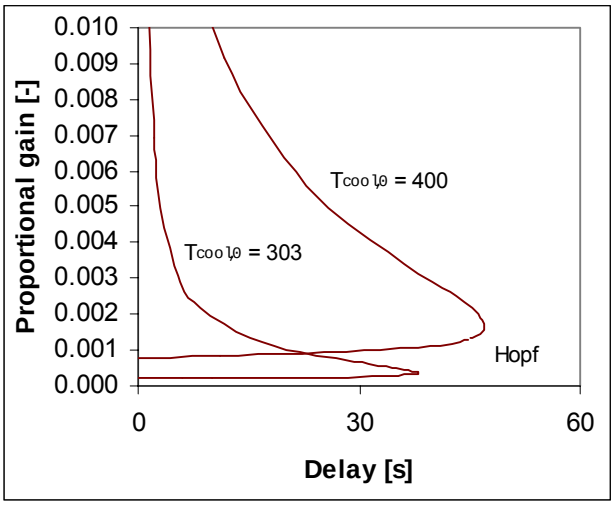

Figure 94a,b Reactor controller stability map. Hopf curves for $T_{cool,0}$ = 303 [K] and $T_{cool,0}$ = 400 [K]. Proportional gain versus delay. The process is stable at the left-hand side of each Hopf curve and unstable at the right-hand side.

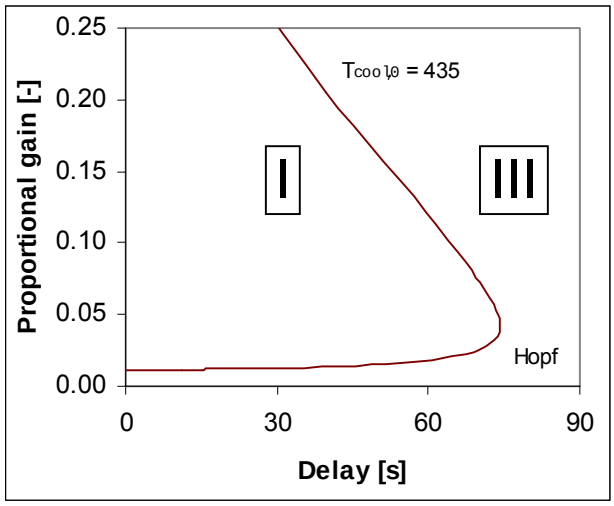

Figure 94c Reactor controller stability map. Hopf curves for $T_{cool,0}$ = 435 [K]. Proportional gain versus delay. The process is stable at the left-hand side of each Hopf curve and unstable at the right-hand side. The LOCBIF source LOCBIF rhs 15 is included in Appendix 7.

Discussion of the reactor controller stability map:

- In case delay is implemented in the model with respect to the proportional controlled coolant flowrate, a proportional gain can be found in between a particular range, in which a stable process without limit cycles can be acquired.
- The area at the left hand side of each Hopf curve encloses the stable region I, at the right hand side the unstable region III. For $T_{cool,0}$ = 303 [K] this results to Figure 94c.
- In Table 29 the range is printed in which stability is concerned. The K_c regarding Figure 93, in which the system appears to be stable, matches with the results in Table 29.
- The delay is less dangerous for larger inlet coolant temperatures.

Table 29 P-control coolant flowrate. Presumed delay τ_d = 30 [s].

Inlet coolant temperature $T_{cool,0}$ [K]	K_c (min)	K_c (max)
303	0.00036	0.00065
400	0.00088	0.0046
435	0.011	0.25

Summarising

In case of proportional controlled coolant flowrate, delay makes a process less stable. In case the non-ideal presumed delay added to the mathematical model, the proportional gain has to be increased to remove limit cycles. However, too large delay means extinction and subsequently the lower steady state.

11.1.3 Controlling the throughput

Mathematical model

$$V_R \frac{d[A]}{dt} = \Phi_V ([A]_0 - [A]) - V_R k_0 e^{-E_{act}/RT}[A] \quad (2)$$

$$\rho C_P V_R \frac{dT}{dt} = \rho C_P \Phi_V (T_0 - T) + (-\Delta H_R) V_R k_0 e^{-E_{act}/RT}[A] - UA(T - T_{cool}) \quad (3)$$

$$\Phi_V = \Phi_{V,sp} - K_c (T_{sp} - T_d) \quad (43b)$$

$$\tau_d \frac{dT_d}{dt} = T - T_d \quad (49)$$

Reactor controller stability map

The following reactor controller stability map has been constructed using active parameters K_c and the delay τ_d.

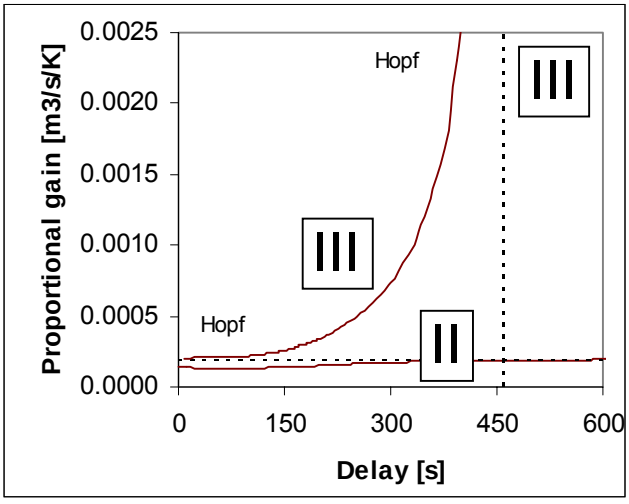

Figure 95 Reactor controller stability map. Proportional controlled throughput with delay. The maximum delay is τ_d = 458 [s].

Discussion of the reactor controller stability map:

- Figure 95 consists more than one Hopf curve, which confirm the appearance of multiplicity.
- K_c > 0.00014 [m^3 s^{-1} K^{-1}] indicates the transition from region II to region III.
- Larger delay implies larger K_c values. Asymptotic value: τ_d = 458 [s]. Nonetheless, because throughput control is difficult and transition is always to be concerned with, this value is not as useful as in case of coolant temperature control, because at the left hand side no region I can be found.
- In the previous section through Figure 73, a K_c > 0.002 [m^3 s^{-1} K^{-1}] is pointed out to acquire a stable process. Figure 95 does not confirm this. This can be due to the fact that LOCBIF sometime has problems with finding an initial point. This is probable because of the occurrence of multiplicity.

Orbit curves

To study the effect of delay, several orbits curves are produced with LOCBIF. Again, the proportional gain has been chosen K_c = 0.002 [m^3 s^{-1} K^{-1}] for all the to examine situations. In Figure 96 a delay τ_d = 30 [s] cannot provoke a system become unstable after an external temperature disturbance. In Figure 97 the flowrate fluctuates in the first minute and becomes quickly stabilised, however the flowrate fluctuations are too large. The initial error (constrained temperature disturbance) causes a flowrate deviation of –75%. The controller corrects primarily in the right direction but oscillates sincerely resulting in a overshoot of +18% and accordingly –82%, 56% etc and is finally after about 1 hour at the desired steady state, which adversely is not the base case steady state situation i.e. a steady state with higher temperature although with lower conversion. In Figure 98 the delay is slightly increased to τ_d = 32 [s] and causes the system to runaway.

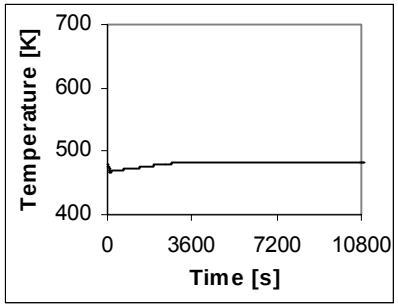

Figure 96 K_c = 0.002 [m^3 s^{-1} K^{-1}] ΔT = 10 [K], τ_d = 30 [s], Stability. Higher steady state.

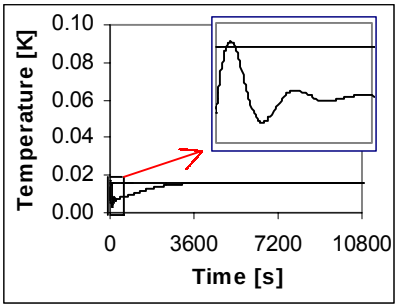

Figure 97 K_c = 0.002 [m^3 s^{-1} K^{-1}] ΔT = 10 [K], τ_d = 30 [s], A higher stable steady state is reached τ_R = 350 [s] ζ = 0.47 and T = 472 [K].

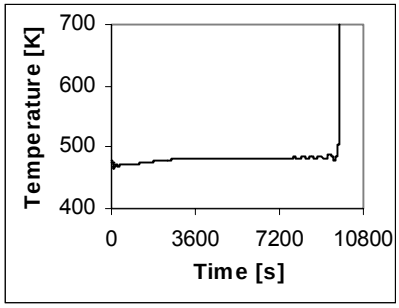

Figure 98 K_c = 0.002 [m^3 s^{-1} K^{-1}] ΔT = 10 [K], τ_d = 32 [s]. Runaway.

In Figure 99 the delay is again increased to τ_d = 60 [s] but no disturbance is constrained. The system remains scarcely stable. The flowrate causes the jump to a higher steady state with lower conversion (Figure 100).

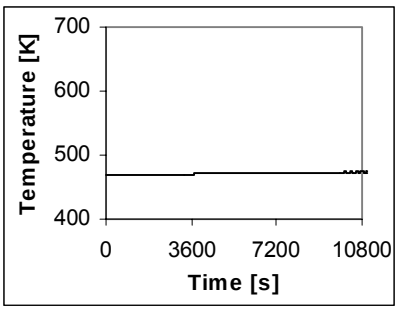

Figure 99 K_c = 0.002 [m^3 s^{-1} K^{-1}] ΔT = 0 [K] delay = 60 [s]. The system is considered stable.

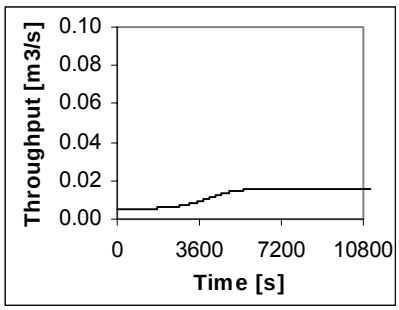

Figure 100 K_c = 0.002 [m^3 s^{-1} K^{-1}] ΔT = 0 [K] delay = 60 [s]. A higher steady state however is reached τ_R = 350 [s] ζ = 0.47 and T = 472 [K].

In case in Figure 99 is simulated with a disturbance, runaway pursues (Figure 101) caused by the flowrate fluctuations (Figure 102).

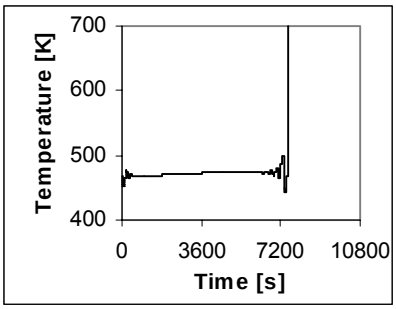

Figure 101 K_c = 0.002 [m^3 s^{-1} K^{-1}] ΔT = 10 [K] delay = 60 [s]. Runaway. The LOCBIF source LOCBIF rhs 17 is included in Appendix 7.

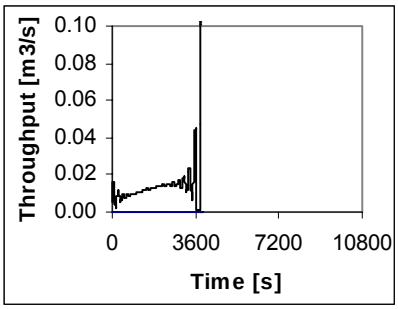

Figure 102 K_c = 0.002 [m^3 s^{-1} K^{-1}] ΔT = 10 [K] delay = 60 [s]. Flowrate varies suchlike that the process cannot be controlled reliable.

Summarising

In previous sections is became clear that controlling the throughput had the disadvantage that it is not possible to preserve the base case situation. Due to the dynamical instability, on the one hand, a large K_c is necessary, however on the other hand, large K_c cause in particular after a disturbance a considerable overshoot causing often transition. Even if transition does not occur, the flowrate fluctuation is sincere and one cannot preserve the commitment to keep the flowrate deviation between only a few percent. The introduction of delay principally deteriorates the stability in general.

11.2 Proportional-integral control

11.2.1 Controlling the coolant temperature

Mathematical model

The mathematical system consist of the following equations:

$$V_R \frac{d[A]}{dt} = \Phi_V \left([A]_0 - [A]\right) - V_R k_0 e^{-E_{act}/RT}[A] \tag{2}$$

$$\rho C_P V_R \frac{dT}{dt} = \rho C_P \Phi_V \left(T_0 - T\right) + \left(-\Delta H_R\right) V_R k_0 e^{-E_{act}/RT}[A] - UA\left(T - T_{cool}\right) \tag{3}$$

$$T_{cool} = T_{cool,sp} + K_c\left(T_{sp} - T_d\right) + \frac{K_c}{\tau_I}\int_0^1 \left(T_{sp} - T_d\right) dt \tag{46}$$

$$\tau_d \frac{dT_d}{dt} = T - T_d \tag{49}$$

Reactor controller stability map

A stability map is created (Figure 103) similar to the proportional controlled base case model (Figure 88).

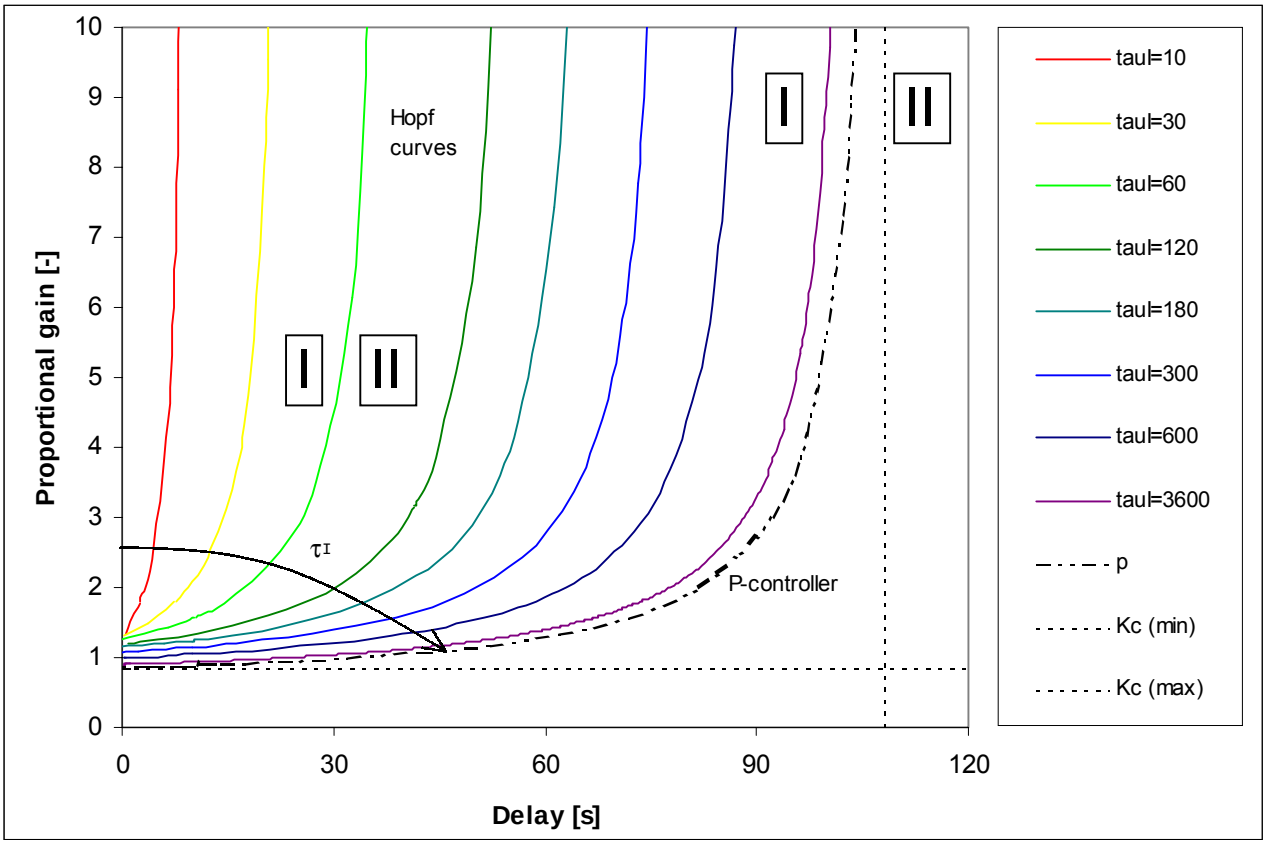

Figure 103 Reactor controller stability map with Hopf curves for increasing integral time vales. The dotted line ($\tau_I \rightarrow \infty$) is similar to the proportional controlled base case model Figure 88. If τ_d > 108 [s] limit cycles will certainly appear regardless the extent of delay. At the left-hand side of one particular Hopf curve the behaviour is dynamically stable and ate the right-hand side ergo unstable. The LOCBIF source LOCBIF rhs 14 is included in Appendix 7.

Discussion of the reactor controller stability map:

- In the actual stability map, Hopf curves are drawn for increasing values of the integral time. The dotted line ($\tau_I \rightarrow \infty$) is similar to the Hopf curve in Figure 88 and coincides with the ordinate for the formerly found value K_c = 0.9.
- To determine the stable and unstable regions in Figure 103, one has to select a particular Hopf curve in accordance with a specific integral time. The region on the left hand side is the stable region and on the right hand side the region in which limit cycles occur.
- In case the delay is increased, the K_c value rises severely to preserve stability. For ($\tau_I \rightarrow \infty$) the same delay τ_d =108 [s] is found (Figure 88) if merely P-controller is considered. For smaller integral times, the asymptotic value decreases.
- Figure 103 proves that the integral action n combination with delay can adversely affect the stability. The shorter the integral time, the higher the proportional gain. An arbitrary integral time constant is chosen e.g. τ_I = 60 [s].

Orbit curves

Through Figure 74 it was determined that K_c = 1.35 is robust enough to preserve stability. Introducing an estimated delay τ_d = 10 [s] disrupts the stability and causes limit cycles (Figure 104a). Decreasing the integral time close to the assumed delay, nevertheless larger, causes limit cycles (Figure 104b). In case the delay exceeds the integral time, the system becomes seriously unstable (Figure 104c). Therefore, it is

essential to acquire an integral time considerably larger than the assumed delay. Several simulations indicate that approximately $\tau_I \geq 10 \times \tau_d$ has good results, because the integral time amply overlaps the delay. Subsequently a proportional gain can be selected in which the overshoot is optimal i.e. ratio a/b = 4/1, (§5.6.2). The main conclusion is that large K_c values are needed to eliminate the self-sustained oscillations. However, too large K_c values in combination with delay can provoke instability. The advantage of the integral action is the fact that the offset is removed. It is desired that the offset is decreased as soon as possible i.e. small τ_I. However, if the assumed delay exceeds the integral time, a very unstable process is definitely resulting.

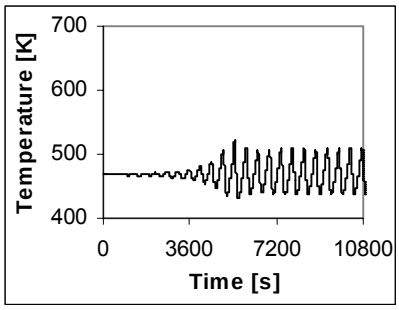

Figure 104a Orbit curve. K_c = 1.35, τ_I = 60 [s], **τ_d = 10 [s]**. Dynamical behaviour: limit cycles.

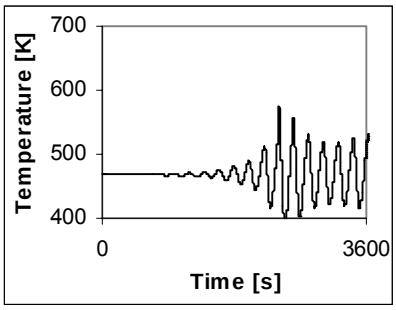

Figure 104b Orbit curve. K_c = 1.35, τ_I = 10 [s], **τ_d = 5 [s]**. Dynamical behaviour: limit cycles.

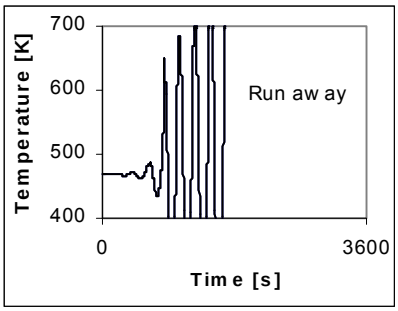

Figure 104c Orbit curve. K_c = 1.35, τ_I = 10 [s], **τ_d = 20 [s]**. Dynamical behaviour: run away i.e. integral windup.

Summarising

Delay can be the cause of instability during a process, which operates at stable steady state. The proportional gain is decisive for its stability. In case of coolant temperature control in which no delay is involved, the integral time has a minor effect on the stability of the process. If delay however is taken into account, it is crucial that the integral time is considerably larger than the delay. Otherwise, instability is inevitable.

11.2.2 Controlling the coolant flowrate

Mathematical model

The PI-controlled coolant flowrate with delay is mathematical described with:

$$V_R \frac{d[A]}{dt} = \Phi_V \left([A]_0 - [A]\right) - V_R k_0 e^{-E_{act}/RT}[A] \tag{2}$$

$$\rho C_P V_R \frac{dT}{dt} = \rho C_P \Phi_V \left(T_0 - T\right) + \left(-\Delta H_R\right) V_R k_0 e^{-E_{act}/RT}[A] - UA\left(T - T_{cool}\right) \tag{3}$$

$$\rho_{cool} C_{P,cool} V_{cool} \frac{dT_{cool}}{dt} = \rho_{cool} C_{P,cool} \Phi_{V,cool} \left(T_{cool,0} - T_{cool}\right) + UA(T - T_{cool}) \tag{12}$$

$$\Phi_{V,cool} = \Phi_{V,cool,sp} - K_c \left(T_{sp} - T_d\right) - \frac{K_c}{\tau_I} \int_0^1 \left(T_{sp} - T_d\right) dt \tag{47}$$

$$\tau_d \frac{dT_d}{dt} = T - T_d \tag{49}$$

Orbit curves

The destabilising effect of delay will be demonstrated through the following orbit curves. Lets consider the proportional-integral controlled base case, which primarily behaves dynamical stable. After an external disturbance, a small delay τ_d = 1 [s] cannot disturb the stable situation (Figure 105a). A larger delay τ_d = 10 [s] disorders the process which exhibits limit cycles (Figure 105b). Larger delay eventually causes extinction (Figure 105c).

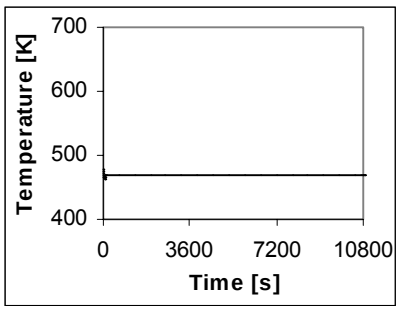

Figure 105a $T_{cool,0}$ = 303 [K], K_c = 0.00025 [m^3 s^{-1} K^{-1}], τ_I = 600 [s], ΔT = +10 [K], **τ_d = 1 [s]**

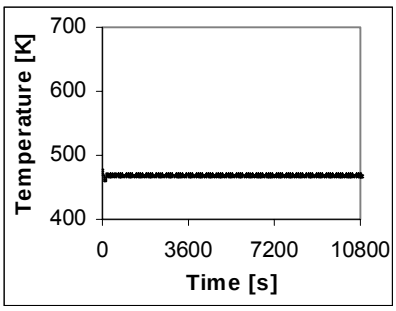

Figure 105b $T_{cool,0}$ = 303 [K], K_c = 0.00025 [m^3 s^{-1} K^{-1}], τ_I = 600 [s], ΔT = +10 [K], **τ_d = 10 [s]**.

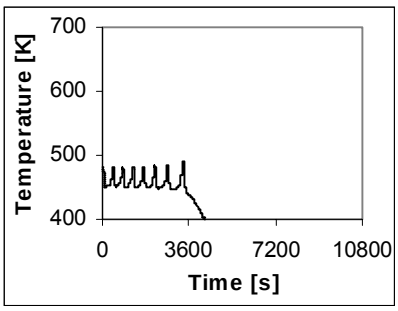

Figure 105c $T_{cool,0}$ = 303 [K], K_c = 0.00025 [m^3 s^{-1} K^{-1}], τ_I = 600 [s], ΔT = +10 [K], **τ_d = 30 [s]**.

Reactor controller stability map

For the stability map (Figure 106), active LOCBIF bifurcation parameters K_c and the delay are used. Due to the fact that LOCBIF couldn't find a (initial) solution, the stability map is exclusively created for $T_{cool,0}$ = 303 [K]. The principles remain the same for $T_{cool,0}$ = 400 [K] and $T_{cool,0}$ = 435 [K].

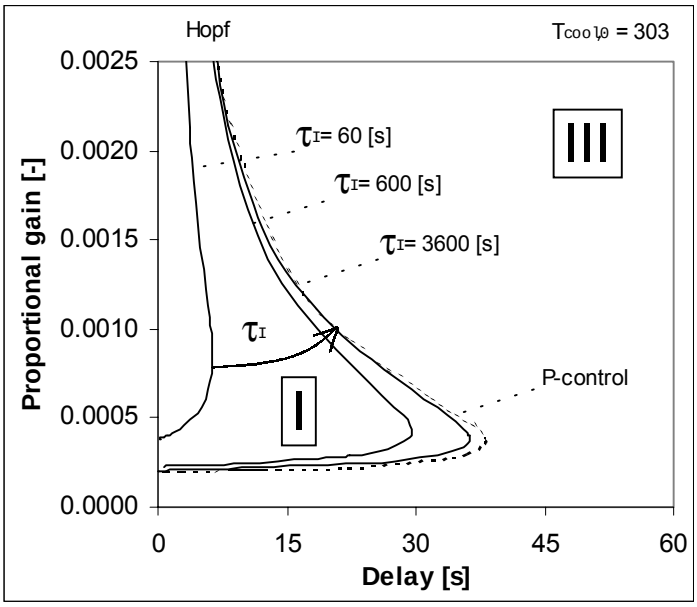

Figure 106 Reactor controller stability map with Hopf curves for $T_{cool,0}$ = 303 [K]. Proportional gain versus delay. The LOCBIF source LOCBIF rhs 16 is included in Appendix 7. The left-hand side of each Hopf curve for one particular inlet coolant temperature indicates stability and vice versa the right hand side instability.

Discussion of the reactor controller stability map:

- The area at the left-hand side of each Hopf curve encloses the stable region I, at the right-hand side the unstable region III.
- The figure shows that for smaller integral time, a considerably larger proportional gain is needed.
- The dotted line matches Figure 94 for merely proportional control.
- For particular small integral times, a considerable large proportional gain is required to maintain stability.
- Beyond a particular value, instability is inevitable.

Summarising

In case of the integral action is considered combined with delay instability can be the consequence. Large integral time values increase the stable region.

11.2.3 Controlling the throughput

Mathematical model

The mathematical notation with regards to the PI-controlled throughput with delay:

$$V_R \frac{d[A]}{dt} = \Phi_V \left([A]_0 - [A]\right) - V_R k_0 e^{-E_{act}/RT}[A] \tag{2}$$

$$\rho C_P V_R \frac{dT}{dt} = \rho C_P \Phi_V \left(T_0 - T\right) + \left(-\Delta H_R\right) V_R k_0 e^{-E_{act}/RT}[A] - UA\left(T - T_{cool}\right) \tag{3}$$

$$\Phi_V = \Phi_{V,sp} - K_c \left(T_{sp} - T_d\right) - \frac{K_c}{\tau_I}\int_0^1 \left(T_{sp} - T_d\right) dt \tag{48}$$

$$\tau_d \frac{dT_d}{dt} = T - T_d \tag{49}$$

Reactor controller stability map

For the stability map, K_c has been drawn versus τ_d.

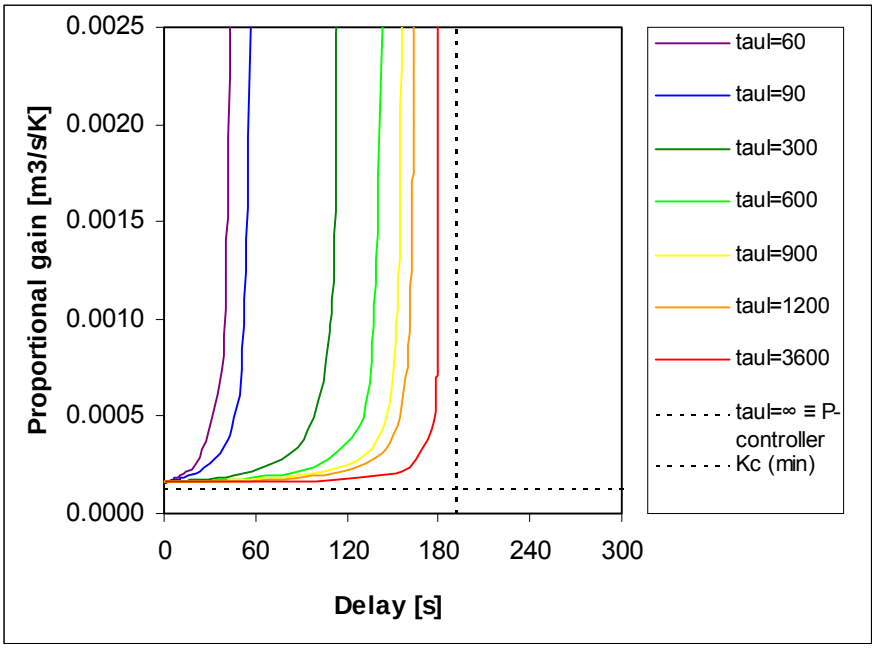

Figure 107 Reactor controller stability map. Proportional + integral control flowrate with delay. The LOCBIF source LOCBIF rhs 18 is included in Appendix 7.

Discussion of the reactor controller stability map:

- The implementation of delay in the model resulting in the stability map Figure 107 shows that for small integral time the proportional gain increases dramatically from which can be concluded that the integral time should be larger than the delay with respect to stability.
- Increasing the integral time results in shifting the Hopf curve to the right. In fact $\tau_I \rightarrow \infty$ the curves matches the lower curve of Figure 95 (K_c = 0.00014 [m^3 s^{-1} K^{-1}]). Therefore, the upper Hopf curve in Figure 95, for varying integral times, cannot be found with LOCBIF. This is due to the existence of multiplicity. LOCBIF requires suitable initial numerical values, which are sometime not obtainable.
- The asymptotic delay value for $K_c \rightarrow \infty$ states τ_d = 192 [s]. In case τ_d > 192 [s] LOCBIF provides no solutions for Figure 107. One can expect, despite the lack in Figure 107, that at the right-hand side for considerably large delay, the process behaves unstable.
- In exclusively P-control (Figure 95), an asymptotic value: τ_d = 458 [s] has been found. For PI-control, the asymptotic value is τ_d = 192 [s] has been found, whereas for $\tau_I \rightarrow \infty$ the asymptotic τ_d = 458 [s] should be expected.
- Apparently, the combination of delay and integral time together with multiplicity can sometimes give some simulation problems. This is perhaps due to the appearing of more asymptotic Hopf curves (maximum values), which might interfere with other Hopf, curves. It could be so that the asymptotic value of one predominate the other. Therefore, another asymptotic value will be found.

Summarising

Controlling the throughput, using PI-action, combined with presumed delay confirms the formerly presented conclusion: which is that throughput control compared to cooling control is not a suitable method to eliminate limit cycles and preserve stability with the same reactor temperature and conversion.

11.3 Process capacity

The process capacity is explained in paragraph 5.5.

11.3.1 Process time constant

Mathematical model

The mathematical model for the CISTR states:

$$\tau_R \frac{d[A]}{dt} = ([A]_0 - [A]) - \frac{V_R}{\Phi_V} k_0 e^{-E_{act}/RT}[A] \tag{33}$$

$$\tau_R \frac{dT}{dt} = (T_0 - T) + \frac{V_R}{\Phi_V} \frac{(-\Delta H_R)}{\rho C_P} k_0 e^{-E_{act}/RT}[A] - \frac{UA}{\Phi_V \rho C_P}(T - T_{cool}) \tag{34}$$

In which the process time constant becomes:

$$\tau_R = \frac{V_R}{\Phi_V} + \frac{m_{equipment} C_{P,equipment}}{\rho C_P \Phi_V} + \ldots \tag{51}$$

Reactor controller stability map

If the reactor controller is interested in the influence of process equipment on the dynamical behaviour of a process, a plot like Figure 108 can be constructed.

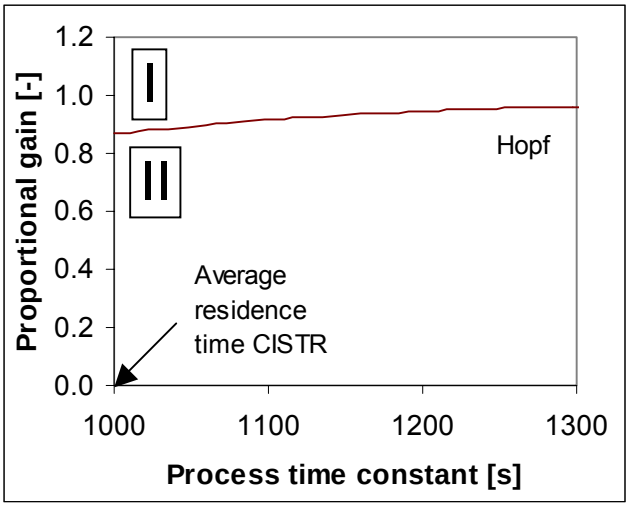

Figure 108 Reactor controller stability map with Hopf curve. The proportional gain has to be increased slightly to preserve stability, if the influence of the CISTR equipment is taken into account.

Discussion of the reactor controller stability map:

- If exclusively the base case is considered, the particular time constant is equal to the average residence time of the CISTR. $\tau_R = V_R/\Phi_V = 1000$ [s]
- If the external elements are concerned with through equation 35, a slower responding process is to be expected e.g. heating up of the CISTR wall etc. Consequently, a larger proportional gain is then required to maintain stability.

- If the process time is increased as Hopf bifurcation parameter, Figure 108 confirms the increase of K_c. Nevertheless, if the time constant is composed of reactor wall, cooling equipment, stirrer etc., its maximum value states approximately $\tau_R \approx 1200$ [s] compared with $\tau_R = 1000$ [s], which means according to Figure 108 that K_c should be increased with 9%. Therefore, the influence of process equipment moderate affects the value of the proportional gain.

11.3.2 Cooling time constant

In §5.5.2 the coolant differential equation 36 has been postulated in which τ_{cool} represents the cooling time constant.

Mathematical model

The mathematical model states:

$$\tau_{cool}\frac{dT_{cool}}{dt} = \left(T_{cool,0} - T_{cool}\right) + \frac{UA}{\rho_{cool}C_{P,cool}V_{cool}}(T - T_{cool}) \tag{36}$$

In which the cooling time constant becomes:

$$\tau_{cool} = \frac{V_{cool}}{\Phi_{V,cool}} + \frac{m_{equipment}C_{P,equipment}}{\rho_{cool}C_{P,cool}\Phi_{V,cool}} + \ldots \tag{38}$$

Equation 38 clearly demonstrate that τ_{cool} increases if the physical properties of the equipment is concerned with. A larger τ_{cool} implies that the response of the process becomes slower. The latter can perhaps affect the behaviour of the system. According to Roffel[68] through the lack of information, the physical meaning of equation 38 is difficult to determine. Therefore, analysing exclusively the parameter τ_{cool} can provide some information with respect to the dynamical behaviour of the process.
Based on the data printed in Appendix 3 (Table 38) and equation 38 the value of the cooling time constant can be estimated. It is presumed that the cooling equipment has been constructed from stainless steel. The results from Table 30 confirm the capability of the cooling equipment to store energy which is obvious considering that if the reactor temperature increases it takes time to bring the cooling equipment to the same temperature as the reactor contents resulting in a slower response to changes.

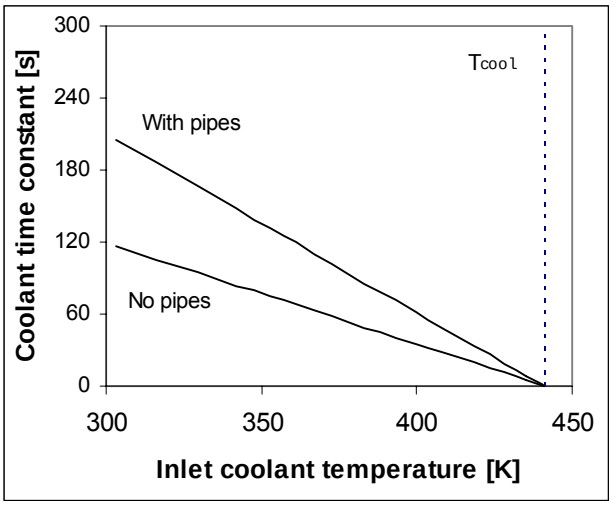

Figure 109 Coolant time constant versus inlet coolant temperature.

Table 30 Time constants coolant. Results (dotted lines in Figure 110).

Time constant coolant	$T_{cool,0}$ = 303 [K]	$T_{cool,0}$ = 400 [K]	$T_{cool,0}$ = 435 [K]
τ_{cool}(no pipes)	117	35	5
τ_{cool}(with pipes)	205	61	9

Reactor controller stability map proportional control

If coolant flowrate proportional control is considered, the following stability map can be drawn. In Figure 110 the proportional gain is drawn against the cooling time constant.

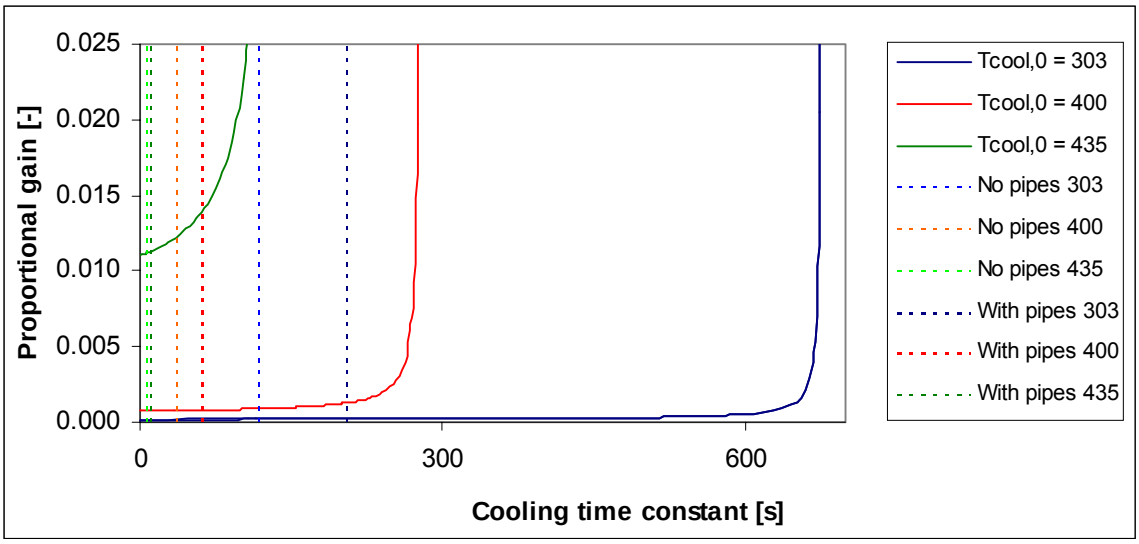

Figure 110 Reactor controller stability map. Influence cooling time constant for various inlet coolant temperatures.

Discussion of the reactor controller stability map:

- The magnitude of the cooling time constant becomes considerably relevant in case
  For $T_{cool,0}$ = 303 [K] τ_{cool} > 650 [s]
  For $T_{cool,0}$ = 400 [K] τ_{cool} > 250 [s]
  For $T_{cool,0}$ = 435 [K] τ_{cool} > 0 [s].
- The latter can be explained by the fact that due to the minor temperature difference between the cooling set point and the coolant inlet temperature even the slightest disturbance has a tremendous effect.

Orbit curves

The cooling time constant in fact causes a particular delay. Figure 111 and Figure 112 prove that the cooling device can cause instability.

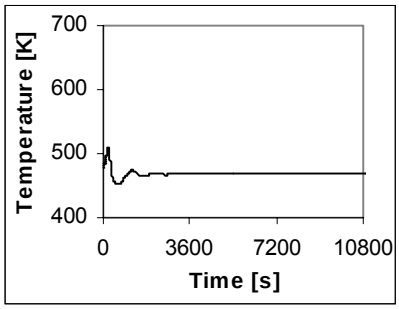

Figure 111 Orbit curve. K_c = 0.00025 [$m^3\ s^{-1}\ K^{-1}$], $T_{cool,0}$ = 303 [K], ΔT = 10 [K], $\Phi_{V,cool}$ (set point) = **5.6×10^{-3}** [$m^3\ s^{-1}$]. τ_{cool} = **56** [s].

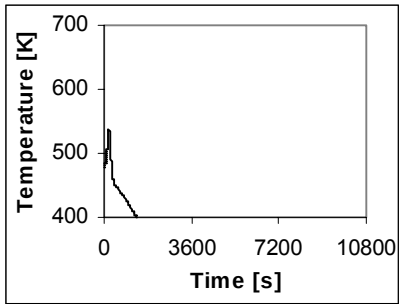

Figure 112 Orbit curve. K_c = 0.00025 [$m^3\ s^{-1}\ K^{-1}$], $T_{cool,0}$ = 303 [K], ΔT = 10 [K], $\Phi_{V,cool}$ (set point) = **2.6×10^{-3}** [$m^3\ s^{-1}$]. τ_{cool} = **98** [s]

Reactor controller stability map proportional-integral control

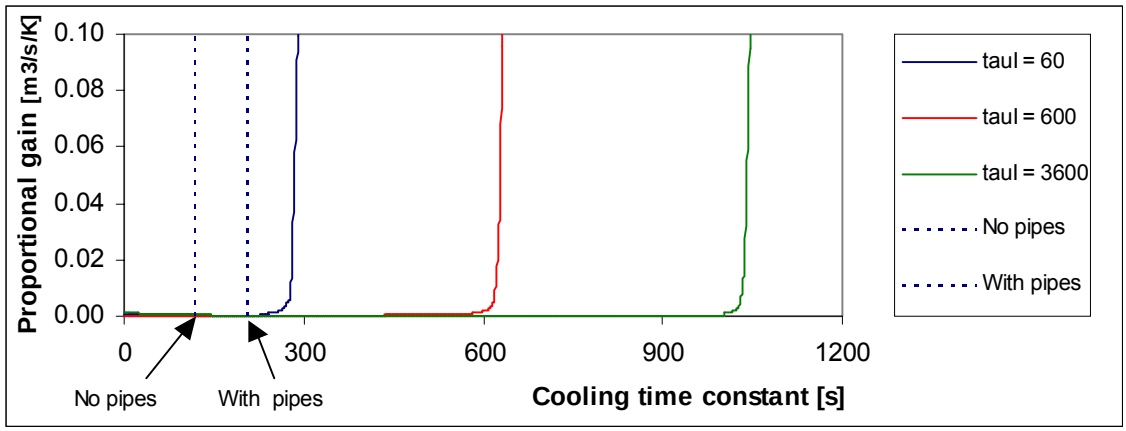

Figure 113 Reactor controller stability map. The influence of the coolant time constant.$T_{cool,0}$ = 303 [K].

Discussion of the reactor controller stability map:

- The values have been retrieved from Table 30 results (dotted lines in Figure 113, Figure 114 and Figure 115).
- If the $\tau_I \rightarrow \infty$ the curves from Figure 110 are again acquired (proportional control only).
- The figures demonstrate that in case a small integral time is chosen, the coolant time constant becomes more crucial.

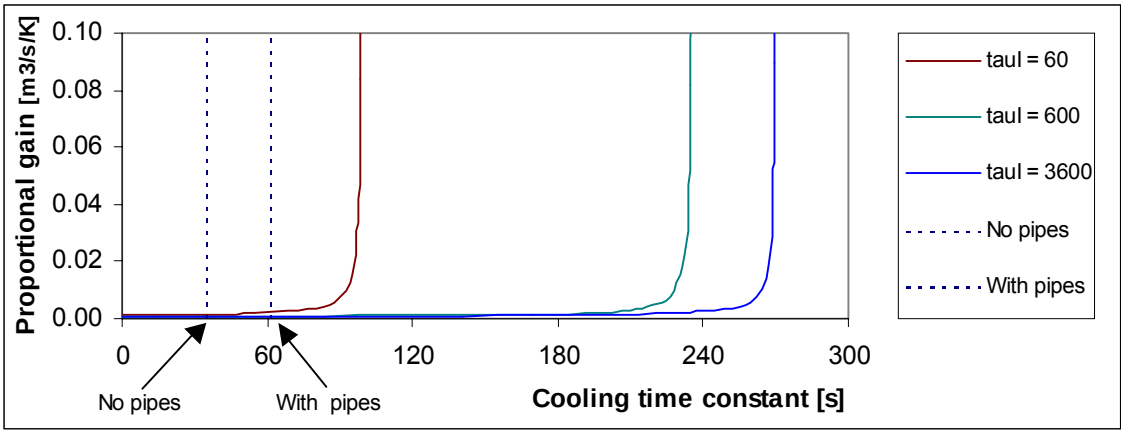

Figure 114 Reactor controller stability map. The influence of the coolant time constant.$T_{cool,0}$ = 400 [K].

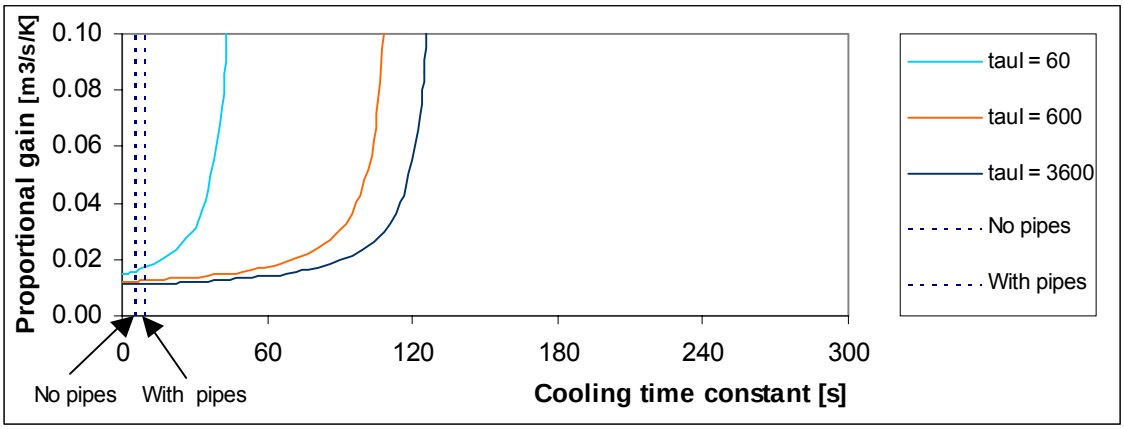

Figure 115 Reactor controller stability map. The influence of the coolant time constant.$T_{cool,0}$ = 435 [K].

Summarising

In fact, the process time constant acts as a certain delay. If of a particular process the mathematical description is available, the process engineer can easily modify the time constant of the actual differential equations, in which the influence of process equipment can be examined. With respect to the base case, if the base case is adequately controlled i.e. not too low K_c and τ_I, in which a low inlet coolant temperature is chosen, the process capacity does not affect the overall stability.

Chapter XII

12 CONTROLLER CONFIGURATION TUNING

In this chapter, a suitable controller configuration is searched for the base case to eliminate limit cycles and preserve stability. Therefore the reactor temperature is disturbed ΔT = 20 [K] and an arbitrary chosen delay τ_d = 30 [s] is concerned with to improve the physical realism. Firstly, the Ziegler Nichols controller tuning method (explained in §5.6.3) is examined. Accordingly, the proportional gain and the integral time are varied to study the effect on the process stability. Finally, the important issues and strategy regarding stability control is to be considered (presented in (§5.6.4).

12.1 Controlling the coolant temperature

12.1.1 Ziegler Nichols tuning method

If the Ziegler Nichols methodology is applied for proportional control only, the self-sustained oscillations have been acquired (Figure 116a). According to the method the integral time is set to infinite $\tau_I \rightarrow \infty$. A proportional gain K_U = 0.96 is obtained and an ultimate period of sustained cycling P_U = 16 [min]. The contradiction appears due to the fact that limit cycles system exhibit even if K_c = 0. Therefore, a proportional gain is searched for the transition between limit cycles and spiral point. The resolved Ziegler Nichols controller-tuning configuration becomes:

K_c = 0.43 [-] and τ_I = 760 [s].

According to Figure 116b this configuration is not robust enough to eliminate limit cycles. In this particular case the Ziegler Nichols tuning method is not suitable to provide a stable system. Apparently, this tuning method does not take into account dynamically instabilities like limit cycles and is developed for static instability problems only.

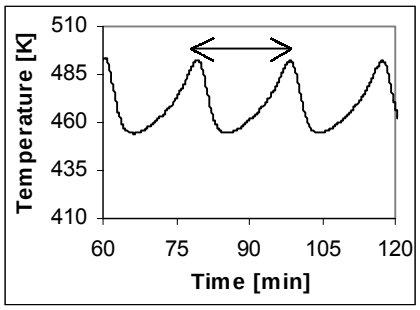

Figure 116a K_U = 0.98 [-], $\tau_I \rightarrow \infty$ [s], ΔT = +20 [K], τ_d = 30 [s], P_U = 15.2 [min].

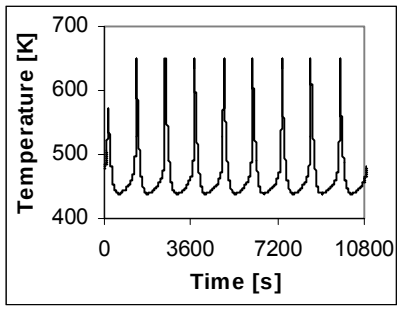

Figure 116b K_c = 0.43 [-] τ_I = 760 [s]., ΔT = +20 [K], τ_d = 30 [s].

12.1.2 Controller parameter variation

The following directives can provide a reasonably appropriate controller configuration, which preserves stability:

- The generally accepted ¼-decay criteria (§5.6.2) is qualitatively applied to determine a proportional gain, which minimises the settling time i.e. time needed for the response to settle within ±5% of the desired value.
- Because delay can be the occasion of instability during a process, the integral time must be considerably larger than the delay.
- Overshoot cannot be avoided, however peaks, which are too strong, are undesirable.
- The frequency of oscillation cannot be too high due the practical limitations of the actual process controller.

Table 31 Results various controller parameters. Step disturbance ΔT =20 [K], delay τ_d = 30 [s].

Proportional gain	Integral time		
	τ_I = 60 [s]	τ_I = 600 [s]	τ_I = 3600 [s]
K_c = 1 [-]	Figure 117	Figure 118	Figure 119
K_c = 5 [-]	Figure 120	Figure 121	Figure 122
K_c = 10 [-]	Figure 123	Figure 124	Figure 125
K_c = 100 [-]	Figure 126	Figure 127	Figure 128

Figure 117-Figure 119 show visibly that the proportional gain K_c = 1 [-] is not robust enough to reduce the self-sustained oscillations.

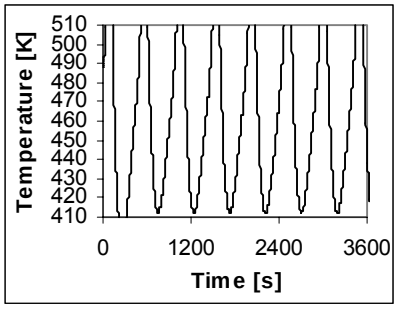

Figure 117 K_c = 1, τ_I = **60**.

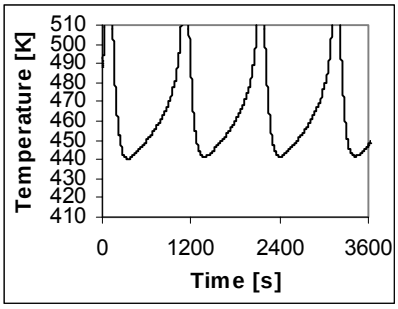

Figure 118 K_c = 1, τ_I = **600**.

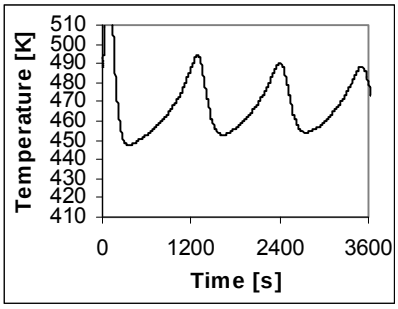

Figure 119 K_c = 1, τ_I = **3600** [s].

In case the proportional gain is increased to K_c = 5 [-] the limit cycles can be repressed. However, a small integral time results in a long settling time (Figure 120). An integral time τ_I = 600 [s] conversely offers rapidly a stable system with a small settling time and without too excessive overshoot (Figure 121). Larger integral time has no improvement effect on the stability (Figure 122).

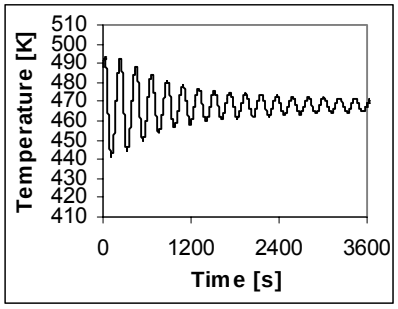

Figure 120 K_c = 5, τ_I = **60** [s].

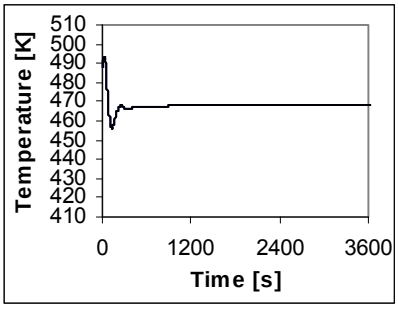

Figure 121 K_c = 5, τ_I = **600** [s].

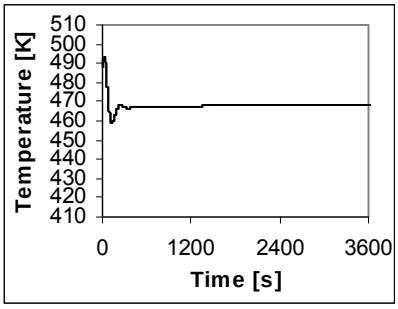

Figure 122 K_c = 5, τ_I = **3600** [s].

A larger proportional gain K_c = 10 [-] Figure 123- Figure 125, decreased the settling time. Although this improvement, it is not recommended tot chose a too large proportional gain due to the fact that the in case the assumed delay τ_d = 30 [s] has been underestimated, the stability of the process could be at risk.

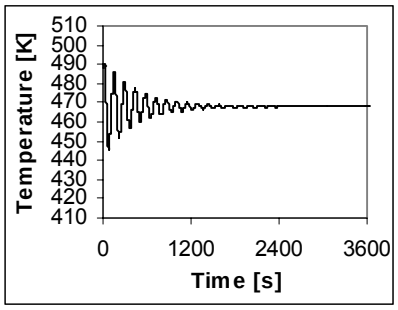

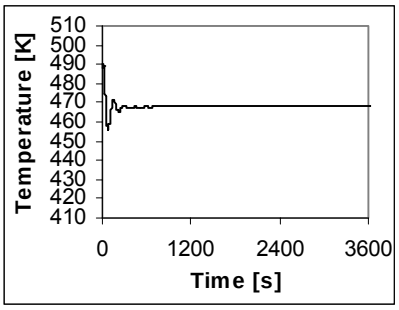

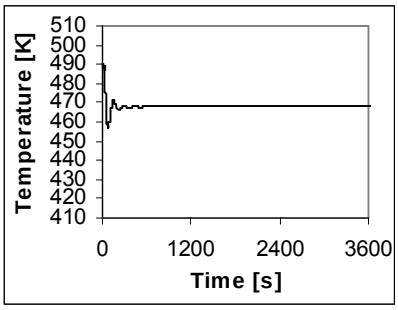

Figure 123 K_c = 10, τ_I = **60** [s]. **Figure 124** K_c = 10, τ_I = **600** [s]. **Figure 125** K_c = 10, τ_I = **3600** [s].

Further increasing the proportional gain (Figure 126-Figure 128) however decreases the settling time nevertheless raises the oscillation frequency. A process controller has a practical limited response time after an exhibiting disturbance, therefore too large K_c are unlikely.

Literature

The literature raises several directives to acquire controller parameters.
According to Shinskey[72] $\tau_I > 4\ \tau_d$. to achieve a self-regulating process, hence $\tau_I > 120$ [s].

$$\tau_I = \frac{m_R C_P}{UA} \tag{52}$$

According to Perry[59] the magnitude of the integral time can be estimated using correlation 52, consequently: $\tau_I \approx 160$ [s]. These values are clearly too small to acquire stability. An integral time τ_I = 600 [s] however is more appropriate value for this particular base case.

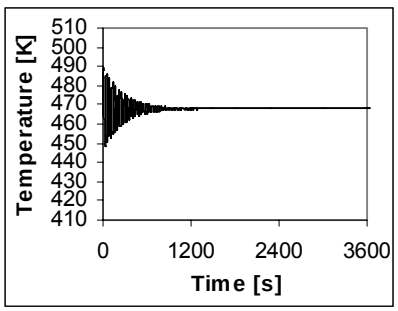

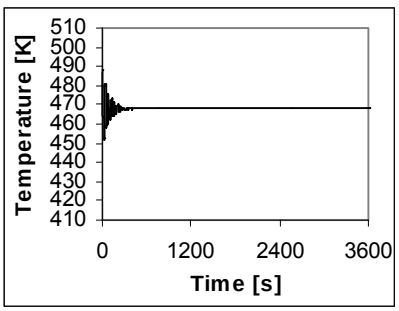

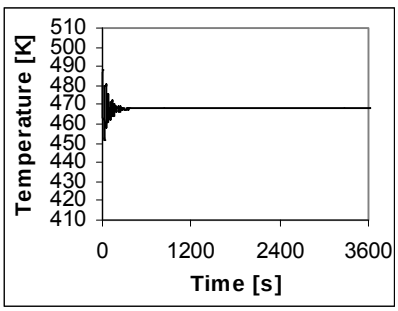

Figure 126 K_c = 100, τ_I = **60** [s]. **Figure 127** K_c = 100, τ_I = **600** [s]. **Figure 128** K_c = 100, τ_I = **3600** [s].

12.2 Controlling the coolant flowrate

12.2.1 Ziegler Nichols tuning method

A proportional gain K_U = 0.00052 [m^3 s^{-1} K^{-1}] is acquired and an ultimate period of sustained cycling P_U = 9 [min] (Figure 129). Therefore, the Ziegler Nichols controller-tuning configuration becomes:

K_c = 0.00023 [m^3 s^{-1} K^{-1}] and τ_I = 444 [s].

This configuration is not robust enough to eliminate limit cycles (Figure 130), although the provoked disturbance can be removed. Apparently, the Ziegler Nichols tuning method is suitable to provide a stable system in which external disturbances can be eliminated. Nevertheless does not take into account the internal disturbances like exhibiting limit cycles. Therefore, the Ziegler Nichols tuning method has to be applied with caution.

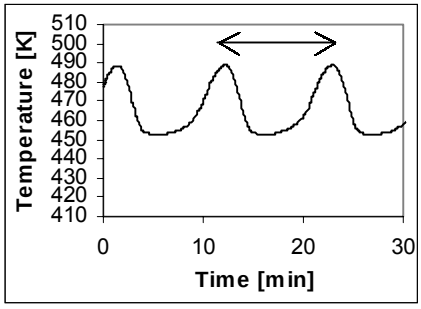

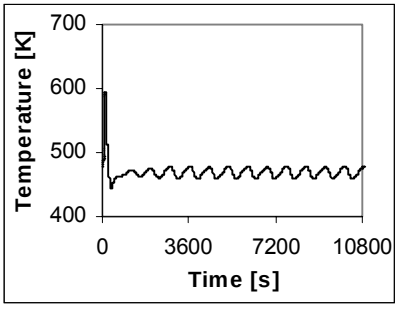

Figure 129 K_U = 0.00051908 [m^3 s^{-1} K^{-1}], $\tau_I \rightarrow \infty$ [s], P_U = 9 [min].

Figure 130 K_c = 0.000234 [m^3 s^{-1} K^{-1}] τ_I = 444 [s].

12.2.2 Controller parameter variation

To acquire a suitable controller configuration, the distinct parameters are varied and evaluated on basis of its dynamical behaviour.

Table 32 Results various controller parameters. Presumed delay τ_d = 30 [s].

Proportional gain, perturbation	Integral time		
	τ_I = 60 [s]	τ_I = 600 [s]	τ_I = 3600 [s]
K_c = 0.00020 [m^3 s^{-1} K^{-1}] ΔT =20 [K]	Figure 131	Figure 132	Figure 133
K_c = 0.00025 [m^3 s^{-1} K^{-1}] ΔT =20 [K]	Figure 134	Figure 135	Figure 136
K_c = 0.00030 [m^3 s^{-1} K^{-1}] ΔT =20 [K]	Figure 137	Figure 138	Figure 139
K_c = 0.00050 [m^3 s^{-1} K^{-1}] ΔT =20 [K]	Figure 140	Figure 141	Figure 142

Figure 131 and Figure 132 show clearly that the proportional gain K_c = 0.0002 [m^3 s^{-1} K^{-1}] is not robust enough to reduce the self-sustained oscillations. In case of Figure 133 the integral time is too large resulting in extinction.

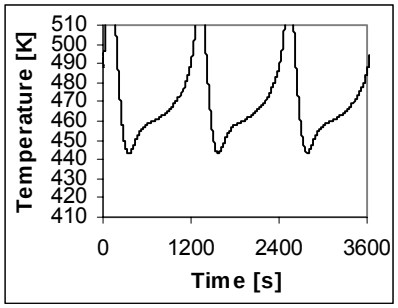

Figure 131 K_c = 0.0002 [m^3 s^{-1} K^{-1}], τ_I = **60** [s].

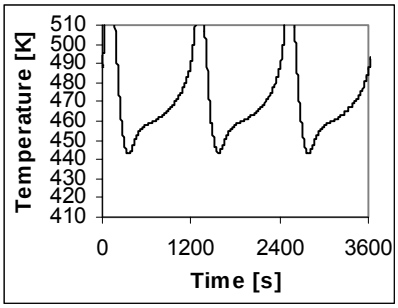

Figure 132 K_c = 0.0002 [m^3 s^{-1} K^{-1}], τ_I = **600** [s].

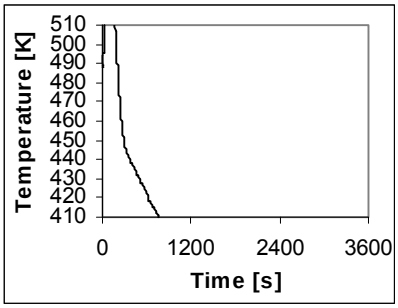

Figure 133 K_c = 0.0002 [m^3 s^{-1} K^{-1}], τ_I = **3600** [s].

In case the proportional gain is increased to K_c = 0.00025 [m^3 s^{-1} K^{-1}], the overshoot is reduced. However, limit cycles still emerge (Figure 134 and Figure 135). An integral time τ_I = 3600 [s] again is too large (Figure 136).

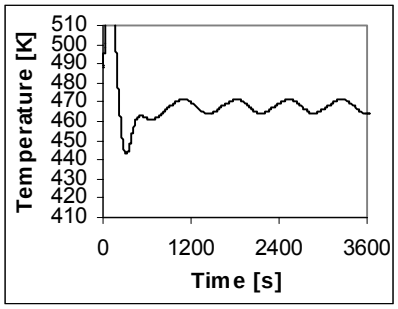

Figure 134 K_c = 0.00025 [m^3 s^{-1} K^{-1}], τ_I = **60** [s].

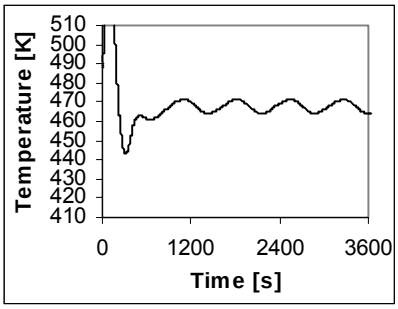

Figure 135 K_c = 0.00025 [m^3 s^{-1} K^{-1}], τ_I = **600** [s].

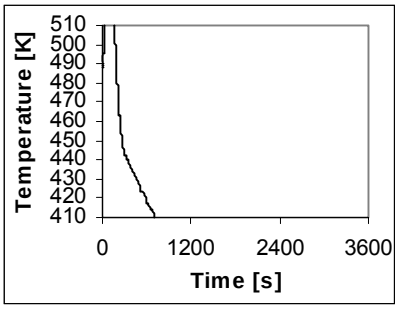

Figure 136 K_c = 0.00025 [m^3 s^{-1} K^{-1}], τ_I = **3600** [s].

A larger proportional gain K_c = 0.0003 [m^3 s^{-1} K^{-1}], (Figure 137 and Figure 138) is robust enough to eliminate the constrained disturbance and the self-sustained oscillations i.e. spiral point. However if the integral; time becomes too long instability is inevitable (Figure 139).

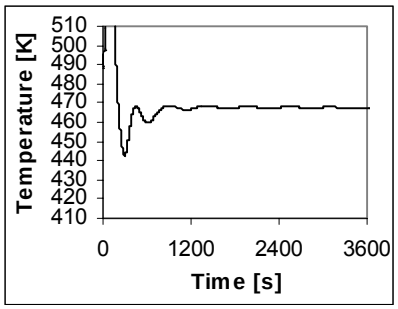

Figure 137 K_c = 0.0003 [m^3 s^{-1} K^{-1}], τ_I = **60** [s].

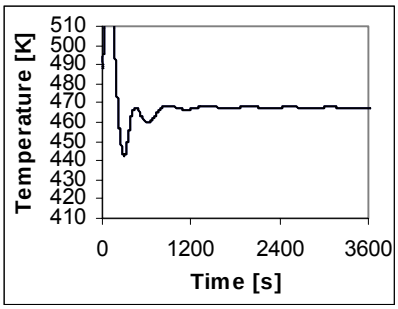

Figure 138 K_c = 0.0003 [m^3 s^{-1} K^{-1}], τ_I = **600** [s],

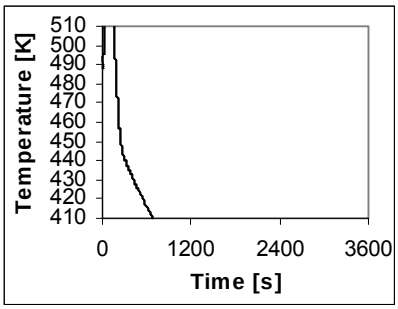

Figure 139 K_c = 0.0003 [m^3 s^{-1} K^{-1}], τ_I = **3600** [s].

Further increasing the proportional gain to K_c = 0.0005 [m^3 s^{-1} K^{-1}], can preserve stability for a small integral time (Figure 140) however for larger integral times (Figure 141 and Figure 142) the reaction irrevocably extinguishes.

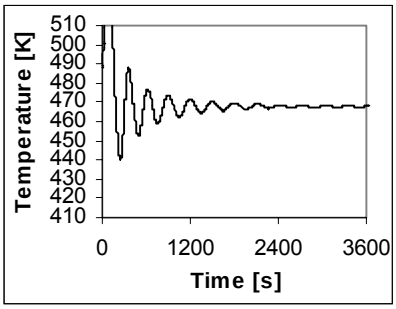

Figure 140 K_c = 0.0005 [m^3 s^{-1} K^{-1}], τ_I = **60** [s].

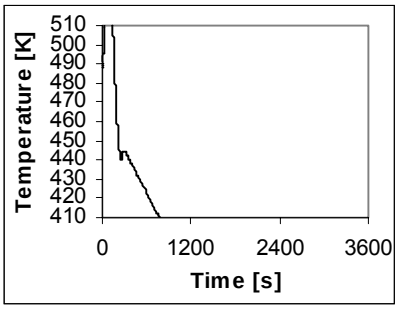

Figure 141 K_c = 0.0005 [m^3 s^{-1} K^{-1}], τ_I = **600** [s].

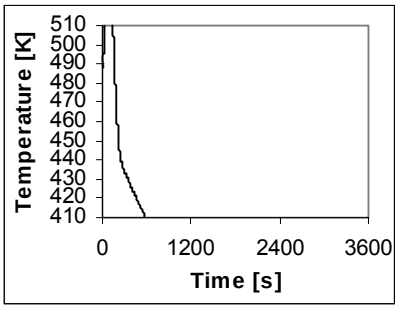

Figure 142 K_c = 0.0005 [m^3 s^{-1} K^{-1}], τ_I = **3600** [s].

In case of coolant temperature control, a larger integral time implies more stability. Due to the extra cooling equation 36 multiplicity is concerned, which can cause the reaction to extinguish.
The best controller configuration regarding the PI-control coolant flowrate has been given in Figure 138 i.e. K_c = 0.0003 [m^3 s^{-1} K^{-1}], τ_I = 600 [s].
The constrained disturbance has a tremendous effect on the controlled coolant flowrate. However due to the considerable cold coolant inlet temperature, the maximum fluid velocity will not become critical. In case of a recycle stream (10×) v_{cool} < 2 [m s^{-1}].
Considered the best controller configuration K_c = 0.0003 [m^3 s^{-1} K^{-1}], τ_I = 600 [s] (Figure 138) the dynamical behaviour of the coolant flowrate is portrayed in Figure 143. Despite the large overshoot, in case of steady state and minor disturbances, the coolant flowrate will vary much less.

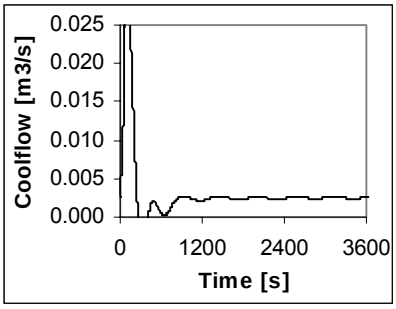

Figure 143 K_c = 0.0003 [m^3 s^{-1} K^{-1}], τ_I = 600 [s], ΔT = +20 [K], τ_d = 30 [s].

12.3 Controlling the throughput

12.3.1 Ziegler Nichols tuning method

A proportional gain K_U = 0.00012 [m^3 s^{-1} K^{-1}] and an ultimate period of sustained cycling P_U = 52 [min] is acquired (Figure 144). According to the Ziegler Nichols method the controller-tuning configuration becomes:

K_c = 0.000054 [m^3 s^{-1} K^{-1}] and τ_I = 2600 [s].

In previous chapters, it has been obvious that the Ziegler Nichols method was not suitable to determine appropriate controller setting. In addition, for throughput control, this method is not applicable (Figure 145).

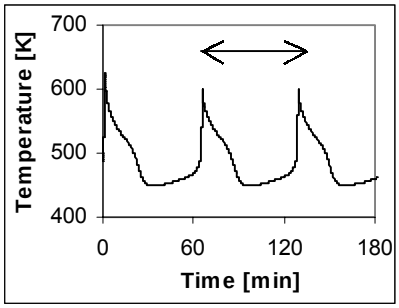

Figure 144 K_U = 0.00012 [m^3 s^{-1} K^{-1}], $\tau_I \rightarrow \infty$ [s], ΔT = +20 [K], τ_d = 30 [s], P_U = 52 [min].

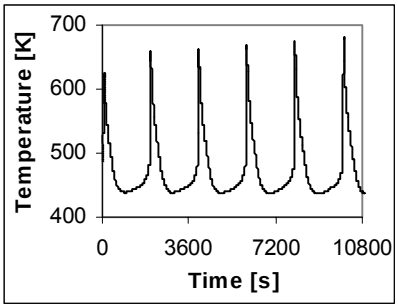

Figure 145 K_c = 0.000054 [m^3 s^{-1} K^{-1}] τ_I = 2600 [s], ΔT = +20 [K], τ_d = 30 [s].

12.3.2 Controller parameter variation

Consider a constrained disturbance in the reactor temperature ΔT and a presupposed delay of τ_d = 30 [s]. The proportional gain and the integral time are varied to study the effect on the stability.

Table 33 Results various controller parameters. Presumed delay τ_d = 30 [s].

Proportional gain, perturbation	Integral time		
	τ_I = 60 [s]	τ_I = 600 [s]	τ_I = 3600 [s]
K_c = 0.0001 [m^3 s^{-1} K^{-1}] ΔT =20 [K]	Figure 146	Figure 147	Figure 148
K_c = 0.001 [m^3 s^{-1} K^{-1}] ΔT =20 [K]	Figure 149	Figure 150	Figure 151
K_c = 0.01 [m^3 s^{-1} K^{-1}] ΔT =20 [K]	Figure 152	Figure 153	Figure 154
K_c = 0.1 [m^3 s^{-1} K^{-1}] ΔT =20 [K]	Figure 155	Figure 156	Figure 157
K_c = 0.01 [m^3 s^{-1} K^{-1}] ΔT =2 [K]	Figure 158	Figure 159	Figure 160

Figure 146, Figure 147 and Figure 148 show visibly that the proportional gain K_c = 0.0001 [m^3 s^{-1} K^{-1}] is not robust enough to reduce the self-sustained oscillations. Actually, the temperature perturbation causes the reaction immediately to runaway.

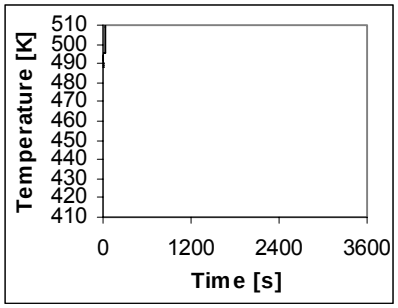

Figure 146 K_c = 0.0001 [m^3 s^{-1} K^{-1}], τ_I = **60** [s].

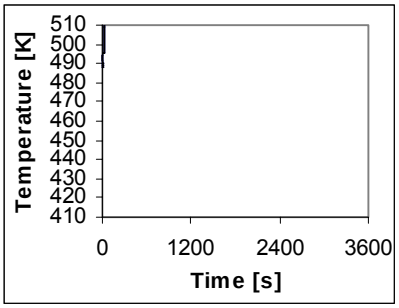

Figure 147 K_c = 0.0001 [m^3 s^{-1} K^{-1}], τ_I = **600** [s].

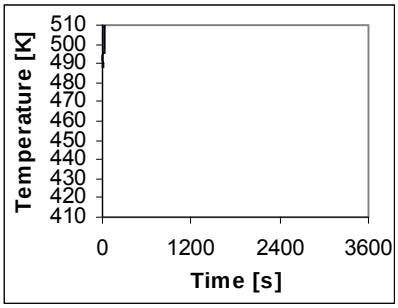

Figure 148 K_c = 0.0001 [m^3 s^{-1} K^{-1}], τ_I = **3600** [s].

In case the proportional gain is increased with a factor 10 to K_c = 0.001 [m^3 s^{-1} K^{-1}] (Figure 149) initially the controller corrects the flowrate in the right direction towards the base case value, however cannot avoid runaway directly after the first peak. Increasing the integral time has a considerable stabilising effect (Figure 150). Actually, after a reasonable short time the reaction is stabilised with the desired reactor temperature T = 468 [K] however with a poorer conversion ζ = 0.48 [-] which is 25% lower than the required base case conversion ζ = 0.68 [-]. The lower conversion is due to the fact easily another steady state is reached corresponding with a throughput Φ_V = 0.001 [m^3 s^{-1}] which is 5 times lower than the base case value. An integral τ_I = 3600 [s] is conversely too large and causes once more runaway (Figure 151).

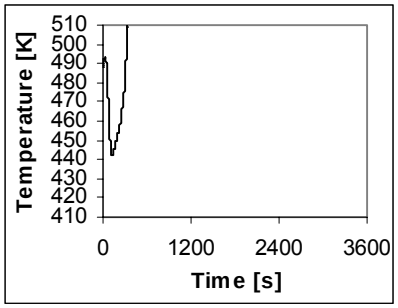

Figure 149 K_c = 0.001 [m^3 s^{-1} K^{-1}], τ_I = **60** [s].

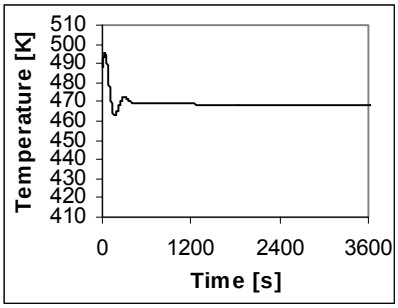

Figure 150 K_c = 0.001 [m^3 s^{-1} K^{-1}], τ_I = **600** [s]. ζ = 0.48, Φ_V = 0.012 [m^3 s^{-1}].

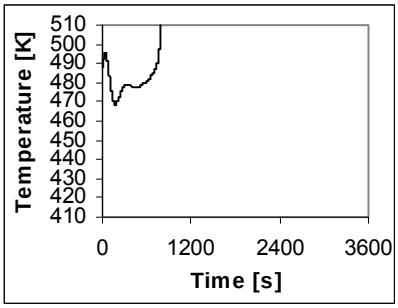

Figure 151 K_c = 0.001 [m^3 s^{-1} K^{-1}], τ_I = **3600** [s].

Increasing K_c 10 times to K_c = 0.01 [m^3 s^{-1} K^{-1}] however with a short integral time implies substantial instability (Figure 152). A larger integral time conversely preserves stability, unfortunately again with a lower conversion (Figure 153). Larger integral times do not change anything in view of the stability (Figure 154). These figures prove that the integral time should not be too small i.e. the influence of the delay can be reduced by choosing a considerably larger integral time, which overlaps abundantly the delay. Because a change in the flowrate, caused by the proportional gain, affects directly the dynamical behaviour of the system, the integral time spreads the large peaks in which risk for transition to other steady states is decreased.

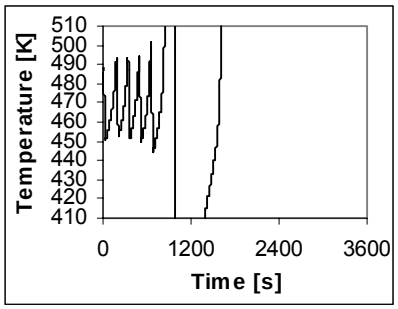

Figure 152 K_c = 0.01 [m^3 s^{-1} K^{-1}], τ_I = **60** [s].

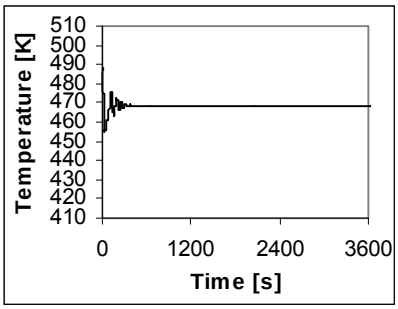

Figure 153 K_c = 0.01 [m^3 s^{-1} K^{-1}], τ_I = **600** [s], ζ = 0.48.

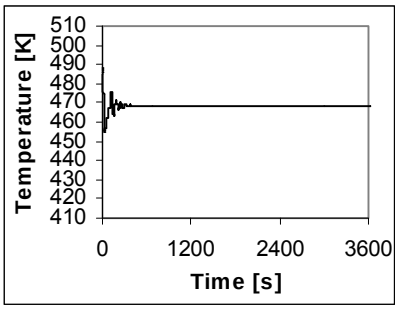

Figure 154 K_c = 0.01 [m^3 s^{-1} K^{-1}], τ_I = **3600** [s], ζ = 0.48.

Further increasing the proportional gain (Figure 155) once more causes runaway, although it takes more time to reach that critical situation. Increasing the integral time provides stability although with high oscillation frequencies, which are practically unlikely to realise i.e. opening and closing the throughput valve (Figure 156). Further increasing the integral time has no effect on the stability (Figure 157).

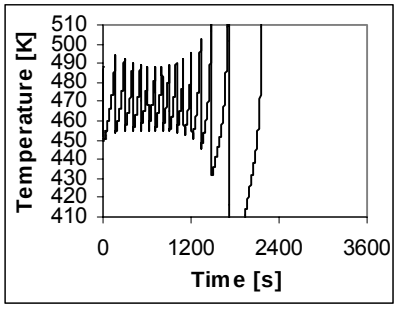

Figure 155 K_c = 0.1 [m^3 s^{-1} K^{-1}], τ_I = **60** [s].

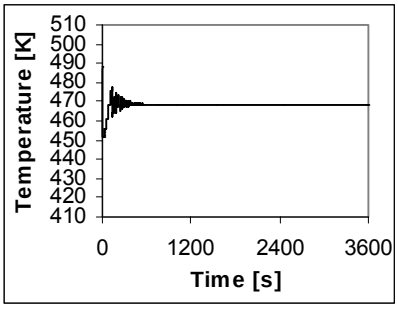

Figure 156 K_c = 0.1 [m^3 s^{-1} K^{-1}], τ_I = **600** [s, ζ = 0.48.

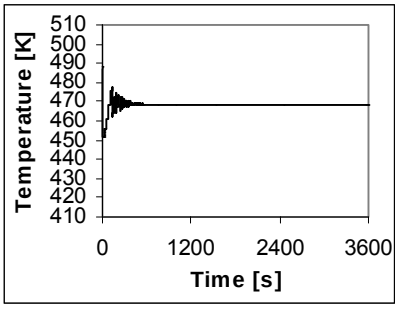

Figure 157 K_c = 0.1 [m^3 s^{-1} K^{-1}], τ_I = **3600** [s], ζ = 0.48.

The previous cases, demonstrate that a considerable disturbance on the one hand can cause instability in the reactor and on the other hand imply stability however corresponding with a lower conversion i.e. the base case situation can not be preserved.
If the actual disturbance is decreased $\Delta T = +2$ [K], the steady state temperature can be remained. (Figure 158, Figure 159 and Figure 160). Unfortunately, due to the unstable operating point the conversion is only temporarily close to the base case steady state value and is irrevocable attracted to the closest steady state, i.e. the steady state corresponding with lower throughput and consequently lower conversion.

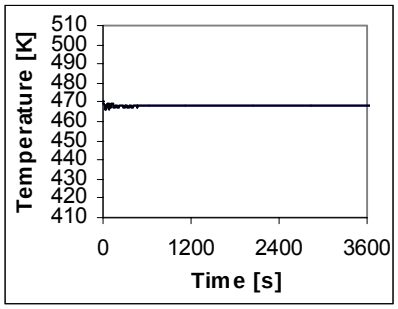

Figure 158 $K_c = 0.01$ [$m^3 s^{-1} K^{-1}$], $\tau_I = 60$ [s] $\Delta T = +2$ [K].

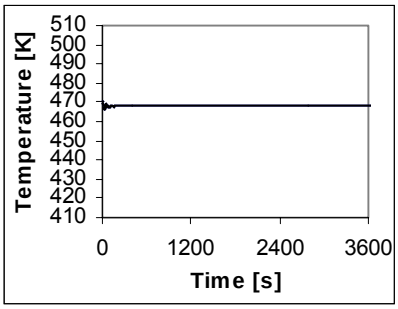

Figure 159 $K_c = 0.01$ [$m^3 s^{-1} K^{-1}$], $\tau_I = 600$ [s] $\Delta T = +2$ [K].

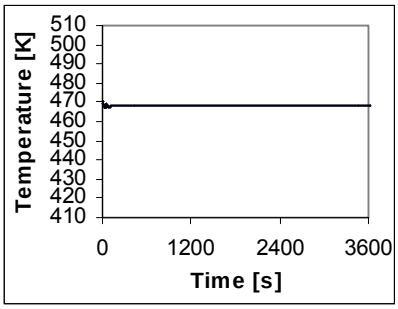

Figure 160 $K_c = 0.01$ [$m^3 s^{-1} K^{-1}$], $\tau_I = 3600$ [s] $\Delta T = +2$ [K].

Figure 159 and Figure 160 show that the reactor temperature can be remained at base case temperature however with a lower conversion.

Finally, if the two possible steady state situation in which or the reactor temperature or the conversion is maintained are compared:

Production = $\Phi_V \times [A]_0 \times \zeta = 0.005 \times 5000 \times 0.68 = 17$ [$m^3 s^{-1}$]
Production = $\Phi_V \times [A]_0 \times \zeta = 0.012 \times 5000 \times 0.48 = 28$ [$m^3 s^{-1}$]

It is apparent that the controller, which uses the reactor temperature as set point, has the largest production, although it is not certain if the larger flowrate is allowed. Besides, in case of conversion as set point the reactor temperature is higher. In view of safety, the latter is perhaps not allowed. Nevertheless, it is not the scope of this report to decide which choice must be made.

12.4 Base case controller configuration

To obtain a suitable controller configuration, on the one hand a robust proportional controller gain is needed to restrain evolving limit cycles, however in addition, too large K_c can cause a certain overshoot, which can cause unwanted or even dangerous situations. If multiplicity is concerned with, transition is inevitable like if the throughput control.
The integral time has to be chosen in such a way that the assumed delay is inferior. A too large integral time has hardly any improvement towards the stability.
The conventional controller tuning methods like the Ziegler Nichols method are not adequate to adopt for processes with distinct dynamically unstable behaviour like the base case.

Consider the base case situation, with an initial temperature disturbance of ΔT = 20 [K] and a presumed delay τ_d = 30 [s] to improve the physical realism, the following controller configuration preserved a stable process:

Table 34 Suitable PI-controller settings coolant temperature control

Description	Value
Presumed delay	τ_d = 30 [s]
Perturbation	ΔT = 20 [K]
Proportional gain	K_c = 5 [-]
Integral time	τ_I = 600 [s]
Desired base case reactor temperature	T = 468 [K]
Required conversion	ζ = 0.68 [-]

Table 35 Suitable PI-controller settings coolant flowrate control

Description	Value
Inlet coolant temperature	$T_{cool,0}$ = 303 [K]
Presumed delay	τ_d = 30 [s]
Perturbation	ΔT = 20 [K]
Proportional gain	K_c = 0.0003 [$m^3 s^{-1} K^{-1}$]
Integral time	τ_I = 600 [s]
Desired base case reactor temperature	T = 468 [K]
Required conversion	ζ = 0.68 [-]

Table 36 The best achievable PI-controller settings throughput control

Description	Value
Presumed delay	τ_d = 30 [s]
Perturbation	ΔT = 2 [K]
Proportional gain	K_c = 0.01 [$m^3 s^{-1} K^{-1}$]
Integral time	τ_I = 600 [s]
Desired base case reactor temperature	T = 468 [K]
Required conversion	ζ = 0.48 [-]
Throughput	Φ_V = 0.012 [$m^3 s^{-1}$]

It is obvious that these values have no practical significant importance, merely give a qualitative impression of the magnitude.

Chapter XIII

13 THE EFFECT OF FOULING ON THE BASE CASE STABILITY

13.1 Introduction

In existing industrial processes, reactor vessels with exothermic chemical reaction are cooled continuously. Simultaneously, the cooling apparatus is contaminated called fouling (Foust[27]). As a consequence of fouling the cooling capacity can decrease during the process. Consider the UA reduction per time.

$$\frac{dUA}{dt} = -UA\mathrm{f} \tag{53}$$

In correlation 53, f stands for the fouling factor i.e. the amount of reduction of the cooling capacity per unit of time. An arbitrary chosen f is to be assumed.

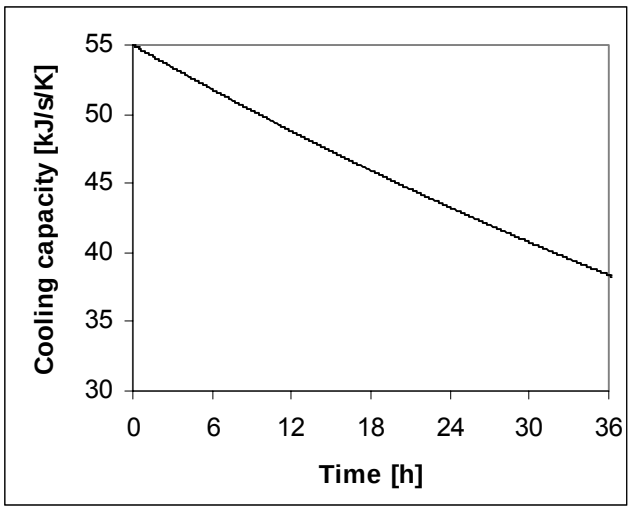

Figure 161 Presuppose that every hour 1% of the cooling capacity is reduced. According equation 53 f = -(1-0.99)/3600 = -2.8×10^{-6} [s^{-1}].

Consider the controlled base case process, operating at a stable point. From the moment t = 0 the process of fouling depletion according equation 53 is to be considered. The simulation starts using the default base case values, however with an initial temperature disturbance of ΔT = +10 [K]. The following systems will be considered:

1. Coolant temperature proportional control
2. Coolant temperature proportional-integral control
3. Coolant flowrate proportional control
4. Coolant flowrate proportional-integral control

13.2 Coolant temperature proportional control

The process is proportional controlled (K_c = 0.95). It has been previously found through Figure 27 that the minimum required proportional gain to provide stability is K_c = 0.9. During the process, the cooling capacity declines as has been portrayed in Figure 161. Initially, Figure 162 confirms that the controller is suitable to eliminate the disturbance. Nevertheless, after approximately 6 hours, the system becomes unstable and exhibits undesired limit cycles. The example demonstrates that a controlled real process, which is marginal stable, can definitely become unstable in case the process variables change.

1 Coolant temperature proportional-integral control

Through Figure 74 it was determined that K_c = 1.35 is sufficient to preserve stability no matter the value of the integral time. Nonetheless, an arbitrary integral time constant is chosen τ_I = 60 [s]. The controller initially removes the constrained disturbance, but after approximately 7 hours, the system becomes unstable which has been shown in Figure 163.

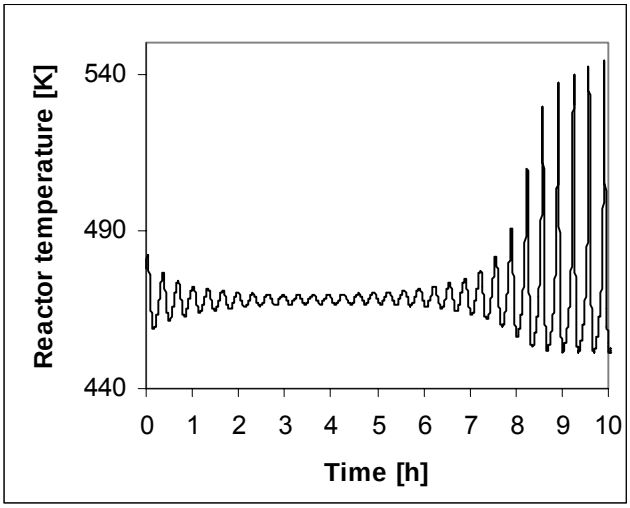

Figure 162 T_{cool} P-control. Initial step disturbance ΔT = 10 [K]. After approximately t = 6 [h], the process becomes unstable and exhibits large limit cycles. The LOCBIF source LOCBIF rhs 9 is included in Appendix 7.

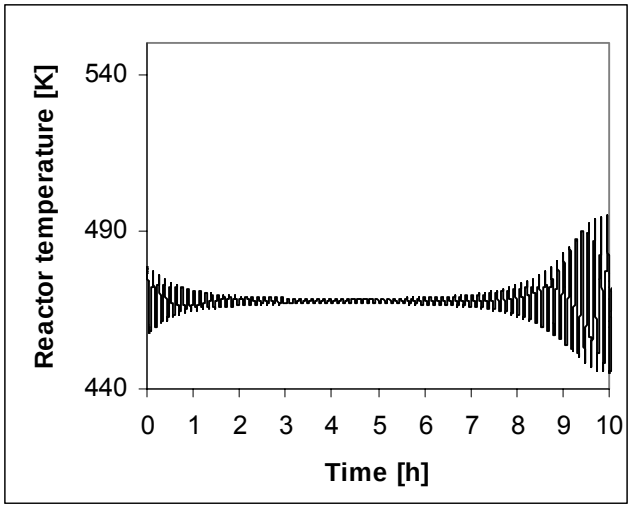

Figure 163 T_{cool} PI-control. Initial step disturbance ΔT = 10 [K]. After approximately t = 7 [h], the process becomes unstable. The LOCBIF source LOCBIF rhs 9 is included in Appendix 7.

Because the offset is not removed in case a P-controller is applied which is clearly visible in Figure 162, the process becomes unstable more early according Figure 163. Correspondingly, in case of coolant temperature control, the advantage of the integral action is demonstrated.

13.3 Coolant flowrate proportional control

A proportional gain K_c = 0.00025 [m^3 s^{-1} K^{-1}] is selected (derived from Figure 37) at which narrowly a stable system is achieved. The proportional controller does not remove the offset which is confirmed in Figure 164a. After approximately 50 hours, the process becomes unstable and exhibits limit cycles. Due to the reduced cooling capacity, more heat has to be removed through the coolant flowrate, which will consequently increase (Figure 164b) whereas the coolant temperature decreases (Figure 164c).

13.4 Coolant flowrate proportional-integral control

The same K_c = 0.00025 [m^3 s^{-1} K^{-1}] is selected at which a stable system is acquired. The integral action clearly removes the offset (Figure 165a). Due to UA decline, the coolant flowrate has to be increased to remove the surplus heat Figure 165b although less compared to P-control only. After approximately 32 hours, the system becomes unstable. In case of proportional control, only it took 50 hours before the system became unstable. The proportional + integral action ($\tau_I \rightarrow$ 600 [s]) makes the system more quickly unstable compared the proportional control action exclusively ($\tau_I \rightarrow \infty$). This can be derived from Figure 80 in which K_c has been plotted against τ_I.

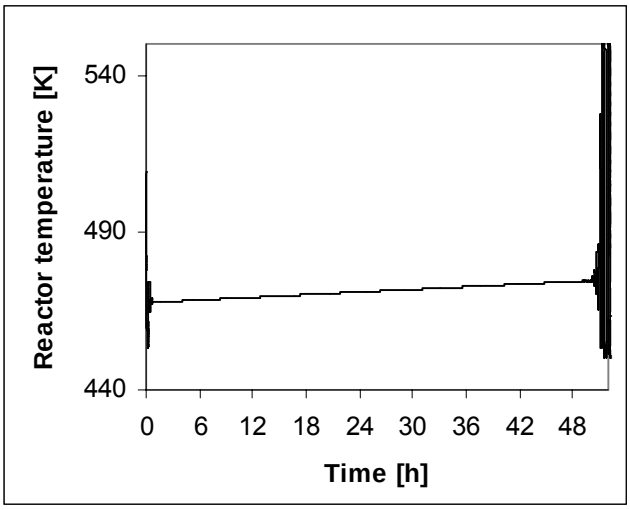

Figure 164a $T_{cool,0}$ = 303 [K]. Initial step disturbance ΔT = 10 [K]. The process becomes unstable after approximately t = 50 [h].

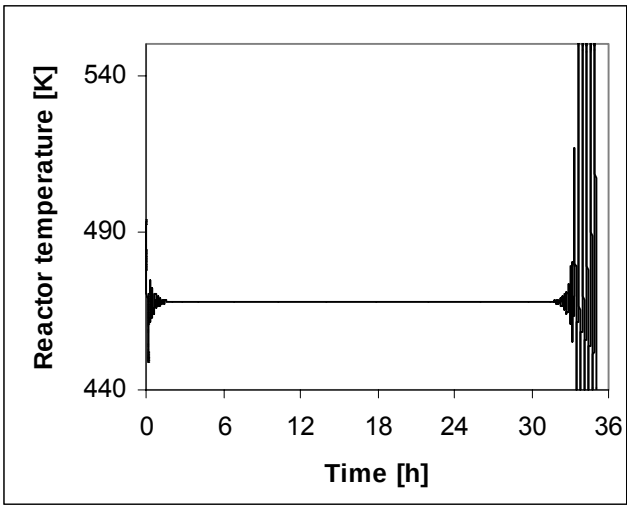

Figure 165a $T_{cool,0}$ = 303 [K], τ_I = 600 [s]. Initial step disturbance ΔT = 10 [K]. The process becomes unstable after approximately after t = 32 [h].

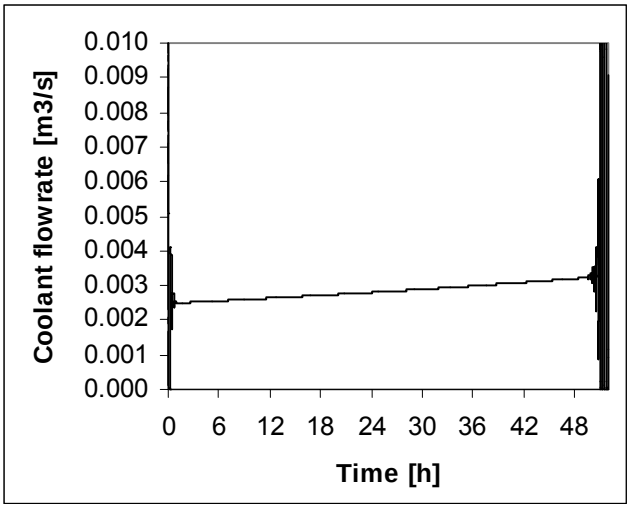

Figure 164b $\Phi_{V,cool}$ P-control. Initial step disturbance ΔT = 10 [K]. The coolant flowrate increases due to UA decline.

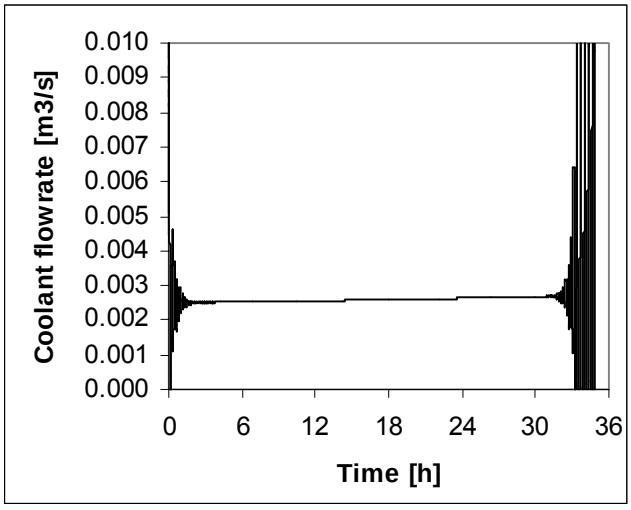

Figure 165b $T_{cool,0}$ = 303 [K], τ_I = 600 [s]. Initial step disturbance ΔT = 10 [K]. The coolant flowrate increases less than P-control.

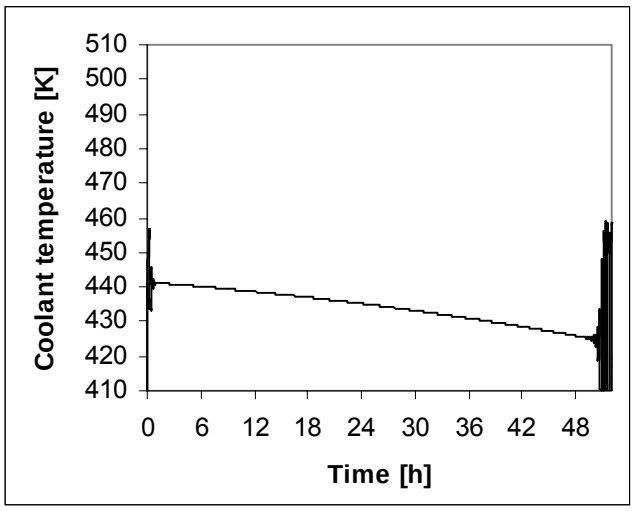

Figure 164c $T_{cool,0}$ = 303 [K]. Due to the increasing coolant flowrate the coolant temperature declines. The LOCBIF source LOCBIF rhs 11 is included in Appendix 7. The influence of the heat capacity of the tube wall is discussed by Roffel[68].

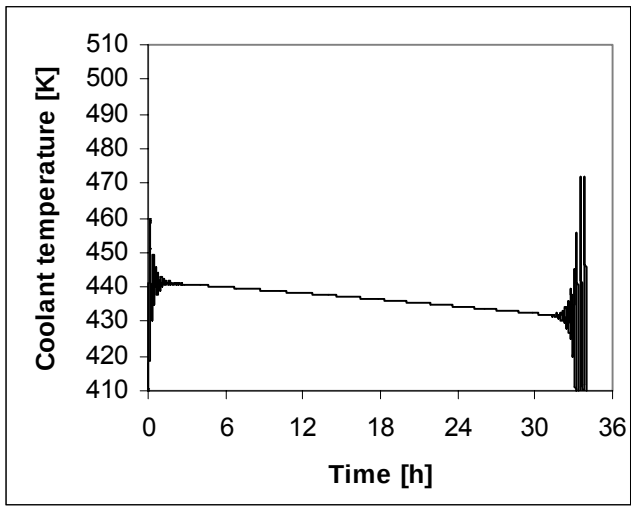

Figure 165c $T_{cool,0}$ = 303 [K]. Due to the increasing coolant flowrate the coolant temperature declines. The LOCBIF source LOCBIF rhs 12 is included in Appendix 7.

CONCLUSIONS

Limit cycles which exhibit in a cooled CISTR with irreversible exothermic reaction A $\rightarrow$ P can completely be eliminated through the application of a proportional-integral controller. This can be achieved successfully if the PI-controller regulates the extent of cooling.
The key to success is the software program LOCBIF in which distinct stability maps and orbit curves can be produced based on the mathematical descriptions. A stability map can give valuable information about the static and dynamical behaviour of a considered process.
Throughput control is not a suitable control method due to the fact that adjusting the flowrate decreases the reactor temperature by the supply of cold feed but on the other hand increases the reaction rate due to the fresh reactant. To match both internal disturbances (self-sustained oscillations) and external disturbances (irregularities) the controller must be robust enough. Nevertheless, too drastic manipulation will on the contrary disrupt the dynamics of a process. If a dynamical unstable process is considered, like the base case, the proportional gain is certainly too large and can cause transition. An inevitable lower proportional gain means either the reactor temperature is chosen as set point with lower conversion, or the conversion is chosen with a higher reactor temperature. With respect to the base case with throughput control, no appropriate control configuration could be obtained.
Cooling control implies practically the regulation of the temperature of a cooling fluid. In this report, two distinguished models have been examined. At first the instantaneously manipulation of the coolant temperature and secondly the implementation of a cooling differential equation which the latter describe the coolant temperature as function of the coolant flow. Considered the first model, it is relatively simple to elucidate limit cycles and preserve stability. In the worst case scenario, limit cycles emerge. Regarding the second model, suitable control can be achieved, although the configuration of the controller parameters must be tuned adequately. Inaccurate control can imply for instance too much heat withdrawal from the reactor causing extinction.
To enlarge the physical realism, the apparent delay is introduced. Small delay cannot destabilise a proper controlled process. Conversely, large delay provokes dynamical instability and if multiplicity is involved even static instability (extinction or runaway). Beyond a certain delay, instability is inevitable in which no controller can provide a stable process. The simulated delay is apparently less dangerous for higher inlet coolant temperatures. In the contrary, the influence of process equipment on the stability of a process, which in fact represents a certain delay, is less affecting the stability for low coolant inlet temperatures.
The integral time removes any offset and is therefore a welcome supplement. The conditions are that the integral time constant is considerable larger than the apparent delay.
Traditional control configuration tuning methods like the Ziegler and Nichols technique are not appropriate to deal with dynamical instabilities.
Large cooling capacity, in general has a positive effect on the stability of a process[80]. However too large UA values, which are practically not thinkable due to economic aspects, can contribute to a process in which too much heat is removed from the system if the controller manipulates too drastic.
If a controller is accurate and can safely preserve stability, a larger proportional gain may imply less UA i.e. installed heat transfer area (cost reduction).
In the literature in general, stability maps are composed in which one focuses on process variables such as the reactor temperature or conversion. In this report, such stability maps are called *reactor designer stability maps*. This is because the influence of important process parameters on the process stability can be analysed in the stability map. Due to the complex structure of the mathematical description and the fact that more than 2 variables are varied in a 2D plot, the curves in these stability maps become rather entangled and are therefore often difficult to interpret, in which the advantage of such maps in fact perishes. The directly study of particular process parameters such as proportional gain or cooling capacity through Hopf curves is less elaborate and often much more easy to interpret. Besides asymptotic limits can also be obtained. Additionally, stable and unstable regions can be indicated easier. Therefore, another stability map is introduced in this report, called the *reactor controller stability map*, in which easily one can determine the controller settings in which stability can be maintained or acquired, in particular after the process has been changed.

RECOMMENDATIONS

Validation

Although in this report it has been demonstrated that the base case, which exhibits limit cycles, can be controlled adequately, it is of crucial importance that the developed models will be validated for real physical existing processes.

This report is part of the research to the stability of process-operation of gas-liquid reactors. The next and logical step in research is the extension of the model with respect to a two-phase reactor.[23 22 78 26]

Model enhancement and extension

In this report, throughput control for one reactant is not recommended. From literature[17 19 38 76], it is know that in case more reactants are concerned with, which the latter is practically mostly the case, flowrate control of one or more inlet flowrate streams might contribute to stabilising a process.

The application of n CISTRs in series with the same total volume n $V_{R,i}$ may be in advantage compared to the use of 1 CISTR. This has to be investigated. [46 55 26 68 67]

The volume in the CISTR can be modified by changing the liquid height in the reactor. Consequently, the heat transferred through the cooling pipes changes. Through regulating the height, flowrate control is perhaps possible[25].

In case of cooling control, the assumption is made that the coolant temperature is constant. In practise, this is not always the case. If the flow pattern though the cooling device (e.g. pipes) is taken into account, one can make the outgrowth probably more realistic. [60 59 4 37 55 26 68]

The accuracy regarding the coolant temperature can be improved in case the logarithmic mean temperature according equation 17, is implemented in the mathematical model. [80 68]

In the models, the assumption is made that the reactor is perfectly mixed. According to[37 4 49] the stirrer affects both the conversion as the heat capacity. A more advanced description of this influence on the conversion and UA value can be an improvement to the model.

Process control improvement

Derivative control can make a control much more stable than a controller with merely proportional or proportional-integral action. Derivative control involves an extra integral equation. Unfortunately, implementation of derivative control action is not possible in LOCBIF, because this package is not adopted for the use of integral equations; conversely, the UNIX package AUTO has special features, which can handle integral equations. The PID controller can then be examined.

In case of substantial deviation of essential system variables, feed forward control can be a suitable solution, or conceivably the combination of feed forward and feedback. [74 9 10 14 75 35 55 59 72 53]

All the considered controller tuning methods have been developed to deal with static instability. Methods[74] have to be acquired or developed to determine suitable controller parameters which preserve a both static as dynamical stable process. The new and advanced kind of process control is the non-linear process control which provides extraordinarily new features. [35 35 74 53 10 51 16]

The control objective of the controller is to keep the temperature T of the reacting mixture constant at a desired value. Possible disturbances to the reactor include the feed temperature T_0 and the coolant temperature T_{cool}. The temperature in the reactor responds much faster to changes in T_0 than to changes in T_{cool}, in case of a coolant flow control method. [74]

NOMENCLATURE

Symbol	Description	Dimension
A	Heat transfer or exchanger area	[m^2]
A_s	Surface area available for heat transfer per unit length	[m^2 m^{-1}]
c	Controlled variable (equation 25)	[.]
c'(t)	Output signal (equation 26)	[.]
C_P	Heat capacity	[J Kg^{-1} K^{-1}]
$C_{P,cool}$	Heat capacity of cooling fluid	[J Kg^{-1} K^{-1}]
D_{imp}	Impeller diameter	[m]
D_{pipe}	Pipe diameter / thickness	[m]
D_{vessel}	Vessel diameter	[m]
E	Total energy of reacting mixture	[J]
E_{act}	Activation energy (equation 1)	[J mol^{-1}]
f	Fouling factor, rate of UA depletion (equation 53)	[s^{-1}]
$f(x)$	Mathematical function description	[-]
g	Gravitational acceleration	[m s^{-2}]
$G_c(s)$	Transfer function (for a controller)	[-]
$\tilde{H}_{subscript}$	Partial molar enthalpies of component subscript (equations 61)	[-]
ΔH_R	Reaction heat / enthalpy of reaction based on R	[J mol^{-1}]
k_0	Arrhenius pre-exponential factor or frequency factor (equation 1)	[s^{-1}]
K_c	Proportional control gain	[-] or [m^3 s^{-1} K^{-1}] or [m^3 s^{-1}]
K_e	Estimated gain conversion parameter (equations 42 and 47)	[m s^{-1} K^{-1}]
K_i	Integral control gain	[-]
$k_{R,m,n}$	Reaction rate constant	[$m^{3(m+n-1)}$ / $mol^{(m+n-1)}$ s]
K_U	Ultimate gain of final control element	[-]
K_x	Mass transfer coefficient of phase x	[m s^{-1}]
L_{pipe}	Pipe length in reactor	[m]
ΔL_{2pipes}	Distance between two pipes in square vessel	[m]
M	Ziegler Nichols amplitude ratio	[-]
$n_{subscript}$	Number of moles (equation 55)	[mole]
N_{imp}	Stirring speed	[# s^{-1}]
NTU	Number of transport units (equation 6)	[-]
NTU_{cool}	Number of transport units coolant (equation 15)	[-]
Nu_R	Nusselt number reaction mixture	[-]
Nu_{cool}	Nusselt number coolant	[-]
p_i	Bifurcation parameter (equation 24)	[-]
P	Potential energy	[J]
P	Pressure	[N m^{-2}] [Pa]
Pr_R	Prandtl number reaction mixture	[-]
Pr_{cool}	Prandtl number coolant	[-]
P_U	Ziegler Nichols ultimate period of sustained cycling	[min]
Q	Amount of removed heat	[J s^{-1}]
Q_p	Heat generation potential Perry *et.al.*[59]	[-]
Q_{feed}	Required heat to bring the feed to operation temperature (equation 65)	[J s^{-1}]
$Q_{reaction}$	Heat produced by reaction (equation 66)	[J s^{-1}]
$Q_{transfer}$	Heat transferred through cooling/heating area (equation 67)	[J s^{-1}]
Q_{cool}	Heat, which is removed by coolant (equation 68)	[J s^{-1}]
R	Ideal gas constant	[J mol^{-1} K^{-1}]
Re_R	Reynolds number reaction mixture	[-]
Re_{cool}	Reynolds number coolant	[-]
R_i	Scale resistance	[m^2 K s J^{-1}])
r_i	Reaction rate	[$m^{3(m+n-1)}$ / $mol^{(m+n-1)}$ s]
S	Cross-section area	[m^2]

St'	Stanton number = NTU	[-]
t	Simulation time variable	[s]
T	Temperature	[K]
T_{cool}	Coolant temperature	[K]
T_{delay}	Temperature after an apparent delay	[K]
T_{∞}	Temperature of the fluid around the wall	[K]
ΔT_{ad}	Adiabatic temperature difference	[K]
ΔT_{log}	Logarithmic temperature mean (equation 17)	[K]
t_d	Time (delay or dead)	[s]
t_U	Ultimate period	[s]
UA	Cooling capacity	[J s^{-1} K^{-1}]
U	Internal energy	[J]
U	Overall heat transfer coefficient	[J m^{-2} s^{-1} K^{-1}]
u_G	Gas velocity	[m s^{-1}]
u_L	Average liquid velocity based on cross section	[m s^{-1}]
V_{cool}	Cooling fluid volume	[m^3]
V_R	Reactor volume	[m^3]
V_{vessel}	Vessel volume	[m^3]
x	Mathematical variable (equation 32, 24)	[-]
X_i	Conversion rate	[s^{-1}]

Greek	**Description**	**Dimension**
α	Angle	[-]
α_R	Heat transfer coefficient reactor	[J m^{-2} s^{-1} K^{-1}]
α_{cool}	Heat transfer coefficient coolant	[J m^{-2} s^{-1} K^{-1}]
δ	Thickness of cooling pipe (equation 84)	[m]
δ_{pipe}	Thickness of pipe in a cooled vessel (equation 84)	[m]
δ_{vessel}	Thickness vessel wall	[m]
ε	Hold-up	[m^3 m^{-3}]
$\boldsymbol{\varepsilon}$	Error or deviation	[-]
ϕ	Time transformation	[-]
γ	Parameters used for ecological-bifurcation model	[-]
η	Liquid viscosity	[kg m^{-1} s^{-1}]
η_{cool}	Coolant viscosity	[kg m^{-1} s^{-1}]
η_{wall}	Viscosity at pipe wall	[kg m^{-1} s^{-1}]
Θ	Dimensionless temperature	[-]
θ	Dimensionless time	[-]
λ	Bifurcation active parameter (equation 18)	[-]
λ	Thermal conductivity	[J m^{-1} s^{-1} K^{-1}]
λ_R	Thermal conductivity reaction mixture	[J m^{-1} s^{-1} K^{-1}]
λ_{pipe}	Thermal conductivity cooling coil / pipes	[J m^{-1} s^{-1} K^{-1}]
λ_{cool}	Thermal conductivity coolant	[J m^{-1} s^{-1} K^{-1}]
σ_T	Temperature sensibility E/RT^2 Perry *et.al.*[59]	[K^{-1}]
τ	Time constant in a process (equation 32)	[s]
$\tau_{coolant}$	Average residence time of a coolant particle in cooling device	[s]
τ_{cool}	Time constant of the cooling fluid (equation 38)	[s]
τ_R	Average resident time (equation 4)	[s]
τ_{dead}	Dead time constant	[s]
τ_d	Presumed dead time	[s]
τ_D	Derivative time constant	[s] [min]
τ_I	Integral time constant / reset time	[s] [min]
τ_m	Measuring time constant	[s]
τ_U	Apparent time constant	[s]
φ	Integral control state variable	[K]
ω_{∞}	Ziegler Nichols crossover frequency	[s^{-1}]
Φ_j	Production rate	[mol s^{-1}]

Φ_v	Volumetric flow rate	[m^3 s^{-1}]
$\Phi_{v,cool}$	Flowrate cooling fluid	[m^3 s^{-1}]
Ψ	Place transformation	[-]
Ψ	Ratio height and diameter vessel (equation 75)	[-]
ρ	Fluid density	[kg m^{-3}]
ρ_{cool}	Density of cooling fluid	[kg m^{-3}]
ζ	Relative conversion	[-]
$\xi_{subscript}$	Absolute conversion	[mol]

Subscripts

0	Inlet or fresh feed
1, 2,…	Reactor 1, 2,…
a, b	Component A, B
ana	Analytic solution
act	Activation
bc	Base case
c	Controller
cool	Coolant / cooling (media)
conv	Converted
crit	Critical
d	Dead time
e	External
(g)	Gas phase
i	Initial / species i / inlet
(l)	Liquid phase
lm	Linear median / mean
log	Logarithmic mean
m	Measured
meas	Measuring device
min	Minimum
max	Maximum
num	Numerical
p	Process
pipes	Cooling pipes
s	Specific / steady state
sp	Set point
stst	Steady state
t	Total
u	Ultimate

Abbreviations

ART	Average residence time
BR	Batch reactor
CISTR	Continuously ideally stirred tank reactor
CORR	Corrective
D	Derivative
G	Gas
HPR	Heat production rate
HWR	Heat withdrawal rate
I	Integral
IAE	Integral of the absolute error
ITAE	Integral time absolute error
L	Liquid
ODE	Differential equations
PDE	Partial differential equations
PFR	Plug flow reactor
P	Proportional
PI	Proportional integral
PID	Proportional integral derivative
PB	Proportional band
RCSM	Reactor controller stability map
RDSM	Reactor designer stability map
RHS	Right hand side
RT	Residence time

Symbols

$\oplus$	Base case

LOCBIF List of symbols

Printed in Appendix 6 at p123.

REFERENCES

[1] Aris, R. and Amundson, N.R., 1958, “An analysis of chemical reactor stability and control - part I to III”, *Chem. Eng. Sci.* **7**, p121-155.

[2] Aris, R, 1969, “Elementary chemical reactor analyses”, Prentice-Hall, Englewood Cliffs, NJ.

[3] Bazykin, A.D., 1985, “Mathematical biophysics of interacting populations”, Nauka Moscow Russia.

[4] Beek, W.J. and Muttzall, K.M.K.,1983, “Transport phenomena”, Wiley Intersscience Publication, ISBN: 0-471-06173-5.

[5] Bush, S.F., 1969, *Proc. Royal. Soc.*, **309**A, p1-26.

[6] Bykov, V.I., Yablonskii, G.S. and Kim, V.S., 1978, “On the simple model of kinetic self-oscillations in catalytic reaction of CO oxidation”, *Dokl. Sov. Math.*, p637-639.

[7] Bilous, O. and Amundson, N.R., 1955, “Chemical reactor stability and sensitivity”, *A.I.Ch.E. J.* **1**, p513-521.

[8] Bykov, V.I., Yablonskii, G.S., Kim, V.F., 1978, “On the simple model of kinetic self-oscillations in catalytic reaction of CO oxidation”, *Dokl. Sov. Math.*, p637-639.

[9] Calvet, J.P. and Arkun, Y., 1988, “Feedforward and feedback linearisation of non-linear systems and its implementation using internal model control”, *Ind. Eng. Chem. Res.* **27** p1822-1831.

[10] Calvet, J.P. and Arkun, Y., 1990, “Design of P and PI stabilizing controllers for quassi non-linear systems.”, *Comp. Chem. Eng.* **14**, p415-426.

[11] Cohen, G.H. and Coon, G.A., 1953, “Theoretical consideration of retarded control”, *Trans. A.S.M.E.*, **75**, p827.

[12] Coughanowr, D.R., and Koppel, L.B., 1965, “Process systems analysis and control”, McGraw-Hill, 64th ed.

[13] Coulson, J.M., Richardson, J.F., Backhurst, J.R. and Harker, J.H., 1993, “Chemical Engineering”, Pergamon Press, Volume 1, 4th edition, ISBN: 0-08-037948-06.

[14] Coulson, J.M., and Richardson, J.F., 1979, “Chemical Engineering”, Pergamon Press, Volume 3, 2nd edition, ISBN: 0-08-023818-1.

[15] Coulson, J.M., Richardson, J.F. and Sinnott, R.K., 1991, “Chemical Engineering”, Pergamon Press, Volume 6, 1th edition, ISBN: 0-08-022969-0.

[16] Daoutidis, P. and Kravaris, C., 1991, “Dynamic output feedback control of minimum-phase non-linear processes”, *Chem. Eng. Sci.*, **47-4**, p837-849.

[17] Ding, J.S.Y., Sharma, S. and Luss, D., 1973, “Steady state multiplicity and control of the chlorination of liquid n-decane in an adiabatic continuously stirred tank reactor”, *Ind. Chem. Eng.* **13**, p76-82.

[18] Doedel, E.J. and Heinemann, R.F., 1983, “Numerical computations of periodic solutions branches and oscillatory dynamics of the stirred tank reactor”, *Chem. Eng Sci.*, **38** ,p1493-1499.

[19] Dolnik, M., Banks, A.S. and Epstein, I.R., 1997, “Oscillatory chemical reaction in a CISTR with feedback control of flowrate.”, *J. Phys. Chem.,* **101**, p5148-5154.

[20] Dougles, J., 1972, “Process dynamics and control, volume 1, Analyses of dynamic systems”, Prentice-Hall, Englewood Cliffs.

[21] Doherty, M.F. and Ottino, J.M., 1988, “Chaos in deterministic systems: strange attractors, turbulence and applications in chemical reactors ”, *Chem. Eng. Sci.*, **43-2**, p139-183.

[22] Elk, E.P., van, Borman, P.C., Kuipers, J.A.M. and Versteeg, G.F., 1999, “Modelling of gas-liquid reactors – Stability and dynamic behaviour of gas-liquid mass transfer accompanied by irreversible reaction“, *Chem. Eng. Sci.*, **54**, p4869-4879.

[23] Elk, E.P., van, Borman, P.C., Kuipers, J.A.M. and Versteeg, G.F., 1999, “Modelling of gas-liquid reactors – Implementation of the penetration model in dynamic modelling of gas-liquid processes with the presence of a liquid bulk“, *Chem. Eng. J.*, **76**, p223-237.

[24] Elk, E.P., van, Borman, P.C., Kuipers, J.A.M. and Versteeg, G.F., 2001, “Modelling of gas-liquid reactors – Stability and dynamical behaviour of a hydroformylation reactor“, *Chem. Eng. Sci.*, **56**, p1491-1500.

[25] Erickson, K.T., and Hedrick, J.L., 1999, “Plantwide process control”, John Wiley & Sons, ISBN: 0-471-17835-7.

[26] Fogler, H.S., 1992, “Elements of chemical reactor engineering”, Prentice Hall Int., 2nd ed., ISBN 0-13-263534-8.

[27] Foust, A.L., Wenzel, L.A., Clump, C.W., Maus, L. and Andersen, L.B., 1980, “Principles of unit operations”, John Wiley & Sons, New York, ISBN 0-471-26897-6.

[28] Franks, G.E.F., 1966, “Mathematical modelling in chemical engineering”, John Wiley & Sons, Inc.

[29] Giona, M, and Paladino, O, 1994, “Bifurcation analysis and stability of a controlled CSTR”, *Computers and chem. eng. J.*, **18**, p877-887.

[30] Hancock, M.D., Kenney, C.N., 1976, “The stability and dynamics of a gas-liquid reactor”, *Chem. Eng. Sci.* **32**, p629-636.

[31] Harold, M.P. and Luss, D., 1984, "An experimental study of steady state multiplicity features of two parallel catalytic reactors", *Chem. Eng. Sci.*, **40**, p35-52.
[32] Harold, M.P., Ostermaier, J.J., Drew, D.W., Lerou, J.J. and Luss, D., 1996, "The continously-stirred dacanting reactor: Steady state and dynamic features", *Chem. Eng. Sci.* **51**, p1777-1786.
[33] Heemskerk, A.H., Dammers, W.R., Fortuin, J.M.H., 1980, "Limit cycles measured in a liquid-phase reaction system", *Chem. Eng. Sci.* **35**, p439-445.
[34] Heerden, van, C., 1953, *Ind. Eng. Chem.*, p1242.
[35] Henson, M.A., and Seborg, D.E., 1997, "Nonlinear process control", Prentice Hall PTR., ISBN: 0-13-625179-X.
[36] Heiszwolf, J.J. and Fortuin, M.H., 1997, "Design procedure for stable operations of first-order reaction systems in a CSTR", *A.I.Ch.E. J.* **43**, p1060-1068.
[37] Himmelblau, D.M., & Bischoff, K.B., 1968, "Process analyses and simulation", John Wiley & Sons, Inc.
[38] Hjelmfelt, A. and Ross, J., 1994, "Experimental stabilization of unstable steady states in oscillatory and excitable reaction systems", *J. Phys. Chem.* **98**, p1176-1179.
[39] Hoffman, L.A., Sharma, S. and Luss, D., 1975, "Steady state multiplicity of adiabatic gas-liquid reactors: I. The single reactor case", *A.I.Ch.E. J.* **21**, p318-326.
[40] Hopf, E., 1942, "Abzweigung einer periodischen Losung eines Differentialsystems". Aus den Berichten der Mathematisch-Physikalischen Klasse de Schsischen Akademie der Wissenhaften zn Leipzig XCIV, p1-22.
[41] Horák, J., Belohlav, Z., Rosol, P. and Madron, F., 1987, "Analysis of the oscillatory behaviour of an industial reactor for oxination of propene; combined models", *Coll. Czechoslovak Chem. Cummun.* **52**, 2865-2875.
[42] Huang, D. T.-J. and Varma, A., 1981, "Steady-state and dynamic behavior of fast gas-liquid reactions in non-adiabatic continuous stirred tank reactors", *Chem. Eng. J.* **21**, p47-57.
[43] Huang, D. T.-J. and Varma, A., 1981, "Steady-state uniqueness and multiplicity of nonadiabatic gas-liquid CSTRs", *A.I.Ch.E. J.* **27**, p481-489.
[44] Khibnik, A.I., Bykov, V.I. and Yablonskii, G.S., 1987, "23 phase portraits of the simplest catalytic oscillator", *J. Phys. Khim.*, p1388-1390.
[45] Khibnik, A.I, Kuznetsov, Y.A., Levitin, V.V. and Nikolaev, E.V., 1992, "Interactive LOCal BIFurcation Analyzer".
[46] Kuntha, A. and van Elk, E.P., 1999, "Modelling of gas-liquid reactors: stability and dynamic behaviour of gas-liquid mass transfer accompanied by irreversible reaction in CISTRs in series", Procede Twente b.v..
[47] Kravaris, C. and Palanki, S., 1988, "Robust non-linear state feedback under structured uncertainty", *AIChE J.*, **34-7**, p1119-1127.
[48] Kuznetsov, Y.A., 1995, "Elements of applied bifurcation theory", Springer-Verlag, ISBN: 0-387-94418-4.
[49] Levenspiel, O.,1972, "Chemical reaction engineering", John Wiley & sons, ISBN: 0-471-53019-0.
[50] Li, R.S. and Horsthemke, W., 1991, "Effects of product occupancy on self-organization in heterogeneous catalysis. I. Multiple steady states and temporal oscillations", *J. Chem. Phys.* **95**, 5785-5789.
[51] Limquerco, L.C. and Kantor, J.C., 1989, "Non-linear output feedback control of an exothermic reaction", *Comp. Chem. Eng.*, **14**, p427-437.
[52] Lopez, A.M., Smith, C.L. and Murill, P.W., 1969, "An advanced tuning method", *Brit. Chem. Eng.*, **14**, p1533.
[53] Marlin, T.E., 2000, "Process control, designing processes and control systems for dynamic performance", McGraw-Hill Chem. Eng. Series., 2nd ed., ISBN 0-07-039362-1.
[54] McAuley, K.B., Macdonald, D.A. and McLellan, P.J., 1995, "Effects of operating conditions on stability of gas-phase polyethylene reactors", *A.I.Ch.E. J.* **41**, 868-879.
[55] Mohilla, R. and Ferencz, B., 1982, "Chemical process dynamics", Elsevier 4th ed., ISBN 0-444-99730-x.
[56] Murrill, P.W., 1967, "Automatic control of processes", *International Textbook Co*.
[57] Narendra, K.S. and Monopoli, R.V., 1980, "Applications of adaptive control", Academic Press New York.
[58] Pellegrini, L. and Biardi, G., 1990, "Chaotic behaviour of a controlled CSTR", *Computers and chem. eng. J.*, **18**, p877-887.
[59] Perry, R.H., Green, D., 1984, "Perry's chemical engineers handbook", McGraww-Hill Int. Ed., 50th ed., ISBN 0-07-Y66482-X.
[60] Ogunnaike, B.A., and Ray, W.H., 1994, "Process dynamics modelling and control", Oxford Unversity Press, ISBN: 0-19-509119-1.
[61] Olsen, R.J. and Epstein, I.R., 1993, "Bifurcation analysis of chemical reaction mechanisms. II. Hopf bifurcation analysis", *J. Chem. Phys.* **98**, p2805-2822.
[62] Pinto, J.C., 1995, "The dynamic behavior of continuous solution polymerization reactors - a full bifurcation analysis of a full scale copolymerization reactor", *Chem. Eng. Sci.* **21**, 3455-3475.
[63] Raghuram, S., Shah, Y.T. and Tierney, J.W., 1979, "Multiple steady states in a gas-liquid reactor", *Chem. Eng. J.* **17**, p63-75.

[64] Ratto, M. and Paladino, O., 2000, "Controllability of start-ups in CISTRs under PI control", *Dipartimento di Ingegneria Ambientale, Università di Genova, Italy*.
[65] Ratto, M. and Paladino, O., 1999, "Robust stability and sensitivity of real controlled CSTRs" *Chem. Eng. Sci.*, **55**, p321-330.
[66] Ratto, M., 1998, "A theoretical approach to the analyses of PI-controlled CSTRs with noise", *Computers and chem. eng. J.*, **22**, p1581-1593.
[67] Ray, A.K., 1995, "Performance improvement of a chemical reactor by non-linear natural oscillations", *Chem. Eng. J.*, **59**, p169-175.
[68] Roffel, B. and Rijnsdorp, J.E., 1982, "Process dynamics, control and protection", Ann Arbor Science, ISBN 0-250-40483-4.
[69] Scott, S.K., 1987, "Oscillations in simple models of chemical systems", *Acc. Chem. Res*., **20**, p186-191.
[70] Sharma, S., Hoffman, L.A. and Luss, D., 1976, "Steady state multiplicity of adiabatic gas-liquid reactors: II. The two consecutive reactions case", *A.I.Ch.E. J.* **22**, p324-331.
[71] Shinskey, F.G., 1994, "Feedback controllers for the process industries", McGraw Hill, ISBN 0-07-056905-3.
[72] Shinskey, F.G., 1996, "Process control systems", McGraw Hill, 4th ed., ISBN 0-07-057101-5.
[73] Singh, C.P.P., Carr, N.L. and Shah, Y.T., 1982, "The effect of gas feed temperature on the steady state multiplicity of an adiabatic CSTR with a fast pseudo-first-order reaction". *Chem. Eng. J.* **23**, p101-104.
[74] Stephanopoulos, G., 1984, "Chemical process control: an introduction to theory and practice", Englewood Cliffs, N.J.: Prentice Hall Inc., ISBN: 0-13-128629-3.
[75] Uppal, A., Ray, W.H. and Poore, A.B., 1974, "On the dynamic behavior of continuous stirred tank reactors", *Chem. Eng. Sci.* **29**, p967-985.
[76] Uppal, A., Ray, W.H. and Poore, A.B., 1976, "The classification of the dynamic behavior of continuous stirred tank reactors - Influence of reactor residence time", *Chem. Eng. Sci.* **31**, p205-214.
[77] Vleeschhouwer, P.H.M. and Fortuin, J.M.H., 1990, "Theory and experiments concerning the stabilty of a reacting system in a CSTR". *A.I.Ch.E. J.* **36**, p961-965.
[78] Vleeschhouwer, P.H.M., Garton, R.D. and Fortuin, J.M.H., 1992, "Analysis of limit cycles in an industrial oxo reactor". *Chem. Eng. Sci.* **47**, p2547-2552.
[79] Weast, R.C., 1984, "Handbook of Chemistry and Physics", CRC Press, 64th ed.
[80] Westerterp, K.R., van Swaaij, W.P.M. and Beenackers, A.A.C.M., 1990, "Chemical Reactor Design", John Wiley & Sons, ISBN: 0-471-90138-0.
[81] Ziegler, J.G. and Nichols, N.B., 1942, "Optimum settings for automatic controllers", *Trans. A.S.M.E.*, **64**, p759.

Table 37 References list and categories.

Subject	References
Limit cycles	18 19 33 35 38 48 51 54 61 62 67 69 71 75 76 77 78
Dynamic instability	1 7 16 17 18 21 30 31 32 33 34 35 36 37 38 40 42 47 48 51 54 60 61 62 64 67 68 71 72 75 76 77 78
Bifurcation	1 7 18 19 21 32 36 38 43 48 50 54 61 62 64 67 75 76 77 78
Process control	1 10 11 12 14 16 17 19 25 28 29 35 37 47 51 52 53 56 55 57 58 60 64 65 68 71 72 74
CISTR	1 4 10 14 17 18 19 21 26 30 31 32 33 34 35 38 41 42 43 47 51 54 55 59 60 61 62 63 64 67 68 70 73 75 76 80
Performance	14 60 61 67 50
Dead time / delay	14 25 37 53 60 71 72 74
Dimensionless notation	1 10 32 35 36 42 43 51 60 62 70 73 75 76 77
Experiments	5 14 19 27 30 31 33 38 54 62 69 77 78
General mathematics	Bifurcation theory[3 28 45 48 59 79] Linearisation[68 25 37 74 60] Laplace transforms[25 60 53 68 74] Routh criterium[7 14 60 74] Partial differential equations[55 68] Discretisation and continuisation[68]

APPENDICES

Appendix 1. Derivation CISTR

The continuously ideally stirred tank reactor

A simple exothermic reaction 1 takes place in the Continuously Ideally Stirred Tank Reactor which has been displayed in Figure 1 at p2. A liquid enters the reactor with a flow rate of Φ_V [m^3 s^{-1}] and a temperature T_0 [K]. This feed flow contains component A with concentration $[A]_0$. The tank is considered to be perfectly mixed, which implies that the temperature and concentration of the effluent is equal to the temperature and concentration of the liquid in the tank Φ_V, T, [A] and [P]. The reactor is cooled by a coolant that for example flows through a jacket around the reactor or flows through a system of cooling pipes (see also Appendix 3).

The fundamental dependent quantities for a reactor are:

1 Total mass of the reacting mixture in tank
2 Mass of chemical substance A in the reacting mixture
3 Total energy of the reacting mixture in the tank

Remarks:

1 The mass of component P can be found from the total mass and the mass of component A. Therefore, it is not an independent fundamental quantity and therefore is superfluous.
2 The momentum of the CISTR does not change under any operating conditions for the reactor and will be neglected.

Assumptions (Westerterp *et.al.*[80], Stephanopoulos[74], Roffel[68] and Marlin[53]):

1. The liquid phase is ideally mixed and can be described as a CISTR.
2. The irreversible, elementary first order chemical reaction states $A \rightarrow P$.
3. The potential and kinetic energies of the inlet and outlet streams are equal.
4. The liquid in and out flowrate are assumed equal.
5. The physical parameters are considered constant i.e. $\Delta\rho = 0$ and $\Delta C_P = 0$.
6. The CISTR is well insulated so that negligible heat is transferred to the surroundings
7. The accumulation of energy in the reactor walls, agitator and cooling coil is negligible compared with the accumulation in the liquid. According to Westerterp *et.al.*[80] this is permissible for large industrial reactor.
8. According to Ogunnaike *et.al.*[60] The coolant is at quasi-steady state.
9. The shaft work done by the impeller of the stirring mechanism, has been neglected.

The conservation principles on the three fundamental quantities will be applied:

Total mass balance

$$\frac{\left[\begin{array}{l}\text{accumulation}\\ \text{of total mass}\end{array}\right]}{\text{time}} = \frac{\left[\begin{array}{l}\text{input}\\ \text{of total mass}\end{array}\right]}{\text{time}} - \frac{\left[\begin{array}{l}\text{output}\\ \text{of total mass}\end{array}\right]}{\text{time}} \pm \frac{\left[\begin{array}{l}\text{total mass}\\ \text{generated or consumed}\end{array}\right]}{\text{time}}$$

or

$$\frac{d(\rho V_R)}{dt} = (\rho\Phi_V)_0 - (\rho\Phi_V) = 0 \tag{54}$$

where: ρ_0, ρ = densities of the inlet and outlet streams.
$\Phi_{V,0}$, Φ_V, = volumetric flow rates of the inlet and outlet streams.
V_R = volume of the reacting mixture in the tank.

Mass balance on component A

$$\frac{\left[\begin{matrix}\text{accumulation}\\ \text{of A}\end{matrix}\right]}{\text{time}} = \frac{\left[\begin{matrix}\text{input}\\ \text{of A}\end{matrix}\right]}{\text{time}} - \frac{\left[\begin{matrix}\text{output}\\ \text{of A}\end{matrix}\right]}{\text{time}} - \frac{\left[\begin{matrix}\text{disappearance of A}\\ \text{due to reaction}\end{matrix}\right]}{\text{time}}$$

or

$$\frac{d(n_A)}{dt} = \frac{d(V_R[A])}{dt} = ([A]\Phi_V)_0 - ([A]\Phi_V) - rV_R \tag{55}$$

where: r = rate of reaction per unit volume.
[A], $[A]_0$ molar concentrations of vA in the inlet and outlet streams
n_A = number of moles of A in the reacting mixture.

In expression 55 r represents the overall chemical reaction rate (reaction 1) defined as:

$$r = -r_A = k_R[A] = k_0 e^{-E_{act}/RT}[A] \tag{1}$$

In equation 1, E_{act} is the activation energy and k_0 the Arrhenius frequency factor. Expression 1 was considered by Arrhenius[59 14 26]. It represents the effect of temperature on the rate constants (of simple reactions) i.e. it symbolises the amount of energy in excess of the average energy level, which the reactants must have in order for the reaction to proceed.
The specific state variables are [A] and V_R. Algebraic manipulation on equation 55 leads to:

$$\frac{d(V_R[A])}{dt} = [A]\frac{dV_R}{dt} + V_R\frac{d[A]}{dt} = (\Phi_V[A])_0 - (\Phi_V[A]) - k_0 e^{-E_{act}/RT}[A]V_R \tag{56}$$

this expression becomes:

$$\frac{d[A]}{dt} = \frac{\Phi_V}{V_R}([A]_0 - [A]) - k_0 e^{-E_{act}/RT}[A] \tag{57}$$

Total energy balance

$$\frac{\left[\begin{matrix}\text{accumulation}\\ \text{of total energy}\end{matrix}\right]}{\text{time}} = \frac{\left[\begin{matrix}\text{input of total}\\ \text{energy of feed}\end{matrix}\right]}{\text{time}} - \frac{\left[\begin{matrix}\text{output of total}\\ \text{energy of feed}\end{matrix}\right]}{\text{time}} - \frac{\left[\begin{matrix}\text{energy removed}\\ \text{by coolant}\end{matrix}\right]}{\text{time}}$$

Extensive thermodynamic derivations can be found in Stephanopoulos[74].

$$\frac{dH}{dt} = \rho_0 \Phi_{V,0} h_0(T_0) - \rho \Phi_V h(T) - Q \tag{58}$$

Where Q is the amount of heat removed. The amount of heat supplied by e.g. steam or removed by the coolant per unit time[80] is given by following expressions:

$$Q_{heat} = UA(T_{steam} - T) \tag{59}$$

$$Q_{cool} = UA(T - T_{cool}) \tag{60}$$

In equation 60 U is the overall heat transfer coefficient and A represents the total area of heat transfer. Equations 54, 55 and 58 are not in their final and most convenient form for process control design studies. To bring them to such form the appropriate state variables will be identified.
From the thermodynamics, it is known that the enthalpy of a liquid system is a function of the temperature and its composition:

$$\rho V_R C_P \frac{dT}{dt} = \Phi_{V,0} \rho_0 C_{P,0}(T_0 - T) + (\tilde{H}_A - \tilde{H}_P) r V_R - Q \tag{61}$$

C_P is the specific heat capacity of the reacting mixture and in equation 61 $\tilde{H}_A$ and $\tilde{H}_P$ are the partial molar enthalpies of A and P. Since $\tilde{H}_A - \tilde{H}_P = -\Delta H_R$ which represents the heat of reaction at temperature T and $\rho = \rho_0$, $C_P = C_{P,0}$.

$$V_R \frac{dT}{dt} = \Phi_{V,0}(T_0 - T) + \frac{-\Delta H_R}{\rho C_P} r V_R - \frac{Q}{\rho C_P} \tag{62}$$

From equation 62 the temperature T is the state variable that characterise the total energy of the system. Summarizing all the steps above in the mathematical modelling of a CISTR results in state variables [A] and T and state equations 63 and 64 according

$$\frac{d[A]}{dt} = \frac{\Phi_V}{V_R}([A]_0 - [A]) - k_0 e^{-E_{act}/RT}[A] \tag{63}$$

$$\frac{dT}{dt} = \frac{\Phi_V}{V_R}(T_0 - T) + \frac{-\Delta H_R}{\rho C_P} k_0 e^{-E_{act}/RT}[A] - \frac{UA(T - T_{cool})}{\rho C_P V_R} \tag{64}$$

Heat classification

Heat can be categorised in respectively:

heat, which is needed to bring the feed to operation temperature

$$Q_{feed} = \rho C_P \Phi_V (T - T_0) \tag{65}$$

heat produced by reaction

$$Q_{reaction} = \Delta H_R V_R k_0 e^{-E_{act}/RT}[A] \tag{66}$$

transferred heat

$$Q_{transfer} = UA(T - T_{cool}) \tag{67}$$

heat, which is removed by coolant according:

$$Q_{cool} = \rho_{cool} C_{P,cool} \Phi_{V,cool} (T_{cool} - T_{cool,0}) \tag{68}$$

heat production rate:

$$HPR = \Delta T_{ad} \frac{k_R \tau_R}{1 + k_R \tau_R} \tag{69}$$

and heat withdrawal rate (derived from equations 2, 3, 10, 4, 6 and 7)

$$HWR = (T_0 - T) - NTU(T - T_{cool}) \tag{70}$$

Linearisation of the non-isothermal CISTR

In process control applications, generally differential equations are linearised to examine its dynamic behaviour. The literature[25 37 59 60 72 74] deals often with the linearisation of the non-linear CISTR model according the state equations 2 and 3. According to Stephanopoulos[74] the linearised mass and energy balances could be perceived as a capacity in which energy can be stored. The response of [A] and T to inlet changes is second order. A CISTR is distinguished by the kinetic rate term, which denotes disappearance of component A. Such terms may produce not only overdamped but also underdamped and inverse response.

Appendix 2. Literature

Although many articles can be found regarding CISTRs, stability and process control, little information can be found with respect to limit cycles and process control. The information that can be gathered is concerned with proportional-integral control in which the coolant temperature is adjusted. Not taken into account is, instead of the coolant temperature, the coolant flowrate nor the derivative control action, assumed delay and the non-ideal process behaviour, which can seriously affect the process stability. Besides, the literature often focuses on complex mathematical models, which requires very profound background knowledge. Nevertheless, some articles are refereed which may contribute to understand the limit cycle and stability problem in CISTRs.

Multiplicity and stability in CISTRs

Roffel[68] examined state equations 2 and 3 applying an information flow diagram in which the stable equilibrium points can be derived from specific trajectories. This method however is rather laborious in case model improvements are concerned. Bilous *et.al.*[7] presented the first modern stability analyses of the equilibrium states in a CISTR with a single exothermic reaction. It has been shown that instabilities may exist in the three steady states. Analytical criteria have been for the determination of stability. The article provides much information about the dynamical behaviour of a CISTR. However, in case the model is extended, the methods become very complex. Doherty and Ottino[21] explained in their article through chaos theory the sensitive dependence of solution of differential equations on initial conditions. Hoffman *et.al.*[39] developed a model to determine steady state multiplicity in a gas-liquid CISTR with exothermic reaction. Pellegrini et.al.[58] determined the region of asymptotic stability for, and the chaotic behaviour of a CISTR. Ding *et.al.*[17] demonstrated through chlorination of liquid n-decane experimentally in an adiabatic continuously stirred tank reactor the existence of steady state multiplicity. They investigated the influences of a control scheme. Harold *et.al.*[31] investigated experimentally the steady state multiplicity features of two parallel catalytic reactors. They found methods to determine all possible steady states. Ostermaier *et.al.*[32] compared the CISTR with the decanting reactor for its dynamical behaviour. Huang *et.al.* [43] studied the second order reaction with regards to multiplicity. Vleeschhouwer *et.al.*[78] proposed an analytical perturbation analysis of a cobalt catalysed oxo reactor. They described the process with a pseudo homogeneous pseudo first order system, which can be described by merely two differential equations.
Heiszwolf and Fortuin[36] give a very clear example of a design procedure for stable operation of a first-order system in a CISTR using an analytical perturbation method. Ray[67] discussed the performance improvement of a chemical reaction by non-linear natural oscillations. Li and Horsthemke[50] studied the product occupancy in heterogeneous catalyses in relation with multiple steady states and temporal oscillations.

Limit cycles theoretical results

Aris and Amundson[1], van Heerden[34], Uppal *et.al.*[75], Heemskerk and Dammers[33], published the theoretical treatment of instabilities in continuously ideally stirred tank reactors based on the fundamental mass and energy balance. In these articles the appearance of self-sustained oscillations i.e. limit cycles have been theoretically demonstrated. Scott[69] and Bilous *et.al.*[7] considered the oscillations in simple models in chemical reactors and represented some experimental cases. Doedel and Heinemann[18] used the bifurcation theory to investigate the oscillatory behaviour in a CISTR with consecutive A→B→C reaction. They used a continuation technique to compute response diagrams exhibiting stable and unstable periodic branches that contain multiple limit points. Finally, Westerterp *et.al.*[80] mentioned the work on laboratory scale in which the existence of limit cycles have been demonstrated.

Limit cycles experimental results

Heemskerk *et.al.*[33] described experimental investigations concerning limit cycle behaviour in a one-phase reaction system i.e. the acid-catalysed hydrolyses of 2,3-epoxypropanol-1b and showed a good agreement with theory based on the fundamental mass and energy balance. Hanckock *et.al.*[30] analysed the instabilities in a CISTR with temperature fluctuations in one-phase and two-phase reactors reactor theoretically and carried out experiments e.g. the formation of methyl-chloride from methanol and hydrogen-chloride. They found the principle features of oscillatory behaviour. Bush[5] discovered the consternation of practical engineering in commercial situations. Harold *et.al.*[32] constructed maps with parameter regions with qualitatively different steady state and dynamical bifurcation diagrams. These maps could clearly describe the desirable regions of operation and point out the potential stability. They suggested to maintain a sufficiently small difference between the reactor temperature and the coolant temperature to avoid oscillatory behaviour. Huang *et.al.*[42] did research on predicting the steady state and dynamical behaviour of fast gas-liquid reactions in a non-adiabatic CISTR. The models they developed were experimentally identified i.e. multiplicity in the chlorination of n-decane. Vleeschhouwer and Fortuin[77] have been concerned with the theoretical and experimental aspects with respect to stability in a CISTR. Uppal and Ray[76] investigated theoretically the influence of the average residence time on the dynamical behaviour of a CISTR. Hjelmfelt and Ross[38] used a proportional flow feedback method to stabilise unstable stationary states in experiments with chlorite-iodide reactions. Vleeschhouwer *et al.*[78] demonstrated that sustained temperature oscillations can occur in a commercial scale gas-liquid oxo-reactor.

Process control

Kravaris *et.al.*[47] proposed a robust non-linear feedback control scheme. This article is an improvement of the global input/output linearisation approach. The article is difficult to expand with differential equations. Ratto *et.al.*[64] analysed the PI-controlled CISTR with fluctuating and uncertain parameters. In the article, they applied the Hopf bifurcation plot to determine the stability. Ratto[66] made also a theoretical approach to the analyse of PI-controlled CISTRs with noice. Calvet *et.al.*[10] presented a method to compute gains to design a PI-controller based on perturbations in non-linear systems. In the article, the influence of limit cycles was not considered. Daoutidis *et.al.*[16] are concerned with a different approach of non-linear systems i.e. the state-space approach. Although the author proclaimed stability, the applied methods are rather laborious. Giona and Paladino[29] developed a comprehensive bifurcation analyses and stability consideration of a controlled CISTR in the presence of a νth order exothermic reaction. They studied the PI-control and introduced controller time delay. Paladino and Ratto[65] developed a procedure for stability, robustness and sensitivity of real controlled CISTRs through bifurcation analyses. Paladino and Ratto [64] also studied the controllability of start-ups in CISTRs under PI-control.

Limit cycle control

Limquerco *et.al.*[51] proposed a non-linear output feedback control of an exothermic reaction in a CISTR. In case the system was perturbed, they found both ignition and extinction, however more interesting they measured limit cycles under certain conditions. The disadvantage of this article like the article of Uppal *et.al.*[75] is the fact that instantaneous change of the coolant temperature is assumed. Interesting point of

the article is the non-linear approach. Dolnik *et.al.*[19] studied numerical and experimental the chlorine dioxide-iodide reaction in a CISTR with feedback regulation of flow rate. The difference with this report is the existence of more than one reactant.

Appendix 3. Value estimation

Despite the fact that this report has a qualitative analytical character and the chosen base case, definition has been extracted from the article by van Elk *et.al.*[22] it is indispensable to investigate the magnitudes of the base case parameters; consequently, the chosen values will be compared with regular values and validated. To examine parameters: UA, $-\Delta H_R$, E, k_0, ρ, V_R, C_P.

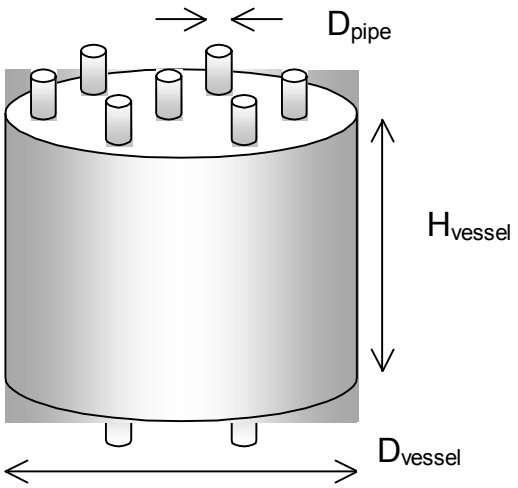

Figure 166 Theoretical cylindrical vessel containing cooled through n pipes.

UA value estimation

In this section, the value of product U and A will be considered.
In the base case definition, the value UA = 55 [kJ s^{-1} K^{-1}] has been chosen. To validate this magnitude, inevitably several calculations will be made.

Assume a chemical reactor has to be cooled through n pipes. Consider a cylindrical vessel with volume V_{vessel}. The vessel contains a reacting substance with volume V_R. Heat is transferred by the pipes and the reactor wall. The base case UA-value states UA = 55 [kJ s^{-1} K^{-1}].
The reactor volume is the sum of the liquid volume and the volume of the cooling pipes:

$$V_{vessel} = V_{pipes} + V_R \qquad (71)$$

In the first place, the number of pipes n is estimated.

The total area regarding heat transfer states:

$$A_{pipes} = n\pi D_{pipe} H_{vessel} \qquad (72)$$

$$A_{vessel} = 2\frac{\pi}{4} D_{vessel}^2 + \pi D_{vessel} H_{vessel} - 2n\frac{\pi}{4} D_{pipe}^2 \qquad (73)$$

$$A_{total} = A_{pipes} + A_{vessel} \qquad (74)$$

The ratio vessel height H_{vessel} and vessel diameter D_{vessel} is introduced:

$$H_{vessel} = \Psi D_{vessel} \tag{75}$$

The volume of the vessel states:

$$V_{vessel} = \frac{\pi}{4} D_{vessel}^2 H_{vessel} \tag{76}$$

The number of pipes in the vessel can be estimated combining equations 72, 73, 74, 75 and 76 under the assumption that $V_{vessel} \approx V_R$.

$$n = \frac{\frac{A_{total}}{\pi} - \left(\frac{4V_R}{\pi\Psi}\right)^{2/3}\left(\frac{1}{2}+\Psi\right)}{\left(\frac{4V_R}{\pi\Psi}\right)^{1/3}\Psi D_{pipe} - \frac{1}{2}D_{pipe}^2} \tag{77}$$

- Subsequently the vessel height and diameter is derived.

The volume of n pipes states:

$$V_{pipes} = n\frac{\pi}{4} D_{pipe}^2 H_{vessel} \tag{78}$$

Combining expressions 71, 75, 76 and 78 provides the following cubic equation:

$$D_{vessel}^3 + a_1 D_{pipe} + a_2 = 0 \tag{79}$$

Where:

$$\begin{aligned} a_1 &= -nD_{pipe}^2 \\ a_2 &= \frac{4V_R}{\pi\Psi} \end{aligned} \tag{80}$$

The vessel diameter can be calculated with:

$$D_{vessel} = \frac{1}{6}\left(108a_2 + 12\sqrt{-12a_1^{\,3} + 81a_2^{\,2}}\right)^{1/3} + \frac{2a_1}{\left(108a_2 + 12\sqrt{-12a_1^{\,3} + 81a_2^{\,2}}\right)} \tag{81}$$

Due to the assumption $V_{vessel} \approx V_R$ in equation 77, a slightly divergent value is obtained, using equation 73. However, merely a few recalculations is sufficient enough to eliminate this discrepancy. Better is to apply a solver e.g. Excel or Maple.
Using equation 82 the volumetric percentage of all the pipes in the reactor can be acquired:

$$Vol\% = n\left(\frac{D_{pipe}}{D_{vessel}}\right)^2 100\% \tag{82}$$

The specific area of the pipes becomes:

$$a_{pipes} = 4n\frac{D_{pipe}}{D_{vessel}^2} \tag{83}$$

Suppose the cooling fluid flows through pipes with thickness δ_{pipe} and with an average fluid velocity u_L,

$$\Phi_{V,cool} = n\frac{\pi}{4}\left(D_{pipe}^2 - \delta_{pipe}^2\right)u_L \tag{84}$$

Coulson *et.al.*[14 15] summarised typical values for the overall heat transfer coefficient U for various types of heat exchanger and specific media. According to Westerterp *et.al.*[80], a general applicable value for the overall heat transfer coefficient for a cold liquid is $U \approx 900$ [J m^{-2} s^{-2} K^{-1}].
The overall heat transfer coefficient value can additionally be verified using several calculation methods according to Perry *et.al.*[59], Heiszwolf *et.al.*[36], Coulson *et.al.*[14] and Roffel[68].

Table 38 represents the essential calculations and results for the UA value estimation.

Table 38 Example UA calculation value in cylindrical vessel.

Description	Calculation	Result
Reactor with volume	Base case value[22] ($\varepsilon = 0$)	$V_R = 5$ [m^3]
Desired UA value	Base case value[22]	UA = 55×10^3 [J s^{-1} K^{-1}]
Thickness of 1 pipe	Assumed value	D_{pipe} = 1" = 0.0254 [m]
Thickness of pipe wall	10% pipe thickness	δ_{pipe} = 0.00254 [m]
Velocity cooling fluid	Based on equation 84	$u_L = 1.7$ [m s^{-1}]
Reynolds number reaction mixture	Default equation[14 36 59 68]	$Re_R = 2 \times 10^5$ [-]
Reynolds number cooling fluid	Default equation[14 36 59 68]	$Re_{cool} = 8 \times 10^4$ [-] turbulent
Prandtl number reaction mixture	Specific correlation[14 36 59 68]	$Pr_R = 4$ [-]
Prandtl number cooling fluid	Specific correlation[14 36 59 68]	$Pr_{cool} = 3.4$ [-]
Nusselt number reaction mixture	Specific correlation[14 36 59 68]	$Nu_R = 106$ [-]
Nusselt number cooling fluid	Specific correlation[14 36 59 68]	$Nu_{cool} = 300$ [-]
Heat transfer coefficient reactor	Specific correlation[14 36 59 68]	$\alpha_R = 1740$ [J m^{-2} s^{-1} K^{-1}]
Heat transfer coefficient coolant	Specific correlation[14 36 59 68]	$\alpha_{cool} = 5920$ [J m^{-2} s^{-1} K^{-1}]
Overall Heat transfer coefficient	Specific correlation[14 15 36 59 68 80]	$U = 900$ [J m^{-2} s^{-1} K^{-1}]
Ratio vessel height and diameter	Assumed value (arbitrary chosen)	$\Psi = 1¼$ [-]
Total area for heat transfer	UA / U	$A_{total} = 61.1$ [m^2]
Vessel diameter	Equation 75	$D_{vessel} = 1.75$ [m]
Vessel height	Equation 76 (first approximation $V_{vessel} \approx V_R = 5$ [m^3])	$H_{vessel} = 2.19$ [m]
Number of pipes in vessel	Equation 77	n = 255 [-]
Vessel volume	Equation 71	$V_{vessel} = 5.28$ [m^3]
Volume of n pipes	Equation 78	$V_{pipes} = 0.23$ [m^3]
Mass of n pipes	$m = \rho V_{pipes}$	m = 1770 [kg]
Pipe volume percentage	Equation 82	Vol% = 5.3 [%]
Specific area pipes	Equation 83	8.4 [m^2 m^{-3}]
Total area n pipes	Equation 72	$A_{pipes} = 44.5$ [m^2]
Total area vessel	Equation 73	$A_{pipes} = 16.6$ [m^2]
UA contribution n pipes	$U A_{pipes}$	UA = 40×10^3 [J s^{-1} K^{-1}]
UA contribution vessel	$U A_{vessel}$	UA = 15×10^3 [J s^{-1} K^{-1}]
Total pipe length	$n H_{vessel}$	$L_{pipes,total} = 558$ [m]
Flowrate cooling fluid	Equation 84	$\Phi_{V,cool} = 13$ [m^3 min^{-1}]
Residence time coolant	$V_{cool} / \Phi_{V,cool}$	1.3 [s]

The first calculation gives n = 263 for V_{vessel} = 5.29 [m^3]. The solver results in n = 255 for V_{vessel} = 5.28 [m^3]. Therefore, the number of pipes has no decisive effect on the vessel volume. The vessel requires approximately 250 pipes to cool the exothermic reaction. Consequently, 5% of the vessel is filled with pipes. Concisely, the base case value UA = 55 [kJ s^{-1} K^{-1}] is allowable.

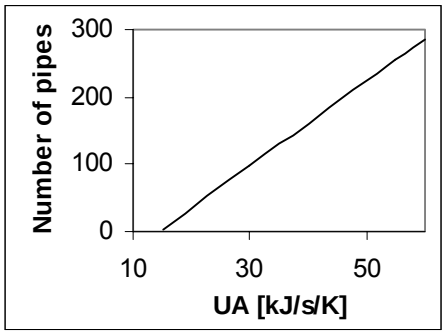

Figure 167 The number of pipes in the vessel (Table 38) rises if the required UA value increases. No cooling pipes are needed if required UA < 15 [kJ s^{-1} K^{-1}] due to the heat transfer through the vessel wall.

$-\Delta H_R$ value estimation

According to Westerterp *et.al.*[80] ΔH_R is defined as the heat absorbed by the system when the reaction proceeds completely in the direction indicated by the arrow, at constant temperature and pressure.
In Weast *et.al.*[79] tables with values of the heat formation at ΔH (T = 25 [°C]) for various species have been given. On account of these tables the reaction enthalpy $\Delta H_R = -1.6 \times 10^5$ [J mol^{-1}] given in the base case definition van Elk *et.al.*[22], can be deduced for instance organic-water mixtures.

E_{act} value estimation

According to Westerterp *et.al.*[80] typical values of Arrhenius activation energy vary globally between $4 \times 10^4 \leq E_{act} < 3 \times 10^5$ [J mol^{-1}]. The value $E_{act} = 9 \times 10^4$ [J mol^{-1}] which has been chosen in the base case definition is a common quantity for organic or organic-water mixtures compounds and therefore acceptable.

k_0 value estimation

In the article by van Elk *et.al.*[22] the value of the Arrhenius pre-exponential factor or frequency factor (equation 1) has been chosen based on a gas-liquid system in a kinetic controlled regime: $k_0 = 5 \times 10^5$ [s^{-1}]. According to the base case definition, no gas is present. Therefore the A-concentration $[A]_{L,bulk}$ = 50.1 [mol m^{-3}] will be integrated in the base case k_0 value i.e.: $k_0 = 50.1 \times 5 \times 10^5 = 2.505 \times 10^7$ [s^{-1}] to obtain the same results published in the articles published by van Elk *et.al*.

ρ value estimation

In the base case definition, the density states ρ = 800 [Kg m^{-3}]. According to Coulson et.al.[14], Fogler *et.al.*[26] and Roffel[68] this value is a common quantity for regular organic compound or organic-water mixtures. The density for stainless steel is assumed[14] to be ρ = 7830 [Kg m^{-3}].

C_P value estimation

In the base case definition, a heat capacity C_P = 2000 [J Kg^{-1} K^{-1}] has been chosen. According to Perry[59] regular value for liquids are on the order of $5 \times 10^2 \leq C_P < 2 \times 10^3$, Therefore the chosen C_P value is acceptable for the base case. The heat capacity for steel is assumed[59] to be C_P = 500 [J Kg^{-1} K^{-1}].

V_R value estimation

The reactor volume discussed in van Elk *et.al.*[22], has been set to V_R = 10 [m^3]. Additionally 50% of the reactor is filled with gas i.e. the hold-up ε = 0.5. According to the base case definition, no gas is present in the reactor i.e. ε = 0, consequently the current reactor volume becomes $V_R = 10 \times (1 - 0.5) = 5$ [m^3].

Appendix 4. Shutting down the input flowrate

In case the stability of the process cannot be maintained, due to e.g. control failure, the possibility of shutdown the feed can than be considered. If has been decided to close the feed flow i.e. not the drain, the state equations 2 and 3 of the CISTR change into respectively equations 85 and 86:

$$V_R \frac{d[A]}{dt} = -\Phi_V [A] - V_R k_0 e^{-E_{act}/RT}[A] \tag{85}$$

$$\rho C_P V_R \frac{dT}{dt} = -\rho C_P \Phi_V T + \left(-\Delta H_R\right) V_R k_0 e^{-E_{act}/RT}[A] - UA\left(T - T_{cool}\right) \tag{86}$$

The reaction will drain ($t \rightarrow \tau_R$) and the reaction will expire (Figure 168). Loss of production is not the only disadvantage of shutdown the reactor. The shutdown operation itself will waste energy and material stored in the process, which must be removed, and the subsequent start-up will require a similar amount of energy and material to be added to reach operating levels again. However, in case the temperature overshoot. More about this subject can be found in Shinskey[71].

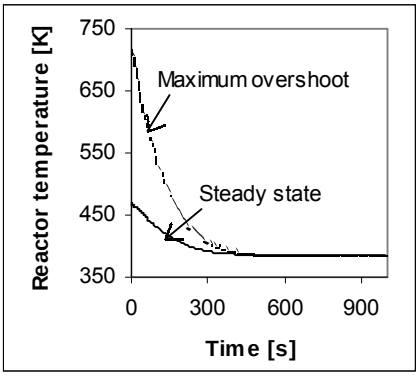

Figure 168 The reactor temperature drops to T=385 [K] in case the input flowrate is halted (equation 86) and is mainly stabilised after $t \approx 500$ [s].

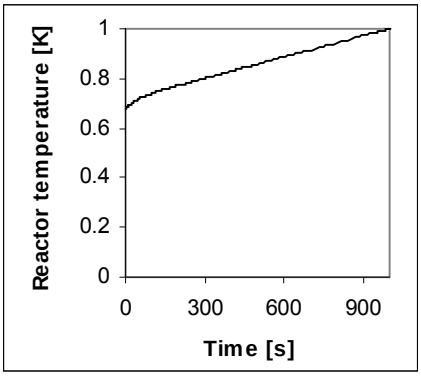

Figure 169 The conversion (equation 86) rises until the maximum value has been reached, which is obviously $\zeta(t = \tau_R) \rightarrow 1$.

Appendix 5. Cooling capacity – coolant flowrate relationship

Foust *et.al.*[27] and Ogunnaike *et.al.*[60] proposed an empirical relationship 87 in which the cooling capacity can be substituted by the cooling flowrate.

$$UA = a_1 \left(\Phi_{V,cool} \right)^{a_2} \tag{87}$$

Table 39 Values empirical heat capacity relation.

Parameter	Value	Dimension
A_1	1.2×10^5	[J s^{-1} K^{-1}]
A_2	0.5	[-]

Combination of equations 13 and 87 can be used to determine the recycle stream ratio. The base case cooling capacity UA = 55 [kJ s^{-1} K^{-1}] corresponds with a recycle ration of approximately 10.

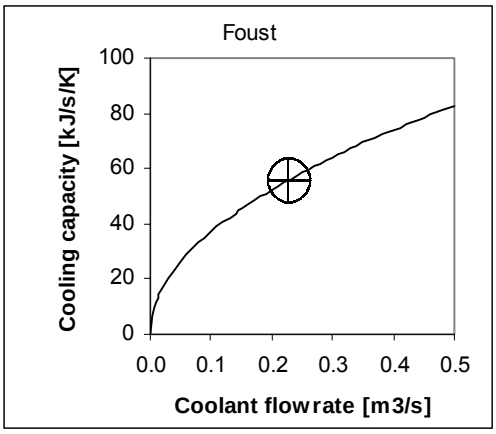

Figure 170 Empirical relationship 87 between the cooling capacity and the coolant flowrate.

More about this subject Aris *et.al.*[2].

Appendix 6. LOCBIF Nomenclature

LOCBIF	Symbol	Description	Dimension
A	A	Heat transfer or exchanger area	[m^2]
cA	[A]	Concentration component A	[mol m^{-3}]
cA0	$[A]_0$	Concentration component A	[mol m^{-3}]
Cp	C_P	Heat capacity	[J Kg^{-1} K^{-1}]
Cpe	$C_{P,cool}$	Heat capacity of cooling fluid	[J Kg^{-1} K^{-1}]
Delay	τ_d	Apparent delay	[s]
Dpipe	D_{pipe}	Pipe diameter	[m]
Eact	E_{act}	Activation energy (equation 1)	[J mol^{-1}]
fouling	f	Fouling factor, rate of UA depletion	[s^{-1}]
g	g	Gravitational acceleration	[m s^{-2}]
dH	ΔH_R	Reaction heat / enthalpy of reaction based on R	[J mol^{-1}]
k	k_0	Arrhenius pre-exponential factor or frequency factor	[s^{-1}]
Kc	K_c	Proportional control gain	[-] or [m^3 s^{-1} K^{-1}]
kr	$k_{R,m,n}$	Reaction rate constant	[$m^{3(m+n-1)}$ / $mol^{(m+n-1)}$ s]
Lpipe	L_{pipe}	Pipe length in reactor	[m]
NTU	NTU	Number of transport units	[-]
NTUe	NTU_{cool}	Number of transport units coolant	[-]
phi	$\int_0^1 (T_{sp} - T)dt$		[K s]
Qfeed	Q_{feed}	Required heat to bring the feed to operation temperature	[J s^{-1}]
Qreaction	$Q_{reaction}$	Heat produced by reaction	[J s^{-1}]
Qtransfer	$Q_{transfer}$	Heat transferred through cooling/heating area	[J s^{-1}]
Qcool	Q_{cool}	Heat, which is removed by coolant	[J s^{-1}]
R	R	Ideal gas constant	[J mol^{-1} K^{-1}]
Spiral	$m_{pipes}C_{p,pipes}$	Additional (cooling device) term in heat balance coolant flowrate	[J K^{-1}]
t	t	Simulation time variable	[s]
T	T	Temperature	[K]
Te	T_{cool}	Coolant temperature	[K]
Tdelay	Tdelay	Temperature after an apparent delay	[K]
thickness	D_{pipe}	Pipe thickness	[m]
dTad	ΔT_{ad}	Adiabatic temperature difference	[K]
td	t_d	Time (delay or dead)	[s]
UA	UA	Cooling capacity	[J s^{-1} K^{-1}]
ve	u_L	Average liquid velocity based on cross section	[m s^{-1}]
Vcool	V_{cool}	Volume cooling fluid	[m^3]
Vr	V_R	Reactor volume	[m^3]
Dpipe	δ	Thickness of cooling pipe	[m]
e	ε	Hold-up	[m^3 m^{-3}]
taue	$\tau_{coolant}$	Average residence time of a coolant particle in cooling device	[s]
taue	τ_{cool}	Time constant of the cooling fluid	[s]
tau	τ_R	Resident time	[s]
taul	τ_I	Integral time constant / reset time	[s] [min]
F	Φ_v	Volumetric flow rate	[m^3 s^{-1}]
Fe	$\Phi_{v,cool}$	Flowrate cooling fluid	[m^3 s^{-1}]
rho	ρ	Fluid density	[kg m^{-3}]
rhoe	ρ_{cool}	Density of cooling fluid	[kg m^{-3}]

Appendix 7. LOCBIF Source codes

```
PHASE zeta, T
PAR UA,Tcool,F
COMMON Vr,rho,cA0,Cp,dH,k,E,R,T0,ret
FUN tau,NTU,dTad
tau=Vr/F
NTU=UA/(rho*Cp*F)
dTad=-dH/(rho*Cp)*cA0
zeta'=(1-zeta)*k*exp(-E/R/T)-zeta/tau
T'=((T0-T)-NTU*(T-Tcool))/tau+dTad*(1-zeta)*k*exp(-E/R/T)
INIT={F=0.005 Vr=5 rho=800 Cp=2000 cA0=5000 dH=-1.6E5 k=2.505E7 E=9E4 R=8.31441 T0=303} ret
```

LOCBIF rhs 2 Bifurcation sample base case.

```
PHASE zeta, T
PAR UA,Tset,Teset,Kc
COMMON F,Vr,rho,cA0,Cp,dH,k,E,R,T0,ret
FUN tau,NTU,dTad,Te,offset
tau=Vr/F
NTU=UA/(rho*Cp*F)
dTad=-dH/(rho*Cp)*cA0
offset=Tset-T
Te=Teset+Kc*offset
zeta'=(1-zeta)*k*exp(-E/R/T)-zeta/tau
T'=((T0-T)-NTU*(T-Te))/tau+dTad*(1-zeta)*k*exp(-E/R/T)
INIT={F=0.005 Vr=5 rho=800 Cp=2000 cA0=5000 dH=-1.6E5 k=2.505E7 E=9E4 R=8.31441 T0=303} ret
```

LOCBIF rhs 3 Base case + coolant temperature proportional control.

```
PHASE zeta, T, phi
PAR UA,Tset,Teset,Kc,taui
COMMON F,Vr,rho,cA0,Cp,dH,k,E,R,T0,ret
FUN tau,NTU,dTad,Te
tau=Vr/F
NTU=UA/(rho*Cp*F)
dTad=-dH/(rho*Cp)*cA0
Te=Teset+Kc*((Tset-T)+phi/taui)
zeta'=(1-zeta)*k*exp(-E/R/T)-zeta/tau
T'=((T0-T)-NTU*(T-Te))/tau+dTad*(1-zeta)*k*exp(-E/R/T)
phi'=Tset-T
INIT={F=0.005 Vr=5 rho=800 Cp=2000 cA0=5000 dH=-1.6E5 k=2.505E7 E=9E4 R=8.31441 T0=303} ret
```

LOCBIF rhs 4 Base case + coolant temperature proportional-integral control.

```
PHASE cA, T, Te
PAR Tset,UA,Kc,Te0,Teset,recycle
COMMON F,Vr,rho,cA0,Cp,dH,k,E,R,T0,Vcool,rhoe,Cpe,Dpipe,thickness,n,pi,spiraal,ret
FUN Qfeed,Qreaction,Qtransfer,Qcool,zeta,Feset,offset,Fe,ve,NTUe
Qfeed=rho*Cp*F*(T0-T)
Qreaction=(-dH)*k*exp(-E/R/T)*cA*Vr
Qtransfer=UA*(T-Te)
Qcool=rhoe*Cpe*Fe*(Te0-Te)
zeta=1-cA/cA0
Feset=-UA*(Tset-Teset)/(rhoe*cpe*(Te0-Teset))
offset=Tset-T
Fe=(sgn(Feset-Kc*offset)+1)*(Feset-Kc*offset)/2
ve=(1+recycle)*(Fe/n/(pi/4*(Dpipe^2-thickness^2)))
NTUe=UA/(rhoe*Cpe*Fe)
cA'=F/Vr*(cA0-cA)-k*exp(-E/R/T)*cA
T'=(Qfeed+Qreaction-Qtransfer)/(rho*Cp*Vr)
Te'=Fe/Vcool*(Te0-Te)+UA/(spiraal+rhoe*Cpe*Vcool)*(T-Te)
INIT={F=0.005 Vr=5 rho=800 Cp=2000 cA0=5000 dH=-1.6E5 k=2.505E7 E=9E4 R=8.31441 T0=303
      Vcool=0.283 rhoe=1E3 Cpe=4200 spiraal=0 Dpipe=0.0254 thickness=0.00254 n=255
      pi=3.1415926536} ret
```

LOCBIF rhs 5 Base case + coolant flowrate proportional control.

```
PHASE cA, T, Te, phi
PAR Tset,UA,Kc,Te0,Teset,recycle,taui
COMMON F,Vr,rho,cA0,Cp,dH,k,E,R,T0,Vcool,rhoe,Cpe,Dpipe,thickness,n,pi,spiraal,Kp,ret
FUN Feset,Fe
Feset=-UA*(Tset-Teset)/(rhoe*cpe*(Te0-Teset))
Fe=Feset-Kc*((Tset-T)+phi/taui)
cA'=F/Vr*(cA0-cA)-k*exp(-E/R/T)*cA
T'=((rho*Cp*F*(T0-T))+((-dH)*k*exp(-E/R/T)*cA*Vr)-(UA*(T-Te)))/(rho*Cp*Vr)
Te'=((UA*(T-Te))+(rhoe*Cpe*Fe*(Te0-Te)))/(spiraal+rhoe*Cpe*Vcool)
phi'=(Tset-T)
INIT={F=0.005 Vr=5 rho=800 Cp=2000 cA0=5000 dH=-1.6E5 k=2.505E7 E=9E4 R=8.31441 T0=303
      Vcool=0.283 rhoe=1E3 Cpe=4200 spiraal=0 Dpipe=0.0254 thickness=0.00254 n=255
      pi=3.1415926536} ret
```

LOCBIF rhs 6 Base case + coolant flowrate proportional-integral control.

```
PHASE cA, T
PAR UA,Te,Tset,Fset,Kc
COMMON Vr,rho,cA0,Cp,dH,k,E,R,T0,ret
FUN tau,Qfeed,Qreaction,Qtransfer,zeta,offset,F,deviation
tau=Vr/F
Qfeed=rho*Cp*F*(T0-T)
Qreaction=(-dH)*k*exp(-E/R/T)*cA*Vr
Qtransfer=UA*(T-Te)
zeta=1-cA/cA0
offset=Tset-T
F=(sgn(Fset-Kc*(Tset-T))+1)*(Fset-Kc*(Tset-T))/2
deviation=(Fset-F)/Fset*100
cA'=F/Vr*(cA0-cA)-k*exp(-E/R/T)*cA
T'=(Qfeed+Qreaction-Qtransfer)/(rho*Cp*Vr)
INIT={Vr=5 rho=800 Cp=2000 cA0=5000 dH=-1.6E5 k=2.505E7 E=9E4 R=8.31441 T0=303} ret
```

LOCBIF rhs 7 Base case + flowrate proportional control.

```
PHASE cA, T, phi
PAR UA,Te,Tset,Fset,Kc,taui
COMMON Vr,rho,cA0,Cp,dH,k,E,R,T0,ret
FUN tau,Qfeed,Qreaction,Qtransfer,zeta,offset,F,deviation
tau=Vr/F
Qfeed=rho*Cp*F*(T0-T)
Qreaction=(-dH)*k*exp(-E/R/T)*cA*Vr
Qtransfer=UA*(T-Te)
zeta=1-cA/cA0
offset=Tset-T
F=(sgn(Fset-Kc*((Tset-T)+phi/taui))+1)*(Fset-Kc*((Tset-T)+phi/taui))/2
deviation=(Fset-F)/Fset*100
cA'=F/Vr*(cA0-cA)-k*exp(-E/R/T)*cA
T'=(Qfeed+Qreaction-Qtransfer)/(rho*Cp*Vr)
phi'=offset
INIT={Vr=5 rho=800 Cp=2000 cA0=5000 dH=-1.6E5 k=2.505E7 E=9E4 R=8.31441 T0=303} ret
```

LOCBIF rhs 8 Base case + flowrate proportional-integral control.

```
PHASE zeta, T, UA
PAR Tset,Teset,Kc
COMMON F,Vr,rho,cA0,Cp,dH,k,E,R,T0,ret
FUN tau,NTU,dTad,Te,fouling
tau=Vr/F
NTU=UA/(rho*Cp*F)
dTad=-dH/(rho*Cp)*cA0
Te=Teset+Kc*(Tset-T)
fouling=-UA*(1-0.99)/3600
zeta'=(1-zeta)*k*exp(-E/R/T)-zeta/tau
T'=((T0-T)-NTU*(T-Te))/tau+dTad*(1-zeta)*k*exp(-E/R/T)
UA'=fouling
INIT={F=0.005 Vr=5 rho=800 Cp=2000 cA0=5000 dH=-1.6E5 k=2.505E7 E=9E4 R=8.31441 T0=303} ret
```

LOCBIF rhs 9 Fouling effect at a coolant temperature proportional controlled base.

```
PHASE zeta, T, phi, UA
PAR Tset,Teset,Kc,taui
COMMON F,Vr,rho,cA0,Cp,dH,k,E,R,T0,ret
FUN tau,NTU,dTad,Te,fouling
tau=Vr/F
NTU=UA/(rho*Cp*F)
dTad=-dH/(rho*Cp)*cA0
Te=Teset+Kc*((Tset-T)+phi/taui)
fouling=-UA*(1-0.99)/3600
zeta'=(1-zeta)*k*exp(-E/R/T)-zeta/tau
T'=((T0-T)-NTU*(T-Te))/tau+dTad*(1-zeta)*k*exp(-E/R/T)
phi'=Tset-T
UA'=fouling
INIT={F=0.005 Vr=5 rho=800 Cp=2000 cA0=5000 dH=-1.6E5 k=2.505E7 E=9E4 R=8.31441 T0=303} ret
```

LOCBIF rhs 10 Fouling effect at a coolant temperature proportional-integral controlled base.

```
PHASE cA, T, Te, UA
PAR Tset,Kc,Te0,Teset,recycle
COMMON F,Vr,rho,cA0,Cp,dH,k,E,R,T0,Vcool,rhoe,Cpe,Dpipe,thickness,n,pi,spiraal,ret
FUN Qfeed,Qreaction,Qtransfer,Qcool,zeta,Feset,offset,Fe,ve,fouling
Qfeed=rho*Cp*F*(T0-T)
Qreaction=(-dH)*k*exp(-E/R/T)*cA*Vr
Qtransfer=UA*(T-Te)
Qcool=rhoe*Cpe*Fe*(Te0-Te)
zeta=1-cA/cA0
Feset=-UA*(Tset-Teset)/(rhoe*cpe*(Te0-Teset))
offset=Tset-T
Fe=(sgn(Feset-Kc*offset)+1)*(Feset-Kc*offset)/2
ve=(1+recycle)*(Fe/n/(pi/4*(Dpipe^2-thickness^2)))
fouling=-UA*(1-0.99)/3600
cA'=F/Vr*(cA0-cA)-k*exp(-E/R/T)*cA
T'=(Qfeed+Qreaction-Qtransfer)/(rho*Cp*Vr)
Te'=Fe/Vcool*(Te0-Te)+UA/(spiraal+rhoe*Cpe*Vcool)*(T-Te)
UA'=fouling
INIT={F=0.005 Vr=5 rho=800 Cp=2000 cA0=5000 dH=-1.6E5 k=2.505E7 E=9E4 R=8.31441 T0=303
Vcool=0.283 rhoe=1E3 Cpe=4200 spiraal=0 Dpipe=0.0254 thickness=0.00254 n=255
pi=3.1415926536} ret
```

LOCBIF rhs 11 Fouling effect at a coolant flowrate proportional controlled base.

```
PHASE cA, T, Te, phi, UA
PAR Tset,Kc,Te0,Teset,recycle,taui
COMMON F,Vr,rho,cA0,Cp,dH,k,E,R,T0,Vcool,rhoe,Cpe,Dpipe,thickness,n,pi,spiraal,Kp,ret
FUN Feset,Fe,fouling,ve
Feset=-UA*(Tset-Teset)/(rhoe*cpe*(Te0-Teset))
Fe=Feset-Kc*((Tset-T)+phi/taui)
fouling=-UA*(1-0.99)/3600
ve=(1+recycle)*(Fe/n/(pi/4*(Dpipe^2-thickness^2)))
cA'=F/Vr*(cA0-cA)-k*exp(-E/R/T)*cA
T'=((rho*Cp*F*(T0-T))+((-dH)*k*exp(-E/R/T)*cA*Vr)-(UA*(T-Te)))/(rho*Cp*Vr)
Te'=((UA*(T-Te))+(rhoe*Cpe*Fe*(Te0-Te)))/(spiraal+rhoe*Cpe*Vcool)
phi'=(Tset-T)
UA'=fouling
INIT={F=0.005 Vr=5 rho=800 Cp=2000 cA0=5000 dH=-1.6E5 k=2.505E7 E=9E4 R=8.31441 T0=303
Vcool=0.283 rhoe=1E3 Cpe=4200 spiraal=0 Dpipe=0.0254 thickness=0.00254 n=255
pi=3.1415926536} ret
```

LOCBIF rhs 12 Fouling effect at a coolant flowrate proportional-integral controlled base.

```
PHASE zeta, T, Td
PAR UA,Tset,Teset,Kc,delay
COMMON F,Vr,rho,cA0,Cp,dH,k,E,R,T0,ret
FUN tau,NTU,dTad,Te
tau=Vr/F
NTU=UA/(rho*Cp*F)
dTad=-dH/(rho*Cp)*cA0
Te=Teset+Kc*(Tset-Td)
zeta'=(1-zeta)*k*exp(-E/R/T)-zeta/tau
T'=((T0-T)-NTU*(T-Te))/tau+dTad*(1-zeta)*k*exp(-E/R/T)
Td'=(T-Td)/delay
INIT={F=0.005 Vr=5 rho=800 Cp=2000 cA0=5000 dH=-1.6E5 k=2.505E7 E=9E4 R=8.31441 T0=303} ret
```

LOCBIF rhs 13 Base case + coolant temperature proportional control with delay.

```
PHASE zeta, T, phi, Td
PAR UA,Tset,Teset,Kc,taui,delay
COMMON F,Vr,rho,cA0,Cp,dH,k,E,R,T0,ret
FUN tau,NTU,dTad,Te
tau=Vr/F
NTU=UA/(rho*Cp*F)
dTad=-dH/(rho*Cp)*cA0
Te=Teset+Kc*((Tset-Td)+phi/taui)
zeta'=(1-zeta)*k*exp(-E/R/T)-zeta/tau
T'=((T0-T)-NTU*(T-Te))/tau+dTad*(1-zeta)*k*exp(-E/R/T)
phi'=Tset-Td
Td'=(T-Td)/delay
INIT={F=0.005 Vr=5 rho=800 Cp=2000 cA0=5000 dH=-1.6E5 k=2.505E7 E=9E4 R=8.31441 T0=303} ret
```

LOCBIF rhs 14 Base case + coolant temperature proportional-integral control with delay.

```
PHASE cA, T, Te, Td
PAR Tset,UA,Kc,Te0,Teset,recycle,delay
COMMON F,Vr,rho,cA0,Cp,dH,k,E,R,T0,Vcool,rhoe,Cpe,Dpipe,thickness,n,pi,spiraal,ret
FUN Qfeed,Qreaction,Qtransfer,Qcool,zeta,Feset,offset,Fe,ve
Qfeed=rho*Cp*F*(T0-T)
Qreaction=(-dH)*k*exp(-E/R/T)*cA*Vr
Qtransfer=UA*(T-Te)
Qcool=rhoe*Cpe*Fe*(Te0-Te)
zeta=1-cA/cA0
Feset=-UA*(Tset-Teset)/(rhoe*cpe*(Te0-Teset))
offset=Tset-Td
Fe=(sgn(Feset-Kc*offset)+1)*(Feset-Kc*offset)/2
ve=(1+recycle)*(Fe/n/(pi/4*(Dpipe^2-thickness^2)))
cA'=F/Vr*(cA0-cA)-k*exp(-E/R/T)*cA
T'=(Qfeed+Qreaction-Qtransfer)/(rho*Cp*Vr)
Te'=Fe/Vcool*(Te0-Te)+UA/(spiraal+rhoe*Cpe*Vcool)*(T-Te)
Td'=(T-Td)/delay
INIT={F=0.005 Vr=5 rho=800 Cp=2000 cA0=5000 dH=-1.6E5 k=2.505E7 E=9E4 R=8.31441 T0=303
      Vcool=0.283 rhoe=1E3 Cpe=4200 spiraal=0 Dpipe=0.0254 thickness=0.00254 n=255
      pi=3.1415926536} ret
```

LOCBIF rhs 15 Base case + coolant flowrate proportional control with delay.

```
PHASE cA, T, Te, phi, Td
PAR Tset,UA,Kc,Te0,Teset,recycle,taui,delay
COMMON F,Vr,rho,cA0,Cp,dH,k,E,R,T0,Vcool,rhoe,Cpe,Dpipe,thickness,n,pi,spiraal,Kp,ret
FUN offset,Feset,Fe
offset=Tset-Td
Feset=-UA*(Tset-Teset)/(rhoe*cpe*(Te0-Teset))
Fe=(sgn(Feset-Kc*(offset+phi/taui))+1)*(Feset-Kc*offset)/2
cA'=F/Vr*(cA0-cA)-k*exp(-E/R/T)*cA
T'=((rho*Cp*F*(T0-T))+((-dH)*k*exp(-E/R/T)*cA*Vr)-(UA*(T-Te)))/(rho*Cp*Vr)
Te'=((UA*(T-Te))+(rhoe*Cpe*Fe*(Te0-Te)))/(spiraal+rhoe*Cpe*Vcool)
phi'=(Tset-Td)
Td'=(T-Td)/delay
INIT={F=0.005 Vr=5 rho=800 Cp=2000 cA0=5000 dH=-1.6E5 k=2.505E7 E=9E4 R=8.31441 T0=303
      Vcool=0.283 rhoe=1E3 Cpe=4200 spiraal=0 Dpipe=0.0254 thickness=0.00254 n=255
      pi=3.1415926536} ret
```

LOCBIF rhs 16 Base case + coolant flowrate proportional-integral control with delay.

```
PHASE cA, T, Td
PAR UA,Te,Tset,Fset,Kc,delay
COMMON Vr,rho,cA0,Cp,dH,k,E,R,T0,ret
FUN tau,Qfeed,Qreaction,Qtransfer,zeta,offset,F,deviation
tau=Vr/F
Qfeed=rho*Cp*F*(T0-T)
Qreaction=(-dH)*k*exp(-E/R/T)*cA*Vr
Qtransfer=UA*(T-Te)
zeta=1-cA/cA0
offset=Tset-T
F=(sgn(Fset-Kc*(Tset-Td))+1)*(Fset-Kc*(Tset-Td))/2
deviation=(Fset-F)/Fset*100
cA'=F/Vr*(cA0-cA)-k*exp(-E/R/T)*cA
T'=(Qfeed+Qreaction-Qtransfer)/(rho*Cp*Vr)
Td'=(T-Td)/delay
INIT={Vr=5 rho=800 Cp=2000 cA0=5000 dH=-1.6E5 k=2.505E7 E=9E4 R=8.31441 T0=303} ret
```

LOCBIF rhs 17 Base case + flowrate proportional control with delay.

```
PHASE cA, T, phi, Td
PAR UA,Te,Tset,Fset,Kc,taui,delay
COMMON Vr,rho,cA0,Cp,dH,k,E,R,T0,ret
FUN tau,Qfeed,Qreaction,Qtransfer,zeta,offset,F,deviation,dcA,dT
tau=Vr/F
Qfeed=rho*Cp*F*(T0-T)
Qreaction=(-dH)*k*exp(-E/R/T)*cA*Vr
Qtransfer=UA*(T-Te)
zeta=1-cA/cA0
offset=Tset-Td
F=(sgn(Fset-Kc*((Tset-Td)+phi/taui))+1)*(Fset-Kc*((Tset-Td)+phi/taui))/2
deviation=(Fset-F)/Fset*100
dcA=F/Vr*(cA0-cA)-k*exp(-E/R/T)*cA
dT=(Qfeed+Qreaction-Qtransfer)/(rho*Cp*Vr)
cA'=F/Vr*(cA0-cA)-k*exp(-E/R/T)*cA
T'=(Qfeed+Qreaction-Qtransfer)/(rho*Cp*Vr)
phi'=offset
Td'=(T-Td)/delay
INIT={Vr=5 rho=800 Cp=2000 cA0=5000 dH=-1.6E5 k=2.505E7 E=9E4 R=8.31441 T0=303} ret
```

LOCBIF rhs 18 Base case + flowrate proportional-integral control with delay

Part I

THEORY

Part II

APPLICATION

Base case model:	Limit cycle system
Source:	Van Elk *et.al.* [22, p4874]
Mechanism:	Irreversible exothermic $A_{(l)} \rightarrow P_{(l)}$
Reactor:	Cooled CISTR
Dynamical behaviour:	Limit cycles
Controllers:	None, P or PI
Manipulated variables:	T_{cool}, $\Phi_{V,cool}$ or Φ_V
Active parameters:	UA, K_c, τ_I and τ_d

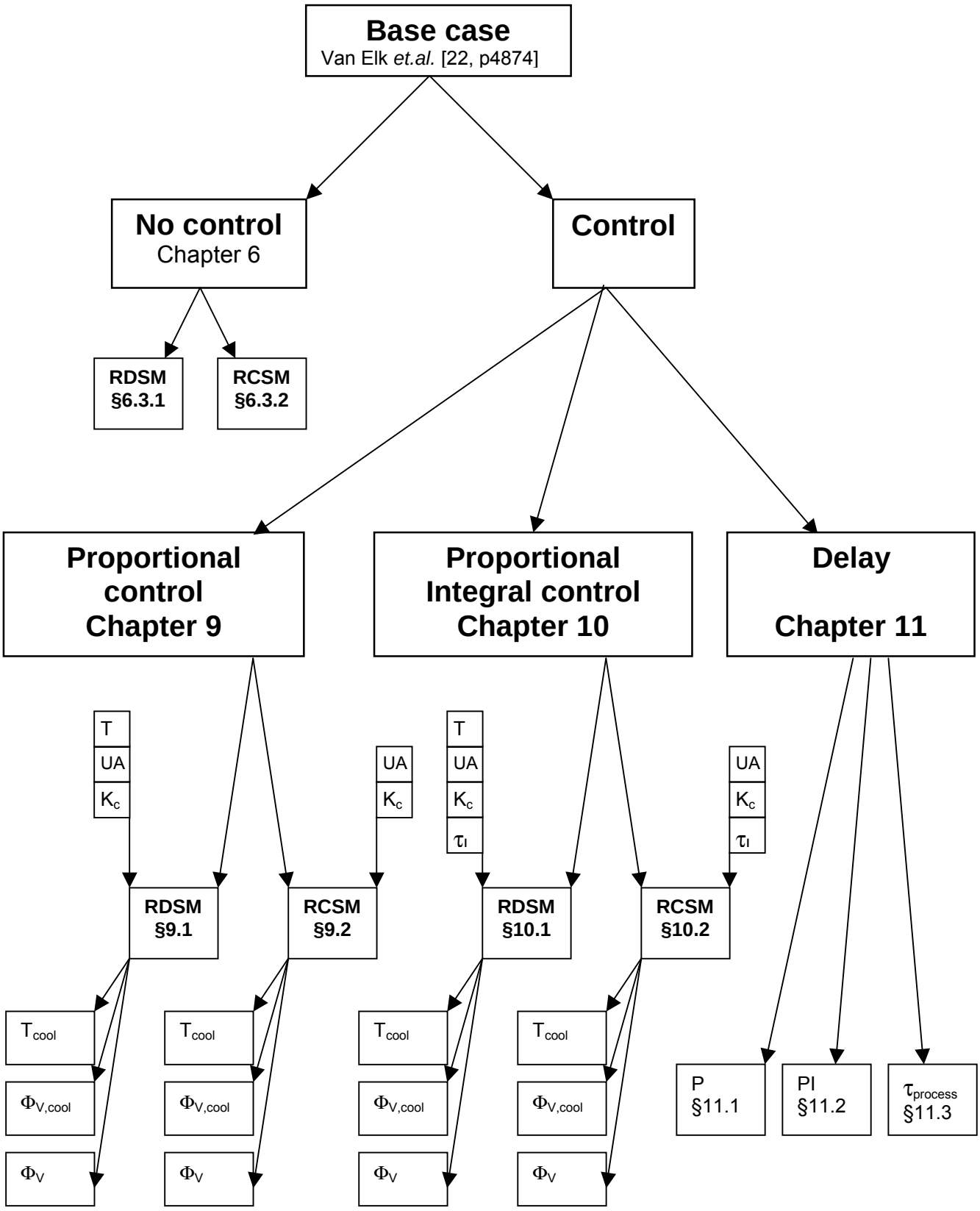
Base case
Van Elk et.al. [22, p4874]
No control
Chapter 6
Control
RDSM
§6.3.1
RCSM
§6.3.2
Proportional control
Chapter 9
Proportional Integral control
Chapter 10
Delay
Chapter 11
T
UA
Kc
UA
Kc
T
UA
Kc
τI
UA
Kc
τI
RDSM
§9.1
RCSM
§9.2
RDSM
§10.1
RCSM
§10.2
Tcool
ΦV,cool
ΦV
Tcool
ΦV,cool
ΦV
Tcool
ΦV,cool
ΦV
Tcool
ΦV,cool
ΦV
P
§11.1
PI
§11.2
τprocess
§11.3

Part III

APPENDICES

FAQ

(Frequently Asked Questions)

- *What is a CISTR?*
  - This is the abbreviation of continuously ideally stirred tank reactor i.e. a chemical reactor frequently applied in the process industry.

- *What is a limit cycle?*
  - A limit cycle is the phenomenon of self-sustained oscillations of the temperature and concentration in a chemical reactor, permanently around an equilibrium point, which never reaches the particular steady state value.

- *What happens if a limit cycle occurs?*
  - In the worst case, the temperature can rise to extreme heights; consequently, the reaction can run away from the desired steady state, which can lead to dangerous situations.

- *Do limit cycles exhibit in the process industry?*
  - Yes, in the literature the existence of limit cycles has been demonstrated and described. It predominantly occurs in cooled CISTRs.

- *What is a stability map?*
  - In a stability map, the stable and unstable regions, in which limit cycles and multiplicity exhibit, can be indicated, based on a mathematical description.

- *When can a limit cycle appear?*
  - A limit cycle appears when the system conditions are such that they can be classified as unstable. This can be derived from a so-called stability map, which is divided into stable and unstable regions.

- *How can a limit cycle exhibit?*
  - In the worst case when the controller device fails and the temperature changes towards an unstable region in which limit cycles can arise. Conversely, when due to long time changes of operation conditions e.g. fouling of the heat transfer unit, the working point has been modified.

- *How long does a limit cycle oscillation take?*
  - The oscillations time varies from minutes to hours. In this report, in the most uncomplicated case, the time between two peaks is on the order of 30 minutes.

- *How can a limit cycle be prevented?*
  - Of course, when a reactor is perfectly designed and nothing goes wrong…

- *What does perturbation and bifurcation mean?*
  - Literally, perturbation means excitement or commotion. In fact, it means an alteration of a specific quantity. A bifurcation point is a point at which two branches of a curve coalesce as a parameter is varied i.e. a critical value.

- *How can a limit cycle be controlled?*
  - With a suitable control device and tremendous appropriate strategy plan.

- *Can a limit cycle be predicted?*
  - If the engineer is capable of making the preferred stability maps. The stable and unstable regions in such a stability map can provide the desired information considering the occurrence of limit cycles.

- *What is an orbit curve?*
  - In an orbit curve an important system variable (temperature, conversion) is plotted against the time, in most cases to investigate the dynamical behaviour of this particular system variable.

- *Waarom heb je geen motto voorin je verslag?*
  - “Een motto is een punt op een lijn.” (Onno Kramer 2001).

END OF REPORT

Printed at: Thursday, 25 April 2002 at 1:11 PM:
Notes:

GLOSSARY

Automatic feedback control	Feedback control in which a controller device monitors the controlled variable of interest and commands a manipulated variable in order to maintain a desired value of the controlled variable.
Autothermal reaction	A system, which is completely self-supporting in its thermal energy requirements. The essential feature of an autothermal reactor system is the feedback of reaction heat to raise the temperature and hence the reaction rate of the incoming reactant stream.
Base case	The mathematical base case model is a collection of mathematical relationships between process variables, which purports to describe the behaviour of the actual physical process.
Bifurcation	This means an alteration of a specific quantity. Bifurcation has been defined as the appearance of topologically phase portraits under variation of parameters. In fact, a bifurcation is a change of the topological type of the system as its parameters pass through a bifurcation i.e. critical value.
Blowout velocity	In case the throughput is too large, the cooling effect of the feed flow is causing the chemical reaction to extinguish because the average reactor temperature drops rapidly.
Cascade control	Control scheme where the manipulated variable output of one controller becomes the set-point of another controller.
Closed loop	See feedback control.
CISTR	Continuously ideally stirred tank reactor.
Continuous process	A process in which material passes in a continuous stream through the processing equipment. Once the process has established in a steady state operating state, the nature of the process does not depend on the length of time the process is operating.
Controlled variable	In a control loop, the variable of which is sensed to originate a feedback signal.
Control state	The current condition of the control entity e.g. process management, unit supervision or process control. The control state defines how the control entity will operate and how it will respond to command.
Control strategy	The control schemes are composed of descriptive information that identifies the process control types of objects i.e. equipment module control, loop, device, indicator and/or status.
Control type	Any of the control that directs, initiates and/or modifies the execution of procedural control and the utilisation of equipment entities.
Damping ratio	The ratio of the second peak to the first peak in the process variable response, only if the process variable response is underdamped.
Dead time	The interval of time between initiation of a input change or stimulus and the start of the resulting observable response.
Derivative action	Calculation of the controller manipulated variable is based on the rate of change of the process variable, also called rate action.
Distance velocity lag	See dead time.
Disturbance	Process influence that affects the process variable but is not manipulated by the controller.
Droop	See offset.
Dynamic model	Mathematic model that attempts to capture the output response of a system as it changes as a function of time.
Equilibrium state	This state refers to a system at rest.
Equilibrium curve	This curve is the steady state solution of the ODE system as a function of one active parameter
Endothermic reaction	A reaction which can maintain exclusively if heat continuously is supplied.
Exothermic reaction	A reaction which produces heat, increasing the reactor temperature, which in turn increases the rate of reaction. This positive feedback loop can result in a thermal runaway.
Feedback control	Control scheme that uses knowledge of the output to take corrective action.
Feed-forward control	Control scheme that eliminates or reduces the disturbance effect on the process variable by using a measurement of the disturbance to modify the manipulated variable.
Fold curve	The Fold bifurcation curve represents the border between static stability and static instability as a function of two active parameters
Fundamental model	A mathematic process model; based on fundamental concepts e.g. the conservation of mass and energy.
Gain	The ratio of the change in the steady state output to a step change in the input provided the output does not saturate.
Heat capacity	The product of the overall heat transfer coefficient U and the area A in which the heat is transferred
Heat production rate	The heat produced in a reactor by a chemical reaction. The HPR is a function of the properties of the reaction mixture.
Heat withdrawal rate	The total heat removal from a reactor is the sum of the heat removed by the cooling medium and the cold feed supply. The HWR depends on the residence time in the reactor
Hopf curve	The Hopf bifurcation curve represents the border between dynamic stability and dynamic instability as a function of two active parameters
Input signal	A signal applied to a device, element or system.
Integral action	The controller manipulated variable is based on the integrated error i.e. the set-point minus the process variable.
Integral time constant	The reciprocal of the integral gain.
Integral windup	When a controller has integral action, a persistent error will cause the integral term to increase or decrease to a value of larger magnitude.
Limit cycle	Self sustained oscillation e.g. reactor temperature or conversion.
Limit point	Fold bifurcation.
Line-out time	See settling time.
Linear system	A system in which the time response to several simultaneous inputs is the sum of their independent time response. A linear system is generally represented by a set of linear differential equations.
Local stability	Using linearised models the stability at the steady state is determined.
Loop	A single-input, single output controller that monitors a transmitter and manipulates a physical quantity, usually a control valve, in order to force a process variable to the desired set-point.
Manipulated variable	A quantity varied by the controller in order to affect the controlled variable.
Mathematical model	A system of equations whose solution, given specific input data, is representative of the response of a process to a corresponding set of input.
Non-linear	A system that is not linear, see linear.
Non-self regulating	A process in which both inflow and outflow are independent of the controlled variable.

Offset	The difference between the set-point and the actual value of the process variable when the system has reached steady state.
Operating point	The normal operating value for the system variable.
Operating state	The currents condition of the equipment entity e.g. process cell, unit or equipment module. The operating state defines how the entity will operate and how it will respond to command.
Orbit curve	In a orbit curve an important system variable is plotted against the time. In most cases to investigate the dynamical behaviour of this particular system variable.
Output signal	A signal delivered by a device, element or system.
Overshoot	The maximum execution beyond the final steady state value of outputs as result of an input change.
Peak time	The time from the set-point step change to the time of the first peak of an underdamped process variable response.
Perturbation	Translated: excitement or commotion. See bifurcation.
PI-control	Abbreviation for proportional plus integral control. A controller whose output is the sum of proportional action + integral action.
PID-control	Abbreviation for proportional plus integral plus derivative control.
Process	Physical or chemical change of matter or conversion of energy e.g. change in temperature or concentration.
Process control	The control entity that encompasses the basic discrete regulatory and equipment module procedural control elements.
Process model	An overall model of the process that describes the processing actions required to convert raw material into finished product.
Process operation	Process operations represent major processing activities, which usually result in a chemical or physical change in the material being processed.
Process variable	The measured variable of the controller variable that, along with the set-point, is used by the controller to calculate a value of the manipulated variable.
Proportional action	The controller manipulated variable is calculated as a constant, called the proportional gain, multiplied by the error, the set-point minus the process variable.
Proportional gain	The ratio of the change in the manipulated variable due to proportional action to the change in the error.
Pure delay	See dead time.
Residence time	The quotient of the reactor volume and the throughput i.e. the average time the species remain in the reactor.
Response time	See settling time.
Ride hand side	LOCBIF source code.
Rise time	The time required for the process variable to go from 0% to 90% of the steady state change.
Runaway	See exothermic reaction.
Saddle node	Fold bifurcation.
Self regulating process	This process has a steady state relationship between the controlled variable and either inflow or outflow. The output variables tend to a steady state after the input variables have reached constant values.
Set-point	An input variable which sets the desired value of the controller variable.
Settling time	The time from the set-point change to the time that the process variable response has settled within a certain percentage band of the final value, usually 2% - 5%.
Stable system	A system is considered to be stable if a bounded input signal always returns in an output signal that is also bounded.
Stability map	In a stability map, the stable and unstable regions, in which limit cycles exhibit, can be indicated
State	The current condition of the physical or control entity. The state also defines how the entity will operate and how it will respond to commands.
Steady state	The long-term output response of a system after it has been disturbed.
Time constant	In an expression for linear system time response, the time constant is the value τ in the response term $e^{-\tau s}$. In a transfer function, the time constant is the value τ in the denominator $1+\tau s$. For the output of a first order system whose input is a step signal, the time constant τ is the time to complete 63.2% of the total output change.
Transfer function	For a continuous time system, the transfer function is the ratio of the Laplace transform of the output variable to the Laplace form of the input variable, with all initial conditions assumed to be zero.
Transportation lag	See dead time.
Underdamped	The time response of the system to a step signal input has overshoot.